

17443

NATIONAL LIBRARY  
OTTAWA



BIBLIOTHÈQUE NATIONALE  
OTTAWA

NAME OF AUTHOR... *N. S. S. S. S.*

TITLE OF THESIS... *Volcanogenesis, Orogenesis  
& Metallogenesis, Cause of  
River Northwest  
Alberta*

UNIVERSITY... *Alberta*

DEGREE FOR WHICH THESIS WAS PRESENTED... *Ph.D.*

YEAR THIS DEGREE GRANTED... *1973*

Permission is hereby granted to THE NATIONAL LIBRARY  
OF CANADA to microfilm this thesis and to lend or sell copies  
of the film.

The author reserves other publication rights, and  
neither the thesis nor extensive extracts from it may be  
printed or otherwise reproduced without the author's  
written permission.

(Signed) *[Signature]*

PERMANENT ADDRESS:  
*East Stowford  
Chittlehampton  
Umberleigh  
N. Devon  
England*

DATED... *3 Oct 1973*

UNIVERSITY OF ALBERTA

VOLCANIC ERUPTIONS, ORIGIN, NATURE AND METALLOGENESIS,  
CANNON RIVER AREA, N.M.T.

by



J.P.H. BADIAM

A THESIS

SUBMITTED TO THE FACULTY OF GRADUATE STUDIES AND RESEARCH  
IN PARTIAL FULFILLMENT OF THE REQUIREMENTS FOR THE DEGREE  
OF DOCTOR OF PHILOSOPHY

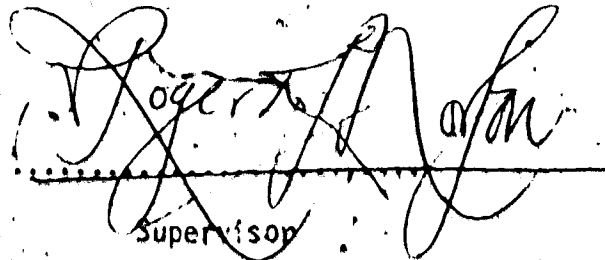
DEPARTMENT OF GEOLOGY

Edmonton, Alberta

Fall, 1973

THE UNIVERSITY OF ALBERTA  
FACULTY OF GRADUATE STUDIES AND RESEARCH

The undersigned certify that they have read, and recommend to the Faculty of Graduate Studies and Research, for acceptance, a thesis entitled "Volcanogenesis, Orogenesis and Metallogenesis, Camsell River Area, N.W.T.", submitted by J.P.N. Badham in partial fulfilment of the requirements for the degree of Doctor of Philosophy.

  
.....  
Supervisor

R. S. Lambert  
.....

J. G. Jacobs  
.....

R. S. Johnson  
.....

E. F. Stoff  
.....  
External Examiner

Date 1 Oct. 1973  
.....

# PREFACE

## From the Author to the Reader.

*YOU who so flit amid various things that you feel it shame to give yourself up even for a few short moments to mirth and joyousness in the land of fancy; you who think that life hath nought to do with innocent laughter that can harm no one; these pages are not for you. Clap to the leaves and go no farther than this, for I tell you plainly that if you go farther you will be scandalized.*

From 'The Merry Adventures of Robin Hood',

by

Howard Pyle.

London Press.

1872.

## ABSTRACT

An area of some 300 sq. miles, in the SE corner of Great Bear Lake, has been mapped and sampled. The predominant lithologies are Aphebian (2200-1700 m.y.) volcanic and plutonic rocks, and the area is interpreted as a roof-pendant of volcanic rocks lying in a keel between plutonic highs. The volcanic rocks are interpreted as comagmatic with, and derivative from the polyphase plutonic rocks, and all are interpreted as the product of late-stage orogenic magmatism.

Chemical analyses of the igneous rocks show them to be typical of the calcalkaline association. These data, together with recently-published data covering other parts of the Great Bear Lake area, lead to the postulate that a typical continent-margin orogen was active on the western edge of the Canadian Shield in Aphebian time.

The complex relationships of post-Aphebian diabase dykes are described. It is shown that these dykes are quartz tholeiites, and that they are the product of one extended phase of intrusion that is not obviously related to any of the Mackenzie swarms to which they have previously been ascribed.

Mineral deposits in the area, including those at the Terra, Norex and Silver Bay Mines, were examined, and three distinct types of mineralisation were recognised. The first, metasomatic sulphide deposits, is common around the margins of early-intermediate stocks. A study of the metamorphism and metasomatism around these stocks shows

the sulphides to have been derived from the intrusions. This conclusion is substantiated by sulphur isotope data.

Secondly, magnetite-apatite-actinolite intrusions, veins and diffusions are also common around the early plutons. Optical and analytical data are reported, and it is concluded that these bodies represent immiscible fractions from the silicate magma that was parent to the early intrusions.

Thirdly, polymetallic hydrothermal veins of the Ni, Co arsenide-silver ore-type are described. Detailed optical and mineralogical studies show these to be similar in most respects to other deposits of this type throughout the world. A long and complex paragenesis is proposed for the veins - a paragenesis dependent upon both the time of deposition and the distance travelled by the ore-fluid.

Analyses of the stable isotopes of oxygen and carbon from vein-carbonates provide little conclusive evidence concerning the source or evolution of the mineralising fluids. Analyses of sulphur isotopes are used to propose a 'magmatic hydrothermal' origin for the sulphur. It is proposed that the hydrothermal veins are the product of the younger intrusions, and that the complex, polymetallic assemblages are the product of 'telescoping' of the hydrothermal sequence.

Analyses of sulphosalts from the mines located no new minerals, but do provide new compositional data. Various hypotheses of metal derivation were tested by analyses of trace elements in both the country rocks and in pre-existing sulphides.

The veins are interpreted as having been deposited over a period

of some 200 m.y., and at temperatures ranging between 100° and 250°C. Other products of the hydrothermal activity include mineralised and barren Giant Quartz Veins and quartz-carbonate veins.

Finally, a model is proposed wherein the metasomatic and hydrothermal mineralisation are the inevitable products of the polyphase intrusive activity, which, in turn, is the inevitable product of the geotectonic evolution of the area. It is shown that, with one notable exception, the Ni-, Co arsenide-silver deposits of the world were formed as a consequence of similar geotectonic processes in similar geotectonic environments.

## ACKNOWLEDGEMENTS

This thesis was undertaken at the suggestion and under the supervision of Dr. R.D. Morton, who not only proved an invaluable councillor, but also footed many of the bills.

Field work was supported by Terra Mining and Exploration Limited (1970), Vestor Explorations Limited (1971), and Saco Mining Limited (1972). In 1972 the author was also able to visit the Silver Bay Mine, while working for Federated Mining Corporation. I am grateful to Messrs. A. Rich, A. Farrell, H. Sanche and R. Syliski of these companies, for their understanding that matters economic and academic may often be inseparable.

In the field Alemu Shiferaw was a most able assistant in 1971, and Messrs. D. Saare, W. Dollery-Pardy, F. Lypka, H. Arden, R. Zablonki, and J. Wilkinson showed me over their properties and lent me their cabins and equipment.

Mr. Robert Hornal of the Department of Indian Affairs, Yellowknife, and his staff have been most helpful and encouraging throughout the project.

At the Geological Survey of Canada, Drs. R. Thorpe, J. McGlynn and P. Hoffman have suffered a barage of argumentative letters and have answered most carefully; I must thank them for their ideas and their assistance. Dr. Hoffman made a number of unpublished analyses available to me.

Dr. R.W. Boyle most generously arranged and financed some of the



whole-rock trace element analyses.

Dr. G. Holland of the University of Durham, kindly analysed the rock samples for the major and some of the trace elements.

Dr. B.W. Robinson, of the D.S.I.R., New Zealand, performed the sulphur isotope analyses after the mass-spectrometer at Alberta became unavailable. For this, for his co-authorship on two (to date) papers, and for his continual and most helpful ideas and criticism, I shall always be grateful.

I would like to thank Dr. D.G.W. Smith for help and advice with the microprobe analyses, for his ability to solve the continual analytical problems I managed to come up with, and for his lack of violent reaction when I oxygenated his machine. In addition, operators D.A. Tomlinson and Mrs. Rene Bliss were invaluable during the analyses.

Dr. S. Pawluk was most helpful in advising on the atomic absorption analyses. Mr. A. Stelmach provided his excellent technical know-how during preparation of the samples, and Mr. Park Yee his during analysis. To all these I am most grateful.

The stable isotope project was set up in discussion with Dr. P. Fritz, who not only taught me the  $\text{CO}_2$  and  $\text{SO}_2$  extraction techniques, but also hovered over me during analysis of the carbon and oxygen isotopes - many thanks. Dr. M. Coleman took over the job of isotope advisor to me in 1972, and I am grateful to him for continual enlightenment. In addition, he and Miss P. Sundstrom analysed a further 10 carbonate samples for me.

I have profited greatly from discussions of the igneous petrology of the Camsell River area with Drs. C. Scarfe, I. McReath, T. Frisch and R. St. J. Lambert. In addition they read and offered helpful advice on early drafts of some of my publications.

The first draft of the thesis was read by Drs. R.D. Morton, R. St. J. Lambert and R.E. Folinsbee, and I am most grateful for their comments.

Mr. S. Winzer kindly investigated the garnets during one of his electron microprobe sessions, and Mr. C.R. Ramsay analysed the muscovite and amphibole. I am grateful for their work, and for their discussions of the results.

Colin Ramsay has been a most helpful and stimulating office companion for the last three years. I am most grateful to him for his advice and ideas on many parts of this thesis.

My thanks to Mr. Frank Dimitrov who did some of the draughting and advised me on the remainder.

My wife, Trisha, has done all the typing and a considerable portion of the editing. Furthermore, she has put up with my absence in the summers and presence in the winters. For all this I shall always be grateful.

Finally, affectionate thanks to Ron Oxburgh, who said I couldn't do it; and Roger Morton, who thought I might!

## TABLE OF CONTENTS

	Page
ABSTRACT	v
ACKNOWLEDGEMENTS	viii
<b>PART I: VOLCANOGENESIS AND OROGENESIS</b>	<b>1</b>
1. INTRODUCTION	2
2. PHYSIOGRAPHY	5
3. REGIONAL GEOLOGY	9
4. DETAILED GEOLOGY OF THE CAMSELL RIVER - CONJUPOR BAY AREA	19
a) General	19
b) Aphebian Lithologies	28
Basalts	23
Andesites	29
Felsic Volcanic Rocks	31
Volcanoclastic Sedimentary Rocks	33
Other Sedimentary Rocks	35
Correlations	36
Hypabyssal Porphyries	38
Plutons	39
Porphyry Dykes	40
c) Aphebian Events	41
Folding	41
Metamorphism	43
5. GEOCHEMISTRY OF APHEBIAN ROCKS	56
a) Analytical Methods	56
Results	59
b) Classification of the Volcanic and Plutonic Rocks	62
6. GEOTECTONIC EVOLUTION OF THE BEAR PROVINCE	80
Some Speculations on Continental Margins	85

	Page
7. POST-APHEBIAN LITHOLOGIES AND EVENTS	88
a) Faulting	88
b) Giant Quartz Veins	93
c) Diabases	94
d) Mineralised Veins	99
e) Alteration	100
f) Geochronology of Events	101
8. A DIGRESSION ON THE METACALCARGILLITE AT TERRA	103
 PART II: METALLOGENESIS	 114
1. INTRODUCTION	115
2. MAGNETITE-APATITE-ACTINOLITE INTRUSIONS AND RELATED BODIES	117
3. SULPHIDE MINERALISATION	129
4. A MODEL OF THE COOLING PLUTONS	140
5. HYDROTHERMAL VEIN DEPOSITS	142
a) Giant/Quartz Veins and Associated Mineralisation	142
b) Barren Quartz-Carbonate Veins	145
c) Quartz-Carbonate Veins containing Silver, Bismuth and/or Arsenides	146
6. THE TERRA MINE	151
a) History	151
b) General	151
c) Wall-Rock Alteration	154
d) Ore-Lenses	155

	Page
e) Details of the Vein Mineralisation	159
Carbonates	159
Quartz	161
Uranium Minerals	163
Silver	165
Arsenides	175
Sulpharsenides	186
Bismuth	186
Sulphides	190
Sulphosalts	194
Fluorite-Green Mica and Feldspar-Mica Veins	205
Haematite	206
Alteration Minerals	209
f) Paragenetic Sequence and Depositional Conditions	209
g) Ore Potential	215
7. THE SILVER BAY MINE	237
a) History	237
b) Geology	237
c) Wall-Rock Alteration	239
d) Location of Ore-Lenses	240
e) Details of the Vein Mineralisation	242
f) Paragenetic Sequence and Depositional Conditions	250
g) Ore Potential	250
8. THE NOREX MINE	253
a) History	253
b) Geology	253
c) Vein Mineralisation	255
d) Paragenetic Sequence and Depositional Conditions	259
e) Ore Potential	261

	Page
9. OTHER SILVER-BEARING VEINS	262
Ivka Veins	262
Republic Vein	
Gunbarrel Veins	265
Blpom Island Vein	265
Paragenesis	266
10. GENESIS OF THE VEIN MINERALISATION	267
a) Nature of the Ore-Fluid	267
b) Mode of Deposition	269
c) Source of the Ore-Fluid	274
d) Time and Duration of Mineralisation	285
e) Summary	287
f) Comparisons with Other Deposits	293
11. SUMMARY AND THE ORIGIN OF THE NICKEL-COBALT-ARSENIDE SILVER ORE TYPE	296
REFERENCES	303
APPENDIX I. Analytical Methods and Sample Descriptions and Locations.	317
APPENDIX II. Summary of Electron Microprobe Data and Operating Conditions.	324
APPENDIX III. Oxygen and Carbon Isotope Analysis. Analytical Methods and Results.	327 328
APPENDIX IV. Sulphur Isotope Analysis. Analytical Methods and Results.	331 332
APPENDIX V. Papers Published or in Preparation by the Author.	Back-pocket

## LIST OF FIGURES

Figure	Page
1. Location of study area/	6
2. Tectonic subdivisions of the NW Canadian Shield	10
3. The geology of the Great Bear Batholith	11
4. The geology of the Camsell River and Echo Bay areas	12
5. Relative and probable absolute ages of events in the Camsell River-Conjuror Bay area	18
6. Geological map of the Camsell River-Conjuror Bay area	20 and Back Pocket
7. Sections across the peninsula near the Terra Mine	22
8. Geology of the Terra Mine area	23
9. Sections east and west of the Bull Fault	24
10. Sketch map of the Balachey Lake area	26
11. Sketch sections showing the evolution of the Balachey Lake area	27
12. Structural and metamorphic map of the Camsell River area	45
13. Sketch sections A-A' and A-B	46
14. AFM diagram for igneous rocks in the Camsell River area	63
15. Alkali-silica diagram for igneous rocks in the Camsell River area	64
16. Harker variation diagrams for the major elements	69
17. Harker variation diagrams for the trace elements	71
18. Ti:Zr diagram for igneous rocks in the Camsell River area	72
19. Ti:Zr diagram for various calcalkaline suites	74
20. Predicted locations of Benioff zones for the Coronation Geosyncline	78

Figure		Page
21.	Development of the Wopmay Orogen and Coronation Geosyncline	84
22.	Sketch cross-sections showing the evolution of the western margin of the Canadian Shield	87
23.	Photolineations for a part of the Camsell River area	89
24.	Sketch maps of some faults in the Camsell River area, compared with geometric predictions for their development	92
25.	Diabases in the Camsell River area	96
26.	Paragenesis of the metacalcargillite at Terra	105
27.	Schematic mineralogy of some metamorphic bands in the metacalcargillite: an ACF diagram and proposed mechanisms for development of these bands	107
28.	Analyses of tuff, siliceous limestone, hastingsite and garnet, and a plot showing the variations of major element oxides between them	110
29.	Magnetite-apatite-amphibole bodies, Camsell River area	119
30.	Paragenesis of the magnetite intrusion	122
31.	Geological map of the Terra Mine	In Back Pocket
32.	Paragenesis of the sulphide skarn at Terra	133
33.	Paragenesis of events forming skarns around the early plutons, with estimated temperatures.	141
34.	Formation of dilatant pods in fault-zones and the location of ore-shoots	147
35.	Sketch maps of some of the Ag-Ni, CoAs showings	149
36.	Carbonate-filled fractures and the location of ore-shoots, Terra Mine	152
37.	Stope assay diagram, 108 Stope, Terra Mine	156
38.	Stope assay diagram, 201 Area, Terra Mine	157
39.	Carbon and oxygen isotope data for Terra Mine carbonates	162
40.	Mercury-Silver diagrams, Terra, Norex and Silver Bay Mines	172



Figure	Page
41. Stability fields and compositional ranges of di- and triarsenides.	176
42. Variation in Ni-Co-Fe across a zoned arsenide	182
43. Bismuth, showing totem-structure, in matildite	188
44. Compilation of electron microprobe data, showing sulphosalts replacing zoned arsenides	188
45. AKF diagram for the green muscovite	208
46. Paragenesis of the Terra veins	210
47. Depositional temperatures and availability of elements during deposition, Terra Mine veins	214
48. Geology of the Silver Bay Mine	238
49. Map and sections of the Silver Bay veins	241
50. Carbon and oxygen isotope data for Silver Bay, Norex and small showings	244
51. Paragenetic sequence of the Silver Bay Mine	245
52. Sketch map and sections of the Norex Mine	254
53. Paragenesis of the Norex vein	260
54. Deduced parageneses for the four mineralised veins	263
55. Idealised development of mineralised lenses in the Terra veins	273
56. Idealised time-distance plot for development of veins around a cooling pluton	284
57. Paragenesis of events around the cooling plutons in the Camsell River area	286
58. Schematic cross-section of the Camsell River area showing probable sites for development of hydrothermal veins derived from the late granites	289
59. Generalised paragenesis of the mineral deposits of SW England	292
60. Location of analysed samples	323

## LIST OF TABLES

Table	Page
1. Partial chemical analyses of rocks from the Camsell River-Conjuror Bay area	60-61
2. Comparisons of Camsell River analyses with those of other similar suites	66
3. Electron microprobe analysis of the amphibole in Sample SX 9.15	108
4. Sulphur isotope values for the Terra skarn sulphides and comparisons with those of sulphide impregnations from other parts of the Camsell River area, and from the Echo Bay area	136
5. Zinc contents of primary and recrystallised sulphides	139
6. Analysis of sphalerites	139
7. Mercury contents in native silver from Terra, Norex and Silver Bay	169
8. Silver content of bismuths	189
9. Sulphur isotope values of vein sulphides and sulphosalts in the Terra Mine	192
10. d-Spacings of principal reflections of ten matildites from the Terra Mine, compared with data from Rämdohr (1969) and the A.S.T.M. Index (1972)	196
11. Electron microprobe analyses for tetrahedrite, bismuthinite and matildite	197
12. Atomic percentages of elements in the tetrahedrite sample	199
13. Apparent analyses after each of the three electron microprobe analyses of the sulphosalts	201
14. Analysis of the green muscovite in Sample TX 24.4	207
16. Sulphur isotope values for vein sulphides from Silver Bay and Norex, and the Lypka veins	247

Table

Page

- |     |   |     |
|-----|---|-----|
| 16. | Whole-rock trace element analyses from the Camsell River area   | 277 |
| 17. | Comparisons of trace element data from the Camsell River area, with other areas in the Great Bear Batholith, and with calcalkaline averages | 279 |
| 18. | Age, chemistry, host-rock and possible sources of Ni, CoAs-Ag deposits in the world   | 297 |

LIST OF PLATES

PLATE	Page
1.	49
2.	51
3.	53
4.	55
5.	218
6.	220
7.	222
8.	224
9.	226
10.	228
11.	230
12.	232
13.	234
14.	236

PART I

VOLCANOGENESIS AND OROGENESIS

## 1. INTRODUCTION

Great Bear Lake is the northernmost of the great lakes that straddle the presently exposed margins of the Canadian craton. Most of the lake is underlain by Palaeozoic strata, but Alpebian (2100-1700 m.y.) and younger Precambrian rocks outcrop on the eastern shores and it is with some of these that this thesis is concerned.

Although the lake was well known to the white man from trappers' reports, from Petitot's cursory mapping and from the journals of Richardson, Rae, Dease and Simpson during their mid 19th Century search for Sir John Franklin, it was not until 1900 that the first scientific expedition was sent to the lake. J. MacIntosh Bell, accompanied by Charles Camsell and others, made topographic and geologic investigations of much of the lake and of the Camsell River. On 24th August, 1900, the party reached Klarondesh Bay (now Conjuror Bay) which is protected from the main lake by Ndutaho (now Richardson) Island, and entered the Camsell River system. Although he noted the 'granites and greenstones' of the lake's eastern shores, and intimated their Precambrian age, it was Bell's (1900) description of the mineral erythrite in carbonate veins that proved to be most significant.

In 1929 Labine and St. Paul followed up Bell's report and staked the property that was later to become the Port Radium Mine at Echo Bay. They also staked in the Camsell River area, where a

showing is still known as 'St. Paul's Showing'. Reports of the mineralisation filtered across to the Klondike and in the early thirties prospectors began to congregate at Great Bear Lake.

Every mineral showing but one known to the author was investigated at this time, but silver was not an attractive proposition and many of the prospectors were looking only for gold. Some small mines were opened and silver ore was high-graded, but by the mid-thirties many of the prospectors had moved south to Great Slave Lake where rumours of a gold strike were rife.

In the thirties the Echo Bay region was investigated in some detail by the Geological Survey, but only Kidd (1936) extended these studies to map - on the broadest of scales - the other Archean areas at Great Bear Lake.

By 1939 interest in the area was dead. A revival of the Port Radium Mine in 1942 to supply the Manhattan Project sparked renewed and detailed geological work in the Echo Bay area, but again the Camsell River area was virtually ignored. It was not until the mid-sixties that an interest in silver caused some of the old mines to be reactivated, and some new mines - including the Terra Mine - to be opened. This revival sparked new research, notably by Robinson (1971) on the by then relatively well-known Echo Bay deposits, and this research project was extended to the Camsell River area by the present study.

In 1970 the author was employed by Terra Mining and Exploration Limited to investigate their Cu-Ag property on the Camsell River.

It was quickly realised that the mineral controls were structural and lithological and it became imperative to map the whole area. The funds and interest for this were not available from Terra, so in 1971 the author was employed by Vestor Explorations Limited to do this. The work was continued for a short time in 1972, under the aegis of Saco Mines Limited, and Federated Mining Limited, but unfortunately not as much time has been spent on the area as the author would have liked. The remoteness and the expenses involved make purely academic research somewhat impractical in this area. However, in 1972 the Department of Indian Affairs and Northern Development at Yellowknife decided to continue and elaborate this author's work in the area, and Mr. Jim Murphy has produced a map which will soon be available. Continuing collaboration between the author and the D.I.A.N.D. has been most beneficial.

Although the original object of this thesis was to study the geology and genesis of the Terra Mine, the scope has widened because of the nature of the geology. Consequently, details of the geology and a scheme for the geotectonic evolution of the area are presented in Part I. Details of the mineral deposits are reported in Part II. A unified concept for the geologic and metallogenic evolution of the area is proposed finally.

Parts of this work have already been presented as Badham, Robinson and Morton (1972), Badham (1972) and Badham (1973). These works are included as Appendix 5 at the end of the thesis.



## 2. PHYSIOGRAPHY

The location of the area is shown in Figure 1. Most of the area consists of rolling hills, with up to 130 m of relief in those areas underlain by the volcanic complexes. Areas underlain by granitic rocks are generally high, but with low relief. The shores of Great Bear Lake (170 m above sea level) are considerably uplifted, with heights over 270 m recorded on Richardson Island - and the country is higher and more rugged to the north.

Rainfall is low and the area is classified as a sub-arctic sub-desert. Snowfall rarely exceeds 1 m. Drainage is by large rivers that flow over short and narrow falls connecting sizeable lakes. Ice persists from October to June and during break-up the rivers may rise by about 1 m. The optimum field season is from June to August, when the weather is usually hot and sunny, and water travel is unhindered by ice. The season is marred by an alarmingly dense and varied population of various biting insects.

The area is well-wooded with black spruce, and occasional stands of excellent timber can be found along the Camisel River; many have now been removed to supply the mines with timber.

Large game is rare and the population is declining rapidly. Wolves are perhaps the most common, although they were, until very recently shot on sight. Black bear are rare and are usually killed when seen. Moose are rare and caribou, common throughout the area fifty years ago, are now reduced to a handful of winter migrants.

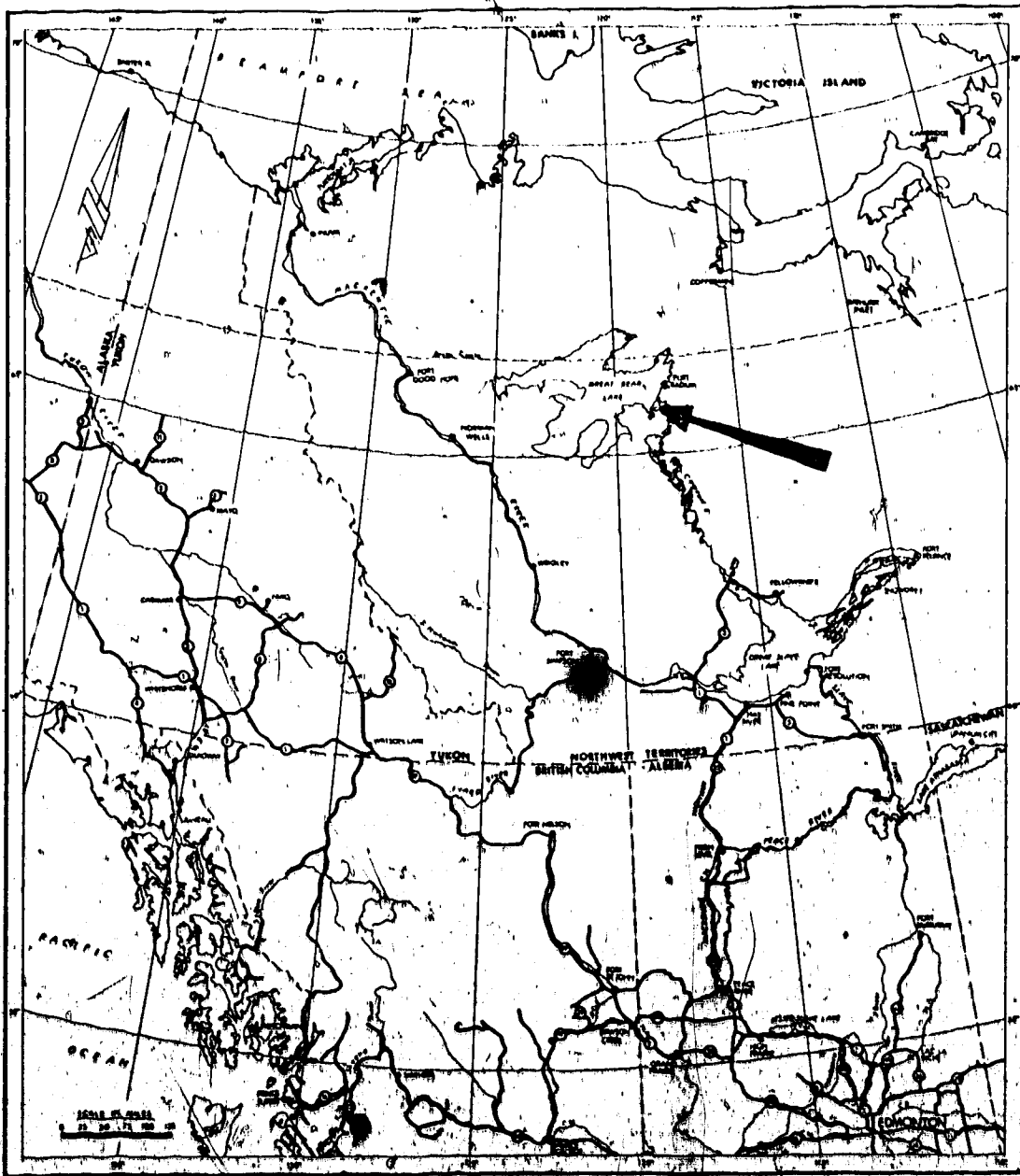


Fig. 1 Location of the study area.

Small game and waterfowl are abundant and appear to be increasing in number, largely due to the decimation of the larger predators.

Fish are plentiful and include northern pike, lake trout, grayling and whitefish. The trout, however, are suffering from overfishing and will soon need stringent protection if the famed trophy stock is to survive the century.

Outcrop is commonly better than 70% of the land areas. The best exposures occur along shorelines, and rocks on the hills, although scraped clean by ice, are usually altered by the chemical activity of lichens. The main Pleistocene ice transport direction was from the east, although apparently older striae trending north-south are occasionally found. Eskers of unsorted sand and gravel, often over 30 m high, are common and often of considerable length. Their courses reflect far more the trends of the underlying bedrock than the ice path. The boulders are usually locally derived.

Erratics are scattered throughout the area and although most are of local provenance, many are derived from the high-grade metamorphic rocks of the Hepburn metamorphic-plutonic belt and some were obviously eroded from greenstones, granites and gneisses of the Slave craton.

Raised beaches of well-sorted pebble conglomerate are common, even on the highest hills. Although many of these are isolated and poorly preserved, one beach that appears to be continuous from lake level to 100 m above the lake up a gentle slope has been found. This beach presumably documents the gradual isostatic response of the area since the departure of the main ice sheet some 10,000 years ago.

The figures are but qualitative and the beach warrants more careful examination, but if the interpretation is correct, this apparent rate of uplift is similar to those indicated around the margins of Wilson's Bay (J. Westgate, Pers. Comm., 1973).

### 3. REGIONAL GEOLOGY

The Bear Province was defined by Joliffe (1948) and is characterised by K-Ar ages around 1700 m.y. It has since been shown to be both a discrete structural province (e.g. Hoffman et al., 1970; Fraser et al., 1972) and a discrete metallogenic (U-Ag-Ni, CoAs-Bi-Cu) province (Joliffe, 1948; Badham et al., 1972). It is considered that the original definition of the province has outlived its usefulness. The radical change in the understanding of the Bear Province, engendered principally by Hoffman, has delimited various tectonic units and has demonstrated their interdependence. It is considered more appropriate now to use the tectonic subdivisions recently proposed by Fraser et al. (1972) - i.e. that the Aphebian of the Bear Province be ascribed to the Wopmay Orogen and that the younger Precambrian rocks be ascribed to the Amundsen Basin. This chapter outlines the regional geology of the Great Bear Batholith, one of three belts that constitute the Wopmay Orogen (Fig. 2). The relationships of these three belts are considered later.

A map showing the principle features of the Great Bear Batholith (Fig. 3) demonstrates the NE-trending, linear nature of the volcanic complexes within the epizonal granitic rocks. Where these complexes outcrop on the shores of Great Bear Lake they are roof-pendants composed of andesite-dacite-rhyolite sequences and associated volcanoclastic sediments. A more detailed map of two of these pendants is shown in Figure 4. The two pendants have been studied

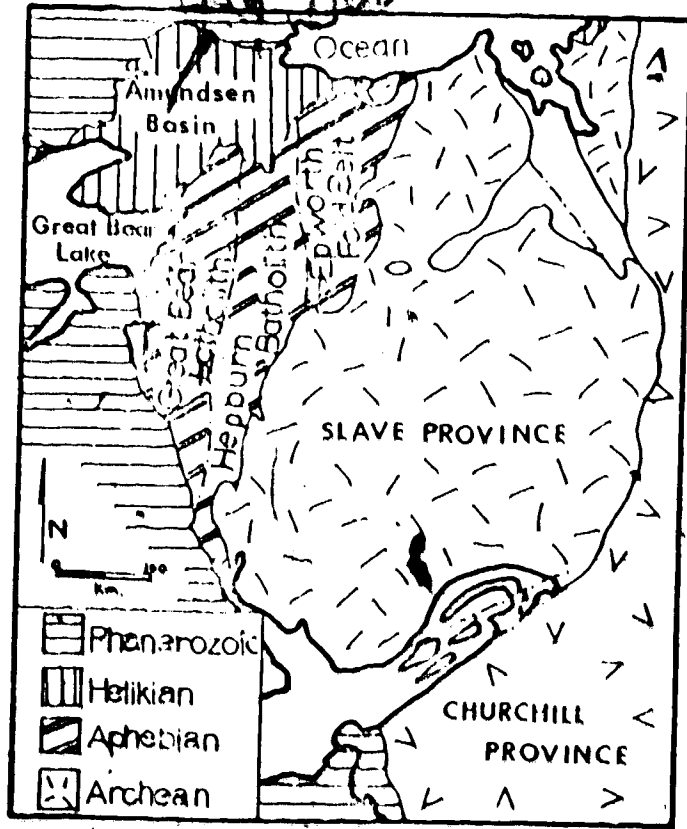


Figure 2. Tectonic subdivisions of the NW Canadian Shield- after Fraser et al (1972).

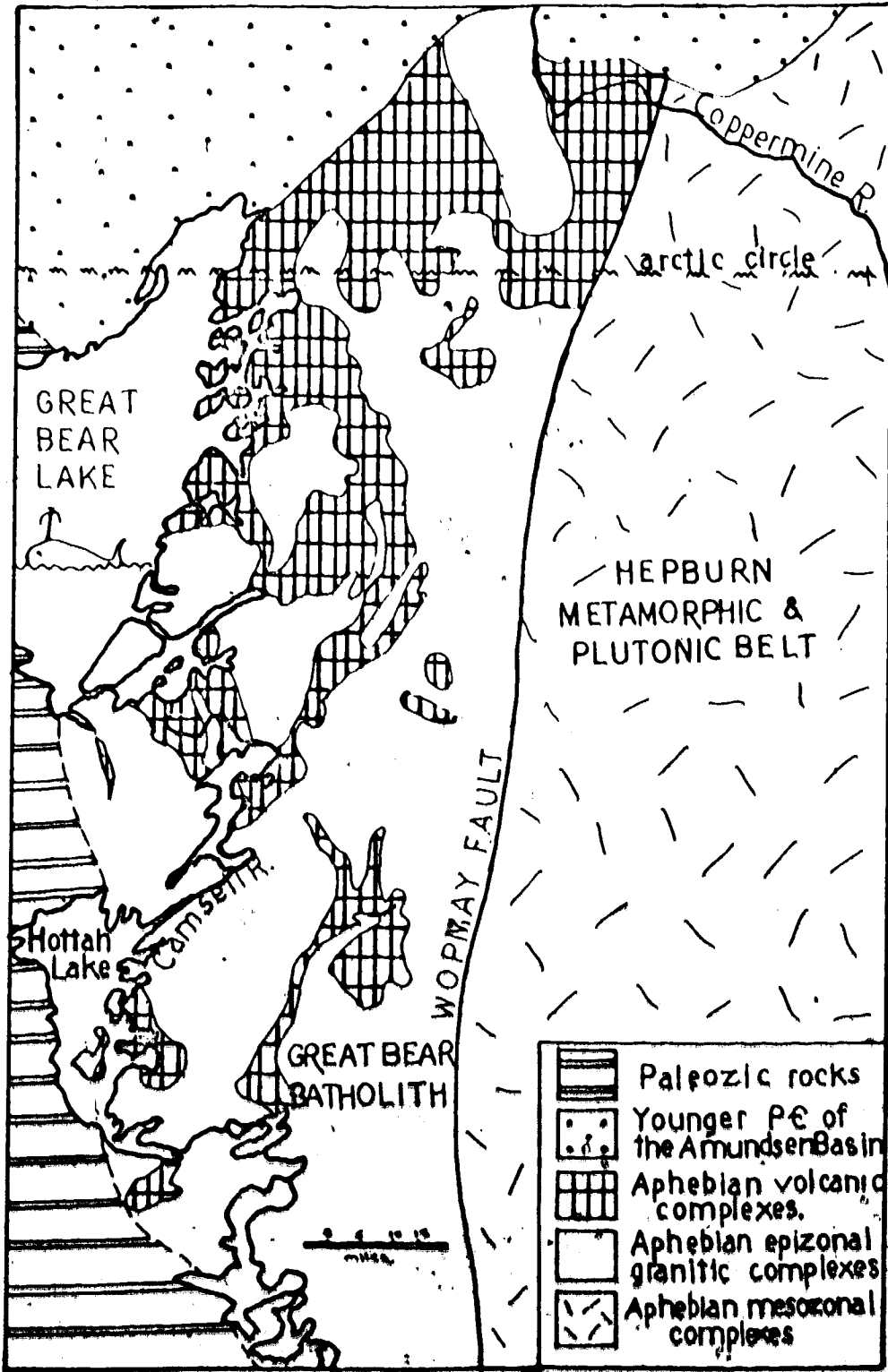


Figure 3. The Geology of the Great Bear Batholith.

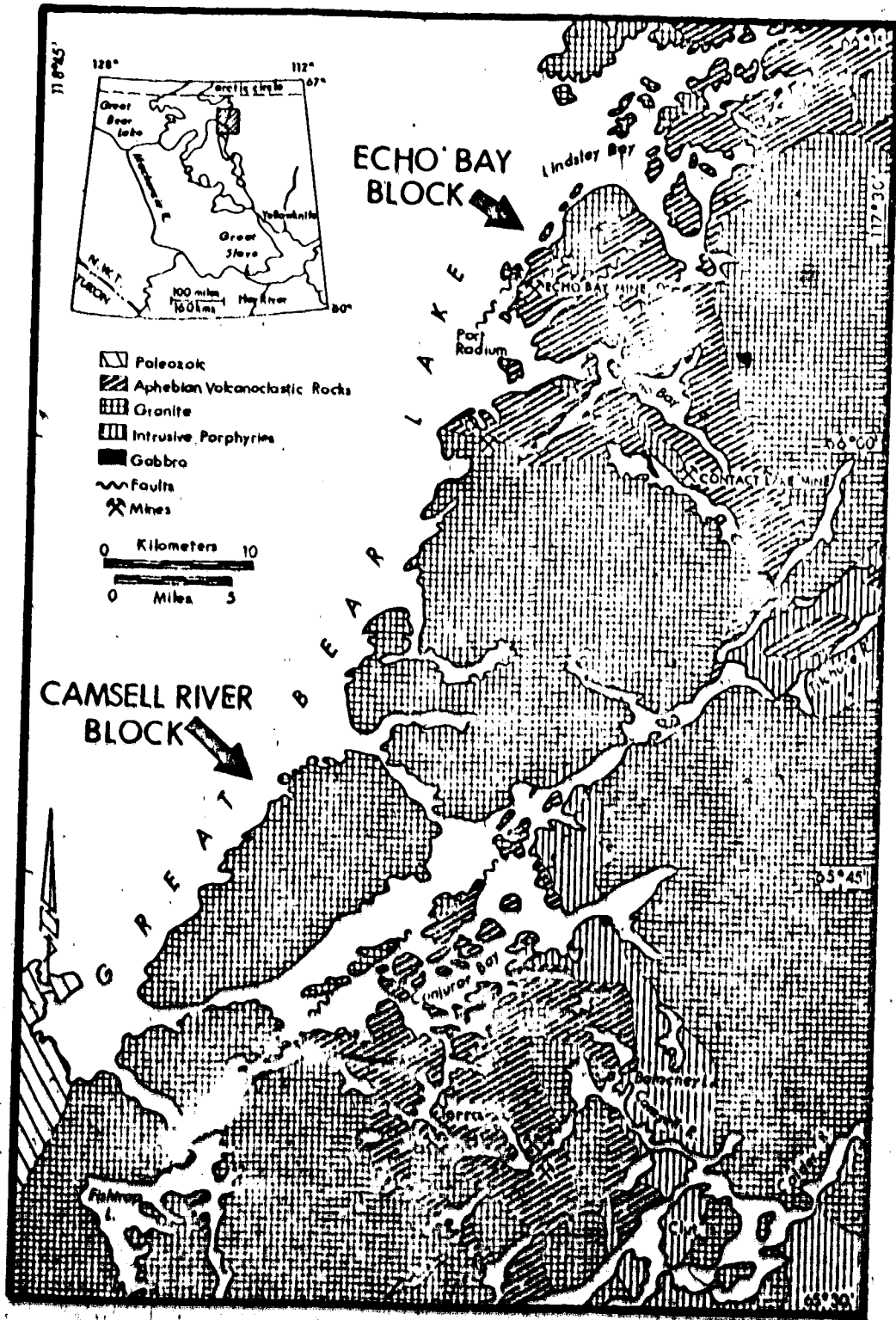


Figure 4. The Geology of the Camsell River and Echo Bay Areas.



and described as the Echo Bay Block and the Camsell River Block (Badham et al., 1972).

The Echo Bay area was first studied by Kidd (1931, 1932, 1936) who divided the complex into an older and dominantly volcanic group (the Echo Bay Group) and a younger, dominantly sedimentary group (the Cameron Bay Group). Kidd intimated that there was unconformity between the two groups, represented by a period of granitic intrusion, but showed clearly that both groups were intruded by granite batholiths.

Feniak (1947) detailed the stratigraphy of the Echo Bay Group, dividing it into a lower sedimentary and pyroclastic unit (1433 m) and an upper volcanic unit (1667 m). Neither top nor bottom of this sequence are exposed. Campbell (1955) further subdivided these units and Robinson (1971) obtained an Rb-Sr age of  $1770 \pm 30$  m.y. for the Upper Echo Bay Group. Although Mursky (1963) described Yellowknife (Archaean) sediments occurring to the northeast of the Echo Bay area, the report has not been substantiated and the Echo Bay Group are the oldest rocks exposed in the area.

All the above authors intimated profound unconformity between the Echo Bay and Cameron Bay Groups. The evidence for this conclusion at Echo Bay is the presence of boulders of Echo Bay Group and granite within Cameron Bay conglomerates. However, the contact is not exposed and there is no bedding discordance; indeed in many parts of the complex rocks typical of both groups are interbedded. The problem of the subdivision will be discussed later, after some

critical exposures have been described. Suffice it to say that the type stratigraphy can only be applied to the Echo Bay area, and that lithological correlations with other areas cannot be made. Attempts to apply the Echo Bay stratigraphy elsewhere have resulted in confusion. Some suggestions for dispelling this confusion are made below.

In general, however, the western volcanic complexes are typified by sequences of andesites-dacites-rhyolites overlain by their derivative sediments. These complexes were intruded at various times by intermediate stocks and hypabyssal porphyries, many of which are texturally indistinguishable from their volcanic equivalents. The whole area was finally intruded by coarse-grained granite (*sensu stricto*) batholiths.

All these Aphebian rocks are unconformably overlain by the Helikian Hornby Bay Group, which thickens and dips to the north. This, and the decreasing size of the volcanic complexes to the south, indicates that the present erosion surface cuts progressively deeper levels of the batholith to the south.

In the eastern parts of the Great Bear Batholith the volcanic complexes differ somewhat. Here vast thicknesses of silicic welded tuffs, with rare intercalations of trachybasalt and volcanoclastic sediment, are intruded by hypabyssal porphyries and by granitic rocks; there being a textural continuum between these three which are thus interpreted as being comagmatic (Hoffman, 1973 and Pers. Comm., 1973). These volcanic sequences are apparently contemporaneous with those in

the west and the differences may reflect a fundamental polarity of the batholith belt. However, Smith (1953) describes similar silicic tuff sequences which overlie granites containing remnants of rocks similar to the Echo Bay sequences at Hottah Lake. This evidence may reflect a difference in age of the 'eastern' and 'western' type sequences. Again, this point will be discussed more fully later.

In all the complexes, the volcanic rocks are broadly folded and generally dip away from the surrounding intrusions. Folding increases in intensity, but decreases in amplitude towards the contacts. Metamorphism to the hornblende-hornfels facies (Turner, 1968) has been recognised, but rarely extends more than a few hundred metres perpendicularly from intrusive contacts. In many of the aureoles various types of magnetite-apatite-actinolite bodies are developed (Kidd, 1936; Furnival, 1939a; Feniak, 1947; Robinson, 1971; Badham, 1972). The nature of these is discussed in Part II.

In the Echo Bay area the deposition of the Cameron Bay Group is fault-controlled (McGlynn, Pers. Comm., 1972). In the Camsell River area the margins of the larger batholiths appear also to be fault-controlled. Aplite and quartz-feldspar porphyry dykes, both related to the granites, also commonly intrude along faults. In all these cases the faults strike northeast and have been active since the Alpebian. The Bear Province is in fact typified by right-lateral NE-trending faults that splay and coalesce frequently, and which were most active between 1700 m.y. and 1400 m.y. ago. There are indications of N- to NW-trending faults that were active after the

final period of plutonism but before the main activity on the NE-trending faults (Feniak, 1949; Badham, 1972); these are not well documented as yet. Drag-folding adjacent to the primary faults is common. These faults have acted as the loci for a variety of minor intrusions.

'Giant Quartz Veins' (Furnival, 1935) are one such intrusive type. Frequently over 150 m wide, these massive quartz veins, containing scattered patches with hematite and uranium and copper minerals, filled dilatant zones in the faults during at least three distinct periods. Each period of intrusion corresponded to a period of movement that brecciated pre-existing material. The two earliest phases of intrusion preceded the deposition of the Hornby Bay Group, but a younger phase has been observed to cut this group (Kidd, 1936).

Diabase dykes occupy many of the primary faults and their secondary splays. Thick diabase sheets also intrude the Aphebian rocks and can be seen to swing into the faults in places. Most of these diabases appear to be older than 1300 m.y. (e.g. Fahrig and Wanless, 1963), but different periods of intrusion seem to be present and the complexity of the dyke swarms in this area will be discussed later.

Quartz-carbonate veins occupy many of the secondary splay-faults and associated tension fractures. These are mineralised in certain lithological and structural facies with the U-Ag-Ni, CoAs-Bi association, and it is these veins which form the basis of the mining industry in the area. Most of the metalliferous mineralisation

appears to have occurred between 1625 m.y. and 1400 m.y. These ages will be discussed later.

Hydrothermal alteration is widespread in the volcanic complexes and can be related mainly to the epizonal plutons. Alteration is common, but more limited, around all the Giant Quartz Veins, the mineralised veins, and the diabase dykes.

Although the area must have been covered by Phanerozoic sediments, there is no evidence of any geological process which might have affected the area between the intrusion of the youngest diabase and the Pleistocene glaciation.

The age relations of the various lithological units and events that affected them are shown in Figure 5.

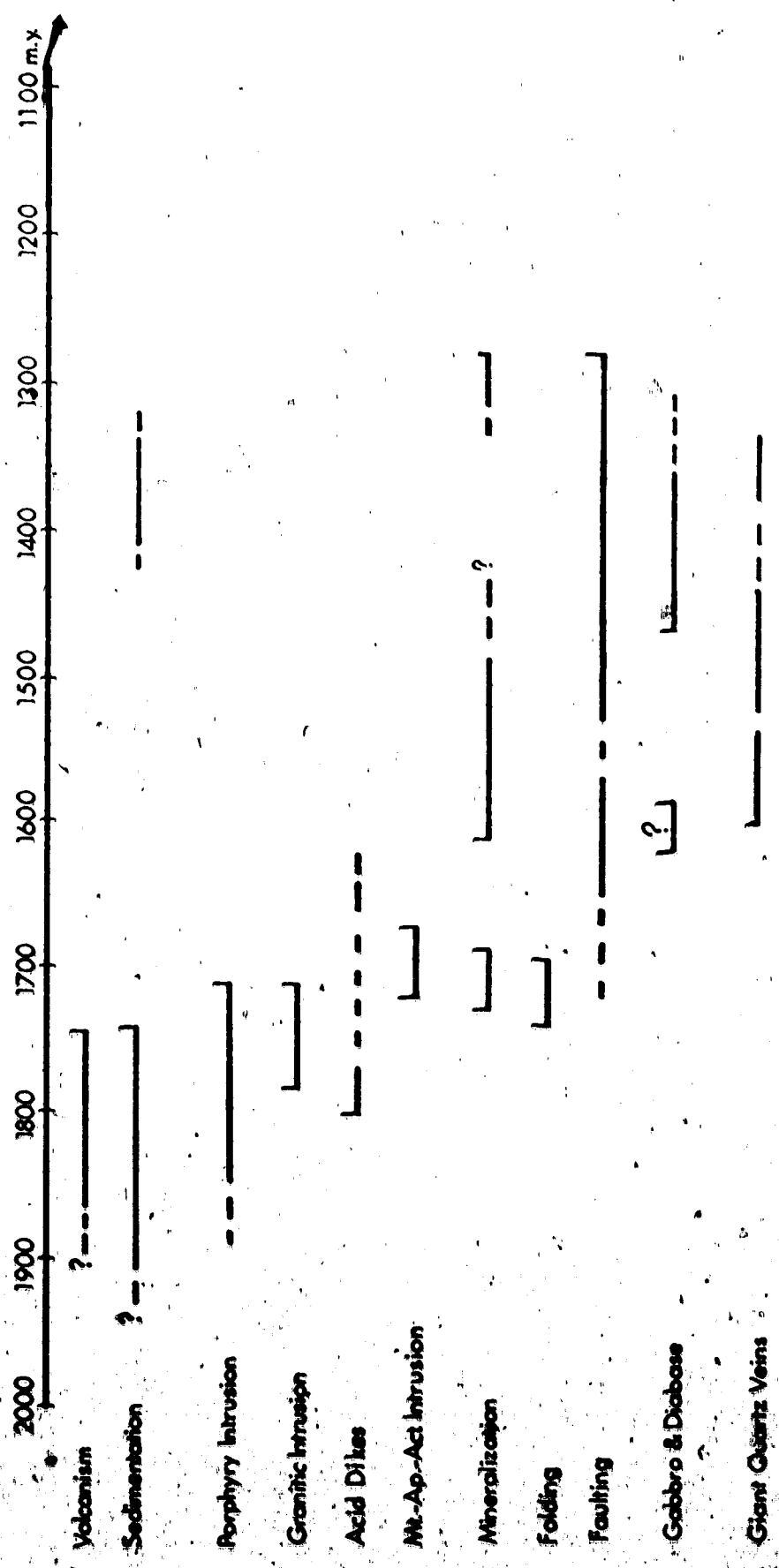


Fig. 5. Relative and probable Absolute ages of events in the Camsell River Conjuror Bay Area.

#### 4. DETAILED GEOLOGY OF THE CAMSELL RIVER-CONJUROR BAY AREA

##### a) General

The author's detailed map of the area is shown both in Figure 6 and in a large foldout in the back pocket. This map was compiled essentially from a four-week mapping season in 1971, but the Terra peninsula had been mapped in detail in 1970 while the author was employed as mine geologist at the Terra Mine. Details of the splaying and movements on the Beach-Bull-Alter Fault System were mapped in 1972. Kidd (1932) mapped the contacts of the volcanic complex with the surrounding granites, and Furnival (1934) mapped parts of the Gunbarrel Gabbro. Parsons and Lord (1947) covered the extreme eastern edges of the area, but no maps of the area were published until Figure 6 was presented in Badham (1972). The mapping is continuing under the auspices of the Department of Indian Affairs and Northern Development, Yellowknife. The only major revision that should be noted (Murphy, Pers. Comm., 1973) is that the 'esker' running east from the Gunbarrel Gabbro is underlain by the continuation of this gabbro. Areas not mapped in detail by the author (i.e. as undifferentiated Echo Bay Group on Fig. 6) have been found to be essentially similar to mapped areas (Murphy, Pers. Comm., 1973).

The volcanic complex is roughly circular, but is partly split by the NW-trending lobes of plutonic rocks and is transected by NE-trending faults, across which correlations are often hard to make. All the rocks are correlated with the Echo Bay Group (Badham,

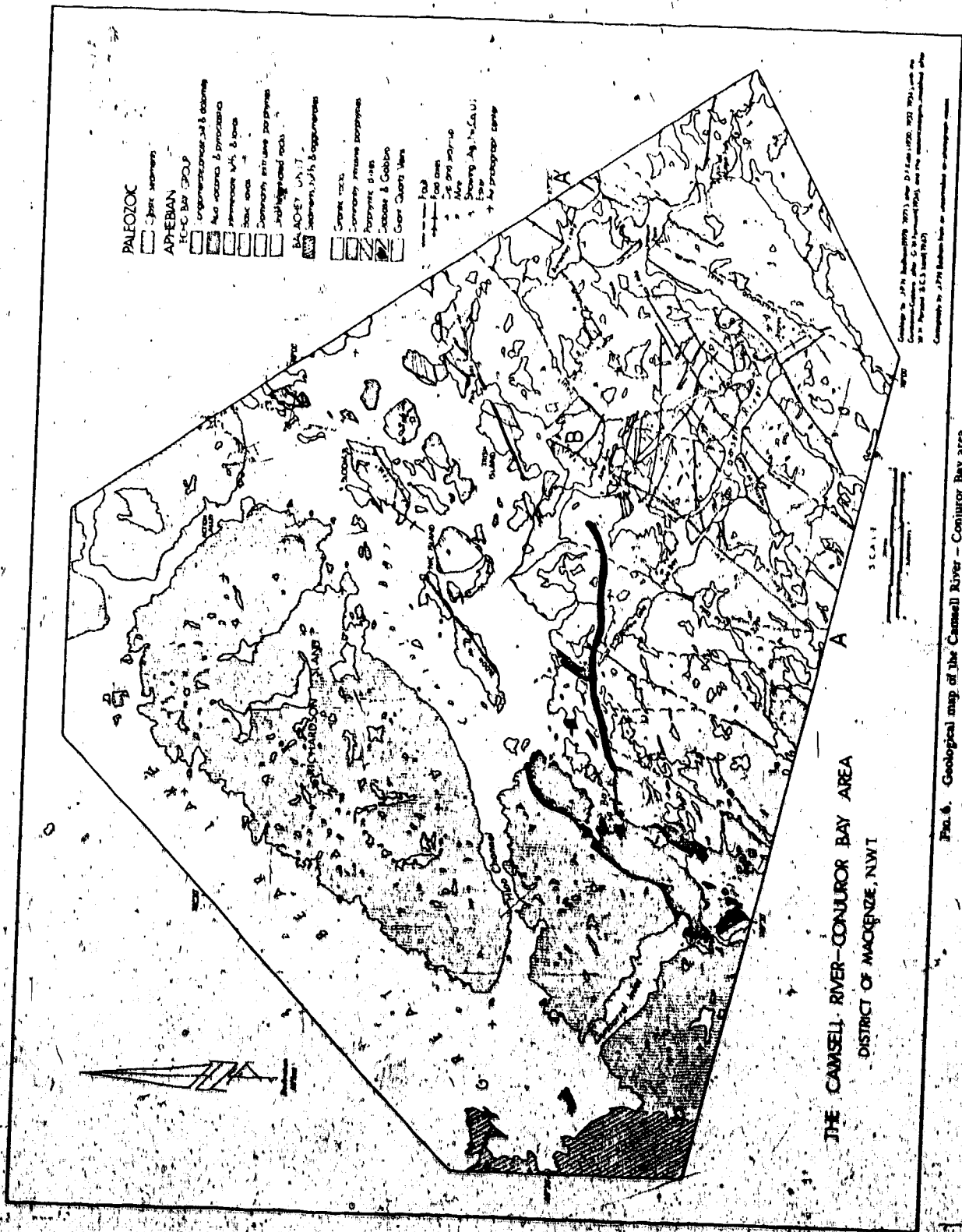


Fig. 6. Geological map of the Cammell River - Conjuror Bay area.



1972). Essentially four main sequences are recognised. The first, between Terra and Alter Arm, consists of about 500 m of andesite flows and tuffs, agglomerates and breccias (the 'Terra Sequence'), overlain by 3300 m of volcanoclastic sediment. The Terra Sequence can be traced along strike to the east, where the thickness of the andesite flows increases, around the nose of a large open syncline, where a few hundred metres of basalt appear, and on up the side of Jason Bay and to the north. There metamorphism is fairly intense and exposures are limited, and the sequence was not followed further. Detailed sections of this lower sequence at Terra are shown in Figure 7 and a map of the peninsula in Figure 8.

The second sequence outcrops to the west of the Bull Fault System. It is truncated by granites at the base and by Conjuror Bay in the north. It consists of at least 5700 m of silicic pyroclastic rocks, with rare volcanoclastic intercalations: lateral facies variations are rapid. This sequence underlies the first, whose basal members appear on the southern shores of Conjuror Bay (Fig. 9).

The third sequence is not known in detail but outcrops on the islands in Conjuror Bay. It consists dominantly of thick welded rhyolite tuffs, with thin intercalations of dolomite, quartz pebble conglomerate, quartzite and argillite, but some islands consist entirely of metamorphosed andesite flows and tuffs. Correlations between these rocks are at best difficult.

The fourth sequence outcrops from Balachey Lake to Pole Bay and consists of at least 100 m (at Balachey Lake) of well-bedded

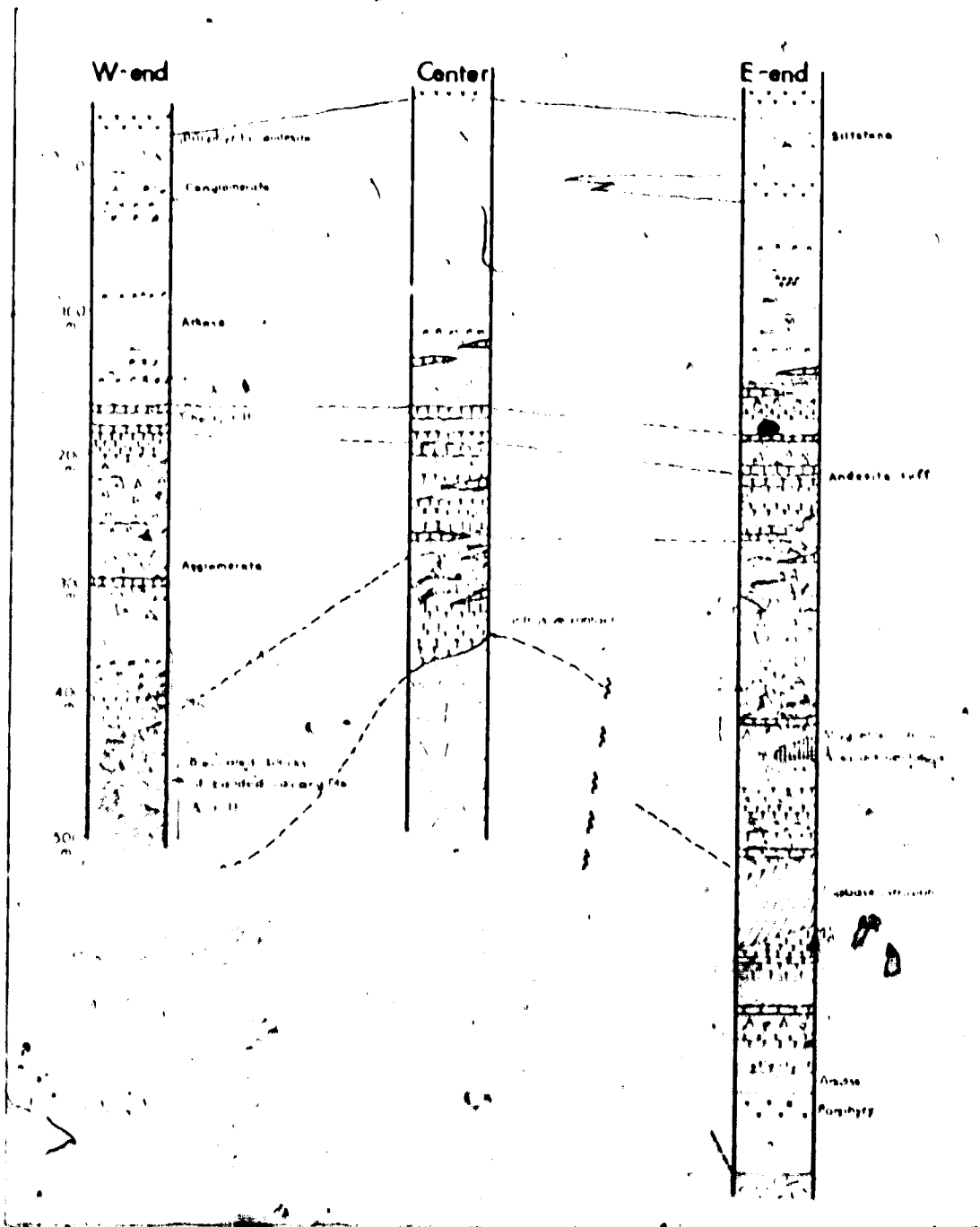


Figure 7. Sections across the peninsula near the Terra Mine.

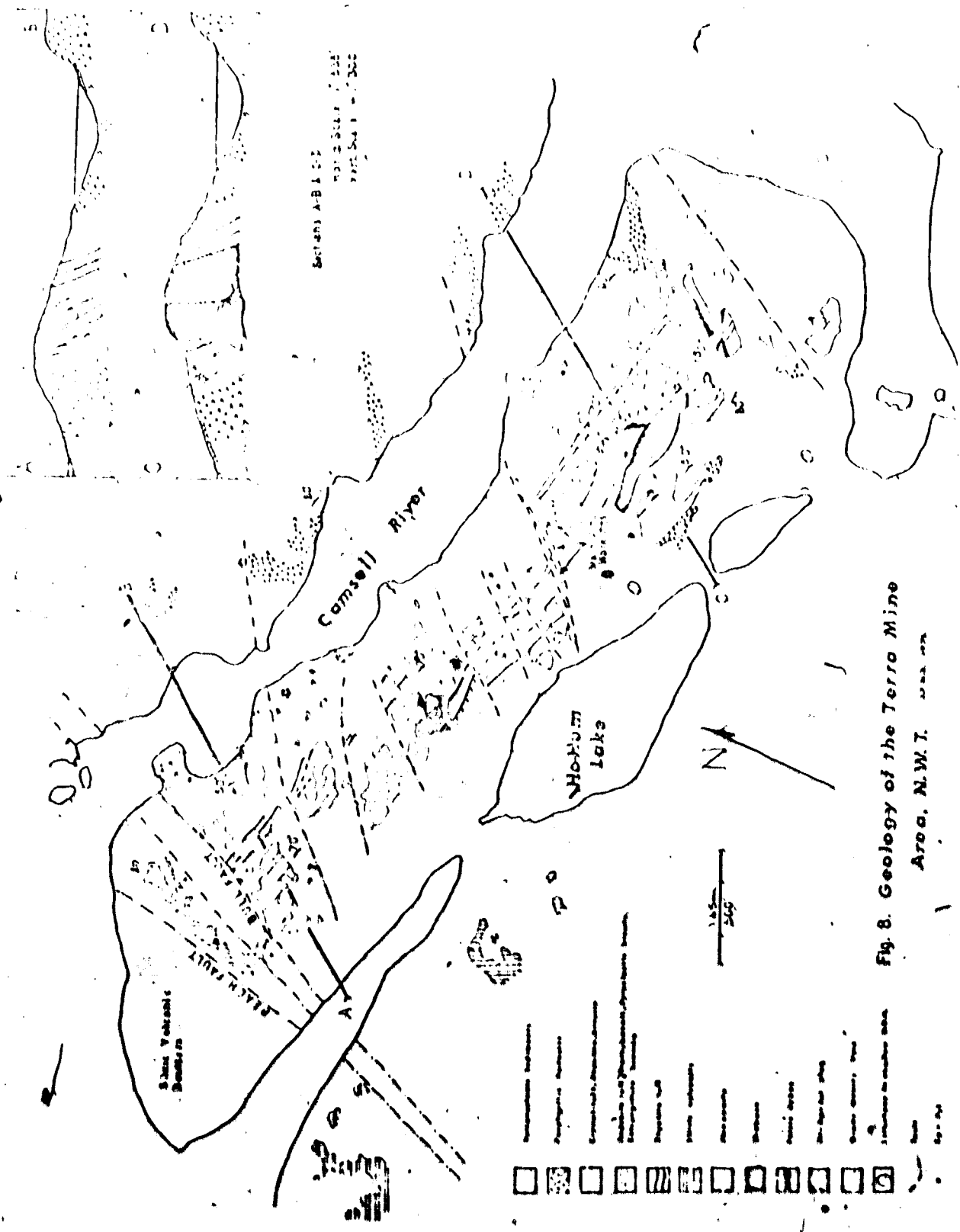
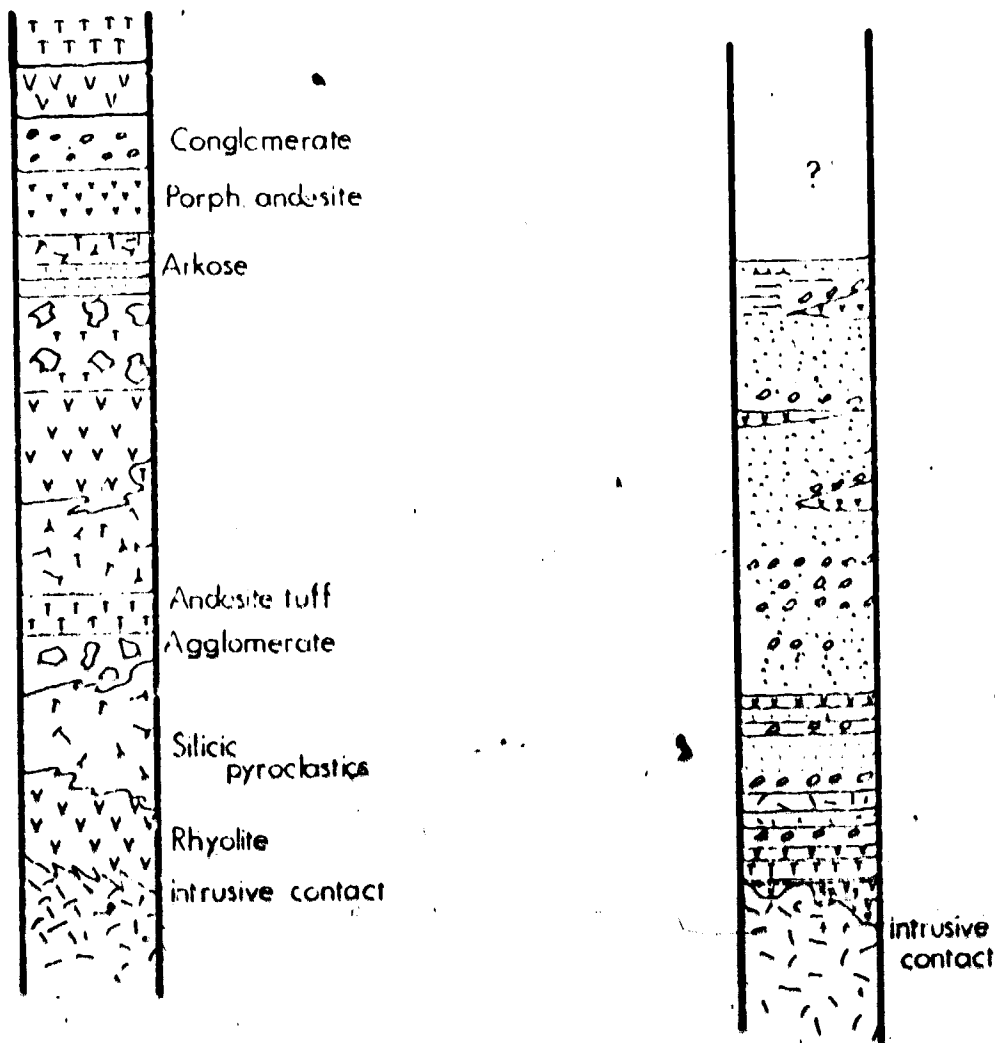


Fig. 8. Geology of the Terro Mine Area, N.W.T.

### Section West of the Bull Fault

### Section from Silver Bear Mine to Alter Arm



SCALE  
2000 meters

Figure 9. Sections East and West of the Bull Fault.

sediments unconformably overlying a highly altered diorite. The basal 5 m consists of a breccia of diorite blocks which grades up into a conglomerate containing diorite and typical Echo Bay Group boulders (Fig. 10). These are overlain by fine-bedded argillites and greywackes and, in the upper parts, silicic tuffs and flows and rare intercalations of dolomite are present. At Balachey Lake typical Echo Bay Group volcanic rocks are intruded by the diorite, but at Pole Bay the Balachey Sequence, though much thinner, is interbedded with typical Echo Bay Group rocks. This apparent dilemma has been explained (Badham, 1972) as the result of penesynchronous volcanism in the one area and local unroofing of an early diorite stock in the other (Fig. 11). All the rocks are intruded by a younger granodiorite at Balachey Lake.

The sequence described above was also described by Kidd (1936) and Parsons (1948), both of whom correlated it with the Cameron Bay Group. Both authors also noted that the sequence was intruded by granitic dykes. The correlation is not valid in the light of the evidence presented above and until its relations to other groups are more clearly defined, this sequence is assigned to the Balachey Unit (Badham, 1972).

All volcanic and sedimentary rocks in the Great Bear Batholith should be assigned to a single 'supergroup' with various local sequences being given local names as 'units'. It is suggested that the 'Echo Bay Group' has priority and should be so redefined.

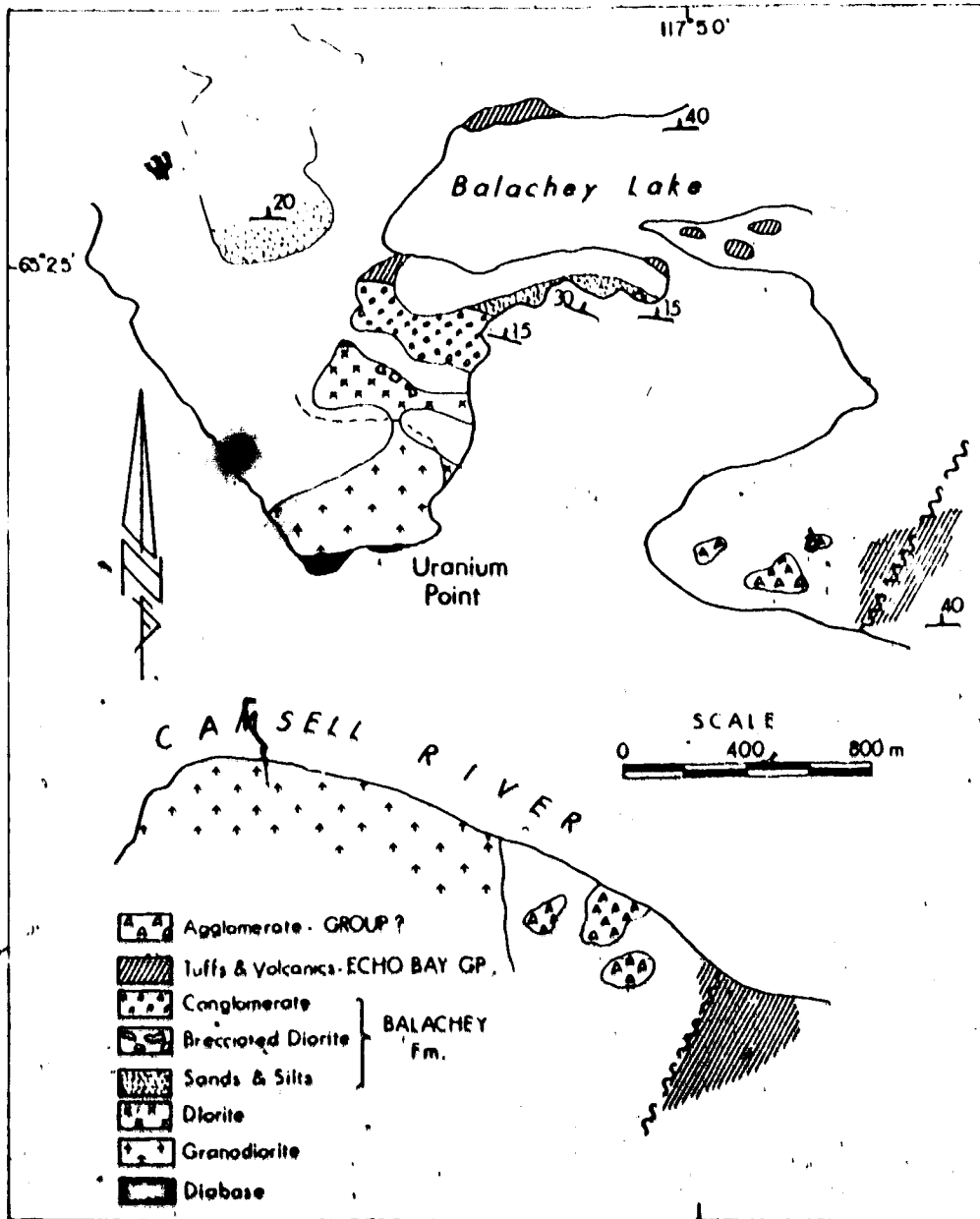


Figure 10. Sketch Map of the Balachey Lake Area.

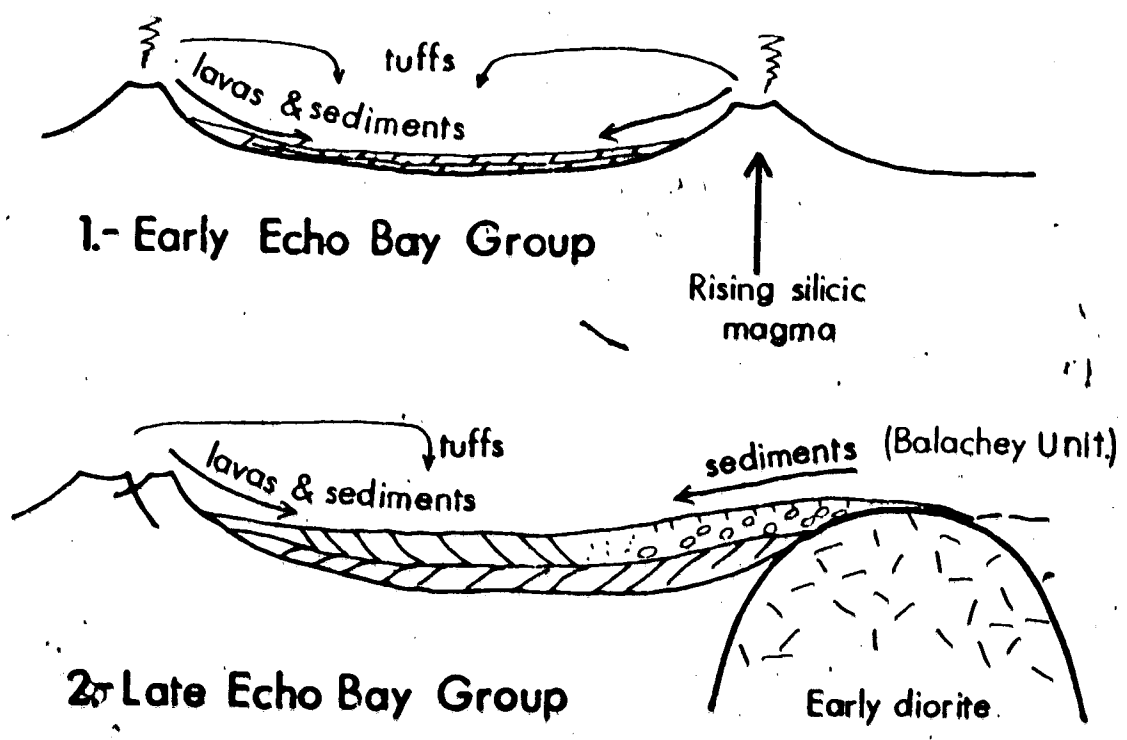


Figure II. Sketch sections showing the Evolution of the Balachey Lake Area.

## b) Aphebian Lithologies

In this section field and petrographic descriptions of the rocks are presented. A general summary of the lithologies has been given in Badham (1972).

### Basalts

Approximately 100 m of basalt outcrop in the core of a large open syncline on both banks of the river at Silver Bay. The unit extends to the north parallel to Jason Bay, becoming thinner and containing intercalated intermediate tuff horizons. Within the Terra Sequence near Terra and in a few other horizons, thin trachybasalts have been observed (Plate 2.1). The contact relations of the latter are obscured and they may in fact be syn-volcanic basic dykes (see Part I:5).

The Silver Bay basalts occur within the Ab-Ep facies aureole of the granites to the east and are altered by the local mineralised veins (Plate 4.7). Nevertheless, the original mineralogy can be deduced. In hand specimen the rocks are fine-grained and dark green with very dark green chlorite patches and small feldspar phenocrysts. Locally they are highly vesicular and contain thin lenses of agglomerate. In thin section most of the chlorite patches are clearly pseudomorphous after amphibole, but some are of dubious origin. Kidd (1936) noted relics of olivine, but none were seen by the author. The feldspar phenocrysts are mostly andesine and are altered to sericite, epidote and carbonate. They are weakly aligned. The phenocrysts are set in a finely crystalline mesh of feldspar laths.



chlorite, carbonate and magnetite. The vesicles are irregularly shaped and rimmed with chlorite and are filled with two generations of quartz and less commonly with carbonate. The agglomeratic horizons consist of angular blocks of the above basalt contained in a yellow-weathering matrix that is made up of trachytic andesine phenocrysts and chlorite, streaked quartz-filled vesicles and devitrified shards (Plate 2.3). These horizons are interpreted to be of flow-top devolatilization origin ('froth-lavas' - Tazieff, 1970) and attest to the highly volatile nature of these basaltic magmas. Generally flow tops are hard to recognise because of the alteration, but three slightly different flows have been identified.

#### Andesites

Nearly all the andesite flows in the area are feldspar, hornblende porphyritic andesites. They are mineralogically and texturally indistinguishable from many of the hypabyssal porphyries and can only be distinguished from the latter by their field relationships. Important criteria for this are:

1. Conformity of bedding.
2. The lack of chilled tops.
3. The lack of contact metamorphism.
4. The presence of rolled bases, aa blocks and trachytic flow textures.
5. The presence of amygdules and scoriaceous tops.
6. The presence of eroded tops.

7. The presence of tuffaceous and agglomeratic horizons.

These flows are commonly over 30 m thick, but often change thickness considerably laterally. Flows on the Terra peninsula were investigated in detail since they had all been previously described as intrusions. Plate 1.1 shows large blocks of porphyritic andesite cracked and surrounded by smaller blocks in a matrix of dark lava that consists of microcrystalline trachytic feldspars in a devitrified matrix. This horizon occurs near the base of a thick flow and is interpreted as a 'rolled base', where earlier partly-crystallised lava was autoclastically fractured by continual flow and the blocks rolled in still-liquid material. Plate 1.4 shows the base of a flow that was extruded onto partially consolidated mudcracked silts. The flow base was chilled and then broken and blocks of silt were incorporated. still-molten lava was injected into the cracks and mixed with wet silt to form an 'emulsion' that was squeezed between the cracks. Sprouting of liquid lava into crystallised and cracked aa flow toes has been described by MacDonald (1953); the mixture of wet sediment and lava to form an emulsion has been proposed by many authors (see Snyder and Fraser, 1963). This same flow must have been thicker than the depth of the water into which it flowed, for the top was weathered sub-aerially before later deepening of the water allowed its own derivative arkose and conglomerate to be deposited upon it.

In thin section the porphyritic andesites consist up to 40% of oligoclase phenocrysts, often cored by chlorite blebs, which replaced glass inclusions (Plate 2.5), 30% of hornblende phenocrysts and rare

corroded quartz crystals, in a fine-grained groundmass of plagioclase chlorite and opaque oxides. The opaque oxides are sometimes replaced by pyrite in the metamorphosed examples. The vesicles are circular and were filled in two stages - firstly by carbonate and chlorite, and secondly by opaline silica, now recrystallised to quartz (Plate 2.4). Variations in the relative proportions of hornblende and plagioclase phenocrysts can be used to distinguish between flows. The andesite tuffs are more variable. Most commonly they consist of well-banded fine crystal tuffs, often partly resedimented, sometimes with intercalated argillaceous bands (Plate 1.2). Coarser lithic crystal tuffs form thick sequences locally, especially in the Terra Sequence, and on the shores of Conjuror Bay. The lithic fragments are always andesite tuff or lava and the crystals are usually cracked and abraded oligoclases or, less commonly, hornblende and quartz. Some fine ash-fall and some vitric-crystal andesite tuffs have been observed.

Breccias consisting of fragments of local lithologies in a porphyritic andesite or tuffaceous matrix are common. These are poorly sorted, chaotic and unstratified (Plate 1.3), but often contain lenses of bedded tuffaceous material. Included are phreatomagmatic breccias, pyroclastic flow breccias and reworked pyroclastic breccias (Fisher, 1961; Parsons, 1968).

### Felsic Volcanic Rocks

Thick sequences of felsic tuffs are common throughout the area.

but flows are less so. In the section to the west of the Bull Fault there are a number of devitrified rhyolite flows, some of which may have been obsidian. They are interbedded with felsic tuffs and fragmental lavas. Distinctions between welded tuffs and devitrified flows are hard to make in the field. The flows contain sparse biotite flecks and rare vugs filled with quartz, possibly pseudomorphous after tridymite. In thin section those samples containing cracked and abraded phenocrysts and lithic fragments were considered to be tuffs.

The tuffs include welded and unwelded varieties and many should be classified as sillars. All combinations of vitric-, crystal- and lithic- varieties have been observed. Crystal fragments include plagioclase, embayed quartz, cristobalite (Plate 2.7), hornblende, K-feldspar (after sanidine?); lithic fragments include andesite and felsic tuff and lava (Plate 2.6).

A crystal-rich welded tuff (ignimbrite) is exposed on the islands east of Bloom Island. It contains shards, collapsed pumice fragments (fiamme); lithic fragments and fractured crystals in a devitrified matrix of hematite-stained microcrystalline material (Plate 2.7). Perlitic devitrification textures (Plate 2.8) are common. Although different parts of the tuff are welded to different degrees (Ross and Smith, 1961), the exposure is not continuous enough, nor the mapping detailed enough to identify individual flows or cooling units. All of these felsic flows and tuffs are sub-aerial.

In the Terra Sequence there are 1-6 m thick beds of what was

mapped as 'chert' (these are also common near Echo Bay, where many authors refer to the 'cherts'). They are well-banded and fairly persistent laterally. They consist of a microcrystalline mesh of sodic plagioclase and quartz with scattered flecks of chlorite and biotite, and are often 'dusted' with haematite. These are ash-fall rhyolite tuffs. They were probably at least partially welded and may be the distal equivalents of the ignimbrites. Some of them show signs of partial reworking, but there is no incontrovertible evidence of sub-aqueous deposition.

#### Volcanoclastic Sedimentary Rocks

Conglomerates and arkoses are commonly interbedded with the lavas and tuffs, and a sequence of 3300 m of these rocks is exposed from the Camsell River northwards to Alter Arm. The conglomerates contain well-rounded boulders (3 cm to 1 m), over 90% of which are porphyritic andesite, in an arkosic matrix. Other boulder materials include rhyolite flows and tuffs, andesite tuffs, Jasper and vein quartz. Boulders of tuff are rare, presumably because the tuffs were not consolidated at the time of erosion. No granitic boulders were found in these rocks. The conglomerates commonly overlie flows and grade upwards into arkoses. In this main sequence many of the flows also grade laterally into conglomerates. The conglomerates are internally structureless, but usually rest on scoured and channelled bases.

The arkoses are often cross-bedded and graded (Plates 1, 5 and

1.6) and contain numerous channels and scours, and lag concentrates of iron oxides. They consist of slightly abraded feldspar crystals in a matrix of finer volcanic debris. Lithic clasts are uncommon.

These feldspars are identical to those in the porphyritic andesites but often appear to be slightly fresher. It may be that many lavas were partially eroded so rapidly after extrusion that the feldspars were 'quenched', whereas those remaining in the still-warm lava underwent some autometasomatic alteration.

Siltstones are less common in the sequence. Where seen, they are well-bedded purple rocks, often interstratified with fine-grained arkoses (Plates 1.6 and 1.8). They are compositionally indistinguishable from the other volcanoclastic sediments and are their more-mature equivalents. The matrices are often very rich in haematite. The siltstones are poorly-sorted and exhibit scours, ripple-marks, grading, mudcracks, mud-chip conglomerates, loading and water escape structures (Plates 1.8, 3.5 and 1.6). In general there is a bimodal distribution of particles in both arkoses and silts. Quartz grains dominate the smaller size fraction and lithic fragments the larger. Feldspar grains are present throughout in all sizes.

These volcanoclastic sediments are predominantly fluvial and the rapid vertical and lateral facies changes suggest they are immature, braided river deposits. Similar deposits are common in mountainous volcanic areas (e.g. Cascades, High Andes) and a similar palaeoenvironment is proposed.

Some of the breccias in the Terra volcanic sequence have a

matrix very similar to the arkoses, although the breccia fragments include all types of volcanic rock in the area. These horizons may be the deposits of volcanic mudflows or lahars (Parsons, 1968).

#### Other Sedimentary Rocks

A banded meta-calcargillite outcrops on the Terra peninsula; it originally consisted of interbedded limestone and andesite ash-fall tuff. The unit is found across the Bull Fault, where it is offset right-laterally over 2000m and is less metamorphosed. In both areas the bed is extensively brecciated and varies in thickness from 6-30 m. The breccia blocks themselves vary from a few centimetres to 15 m and more across. Where smaller, the blocks are rotated and abraded and have a matrix of granulated calcargillite. The larger blocks are often contiguous and only slightly rotated. Bands can be traced between blocks and incipient breaks can be found. The beds below are andesite tuffs and those above are pyroclastic breccias overlain by tuffs and sediments. None of these beds is secondarily brecciated. Lenses of tuff are sometimes found in the calcargillite horizon and blocks of calcargillite are found in the overlying breccias. The horizon is interpreted as having been deposited in calm water (marine or lacustrine?) and brecciated soon after deposition, possibly during quake activity accompanying the volcanic event that produced the overlying breccias and tuffs.

In other parts of the Terra Sequence a number of calcargillite units have been found. These are 1-5 m thick and consist of more or

less brecciated banded dolomite and felsic tuff between unbroken conformable well-banded felsic ash-fall tuffs. All these horizons appear to have been brecciated soon after deposition. They were not deposited as breccias. Each is considered to be the result of a separate volcanic-quake.

Extreme lateral facies variations and the varying degrees of brecciation make these calcareous horizons difficult to interpret. The frequency with which the calcareous horizons are mineralised makes their understanding critical. On Bloom Island there are up to 300 m of banded dolomites with thin siliceous partings, but this sequence thins to some 10 m on the islands to the south (Murphy, Pers. Comm., 1973). These are not brecciated. Some of the siliceous partings may have been algal, but since most of the rock is in the hornblende-hornfels facies, such interpretations are uncertain. No distinctive algal structures were seen.

Thin sequences of white quartzite and quartz pebble conglomerate with a dolomite matrix are found on the southwestern corner of Bloom Island and in the islands to the southwest of Nic Island. Murphy (Pers. Comm., 1973) reports white quartzites near Slapdaw and Black Bear Lakes. These rocks are interpreted as littoral, possibly marine: in all cases they are closely associated and conformable in thick sequences of sub-aerial felsic tuffs.

### Correlations

Although many workers have equated the volcanic sequences at



Echo Bay with those in this area (Kidd, 1933; Badham et al., 1972), direct lithological correlations have not been made.

Briefly, the lower Echo Bay Group at Echo Bay consists of 500 m of bedded felsic tuffs and flows with intercalations of quartzite and dolomite, overlain by 430 m of intermediate pyroclastic rocks, overlain in turn by 530 m of porphyritic andesite and well-bedded andesite tuffs (see Robinson, 1971). These rocks are very similar to the felsic and lower Terra sequences in the Camshell River Block. However, the great disparities in thickness and the lack of detailed similarities of succession suggest that the rocks were not once part of the same sequence, but are the products of very similar processes in neighbouring areas.

This conclusion is strengthened by the fact that the upper Echo Bay Group consists of at least 1700 m of porphyritic andesite flows, whereas the youngest sequences in the Camshell River area consist of at least 3300 m of volcanoclastic sediment. The fact that most of this sediment was derived from porphyritic flows again demonstrates the correlations of process but not of lithology. Indeed, in an attempt to correlate lithologies, Kidd (1936) ascribed this volcanoclastic sedimentary sequence to his Cameron Bay Group, along with the previously-described Balachey Unit.

Consequently, it is proposed that any attempt to make more than very general chronological correlations in this sequence is useless, realising the extreme facies variations characterising this volcano-sedimentary environment.

### Hypabyssal Porphyries

These constitute a group which includes some of the oldest intrusive rocks recognised in the area and which continued to be emplaced throughout the sequence - indeed, the Balachey Unit and Cameron Bay Group are intruded by quartz porphyries. A belt of porphyries outcrops in the southeastern part of the area and small stocks outcrop in the islands and on the north shore of Conjuror Bay. The rocks vary from having dominantly plagioclase and hornblende phenocrysts to having dominantly quartz phenocrysts, but in all cases the feldspathic groundmass is red-pink and very fine-grained. All are clearly intrusive, but no metamorphism has been recognised at their contacts. In many places they have been intruded by younger granites and, because of the recrystallisation, appear to grade into the granites without a break. Elsewhere, where granites have intruded crystal tuffs and porphyritic andesites, recrystallisation has caused these rocks to appear very similar to the porphyry intrusions. Only the presence of palimpsest bedding prevents misinterpretations. The frequency with which these porphyries occur near the edges of the complex suggests that they are supraplutonic, and their similarity, both compositionally and texturally, to the volcanic rocks suggests that they are sub-volcanic. A continuity of process from hypabyssal to plutonic is suggested. An inevitable result of this is that the complexes represent original individual basins while the granites represent the sites of volcanism and erosion to provide the basinal infillings.

## Plutons

The emplacement of the plutons took place over a considerable period of time and in general a sequence from intermediate rocks to true granite can be recognised. The two NW-trending lobes cutting the complex are mostly adamellite, with local gradations into diorite, syenite and even granodiorite. The older intrusion beneath the Balchey Unit is an altered fine-grained hornblende diorite. It is intruded by a hornblende granodiorite. The intrusion to the south of Terra is hornblende monzonite (Plate 3.2) with syenitic and granodioritic patches - these are not separate stocks or composite intrusions. A kilometre to the east of Terra a small stock of diorite cuts the contact of the adamellite and the volcanics. Contact metamorphism is limited in extent and the effects of metamorphism in the hornblende-hornfels facies extend only a hundred metres or so from the contact. The margins of these intrusions are strongly altered and often contain highly porphyritic phases, together with epidote, carbonate and apatite. These margins were the site of shearing and intense hydrothermal activity. Pyrite and pyrrhotite, with lesser amounts of chalcopyrite, are often developed in these zones and skarns of sulphides and magnetite are common in the higher parts of the aureoles (Kidd, 1936; Furnival, 1939a; Badham, 1972).

The large intrusions ringing the complex are all coarse-grained biotite-hornblende granites or granodiorites. These often have aplitic border phases and aplite and quartz porphyritic dykes often extend a short distance from these margins. Some quartz-porphyry

plugs and dykes intrude the edges of the granites, but the contacts are often poorly defined and it is suggested that the various phases are penecontemporaneous.

Contacts with country rock are sharp and again metamorphism is restricted. Some of the contacts are fault-controlled, although later movement on some of these faults (e.g. Bloom Fault) often obscures the contact relations. Near contacts the granites are often strained and sheared (Plate 3.1) and hydrothermal alteration and sulphides are common. Xenoliths of country rock are often seen near the contacts and are scarcely resorbed.

That the intrusions were emplaced at relatively shallow depths (~ 3 km) is indicated by much of the aforementioned data. The frequency of faulted margins suggests that intrusion took place by the upward displacement of country rock, causing rapid erosion above and fast clastic deposition in intervening topographic lows. Similar features in the Peruvian Coastal Batholith have been explained in a similar way (Pitcher, 1972).

#### Porphyry Dykes

Porphyritic dykes, generally of granodioritic composition, cut all the volcanic rocks in the area, as well as the Balachey Unit. They are concentrated near the margins of the plutons, but often strike northeastward. They predate the major transcurrent movements on the NE-trending faults, but were intruded along pre-existing lineaments that were active again later. It is these same

lineaments that often control the margins of the larger plutons. The dykes have not been seen to cut more than the outer fringes of the plutons.

The dykes are variable in colour from dark brown through pink to white, and this change is possibly indicative of progressively more differentiated rocks. They are strongly porphyritic with phenocrysts of quartz, plagioclase, K-feldspar, hornblende and biotite contained in a very fine-grained matrix (Plate 3.3). The dykes are rarely more than 6 m wide and are usually vertical. The margins are chilled and the phenocrysts are often aligned in flow bands parallel to the margins.

These dykes are considered to be supraplutonic and to represent late injections of magma into the fractured roof rocks above the cooling plutons. Detailed studies should reveal separate suites of such dykes associated with each pluton.

### c) Aphebian Events

#### Folding

The broad structural details of the complex are shown in Figure 12. Essentially the volcanic rocks dip homoclinally away from the intrusive contacts and a broad open syncline has developed between the NW-trending intrusive lobes. The dips of the intrusive contacts often appear to be similar to those of the intruded rocks. The contact dips can be interpolated from the extent of metamorphism away from the contacts. At Terra drill and outcrop control are good and

the contact dips at 70-80° and is nearly conformable to the strike of the volcanic rocks.

Microfolding is common in the Terra Sequence and is clearly drag folding related to the main syncline. A few mesofolds of similar type have also been noted (Plate 1.7). Fold axes in Conjuror Bay parallel the Richardson Island granite contact. In general folding is quite intense but of low amplitude close to the intrusive contacts, and dies out rapidly into the complex. The structure of the eastern half of the area is interpreted on two sketch sections (Fig. 13).

The question that needs answering is the usual one when considering folding and high-level intrusion: which came first? Were the intrusions permitted access by anticlinal cores, or did the intrusions generate the folding? The evidence of decreasing degree of folding away from the contacts suggests the latter. The presence of granites where the anticlines might exist suggests the former. In the light of the model to be presented for the structural evolution, the causative agent was clearly the process which generated the granitic magmas. Since, in the Echo Bay area, the Cameron Bay Group is folded to the same degree as the Echo Bay Group, the folding must have occurred after Cameron Bay times. Similarly, the volcanoclastic debris in the Camsell River area is folded, and this must have been eroded from 'highs' over rising granites. The first transcurrent movements on the NE-trending faults offset the fold axes. Consequently, it is proposed that the early

intrusions initiated the folding which terminated with the final emplacement of the granites.

### Metamorphism

All the metamorphism recognised from petrographic studies can be ascribed to contact effects around the intrusions, or to hydrothermal alteration induced by the intrusions, the faults and their associated veins, or the diabases. Robinson (1971) recognised zeolites in the volcanic pile at Echo Bay, but these have not been observed in the Camsell River area.

Metamorphism up to the hornblende-hornfels facies (Turner, 1968) has been recognised around all the plutons, but rarely extends more than 100 m from intrusive contacts, except in calcareous rocks. Recognition of the facies in volcanic and volcanoclastic rocks is not simple. Essentially, at the higher grades the feldspars become more sodic and overgrowths develop, and matrices get coarser grained. In the field a totally subjective judgement of grade has to be made from the 'hardness' and 'greenness' of the volcanic rocks. In the calcareous horizons albite, quartz, garnet, calcite, diopside and a bluish amphibole are common in this facies (Plate 4.4). Very good sections are exposed on Bloom Island.

Identification of the albite-epidote facies (Turner, 1968) is even more subjective. In the andesites the plagioclases become more sodic and are corroded to epidote and carbonate, while micas can be seen to have grown in the matrices of the clastic sediments. Calcite,

tremolite, epidote, quartz, dolomite and chlorite, and rarely green biotite, have been observed in the calcareous rocks (Plate 4.3), and the first appearance of diopside marks the upper limit of the albite-epidote facies. The lower end cannot be defined in the field. Epidote itself has not been recognised more than 1 km from the intrusive margins, but chlorite is common throughout the area. However, it is impossible at present to separate chlorite produced by later hydrothermal events from that produced by the plutons.

In general the outer margin of the albite-epidote hornfels facies is defined by the first appearance of metacrysts of these minerals, even though much of the rock may be totally unaffected. Plate 4.5 shows chlorite metacrysts which have grown in an andesite tuff and Plate 4.6 shows an epidote-chlorite veinlet preferentially replacing coarser bands in volcanoclastic sediments. Both samples are taken about 700 m from the contact on the Terra peninsula, near the outer limits of the albite-epidote facies.

The estimated limits of albite-epidote facies metamorphism are shown in Figure 12. The excessive width of this aureole around the northernmost of the plutonic lobes is used to infer a shallow dip of the plutons (Fig. 13).

Temperatures near the intrusive margins must have been about 600°C with pressures of between 1 and 3 kb (Turner, 1968). Cordierite and andalusite, which might be expected in the metasediments under these conditions, have not been observed. It is concluded that the sediments contain too much calcium (in carbonate and feldspar) for



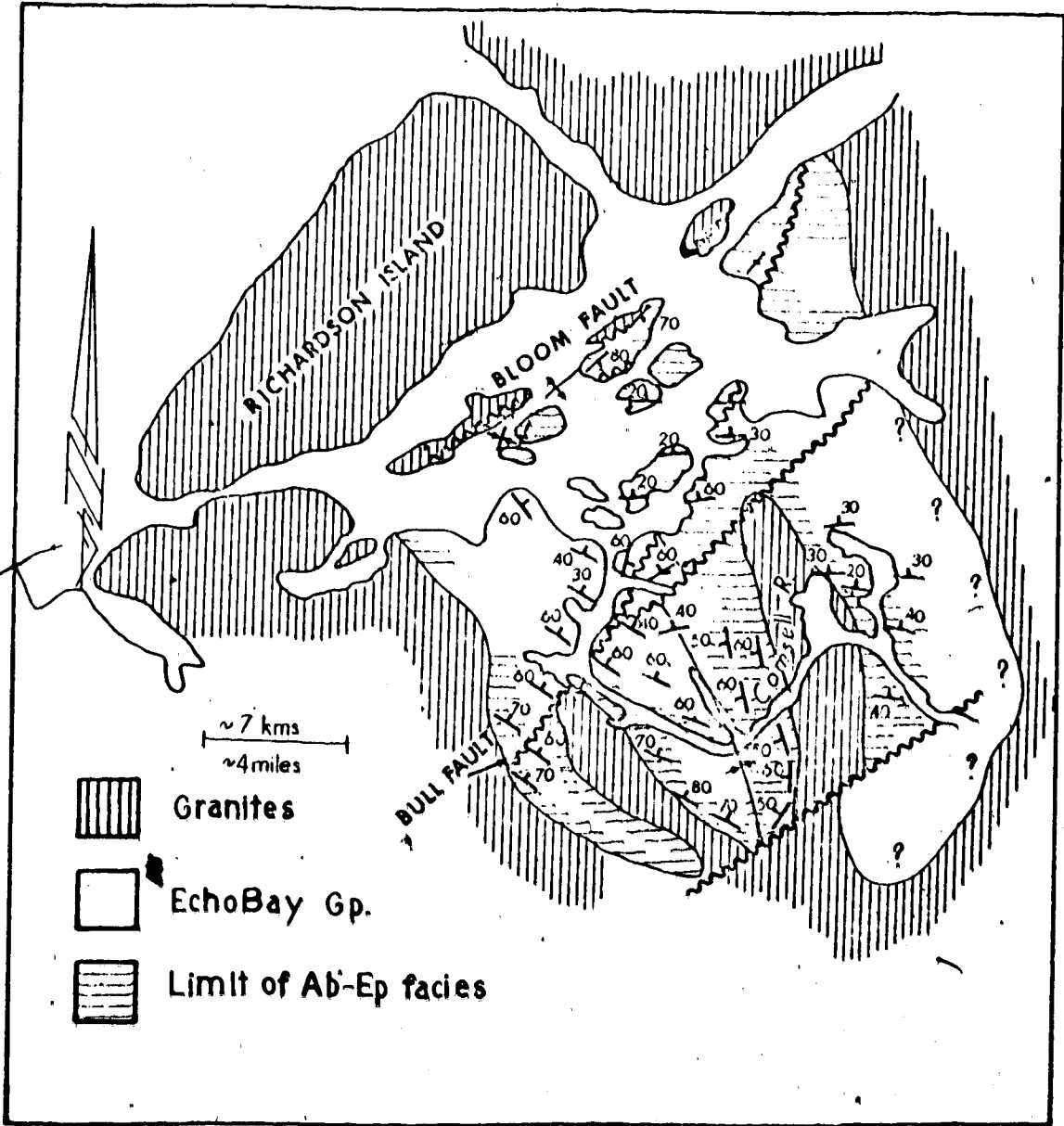
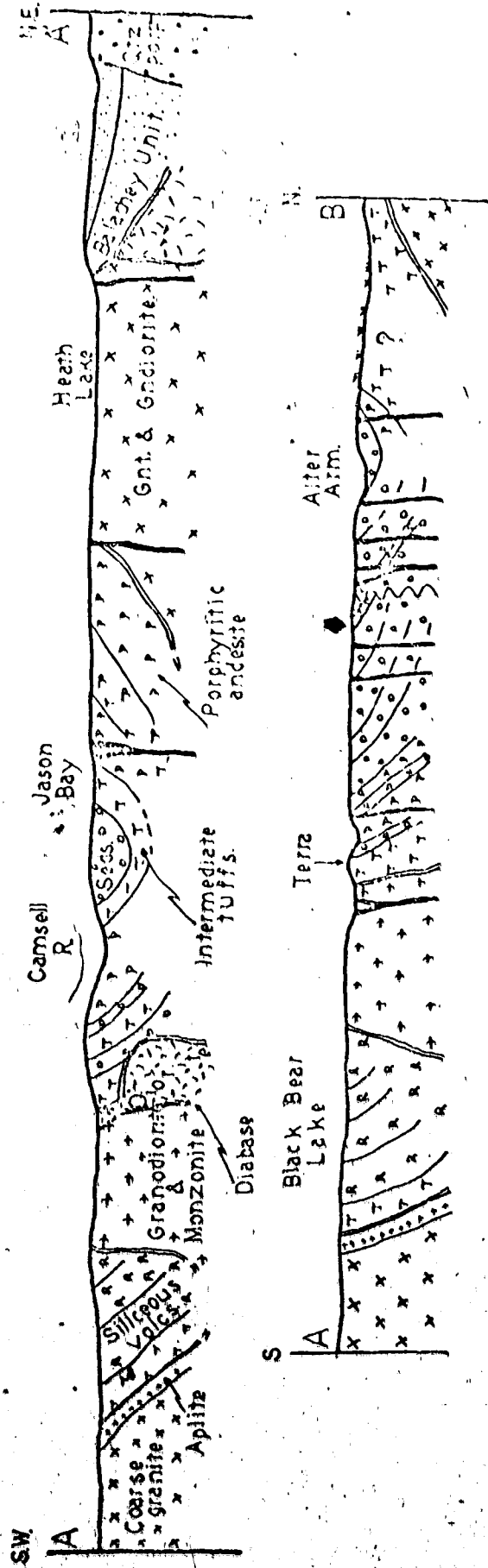


Figure 12. Structural and Metamorphic map of the Camsell River Area.



Sketch Sections A-A' & A-B. Horiz. Scale: 1/4 mile. (cm = 64 km)  
 Figure 13. (See fig. 6)

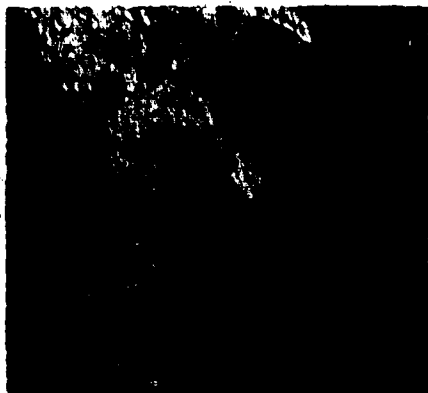
the development of these minerals.

Detailed studies of the metamorphism of the calcargillite at Terra are reported in Part I:8.

## PLATE 1

1. Rolled boulders of chilled porphyritic andesite with interstices filled with glassy and fragmental andesite. Base of flow, north side of Terra Peninsula.
2. Sequence of banded waterlain andesite tuffs, with thin calcareous horizons, overlain by 'cherty' rhyolite, on the right. Terra Peninsula.
3. Volcanic breccia of angular, unsorted clasts, including andesite, rhyolite, tuffs and calcargillite. Terra Peninsula.
4. Base of a porphyritic andesite flow on top of volcanoclastic silt, with some silt:lava 'emulsion'. Terra Peninsula.
5. Cross-bedded, weakly calcareous volcanoclastic sediment. Terra Peninsula.
6. Well-graded, bedded volcanoclastic arkose and silt. Terra Peninsula.
7. Part of a small fold in waterlain andesite tuffs. Terra Peninsula, looking east.
8. Water escape structures, breaking up volcanoclastic silts between graded arkose. Note also shale chips in the coarse beds. Terra Peninsula.

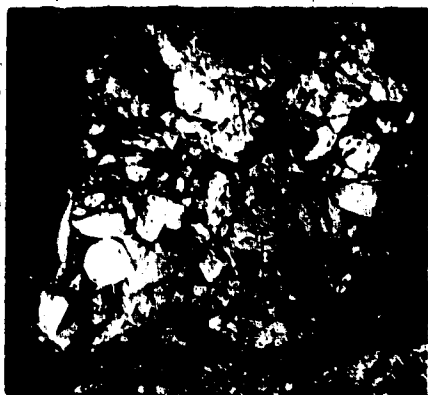
1



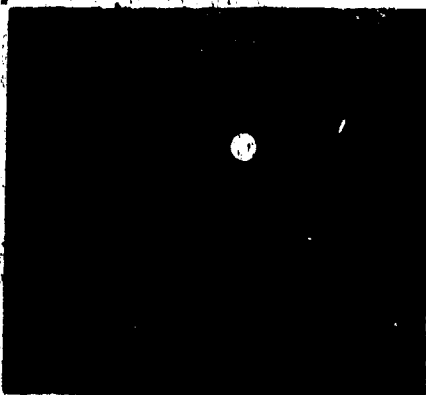
2



3



4



5



6



7



8

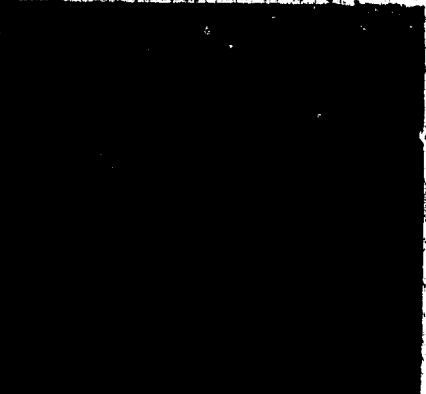


## PLATE 2

1. Andesine porphyritic trachybasalt, with later megacrysts of haematite. Terra Peninsula. P.P.L.
2. Vesicular basalt. Carbonate- and quartz-filled, chlorite-rimmed vesicles. Strongly chloritised 'hornblende' phenocryst on left. Highly altered matrix. Balachoy.
3. Vesicular 'froth-flow' top of trachybasalt. Plagioclase is andesine. Quartz- and carbonate-filled vesicles. Silver Bay. P.P.L.
4. Quartz- and carbonate-filled vugs in porphyritic andesite. Note feldspar needles in groundmass. Terra Peninsula. P.P.L.
5. Oligoclase porphyritic trachyandesite. Phenocrysts contain blebs of chlorite after glass. Terra Peninsula. P.P.L.
6. Rhyolite tuff. Fragments of quartz, feldspar and altered tuff contained in a devitrified, flow-banded matrix. North of Black Bear Lake. P.P.L.
7. Ignimbrite. Embayed quartz (note cubic habit of one - possibly after cristobalite), altered feldspar, hornblende and tuff fragments and pumice flame in streaked, devitrified matrix. Bloom Island. P.P.L.
8. Perlitic devitrification texture in ignimbrite. Bloom Island. P.P.L.

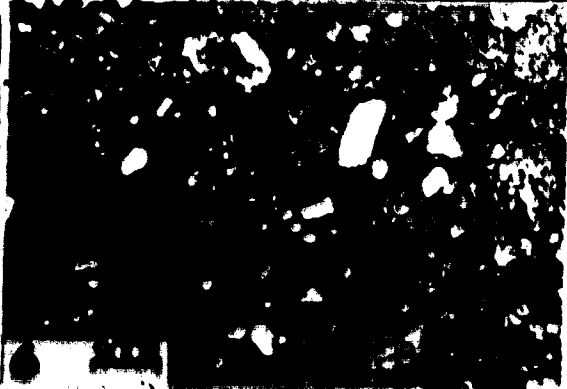
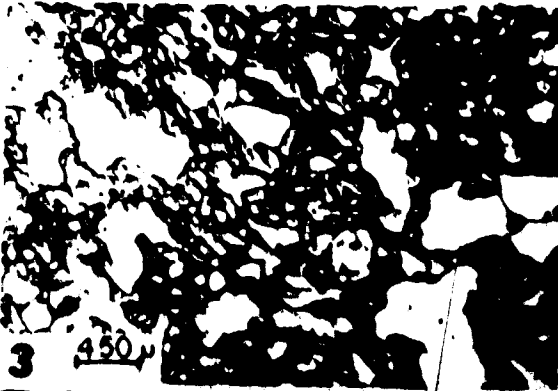


PLATE 2

## PLATE 3

1. Slightly cataclastic and altered hornblende biotite granite. Richardson Island granite, near Bloom fault. Crossed nicols.
2. Pseudomorph of chlorite and haematite after 'amphibole', in altered plagioclase. Terra monzonite. P.P.L.
3. Central phase of quartz-feldspar porphyritic dyke. Terra Peninsula. Crossed polarisers.
4. Contact of diabase (dark, with andesine phenocrysts) with andesite tuff. Cross-cut by quartz (in tuff), carbonate (in diabase) vein. Jason Bay. P.P.L. Green filter.
5. Well-bedded, graded volcanoclastic silt and arkose, the latter containing andesite lava and tuff fragments. Terra Peninsula. P.P.L.
6. Cataclastic tourmaline (grey) overgrowing tuff (on right), cut by quartz stringers (white) and strongly replaced by pyrite. Balachey Lake. P.P.L.
7. Sheared chlorite-muscovite vein, around rolled and strained fragments of quartz on edge of a quartz vein (white). Terra Mine. P.P.L.
8. Progressive vug fill, from a centre of amethystine, zoned quartz (on left) to finer-grained quartz and finally granular, impure dolomite. Silver Bay Mine. Crossed





**PLATE 3**

## PLATE 4

1. Zoned, corroded andradite over quartz and tremolite. Metacalcargillite. Terra Mine. P.P.L.
2. As above. Crossed polarisers.
3. Epidote and tremolite overgrowing a quartz-carbonate band. Metacalcargillite. Terra Mine. P.P.L.
4. Quartz, albite, epidote, diopside, hornblende hornfels. Late metacrysts of haematite replace all but quartz. Bloom Island. P.P.L. Green filter.
5. Anular chlorite metablasts growing in andesite tuff. Albite-epidote facies. Terra Peninsula. P.P.L.
6. Veinlet of epidote and chlorite cutting and banded volcanoclastic sediments and preferentially replacing coarser bands. Terra Peninsula. P.P.L.
7. Highly altered vesicular trachybasalt. Silver Bay Mine. P.P.L.
8. Wall rock alteration around a 20 cm wide carbonate vein, off the right of the picture. On the left, chlorite and sericite replace matrix and alter feldspar phenocrysts in andesite tuff. In centre, the phenocrysts consist of albite-epidote and carbonate in a chlorite and carbonate matrix. On right, the phenocrysts are destroyed and the rock consists of chlorite and carbonate with quartz veinlets. Terra Mine. P.P.L. Green filter.

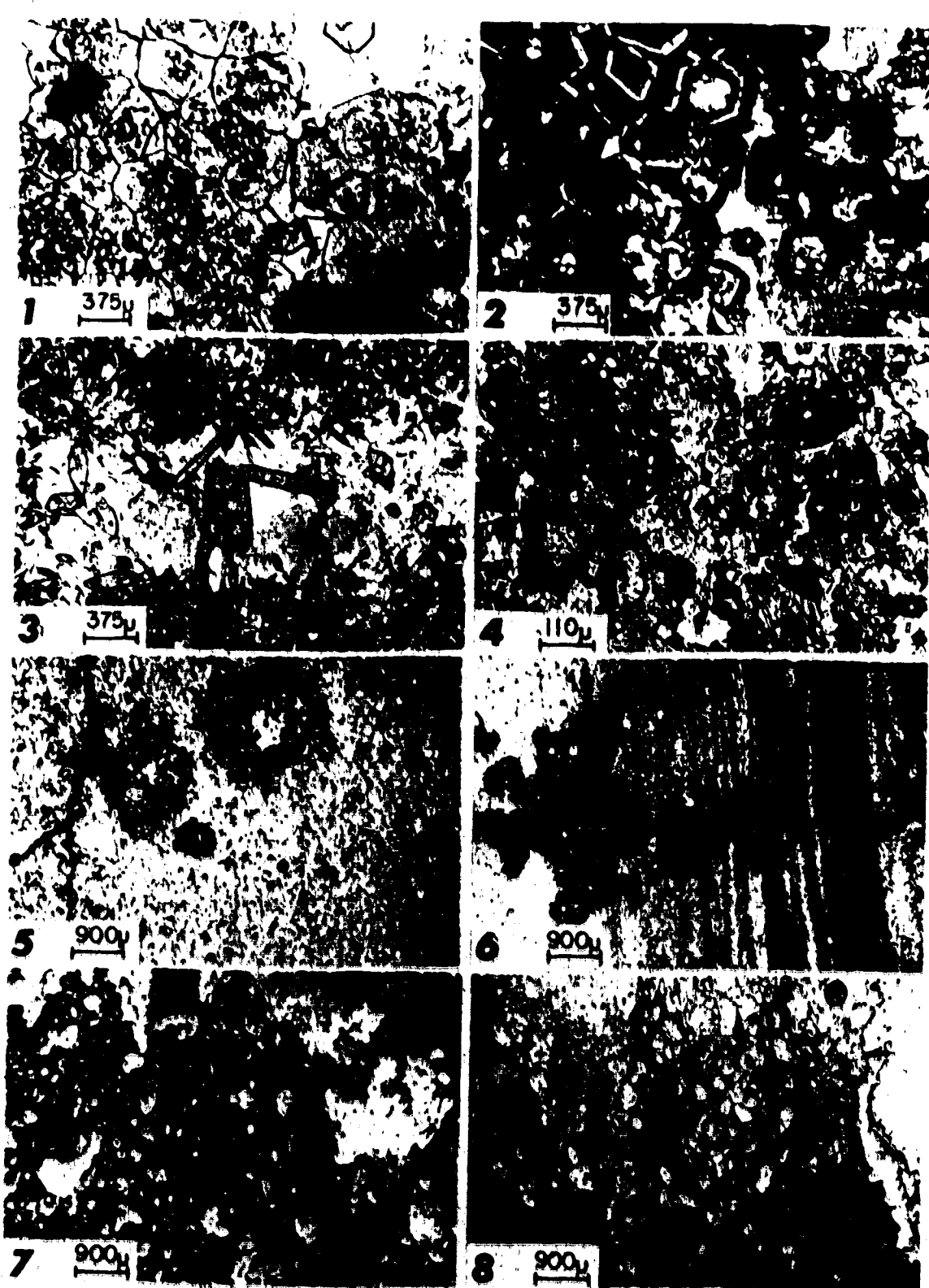


**PLATE 4**

## 5. GEOCHEMISTRY OF APHEBIAN ROCKS

Analyses have been performed on 39 samples (5 basalts, 10 andesites, 8 felsic volcanic rocks, 7 plutonic rocks, 6 sediments and 3 diabases) for up to 25 elements. The analytical techniques are reported in this section together with all the data relevant to a discussion of the nature of the magmatism in the Camsell River area. Results more pertinent to studies on the source and location of mineralisation will be reported later. Inevitably there will be overlap, in which case data are presented in both places. Data reported in this chapter have been presented in Badham (1973).

### a) Analytical Methods

Twenty-five samples (3 basalts, 8 andesites, 2 rhyolites, 6 plutonic rocks, 2 sediments, 1 metasediment and 3 diabases) were kindly analysed for Si, Ti, Al, Fe, Mn, Mg, Ca, Na, K, P, S, Ba, Sr, Rb, Nb, Zr and Y on compacted powder by Dr. G. Holland at the University of Durham, using a Phillips 1212 X-ray fluorescence spectrometer. The results were corrected by him using a computer technique (Holland and Brindle, 1966).

Thirty-two samples (4 basalts, 9 andesites, 5 felsic volcanic rocks, 7 plutonic rocks, 4 sediments and 3 diabases) were analysed by Bondar-Clegg and Company Limited, for Ni, Co, Ag, U and Au, using atomic absorption spectrophotometry. Ni, Co and Ag were extracted with  $\text{HNO}_3$  and HCl, U with  $\text{HNO}_3$ , and Au by fire-assay. This work was

most generously arranged and financed by Dr. R.W. Boyle of the G.S.C., Ottawa.

Thirty-six samples (5 basalts, 10 andesites, 8 felsic volcanic rocks, 6 plutonic rocks, 5 sediments and 2 diabases) were analysed by the author for Cu, Co, Ni, Zn and Mn, employing a Perkin-Elmer Model 303 atomic absorption spectrometer under the direction of Dr. S. Pawluk, Department of Soil Science, University of Alberta, and with the assistance of operator, Mr. Park Yee.

The samples for atomic absorption analysis were prepared by fusing 1 gram of dried rock powder (< 150 mesh) with 3 grams of lithium tetraborate in a Pt-Au crucible. The glass was quenched and dissolved in distilled water and HCl and the resulting solution made up to 100 ml, ensuring that the concentration of HCl remained at approximately 3%. One sample was prepared twice from the same powder to test the reproducibility of the method. Indications from previous studies (Robinson, 1971) were that these sample proportions would give measureable concentrations of the elements being analysed. Five U.S.G.S. standards (G1, W1, AGV-1, BCR-1, GSP-1) were prepared for analysis in exactly the same way, together with a blank sample made up with lithium tetraborate, but no rock powder. A range of internal standards at suitable concentrations was prepared by dissolving metal salts in distilled water and diluting to required concentrations. HCl was added to make acid concentrations the same as in the sample and external standard solutions.

Calibration curves were prepared for each element by running both

internal and external standards twice. Accepted values for the external standards were taken from Flanagan (1969) (G<sub>2</sub>, GSP-1, AGV-1, BCR-1); Taylor and Kolbe (1964) (W1 for Co, Cu); and Fleischer and Stevens (1962) (W1 for Zn).

Errors and detection limits of the study were:

Error	Detection Limit (ppm)
Ni ± 8%	20
Co ± 7%	30
Cu ± 8%	20
Zn ± 1%	15
Mn* up to 7%	30

\*Errors for Mn are hard to estimate because of wide disparities in published values for the U.S.G.S. standards.

There are published zinc values only for W1. Consequently, it is of interest to note the following results for the other standards, corrected from a standard curve of the internal standards and a value for W1 of 82 ppm (Fleischer and Stevens, 1962). Averages of other published analyses for Zn in W1 range from 62-110 ppm with a mean of 78 ppm.

Zn ppm ± 1%	
G2	68
GSP-1	96
AGV-1	78
BCR-1	109

## Results

The results are presented in Table 1. The large scatter in the values of Na, Ca and K and their associated trace elements are clearly demonstrated: these are the result of the alterations discussed in the previous chapter.

None of the samples analysed was apparently weathered. The two analyses of volcanoclastic-sedimentary rock show a close similarity to those of the andesite lavas from which they were derived. However,  $\Sigma\text{FeO}$  is enriched and  $\text{CaO}$  strongly depleted - the alkalis are unchanged. It is concluded that palaeoweathering is responsible for this change. One tuff (SJ 10.1) and one basalt (NK 4.1A) show similar anomalies, but both have apparently also lost potash. It is suggested that this alteration is hydrothermal, and concluded that none of the analysed samples underwent any alteration by palaeoweathering.

From the field relations, petrography and analyses, it is concluded that most of the alteration effects are hydrothermal and correspond to the destruction of mafic minerals to chlorite and magnetite, and feldspars to carbonates, epidote and sericite. The effects of contact metamorphism per se appear to be negligible (compare sample locations in Appendix I with the metamorphic map [Fig. 12]). The petrography of analysed samples is also reported in Appendix I.

Because of the alteration effects, any classification scheme must be used with caution. For instance, schemes based on normative feldspar proportions become meaningless. Total alkali values are, however, less variable (Table 1) and indicate that plots involving  $(\text{Na}_2\text{O} + \text{K}_2\text{O})$  and one or two other components may be more useful.

Sample Number	BASALT			ANDESITE LAVA			ANDESITE TUFF			RHYOLITE			
	SJ29.8	NK1.7B	NK4.1A	SX3.9A	SX7.7F	NK7.13	SJ3.3	SJ5.7	SJ10.1	NK19.6	NK18.8	NK13.2	SX7.2F
% SiO <sub>2</sub>	50.82	48.01	51.19	57.89	57.40	61.14	60.00	61.83	60.82	60.96	64.30	71.51	78.82
TiO <sub>2</sub>	2.60	1.03	0.86	0.64	0.57	0.58	0.32	1.21	0.57	0.53	0.51	0.23	0.17
Al <sub>2</sub> O <sub>3</sub>	14.14	17.18	17.23	19.41	17.81	16.55	12.58	15.28	17.31	19.63	16.70	14.76	11.74
2FeO	14.62	15.50	19.62	5.72	3.60	7.74	7.46	7.88	8.69	4.96	4.96	2.72	1.56
MnO	0.46	0.12	0.15	0.16	1.53	0.15	0.19	0.20	0.18	0.26	0.12	0.13	0.03
MgO	7.95	6.13	7.25	2.24	3.31	3.00	5.40	3.06	6.04	3.75	2.93	1.39	1.25
CaO	3.49	5.79	0.42	5.98	7.07	6.19	5.60	2.79	0.56	4.57	2.39	1.15	0.14
Na <sub>2</sub> O	2.11	4.33	2.94	3.50	6.03	2.98	0.05	2.74	4.29	4.67	3.54	2.69	4.86
K <sub>2</sub> O	3.39	1.61	0.06	4.18	2.37	1.40	8.27	4.52	1.42	3.15	4.40	5.35	1.32
P <sub>2</sub> O <sub>5</sub>	0.25	0.28	0.28	0.29	0.26	0.26	0.10	0.46	0.13	0.21	0.15	0.06	0.06
S	0.16	0.01	0.00	0.00	0.06	0.01	0.03	0.02	0.00	0.01	0.00	0.00	0.05
ppm													
Mn	3100	745	1040	1040	>4000	-	875	-	1165	1645	875	687	305
Ba	1113	246	34	1205	259	652	2749	1572	572	1793	916	1087	216
Rb	153	85	4	164	105	59	368	347	81	83	207	242	58
Sr	103	177	19	383	134	444	63	239	104	309	335	331	71
Nb	37	8	8	12	10	8	13	34	10	13	14	13	14
Zr	196	124	99	162	147	123	132	577	138	191	162	157	125
Y	37	16	17	17	25	15	7	36	17	23	16	14	28
Ni	43	28	53	26	7	8	6	20	16	16	12	8	10
Co	45	32	40	18	5	16	12	26	37	15	18	13	6

TABLE 1. Partial Chemical Analyses of Rocks from the Camsell River-Conjuror Bay Area. All analyses are corrected to 100% on a water and CO<sub>2</sub> free basis, with all iron as FeO



INTRUSIVE ROCKS                      DIABASE

SEDIMENT

Sample Number	SX2.1	SX14.188	NK14.2A	NK19:7	NK19.10	SX3.13B	SX3.1C	NK21.1A	NK15.2A		
%											
SiO <sub>2</sub>	58.65	59.27	62.99	55.95	69.24	68.21	64.54	75.65	47.39	50.88	51.11
TiO <sub>2</sub>	0.71	0.58	0.73	0.84	0.65	0.38	0.57	0.00	2.36	2.36	2.76
Al <sub>2</sub> O <sub>3</sub>	17.41	19.25	15.74	19.51	13.73	15.67	15.25	14.37	14.41	14.19	13.69
ΣFeO	11.40	10.73	4.36	6.38	6.45	3.36	5.88	0.54	16.49	13.75	15.08
MnO	0.12	0.08	0.22	0.15	0.30	0.06	0.16	0.07	1.07	0.23	0.25
MgO	4.54	2.87	3.78	2.66	1.49	1.54	2.60	0.06	8.16	5.21	3.99
CaO	0.46	0.80	3.41	5.37	1.04	2.39	3.83	0.57	4.30	9.89	8.67
Na <sub>2</sub> O	3.99	2.51	1.07	3.92	2.09	2.99	2.23	3.86	1.30	2.32	2.43
K <sub>2</sub> O	2.56	3.83	7.34	4.73	4.78	5.31	4.70	4.85	3.99	0.81	1.53
P <sub>2</sub> O <sub>5</sub>	0.15	0.73	0.24	0.49	0.15	0.10	0.14	0.03	0.24	0.21	0.32
S	0.00	0.01	0.13	0.00	0.07	0.00	0.00	0.00	0.30	0.14	0.21
ppm											
Mn	810	580	1470	950	1790	420	-	450	>4000	1020	-
Ba	978	1027	1476	1616	1152	1238	1059	27	1432	380	283
Rb	83	258	42	171	212	190	188	1279	183	32	42
Sr	49	134	281	612	88	245	213	17	100	185	281
Nb	10	10	14	11	21	15	14	26	15	6	14
Zr	144	167	220	132	388	204	214	54	160	144	220
Y	16	18	51	20	-	23	15	45	32	38	51
Ni	23	28	8	7	14	10	20	4	51	23	20
Co	28	20	13	7	14	42	20	1	44	18	26

All analyses are corrected to 100% on a water and CO<sub>2</sub> free basis, with all iron as FeO

TABLE 1 (continued). Partial Chemical Analyses of Rocks from the Camsell River-Conjuror Bay area

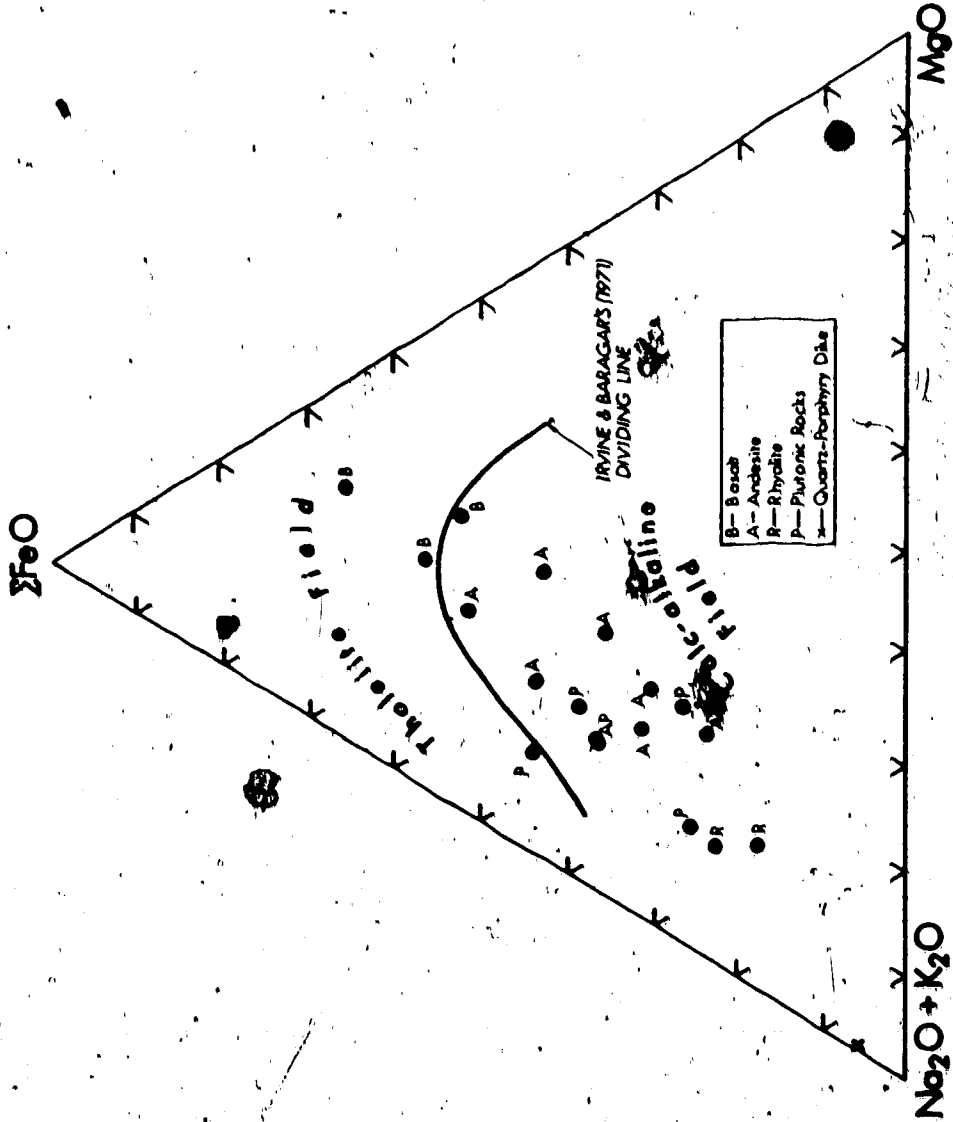
b) • Classification of the Volcanic and Plutonic Rocks

The rocks are classified using the criteria of Irvine and Baragar (1971) where possible. The AFM diagram (Fig. 14) of the suite shows its calcalkaline nature and a typical trend of alkali enrichment to an extreme differentiate - the quartz-porphphy dyke. An alkalis:silica diagram (Fig. 15) demonstrates the marginally sub-alkaline nature of the suite, although the scatter is large. Two of the basalts plot in the alkali field; the alkali values of the third are spurious. The plot of the averages on this diagram shows a typical calcalkaline differentiation trend that can be seen to be slightly more alkaline than those presented by Irvine and Baragar (op. cit.) for example. In neither of these diagrams is there any detectable difference between the volcanic and plutonic rocks and, in spite of the alteration, the suite can readily be classified.

Subdivisions based on rock chemistry are more difficult to make. Attempts to classify the plutonic rocks using the systems of Heitanen (1963) and Smith (1963) produced results sometimes inconsistent with the petrographic data, because of their dependence on alkali values. Consequently, the nomenclature for the plutonic rocks from field and petrographic data is retained.

Irvine and Baragar (op. cit.) recommend the use of a normative colour index: normative plagioclase composition diagram to subdivide the volcanic rocks. Its principle shortcoming is, as they admit, the dependence on the alkali analyses, and attempts to use this method gave inconsistent results.

Figure 14. AFM Diagram for Igneous rocks in the Camsell River Area.



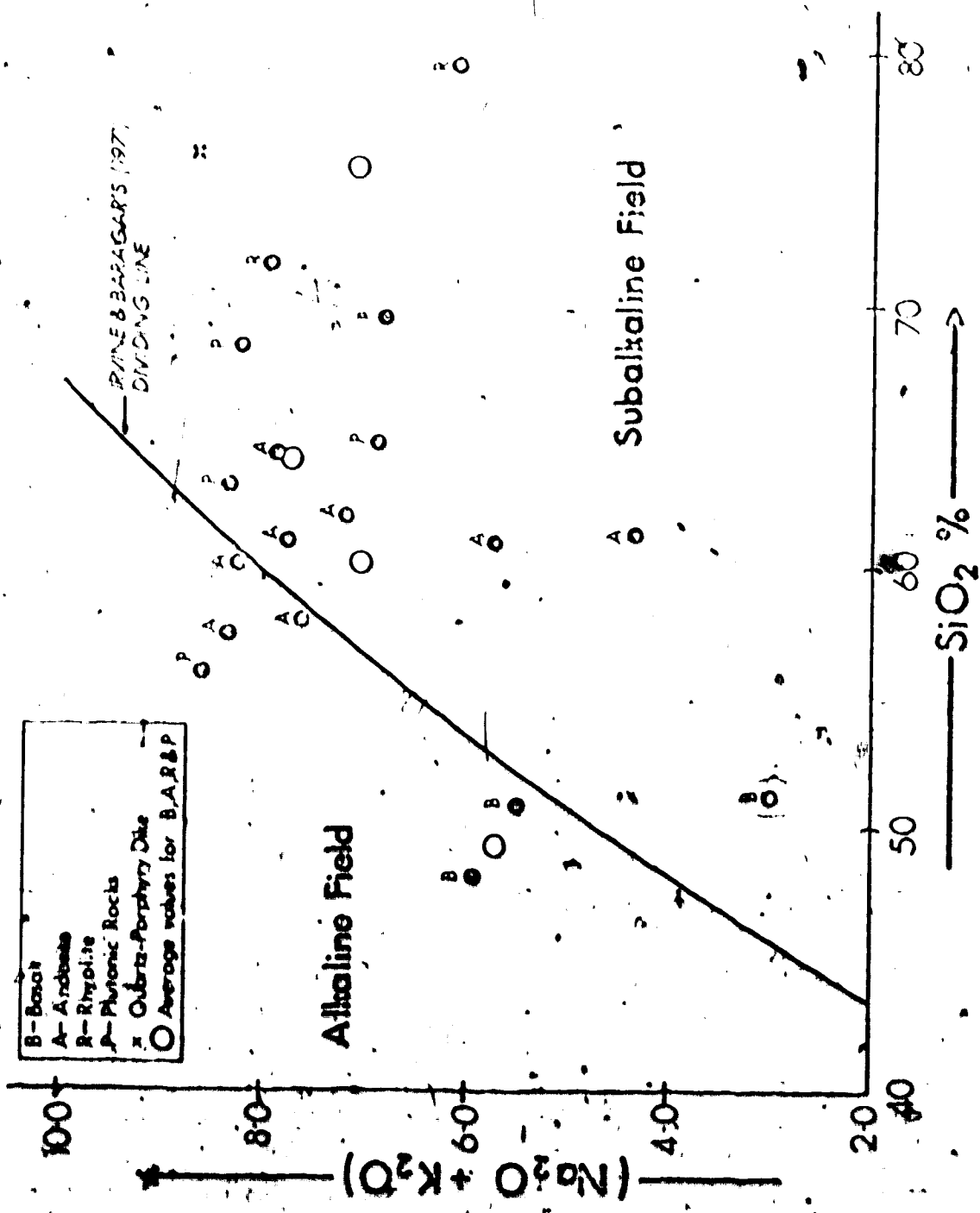


Figure 15. Alkali:Silica Diagram for Igneous rocks in the Cassell River Area.

Consequently, the volcanic rocks are subdivided on the basis of silica alone. The samples analysed fall into three natural groups (basalt:  $\text{SiO}_2$  55%; andesite: 55% -  $\text{SiO}_2$  65%; rhyolite:  $\text{SiO}_2$  > 70%). The absence of dacite (65% -  $\text{SiO}_2$  70%) is almost certainly an accident of sampling. However, the gap between basalts ( $\text{SiO}_2$  maximum 51.19%) and andesites ( $\text{SiO}_2$  minimum 57.40%) is real. Samples identified petrographically as 'basaltic andesite' fell into either 'basalt' or 'andesite' fields. Although this subdivision is unsophisticated, it is justified both by its independence of alkali analyses and by the close similarity of the averages of each subdivision (Table 2) with averages of other suites from similar geotectonic environments.

The basalts can be seen (from Table 2) to be grossly similar to the average alkali basalt (Manson, 1967; Prinz, 1967) apart from enrichments in  $\text{FeO}$ ,  $\text{K}_2\text{O}$  and Rb and depletions in Ni,  $\text{CaO}$  and Sr. Even when the spurious results of the altered sample (NK 4.1A) are omitted, these differences persist and are significant.

The andesite tuffs and lavas are closely similar to an average high-K andesite (Taylor, 1963) and are classified as such. This high K-content is the cause of their marginally alkaline nature on Figure 15.

The rhyolites closely resemble those from many suites of similar geotectonic position - for example those of the Lake Taupo region (Taylor et al., 1968). The close similarity of the intrusive and extrusive rocks is well demonstrated in Table 2.

	BASALT			ANDSITTE			CALC. ALKALI AVERAGE*	INTRUSIVE ROCK		Lake Taupo Average <sup>†</sup>
	Camsell R. Average	Camsell R. Average <sup>‡</sup>	Alkali Basalt Average <sup>§</sup>	Camsell R. Lava	Camsell R. Duff	Camsell R. Average		Camsell R. Average <sup>¶</sup>	Camsell R. Average	
SiO <sub>2</sub>	50.01		47.65	50.81	61.50	63.00	60.00	63.19	73.17	71.10
TiO <sub>2</sub>	1.50		2.54	0.60	0.63	0.62	0.77	0.61	0.20	0.27
Al <sub>2</sub> O <sub>3</sub>	16.13		16.02	17.92	15.76	16.00	16.00	15.93	13.25	13.50
FeO	16.58	15.03	11.02	5.09	6.79	6.34	5.13	5.22	2.14	1.68
MnO	0.24		0.16	0.61	0.40	0.55	-	0.18	0.08	-
MgO	7.11		7.20	2.05	4.24	3.55	2.15	2.41	1.32	3.25
CaO	3.23	4.64	10.24	6.41	3.18	4.80	5.60	3.23	0.65	1.49
Na <sub>2</sub> O	3.1		3.24	4.17	3.06	3.62	4.10	2.46	3.78	4.12
K <sub>2</sub> O	1.69	2.50	1.42	2.65	4.35	3.50	3.25	5.17 <sup>A</sup>	3.34	3.39
P <sub>2</sub> O <sub>5</sub>	0.27		0.51	0.27	0.21	0.24	-	0.22	0.06	-
S	0.06		-	0.02	0.01	0.02	-	0.04	0.03	-
ppm										
Mn	1595		-	-	1140	-	1300	1158	496	400
Ba	461	680	444	705	1420	1113	400	1303	652	870
Rb	61	119	51	109	217	163	68	291	150	108
Sr	100	140	774	320	210	269	620	265	291	125
Nb	11		-	10	17	14	11	15	14	5.6
Zr	140		138	144	240	204	155	232	141	160
Y	23		10-100	19	20	20	20	29	21	23
Th	41		101	14	14	14	3	11	9	n.d.
Co	39		42	13	22	18	13	18	10	n.d.
Ni/Co	1.05		2.41	1.08	0.64	0.78	0.23	0.59	0.90	-

All averages calculated to 100.0% on a water and CO<sub>2</sub> free basis, and with all iron as FeO.

<sup>A</sup>Camsell River basalt averages, ignoring disparate values from Sample 3

<sup>†</sup>Average alkali basalt from Hanson (1968) and Prinz (1960)

<sup>‡</sup>Average high-A andesite from Taylor (1969)

<sup>§</sup>Average Lake Taupo rhyolite from Taylor et al. (1968)

<sup>¶</sup>Average Camsell River intrusive rock, excluding sample S13.130.

TABLE 2. Comparison of Camsell River Analyses with those of Other similar suites.

The intrusive rocks are comparable with many typical orogenic batholith suites, but are particularly enriched in  $K_2O$  and have a high  $K_2O/Na_2O$  ratio. They are similar in many respects to the high-K suite from Yeoval, Australia, discussed by Gulson et al. (1972), but differ from other calcalkaline 'shoshonitic' suites (Joplin, 1968) in having low Ni,  $K_2O/Na_2O > 1$  and a higher content of  $TiO_2$  (Smith, 1972).

In general the suite closely resembles a number of continental late-orogenic calcalkaline suites. The volcanic rocks are closely similar to Cenozoic Andean suites (Hamilton, 1969; Vergara, 1972), although more K-enriched. This K-enrichment is similar to that in the Cenozoic basin and range suite from the Shoshone Mountains (Vitaliano and Vitaliano, 1970). The intrusive rocks are more K-enriched than the volcanic rocks.

The Peacock Index of the whole Camseil River suite (ignoring, for a moment, the basalts) is around 55 ('alkalic-calcic') and is closely similar to the Yeoval, Andean and Shoshone suites discussed previously. The low Ni-contents and low Ni/Co ratios are typical of calcalkaline suites (Taylor, 1969a).

Joplin (1968) intimated that high-K lavas and intrusions were typical of periods of tectonic stabilisation in the waning stages of orogeny. The Yeoval, Andean and Shoshone suites discussed are all typical of such environments, whereas the Papuan suite (Jakes and Smith, 1970; Smith, 1972), while broadly similar, differs in detail both chemically and in its geotectonic position.

Harker variation diagrams for the major (Fig. 16) elements demonstrate the very close similarities of the Camsell River and an Andean suite. The Andean trends are drawn from data assembled by Hamilton (1969) for the Cenozoic rocks of the central Andes. Apart from certain anomalies in the basalts and the higher  $K_2O$  values, the comparisons are remarkable.

The basalts from the Camsell River area are consistently anomalous. Basalts are not common in the late Tectonic calcalkaline suites (for instance, none are described in the Cenozoic Andes), but where they occur they are consistently similar in containing olivine and calcic plagioclase phenocrysts. Published analyses of such basalts (Ewart et al., 1968; New Zealand; Wise, 1969; High Cascades; Vergara, 1972; Mesozoic Andes) are grossly similar and Turner and Verhoogen (1960) conclude that the "chemical features that tend to recur in the basic members of the andesite association are high  $Al_2O_3$ , low  $TiO_2$  and  $\Sigma FeO$  and very low  $K_2O$ ." The Camsell River basalts contain hornblende and intermediate plagioclase phenocrysts and are enriched in  $\Sigma FeO$  and  $K_2O$ , and depleted in  $TiO_2$  and  $CaO$ . They are alkaline, but the low Ni content and Ni/Co ratio suggest a closer affinity with the calcalkaline suite in the area, as does the high  $Al_2O_3$  content.

Considerable alteration of the basalts is evident both in the field and petrographically (Appendix I), and may have exaggerated chemical differences (especially by the loss of  $CaO$  to form carbonate veins), but the chances of areally and texturally different basalts



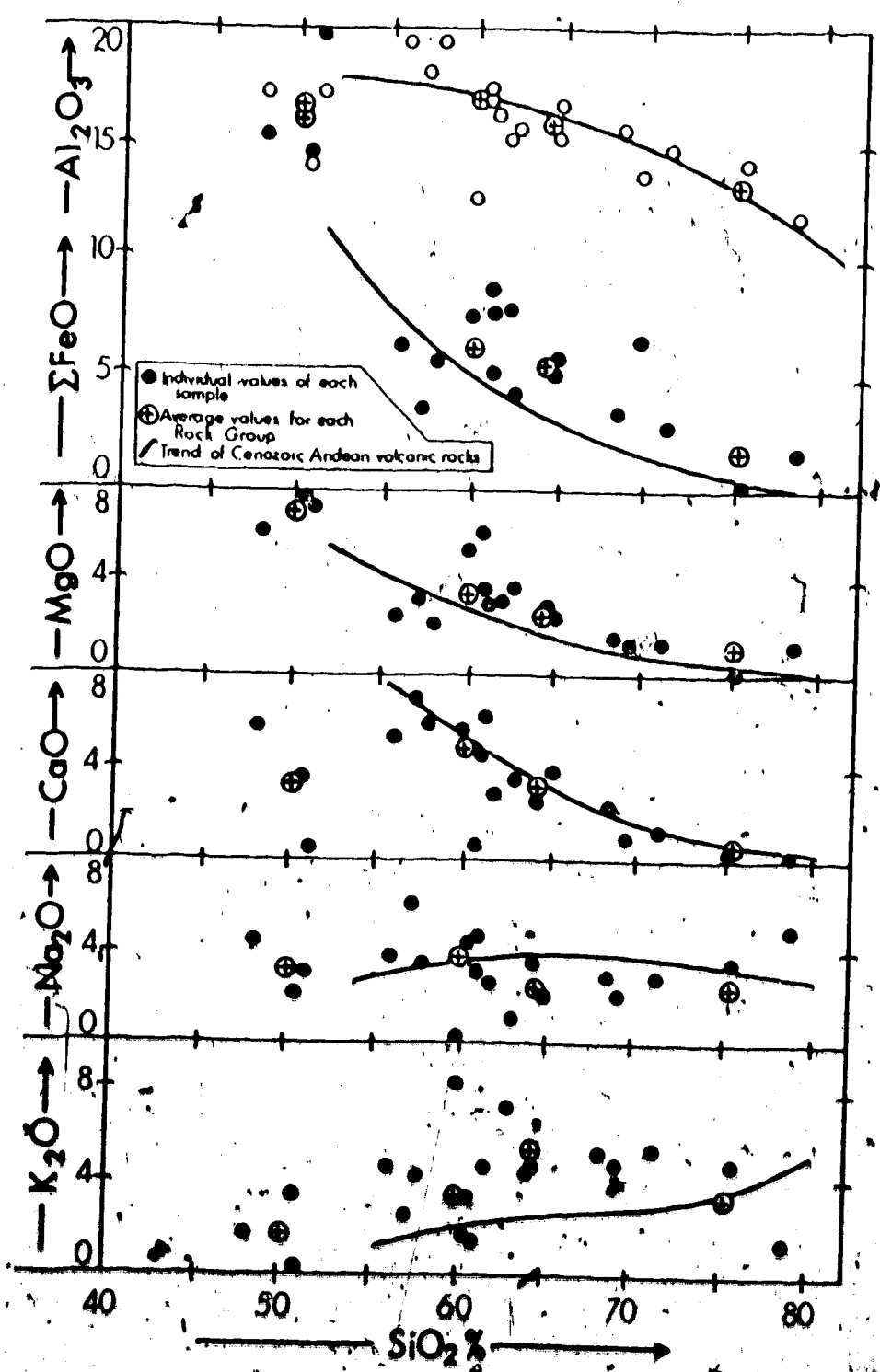


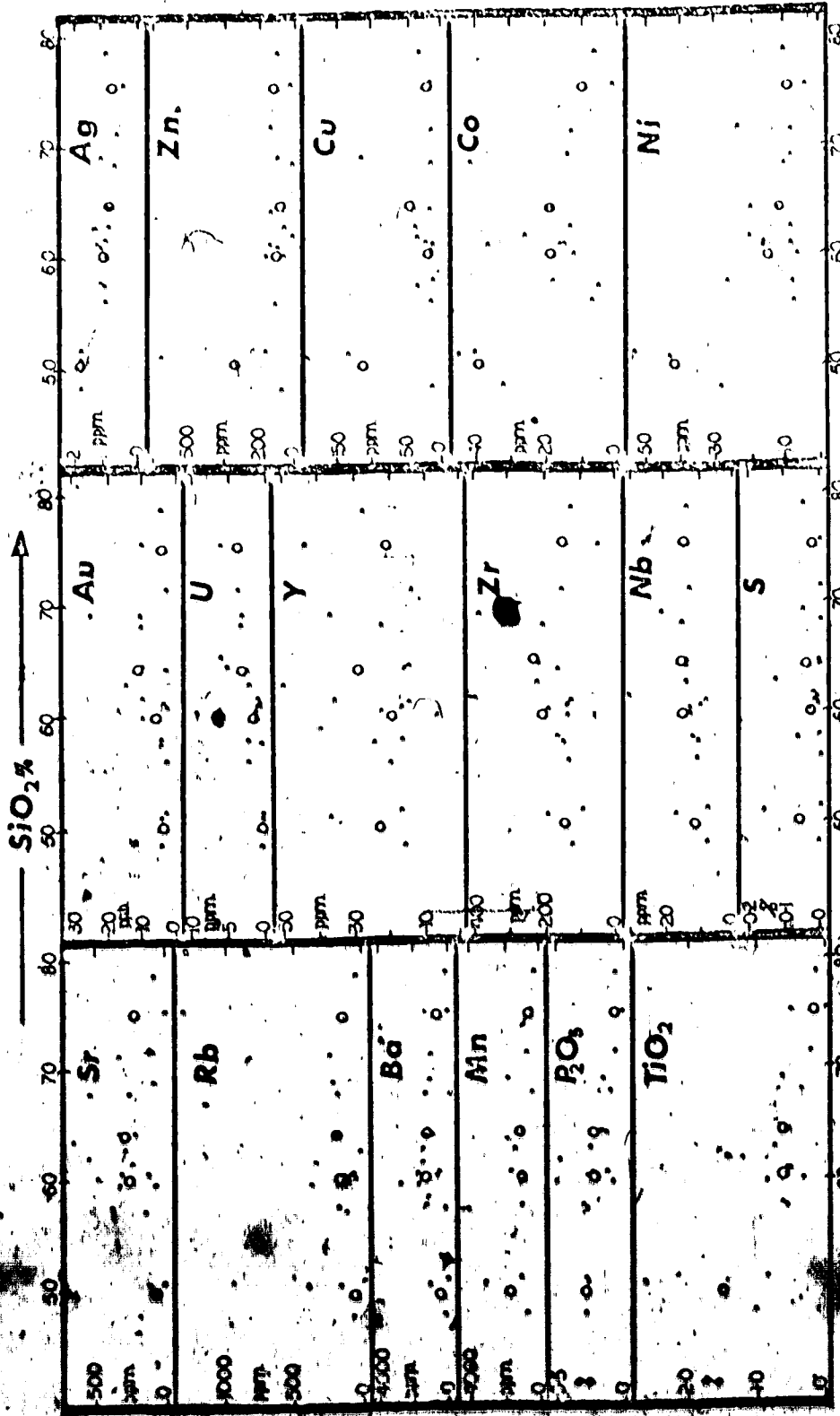
Figure 15. Harter Variation Diagrams of the Major Elements in the igneous rocks of the Cassell River Area, compared with a Cenozoic Andean suite. (Hamilton, 1969).

(and only basalts) showing the same alteration are low.

The low Ni contents of the basalts suggest either a pre-eruptive loss of olivine by fractionation, or a low initial Ni content (Taylor, 1969). Their hornblende porphyritic nature and the tuffaceous, shard-bearing horizons testify to a high water content of the magmas. Hydrous magmas are typically enriched in alkalis over their less hydrous, pyroxene- and olivine-bearing counterparts. These data suggest that the basalts may be related to the rest of the calcalkaline suite, but that this relationship is obscured by alteration.

The variation diagram for the trace elements (Fig. 17) shows that the basalts lie on expected evolutionary curves for many elements - notably Ti, U, Nb, Zr, Y, Zn, Cu, Co and Ni. The relationship may be tested by looking at elements whose distribution is not greatly affected by alteration. Nickel is one such and its content is typically low. Al, Zr and Ti are others. The Al, Ti and Zr contents of Sample SJ 29.8 are suspiciously similar to those of the diabases (Table 2). It was collected near the margin of a young diabase dyke in an area of poor exposure on the Terra peninsula. It is concluded that this may be one of the older, altered diabase dykes, and its analyses for Al, Ti and Zr are not included in the following discussion.

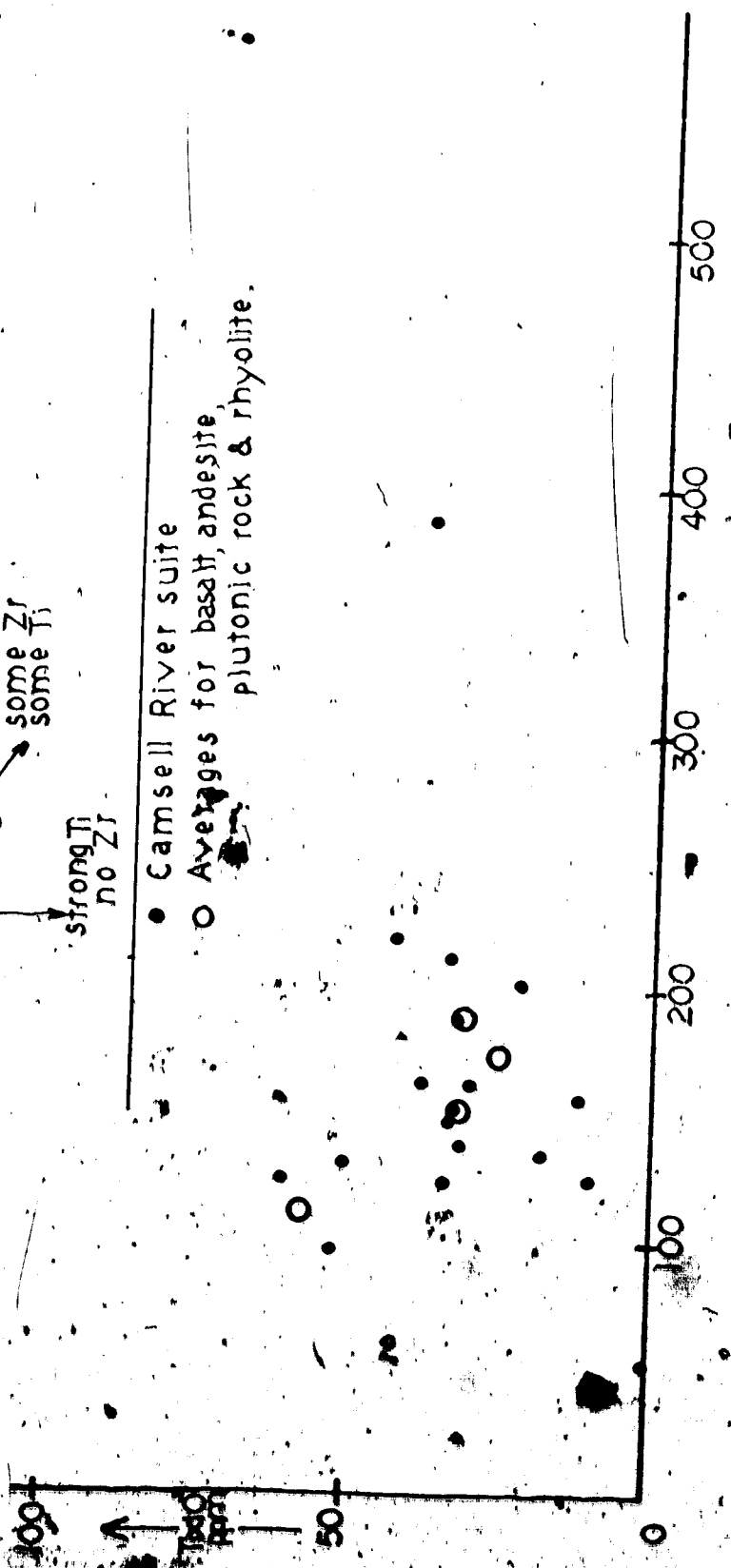
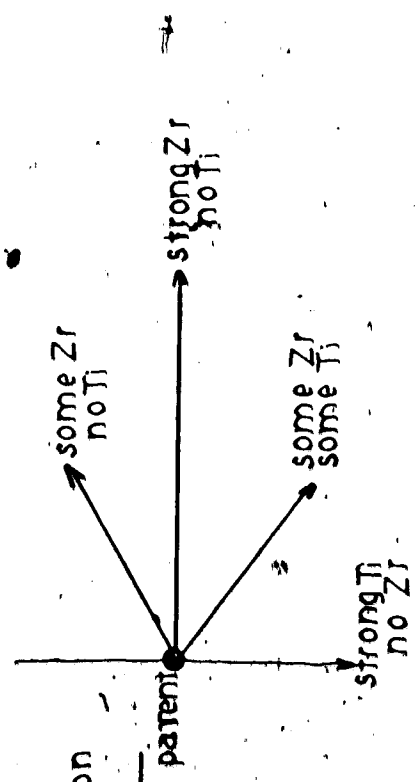
A Ti:Zr plot for the Camsell River suite (Fig. 18) shows a continuous trend from basalt to rhyolite. This does not indicate consanguinity of the basalts and the rest of the suite, but when the



Open circles represent average values for Basalt, Andesite, Intrusive rocks & Rhyolite respectively.

Figure 12  
MARKER VARIATION DIAGRAMS FOR TRACE ELEMENTS

Fractionation diagram.



● Camsell River suite  
○ Averages for basalt, andesite, plutonic rock & rhyolite.

Figure 18. Zr:Ti Diagram for Igneous rocks in the Camsell River Area.

figure is compared with a similar plot for other calcalkaline suites (Fig. 19), where consanguinity is proven, the basalts are closely similar. The alumina values for the basalts are also typical of basic calcalkaline rocks (close to 'high-alumina' series). It is concluded that the basalts are part of the calcalkaline suite, but that their relationship has been obscured by alteration. Nevertheless, they still differ from others in their hornblende-porphyrific nature and high water content.

From the data and arguments presented in this and preceding sections, it is concluded that the Camsell River magmatic rocks are all consanguineous, and part of an alkali-rich calcalkaline suite, having distinct geochemical, petrographic and field affinities with younger orogenic suites. The Ti:Zr diagrams can be used to further these comparisons and to make hypotheses both of magma origin and of magma evolution.

The idea is demonstrated by the 'fractionation diagram' (Fig. 19). Essentially Zr is restricted to amphibole in the earlier-formed minerals of a crystallising basic magma. Various sources indicate Zr contents between 50 and 200 ppm for magmatic amphiboles (e.g. Engel, 1959), although data are scanty. The Zr contents of clinopyroxene are lower. Ti may substitute in early clinopyroxene, amphibole or magnetite, but will enter the oxide preferentially. Titanium, as  $Ti^{4+}$ , substitutes for  $Fe^{3+}$  rather than  $Fe^{2+}$  in both amphiboles and pyroxenes. Thus progressively greater amounts of Ti might be expected in progressively more oxidised amphiboles and

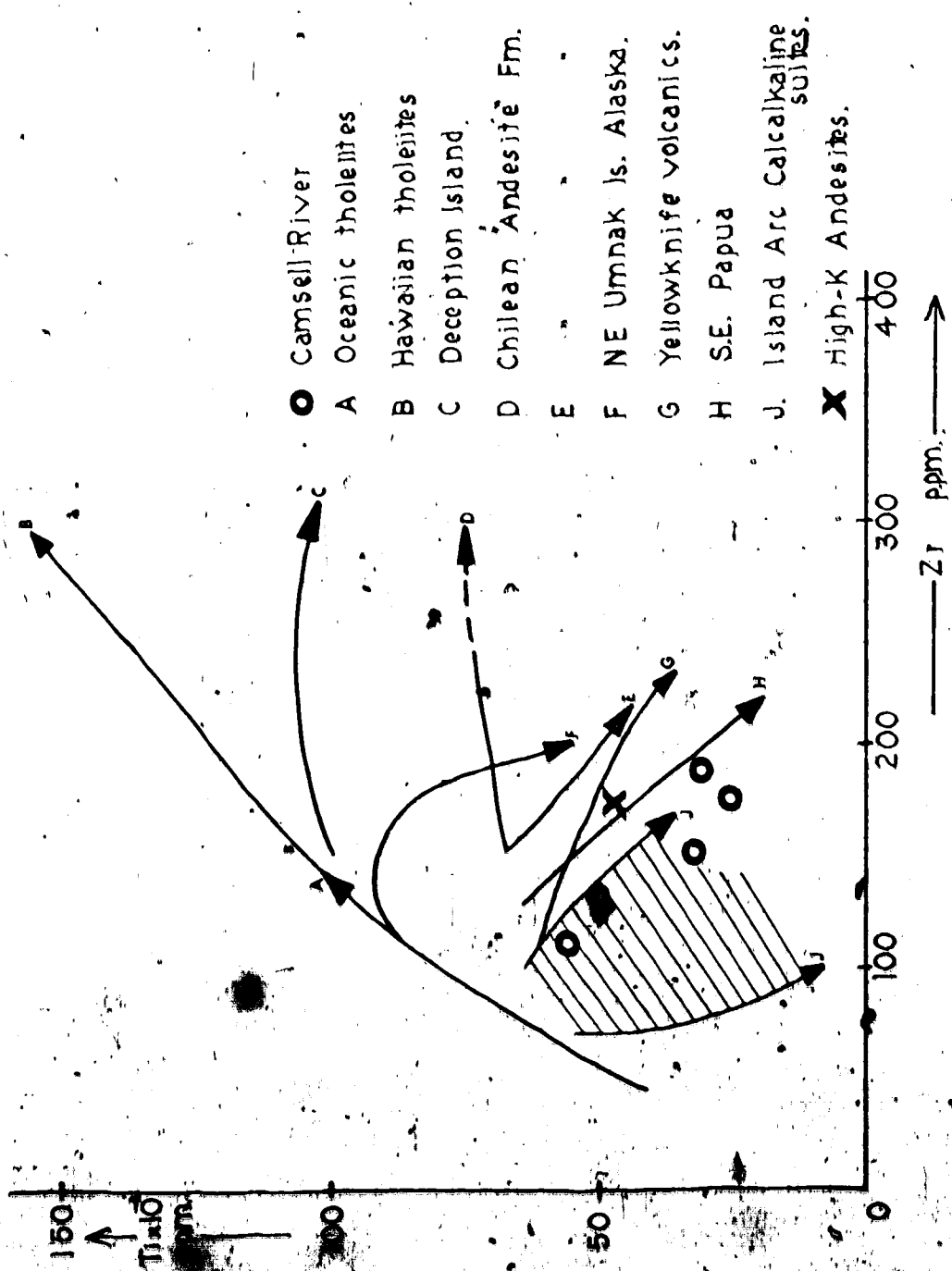


Figure 19. Zr:Tl Diagram for various Calc-alkaline suites:  
 A-B. C. J. from McReath, 1972. D. E. from Siegers et al, 1969.  
 F. from Byers, 1961. G. from Baragar, 1966. H. from Smith, 1972. X. from Taylor, 1969.

pyroxenes, until such time as magnetite forms.

Consequently, Zr fractionation in magmas must be controlled by amphibole. Ti fractionation is controlled by amphibole, clinopyroxene, magnetite and  $fO_2$  (McReath, In Preparation). On the fractionation diagram trends in the NE quadrant are therefore controlled by some amphibole or pyroxene fractionation from the magma, and the steepness of these trends will depend on the amount of Ti both in the original melt and in the crystal phases (i.e. on  $fO_2$ ). Trends in the SE quadrant involve strong amphibole fractionation, and progressively steeper trends will involve more and more magnetite. Finally, a vertical trend can involve magnetite alone. Although the amphibole may carry Ti, weak fractionation will not affect the residual concentration of Ti in the magma: it is too high initially.

Sometime during the course of crystallisation of a tholeiitic magma hornblende and magnetite will start to form. Any trend in the NE quadrant will now turn into the SE quadrant. If the magma evolves to such a point that zircons precipitate, and are fractionated, the trend will reverse into the SW quadrant. A large number of tholeiitic suites have a starting composition around  $50 \times 10^2$  ppm Ti and 50 ppm Zr, and evolve initially into the NE quadrant (McReath, 1972). The distance and steepness of this NE evolution will depend entirely on the amount of Ti in the fractionating phases (i.e. on the  $fO_2$ ). Progressively more oxidised suites should trend progressively closer to the E-axis, and then into the SE quadrant, as shown in Figure 19).

All calcalkaline suites trend either horizontally or into the SE quadrant from a parent containing about 100 ppm Zr and  $60 \times 10^2$  ppm Ti. The difference in steepness of this trend between island arc calcalkaline suites and continental K-rich suites is of interest and would seem to indicate that magnetite plays a more important role than amphibole in the fractionation of island arc magmas. It is also interesting to note the change of trend of both the Deception and Umnak suites as the transition from tholeiitic to calcalkaline is made.

The Camsell River suite plots on the margins between the island arc and K-rich types and shows a similar trend. The parent of the calcalkaline suites falls close to the fractionating tholeiite line and may indicate that the calcalkaline suite may be derived by sudden change in conditions in a fractionating tholeiite magma (i.e. sudden increase in  $fO_2$  or  $pH_2O$ ).

Recent high-K calcalkaline suites are developed in Andean-type orogens and it has often been proposed that the suites are derived by partial melting of a descending slab of lithosphere on the Benioff Zone (McBirney, 1969; Dickinson, 1970) followed by fractionation of hornblende (Jakes and White, 1972). The chemistry, petrography and geology of the Camsell River suite are consistent with such a model. Applications of Dickinson's K-h plots (1970: Fig. 3) to the Camsell River suite indicate that, if the suite originated by partial melting on the Benioff Zone in a similar manner to that proposed for recent circum-Pacific suites, then the magmas were derived from between



250 km (at K 50) and 150 km (at K 65).

Figure 20 shows a plot of the dip of the Benioff Zone against the distance from the trench to the Camsell River area for different depths of magma derivation. Benioff Zones appear to dip at between  $20^{\circ}$  and  $30^{\circ}$  beneath the two cordilleras and application of this figure to the Wopmay Orogen would imply a trench 450-700 km to the west of the Camsell River area (i.e. beneath the Mackenzie Mountains). The areas of major continental-margin Beltian sedimentation lie further to the west. Consequently, either: 1) the model is not applicable; or 2) the Benioff Zone had a shallower dip ( $\sim 15^{\circ}$ ); or 3) the system was not a single trench-Benioff system, but was a complex series of such systems (c.f. the North American Cordillera).

Indications of a polarity of the Great Bear Batholith were discussed in Part I:3 and new chemical data (Hoffman, Pers. Comm. 1973) indicate that this polarity may be a reality. Hoffman substantiates his field observations of interlayered basalts and rhyolites in the eastern part of the batholith, with analyses of the volcanic and plutonic rocks, showing a bimodal distribution with an apparent 'andesite' gap. The basalts are alkali-rich with 1-2%  $\text{Na}_2\text{O}$  and 2-3%  $\text{Na}_2\text{O}$ . The plutons contain 67-77%  $\text{SiO}_2$  and the welded tuff sheets contain up to 80%  $\text{SiO}_2$ . A polarity in suites from andesite-dacite-rhyolite to alkali basalt-rhyolite is evident, and occurs over some 50 miles.

Similar polarities are typical of a number of Andean-type orogens. For example, the polarity across the Cascades is evidenced by the

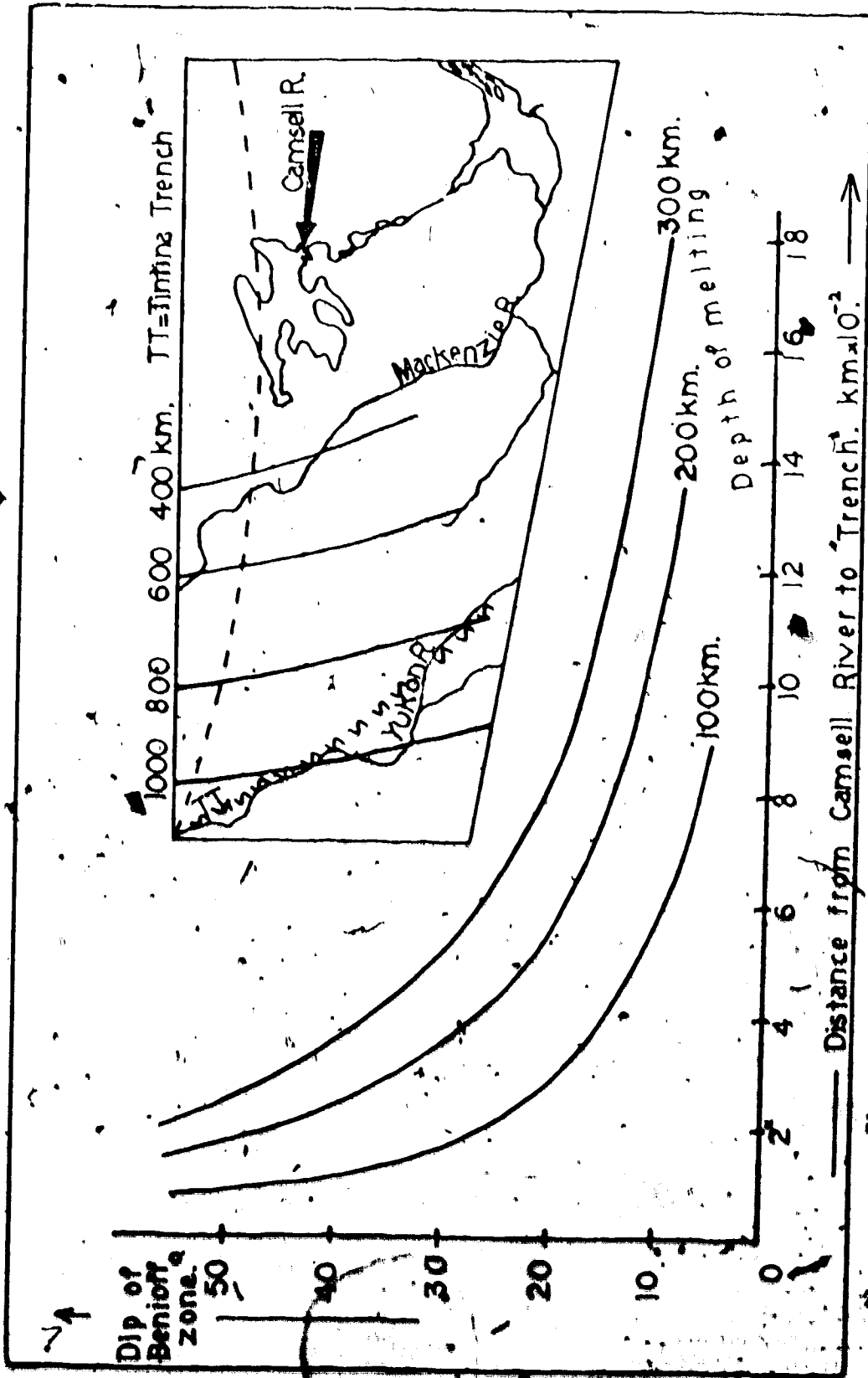


Figure 20. Predicted locations of Benioff Zones for the Coronation Geosyncline.

basalt-andesite-dacite rhyolite suites in the southern Cascades (e.g. Mt. Mazama and Lassen Peak) and the basalt-rhyolite suites on the cratonic margin of the Cascade Range (e.g. Newberry and Medicine Lake Volcanoes). This variation also occurs over some 50 miles. Similar variations occur in the Andes (Vergara, 1972) and in the Avalon Peninsula of Newfoundland (Papezik, 1972). These polarities always occur perpendicular to the trend of orogens, with progressively more K-rich suites lying further from the 'arc'. It is proposed, therefore, from purely chemical and petrographic grounds, that the Great Bear Batholith was an Andean-type continental-margin orogen in which the original margin was considerably to the west of the Camshell River-Echo Bay area.

## 6. GEOTECTONIC EVOLUTION OF THE BEAR PROVINCE

In the past three years there has been a radical change in the interpretation of the Bear Province, engendered by Paul Hoffman of the Geological Survey of Canada.

Hoffman, from mapping of the East Arm of Great Slave Lake (1968, 1969), postulated that the Aphebian Goulburn, Epworth, Snare and Echo Bay Groups and the Great Slave Supergroup (see pre-1965 maps and reports of the G.S.C.) were part of a single geotectonic unit - the Coronation Geosyncline. Later mapping to test this hypothesis showed that in essence Hoffman was correct, but that the Great Slave Supergroup was not actually part of the geosyncline and was set back into the Archaean craton (c.f. Hoffman, 1969, 1970 and 1972). Further work revealed that the Coronation Geosyncline consists of three major units (Fraser et al., 1972; Hoffman, 1972, 1973):

1. The Epworth fold and thrust belt, comprising the Epworth Group sediments which lie unconformably upon the Archaean craton.
2. The Hepburn Batholith, comprising the high-grade metamorphic rocks of the Wopmay and Emile River belts of the Snare Group, and deeply eroded granites and gneisses.
3. The Great Bear Batholith, comprising epizonal granites and derivative volcanics and sediments.

In addition, Hoffman (1973) proposed that the East Arm of Great Slave Lake and Bathurst Inlet were aulacogens, projecting from this geosyncline into the craton. Hoffman realised the continuity of

process from the undeformed cratonal cover, through zones of increasing deformation and metamorphism to areas of major batholith intrusion and recognised that the geosyncline had undergone orogeny remarkably similar to younger continental-margin orogenies (Dewey and Bird, 1970). Hoffman consequently proposed that the units involved in the Aphebian Orogeny be ascribed to the 'Wopmay Orogen'.

At the same time as these hypotheses were being formulated, the author was pondering the palaeogeographic and geotectonic evolution of the Camsell River and Echo Bay areas, and realised that his interpretations were compatible with Hoffman's hypothesis.

Studies of the stratigraphy on the eastern shores of Great Bear Lake revealed that the Aphebian sedimentary and volcanic rocks were initially deposited in fluvial and lacustrine basins between major volcanic 'highs', and that occasional marine incursions caused thin calcareous units to be interlayered. Younger beds became progressively more sub-aerial. A continuity of process but not of lithology was seen between the various 'basins' that are now preserved as roof pendants. Rapid tectonic activity was indicated by the nature of sedimentation, by the rapidity of unroofing of early plutons, and by the syn-depositional faulting. An environment of large volcanic islands being uplifted by block faulting above rising batholiths was proposed (Badham, 1972) and Hamilton and Myers' (1967) model of granitic batholiths, finally intruding their derivative volcanic and sedimentary rocks was deemed applicable. This was substantiated by the geochemical work outlined in the preceding section and by

Badham (1973).

This Andean-type batholith fits well into Hoffman's concept of a continental-margin geosyncline and ensuing orogeny. The evolution of and time relations within this orogenic belt are not yet clearcut. However, the proposed evolution of this continental margin is discussed below.

The Archaean cratons were essentially stabilised by 2390 m.y. (e.g. Green and Baadsgaard, 1971) and they must have been similar to present day continental crust by then, so that similar processes could occur on and around them. There are no data for the time of initiation of sedimentation in the Coronation Geosyncline, but there are indications that before this time there was a 'Lower Aphebian' event which produced the Wilson Island Group in Great Slave Lake (see Reinhardt, 1969; Hoffman, 1969) and which may be correlable with both the Huronian and the Fay Mine Complex (Sassano et al., 1972). Hoffman et al. (1970) propose that sedimentation was initiated a little before 2000 m.y. ago. The Epworth Group was initially derived from the east and consists of quartzites (Odjick Formation) overlain by dolomites (Rocknest Formation) which lie unconformably on Archaean basement and which vary westward into basinal siltstone and mudstone turbidites. After a period of quiescence during which black mudstones were deposited (Lower Recluse Formation) the clastic sediments of the Upper Epworth Group (Recluse Formation, Cowles Lake Formation) were derived from uplift in the Hapburn Batholith area. Emplacement of this 'batholith' caused deformation and metamorphism.

of the lower Epworth sediments and continued uplift and erosion had exposed mesozonal granites by Cowles Lake times. During and after the unroofing of the Hepburn Batholith, 'granites' were being generated and emplaced further to the west, and were in turn generating the late-orogenic volcanism of the Echo Bay Group type. The Great Bear Batholith was emplaced and uplifted by 1750 m.y. ago but remained separated from the far more uplifted and eroded Hepburn Batholith by the Wopmay Fault. These data are summarised in Figure 21.

Thus, there is a polarity of the orogen:

<u>West</u>		<u>East</u>
Epizonal granites	Mesozonal granites	Thrust and folded
Derivative volcanics and sediments	Metamorphic rocks	{ cover rocks on basement
Late orogenic	Intense deformation	

a polarity remarkably similar to that of both north and south American cordilleras, but distinct from the bipolarity of 'continental-collision' orogens, such as the Appalachians (e.g. Dewey and Bird, 1970).

The sedimentary, geochemical and geotectonic evidence combine to indicate that the Wopmay Orogen developed on the margin of the Slave Craton in a similar manner to that in which younger continental-margin orogens have developed. This implies that crustal conditions have remained essentially unchanged since the Archaean.

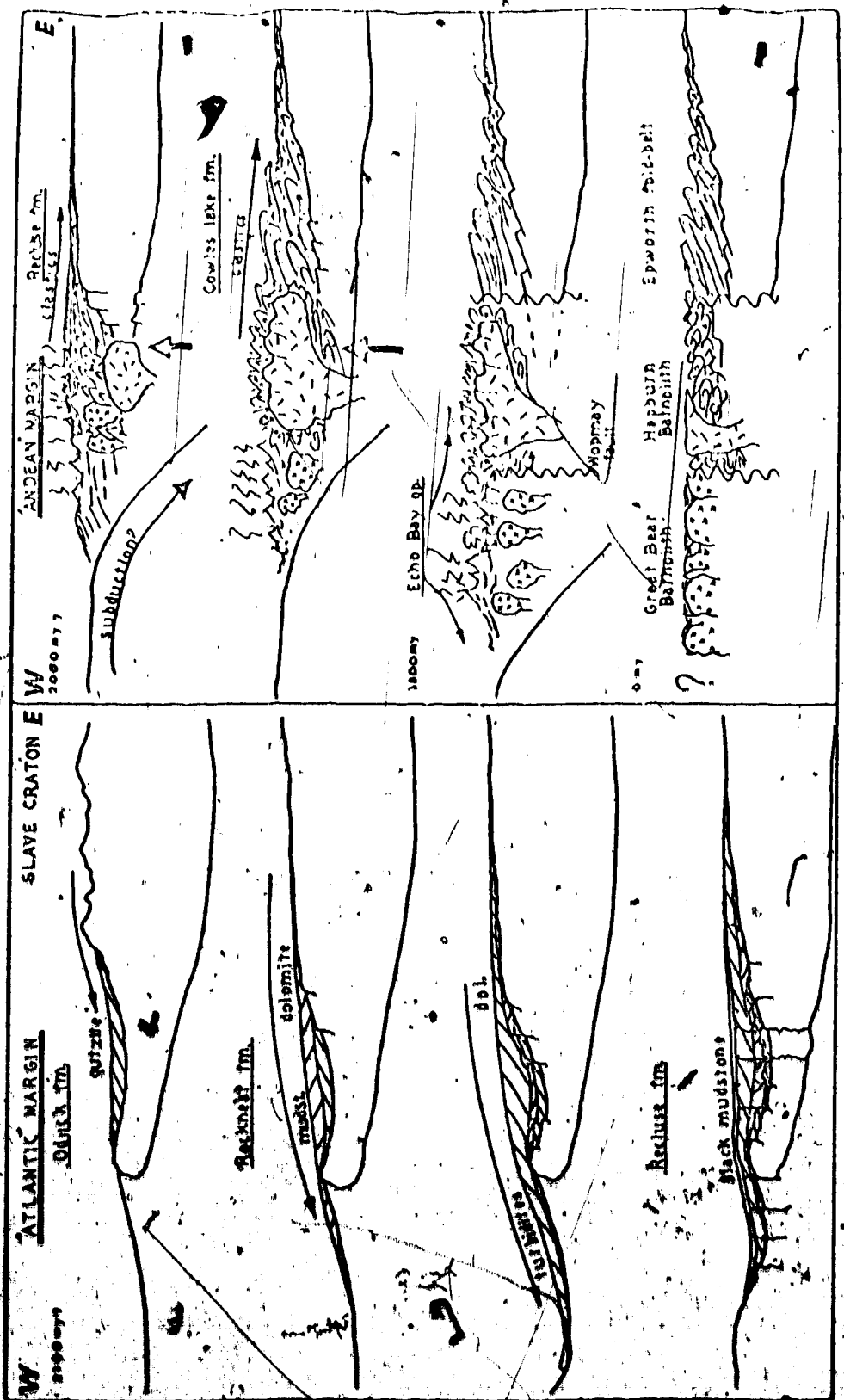


Figure 2. DEVELOPMENT OF THE WOPMAY OROGEN & CORONATION GEOSYNCLINE



The polarity of this orogen is developed on a similar scale to those with which it is compared. The western limits of the orogen are covered by Palaeozoic strata and a strike length of only a few hundred miles is exposed at present. Aphebian volcanic and plutonic rocks are known from drill-hole data beneath Norman Wells and further to the south on the Tathlina Arch (Douglas and Price, 1972), and it is inferred that the Great Bear Batholith extends at least to the Rocky Mountain front, making it of a scale comparable to the Coast Range Batholith, for example.

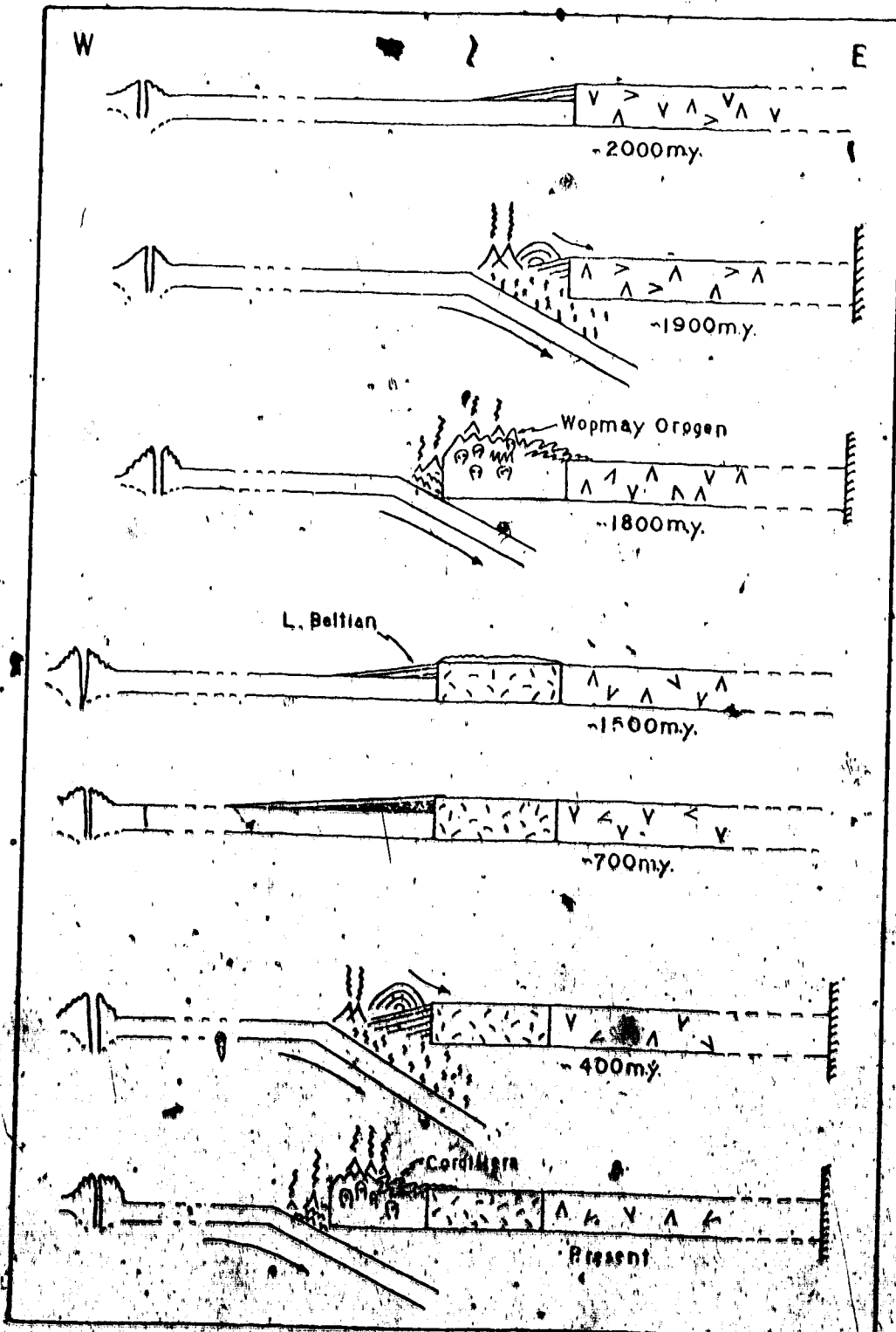
Plate tectonic models involving subduction of ocean-floor beneath a continental margin have been developed to explain Cordilleran geology (e.g. Monger et al., 1972) and it is proposed that they apply equally well to the Wopmay Orogen. As in the Cordillera, a more complex series of events than just a single period of subduction and resultant magmatism is evident (see Fig. 20), but the history of the Wopmay Orogen is far from being worked out yet.

#### Some Speculations on Continental Margins

The Coronation Geosyncline was developed on the margin of the Slave Craton. After the Wopmay Orogeny, Aphebian rocks stretched from the Epworth Group area to at least Norman Wells. It is implied that the sediments of the geosyncline were deposited initially on a trailing or Atlantean-type margin (Mitchell and Reading, 1969) and that later compressive tectonics resulted in rupturing of this margin, subduction and orogeny (shown schematically in Figure 21).

Helikian red beds (Hornby Bay Group) were deposited on the newly stabilised craton in the Great Bear Lake area. Beltian sediments were deposited at this time in large coastal deltas to the west and serve to locate the post-Aphebian continental-margin (Gabrielse, 1972). From Lower Beltian to Lower Palaeozoic times sedimentation continued (with minor interruptions) on an Atlantean-type margin until compression again caused rupturing at this margin and a complex orogen developed to form the Cordillera. This continual process is exemplified in sketch diagrams (Fig. 22) and implies that the western margin of the Canadian Craton has migrated westward continuously since the Archaean. Whether this migration was caused by addition of material from the mantle or by accretion of crustal material (island arcs, continental fragments, etc.) is not known. Such a discussion is beyond the scope of this work and the theoretical possibilities have been discussed at length in the literature (e.g. Dewey and Horsfield, 1970). Likewise, discussions of the strike length of the Aphebian continental-margin and the relationships of the Wopmay Orogen and the Churchill Province are subjects only for speculation at present: subjects that require an immense amount of work before any of this speculation may become meaningful.

Figure 22. Sketch Cross-sections showing the Evolution of the Western margin of the Canadian Shield. (Events in 1500-700 m.y. range are omitted.)



## 7. POST-APHEBIAN LITHOLOGIES AND EVENTS

### a) Faulting

Four sets of air-photograph lineaments have been recognised in the area. Three of these, striking NW, N and NE respectively (Fig. 23), are often of substantial dimensions (Mursky, 1963) and are common to much of the Bear Province. The fourth set is also common throughout the area, but individual lineaments are short. This last set is commonly occupied by the youngest diabase dykes.

The NW-trending lineament represents a set of faults whose movement pre-dates the major transcurrent movement on the NE-trending faults. Furnival (1935) reaches the same conclusion for other areas. Cross-cutting relations are, however, not common. Movements on these faults have not been documented in this area, but other workers have noted small offsets, and Mursky (1963) describes them elsewhere as being complementary to the NE-trending set. At present all that can be said for this area is that dykes in the NW-trending set are sometimes offset by movements on the NE-trending set.

The N-trending lineaments are all joints, with no observed offsets. The scale of this joint system requires a regional event, such as the uplift and cooling of the whole area, to produce them. They pre-date major movements on the NE-trending faults. Fehiak (1949) describes right-lateral offsets on N-trending faults at Hunter Bay, but other authors (Kidd, 1936; Mursky, 1963) have noted no such offsets.

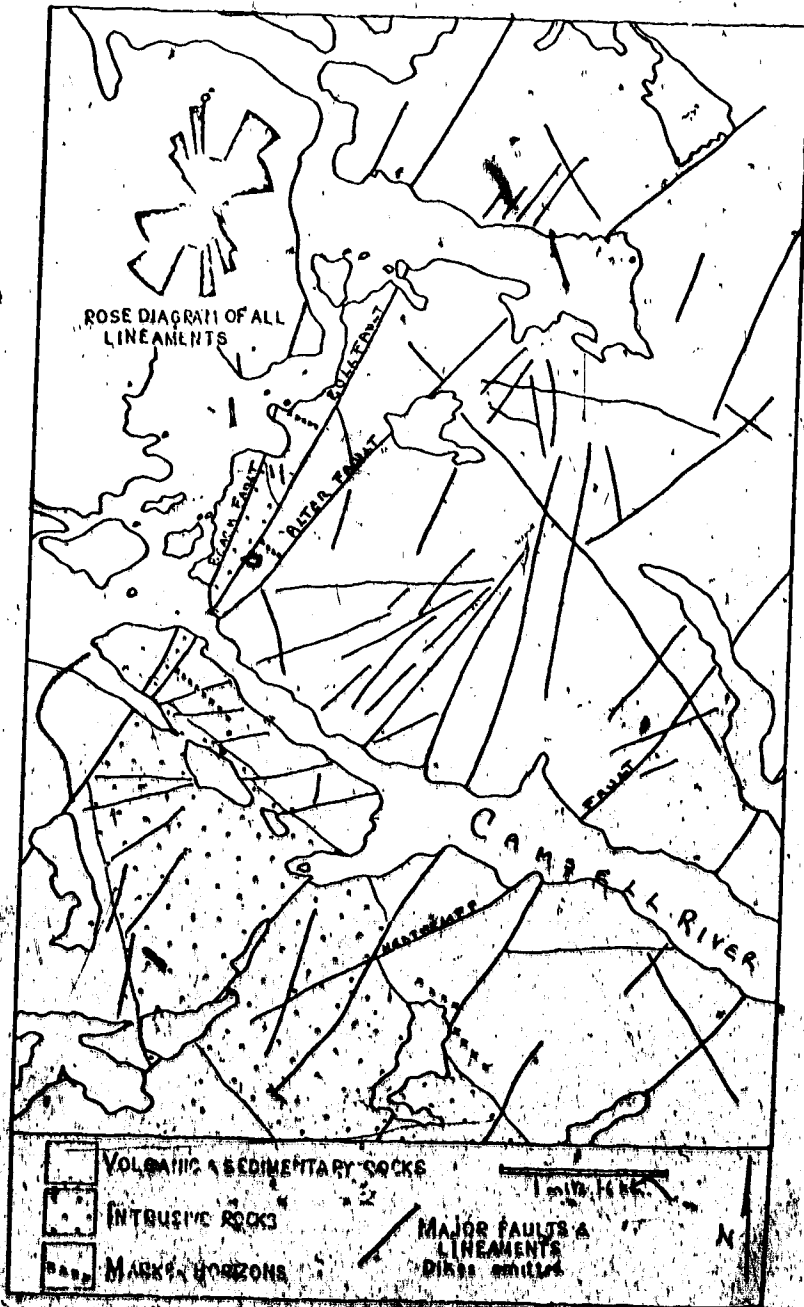


Figure 23. Photo lineaments (Excluding known Diabase Dykes.) for a part of the Campbell River Area.

The NE-trending lineaments represent the major NE-trending complex fault-systems. Evidence has been presented earlier to imply that these faults were active in Archean time, but the major movements took place after the final emplacement of granites. These faults extend throughout the NW Canadian Shield and are often of considerable length. They frequently splay, coalesce and bend. In general the systems can be ascribed to a NE-trending set of master faults on which continuous right-lateral movement developed secondary splays and cross-fractures; the number of such splays is indicative of a number of periods of fault movement (Chinnery, 1966).

Right-lateral movement is the rule on both primary and secondary faults, although apparent left-lateral movement is suspected in some cases (e.g. the Terra Mine fault). No evidence for vertical movements has been seen in this area, but Mursky (op. cit.) documents such movements of a "few hundred feet" elsewhere.

The development of these faults appears to be typical of Chinnery's (op. cit.) 'Type A', and continued movement on them has caused the coalescence of Type A secondary faults with neighbouring primary faults. The geometric problems associated with coalescent junctures have been predicted, but no well-exposed example has been mapped in the required detail.

However, the details at a splaying junction have been well documented. The fault in question is the Bull-Alter-Beach Fault system, which was mapped in detail in 1972. The nature of the movements are illustrated on maps (Figs. 6 and 23) and in a sketch

(Fig. 24). The offsets of 2067 m and 670 m are accurately documented, and the offset on the Beach Fault is probably on the order of 3500 m. Drag-folding and dilatancy associated with these movements is shown on Figure 18 and a comparison of this actual case with some geometric models for the development of such features (Fig. 24) allows predictions of the order of movement of the three splays from the Master Bull Fault. The model implies that the Bull Fault moved first and that a dilatancy, generated at a slight bend in the fault, was filled (during or just after this movement) in this case with a 'Giant Quartz Vein'. Subsequent movement on the Alter Fault generated dilatancy on both faults and disrupted the rocks between the two (Fig. 24, Model 7). Finally, movement on the Beach Fault took place, causing minor drag-folding, but dilatancy only on the Master Fault (Fig. 24, Models 3 and 4).

Minor structures related to the major structures show identical features (e.g. Fig. 24, Outcrop SJ 11.5), and a study of these features can often lead to an understanding of the major features where marker horizons are absent or the fault-planes are not exposed. Study of minor structures has revealed that all of the eight alternative models in Figure 18 do occur, although the geometry and history of the real cases is often far more complicated. The development of dilatancy on these NE-trending faults is the most important post-Aphebian event in the area and permitted the introduction not only of the Giant Quartz Veins and diabase dyke swarms, but also of the mineralised veins. In general the Giant

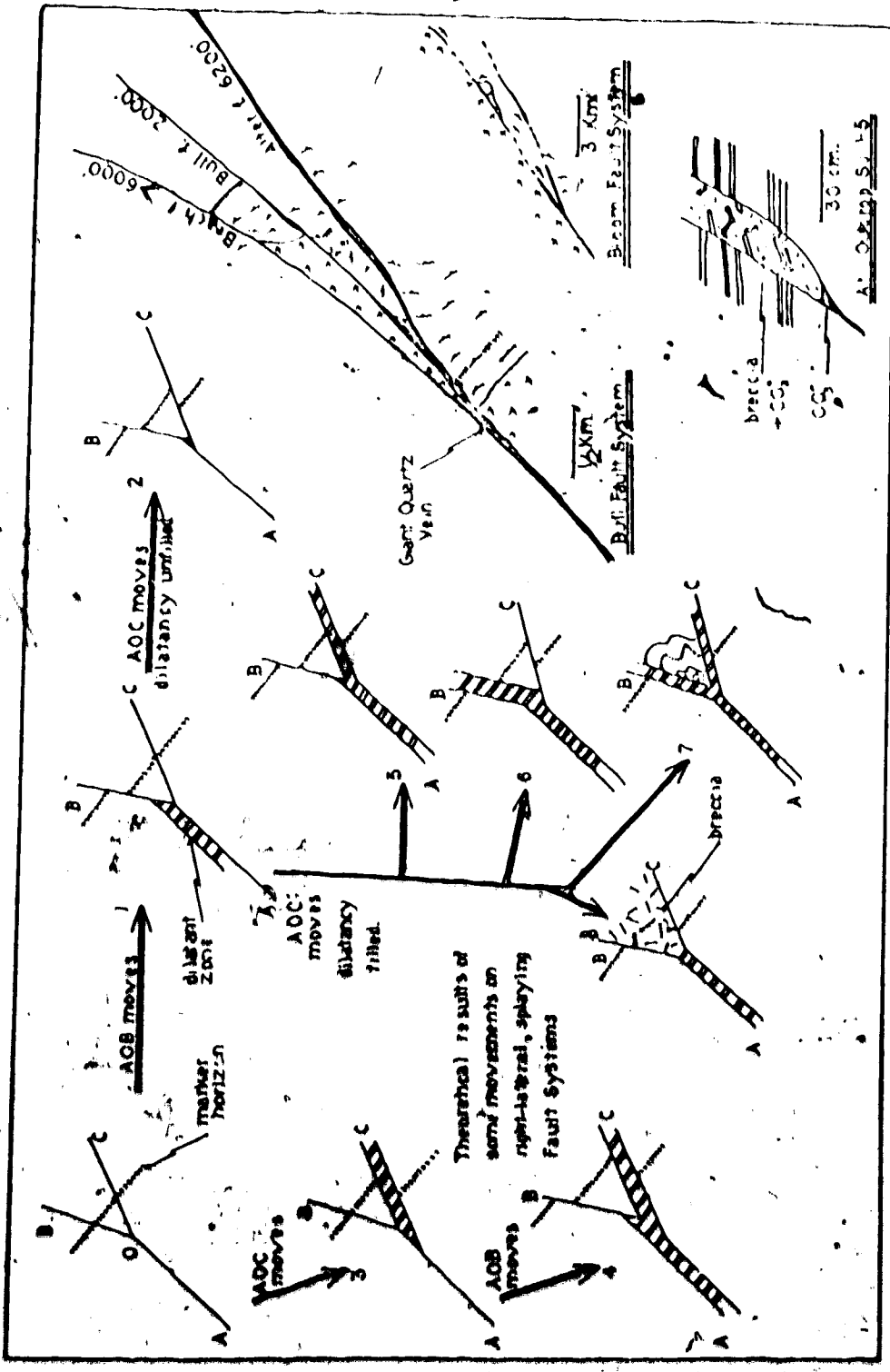


Figure 24. Sketch maps of some Faults in the Camsell River Area compared with Geometric predictions for their development.



Quartz Veins occupy major dilatancies on the Master Faults and the mineralised veins occupy smaller splays from these faults. The development of dilatancies will be discussed more fully in the description of the controls of mineralisation.

The E-striking lineaments are interpreted as joints and cross-tension-fractures related to the NE-trending faults. They commonly run between NE-trending faults, but never through them, and little or no movement is associated with them. They are dilatant and often filled with quartz or carbonate veins and with the youngest set of diabase dykes. In the mineralised areas they join the major NE-trending veins and typically contain the later stages of mineralisation.

#### b) Giant Quartz Veins

Stockworks of quartz, up to 170 m wide, have been seen on the Smallwood, Heathcliff, Bull and Bloom Fault Systems. The Bull Fault itself is filled with quartz for over 10 miles. In all cases the stockworks exhibit progressive filling of dilatant fault zones, interrupted by periods of extensive brecciation of the earlier fill.

The stockworks consist of an inner zone of massive quartz and silicified rock fragments, surrounded by an aureole of silicification in the country rock, which is dissected by numerous quartz stringers. The siliceous zone is enveloped by zones of sericitic and chloritic alteration.

The earliest quartz, now mostly broken fragments cemented by

younger infusions, was white and massive, and constitutes the major part of the veins. This phase was brecciated and a finely-banded chalcedonic quartz was introduced. This was brecciated in turn and a vuggy clear quartz was deposited with local concentrations of copper and uranium minerals and hematite (e.g. at Echo Lake, Jason Bay [Plate 5.7] and Uranium Point).

Furnival (1935) has described these veins in detail. They occur throughout the NW Shield, always in NE-trending faults, and show evidence of three, and sometimes four periods of mineralisation, and hence up to four periods of fault movement. Rarely are the minerals of any economic interest.

Generally the Giant Quartz Veins were emplaced after the granites and before the Hornby Bay Group, but there is good evidence to show that the last phases of quartz mineralisation took place after the Hornby Bay Group sediments had been deposited (Kidd, 1932).

### c) Diabases

The geology and age relations of the diabases of the Bear Province have been in an alarming stage of confusion for many years. There have been a number of phases of diabase emplacement, each on a number of trends, and reports of these together with some completely erroneous data are responsible for the confusion. An attempt is made here to unravel the Gordian Knot after reviewing all the available literature.

The dykes of the Camsell River area are as complex as any

(Fig. 25). Early mapping distinguished NW-, NE- and E-trending sets and a thick sheet - the Gunbarrel Gabbro. All these dykes are two-pyroxene-, quartz-, magnetite-, ilmenite-, plagioclase-bearing diabase, and all have suffered some alteration to assemblages of hornblende, biotite, chlorite, oligoclase, sphene, rutile, maghaemite and haematite. This alteration is controlled by the grain size, the finer rocks being more altered. In addition, the quartz occurs as interstitial anhedral in the fine-grained dykes, but as micrographic intergrowths with feldspar in the coarser ones. There is no consistent mineralogic difference between dykes of different trend. The margins of these dykes are chilled (Plate 3.4) and often contain small carbonate and quartz veins with iron and copper sulphides.

Analyses (Table 2) show that these diabases are typical quartz tholeiites, indistinguishable from other continental dyke-swarms of the Canadian Shield.

The following field relationships have been observed:

1. A NW-trending dyke is cut by an E-trending dyke.
2. Some NW- and E-trending dykes merge into one another.
3. E-trending dykes often cut the NE-trending faults and Giant Quartz Veins.
4. Some E-trending dykes stop at the Bull Fault and cut sheared and quartz-veined rocks, but are not sheared themselves.
5. The Gunbarrel Gabbro varies from a thick sheet to an

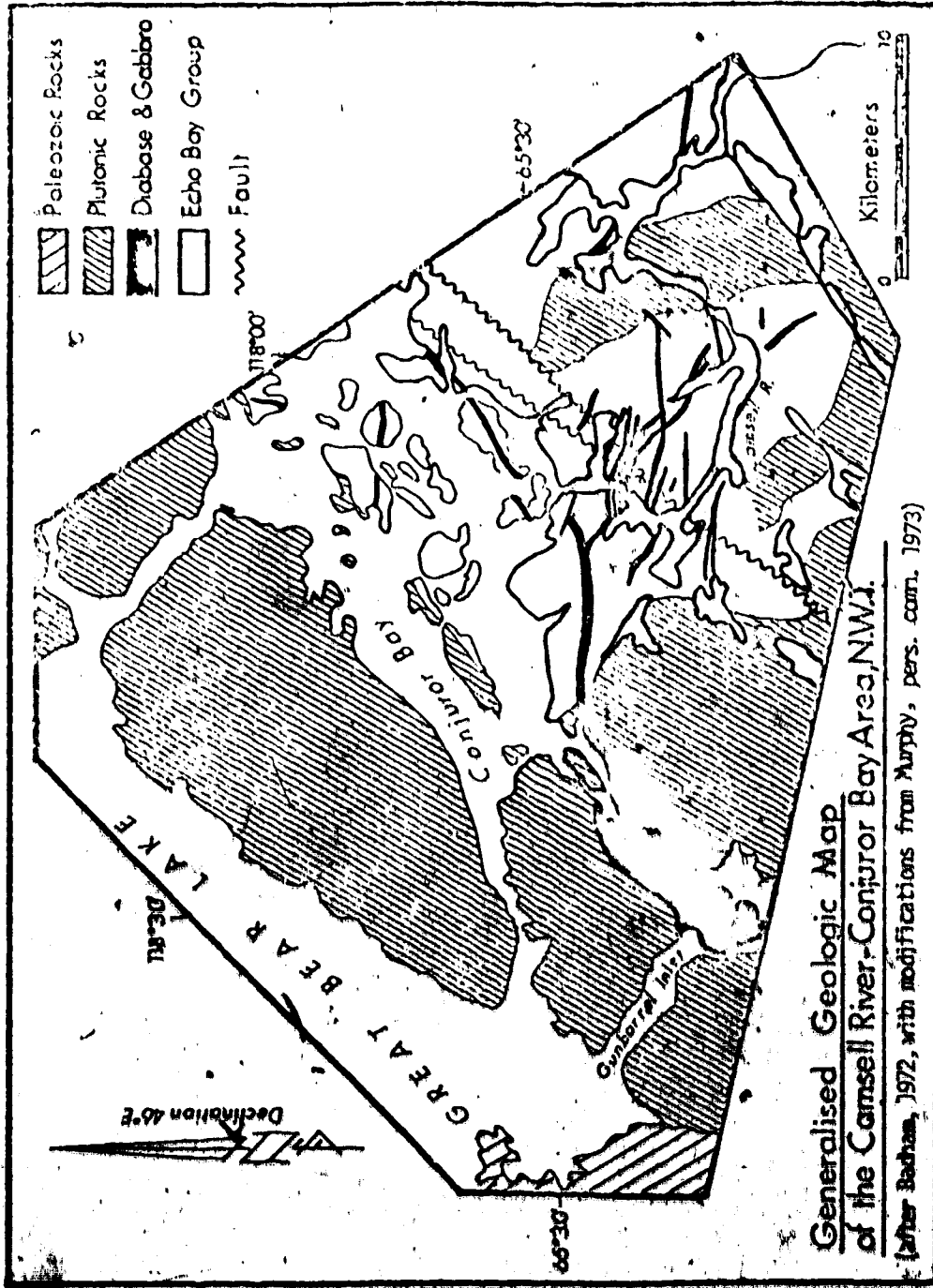


Figure 25. Diabases in the Camsell River Area.

E-striking dyke (Murphy, Pers. Comm., 1973) to a NE-trending dyke.

6. The E-trending dykes do not cut the Gunbarrel Gabbro and the gabbro does not cut the dykes.
7. One remnant of an older 'diabase' was found on the Terra peninsula. It is extremely altered and its feldspars are stained red with haematite. It post-dates the intrusion and the magnetite body, but is cut by an E-trending diabase.

From this data it is concluded that:

1. There may be an old set of dykes which are now extremely altered.
2. The NW-, NE- and E-trending dykes and the gabbro are penecontemporaneous. A major dyking event at some time after the last major NE-trending fault movements caused any 'unsealed' fracture to be filled.

Data from the rest of the Great Bear Batholith is apparently more confusing, mainly because of radiometric and palaeomagnetic studies without proper geologic controls. However, the following relations, synthesised from the references listed, can be seen.

1. Some highly altered 'gabbroic dykes' intrude Aphebian volcanic rocks, but are cut by granites (Furnival, 1934; Kidd, 1936; Smith, 1953).
2. Post-Aphebian dykes with red (altered) feldspar precede the first stages of Giant Quartz Veining (Kidd, 1932, 1936; Kidd and

Haycock, 1935; Feniak, 1949). These dykes often lie in NE-trending faults, pre-date the vein-mineralisation at Echo Bay (Robinson, 1933) and are cut by younger dykes (Feniak, 1949). At Echo Bay these dykes may be about 1625 m.y. old (Thorpe, 1971).

3. All authors but two (Kidd, 1936; Furnival, 1939) agree that events after the earlier dyking were as follows:

- a) Giant Quartz Veins - Phases 1 and 2
- b) Deposition of Hornby Bay Group
- c) Giant Quartz Veins - Phase 3 (and 4) and minerals.

Vein mineralisation is thought to have taken place throughout this time. Kidd and Furnival tentatively identify some dykes as older than c) above.

4. Relations between the 'younger' dykes and the sheets are ambiguous, but when viewed as a whole, indicate their contemporaneity. For example, the sheets often turn into dykes of variable trend, or have dykes as apophyses (Kidd, 1936; Parsons, 1948; Feniak, 1949; Mursky, 1963). These dykes cut the Hornby Bay Group, the Giant Quartz Veins and the Echo Bay vein mineralisation (Kidd, 1932; Robinson, 1933; Parsons, 1948; Feniak, 1949; Mursky, 1963). The sheets are sills in the Hornby Bay Group, but flat-lying sheets in the Aphebian rocks. They often originate from the NE-trending faults (Furnival, 1934; G.S.C. Maps 1014A, 697A, 1224A, A9-19). These dykes and sheets often have carbonate-rich margins containing sulphide minerals, and occasionally have small veins containing remobilised Ni-Co arsenides and silver (Robinson, 1933; Furnival, 1934). The dykes and sheets

have been shown to have approximately the same K-Ar (Wanless et al., 1970) and Rb-Sr (Robinson, 1971) ages (1200-1400 m.y.). Palaeomagnetic work (Irving et al., 1972) shows that the Western Channel diabase and the Port Radium sheets have reversed but equivalent poles that appear to fit the 1200-1500 m.y. interval on apparent polar wandering curves for the Canadian Shield. The Gunbarrel Gabbro and Bell Island Gabbro (Kidd, 1936) are similar. Temperatures near these diabase sheets reached at least 650°C (Irving et al., 1972) and remobilisation of older vein minerals is documented by Thorpe (1971).

It would seem, therefore, that two periods of diabase intrusion (~1625 and ~1400 m.y.) took place in the Proterozoic rocks at Great Bear Lake. There is no evidence that any member of the younger swarms (Numbers 10 [875 m.y.] and 12 [700 m.y.]; Fahrig and Wanless, 1963) outcrops in the area. Relationships beyond the Great Bear Batholith are more complicated and are summarised in Fraser et al. (1972). The work of Fahrig and Wanless (1963) does not apply to this area.

Age relations of the dykes and other features are shown in Figure 5.

#### d) Mineralised Veins

Quartz-carbonate veins containing iron and copper sulphides are associated with the plutons, the Giant Quartz Veins and the younger diabases. Minerals observed include quartz, chlorite, dolomite, ankerite, calcite, barite, haematite, pyrite, uranium oxides, bornite,

chalcopyrite, chalcocite, covellite and arsenopyrite. The veins are vuggy and the minerals were precipitated in vugs in sequential bands. Only the carbonates are ever replaced by other minerals.

A vein containing brecciated and strained black tourmaline (Plate 3:6) cemented by carbonate, quartz and pyrite fills a fault at Balachey Lake. No other veins of this type have been seen.

The ore-bearing veins are documented in greater detail in Part II. Suffice it to say here that all the veins are controlled by faults and related fractures, and all can be related to hydrothermal solutions that were introduced into these faults, or to dykes that intruded the faults.

#### e) Alteration

Four categories of alteration have been recognised in the Camsell River area (Radham, 1973) and were documented further in Section I:5. They are:

1. ~~Recent~~ and recent weathering. Palaeoweathering of flow tops and some tuffs can be seen in the field and typically takes the form of strong haematitisation and leaching. Recent weathering is virtually limited to sulphide-rich rocks which decompose to a crumbly orange gossan. Apart from the surface effects of lichens, other rocks are barely affected.

2. Autometasomatism in the volcanic pile. Zeolites were reported in andesites at Echo Bay (Robinson, 1971) but none has been documented from the Camsell River area. The uraniferous



of diabase has already been discussed, and is clearly autometamorphic.

3. Contact metamorphism. Again the effects of this have been discussed previously.

4. Hydrothermal. Chlorite, epidote, quartz, carbonate, haematite and sulphides have grown at the expense of original minerals adjacent to all the veins, faults and diabase dykes (Plate 4.8). The great number of such features minimises the chances of collecting unaffected samples. In general the rhyolites and sediments appear least affected, essentially because of their low contents of mafic minerals.

#### f) Geochronology of Events

Geochronologic studies of the Great Bear Batholith are, sadly, few and far between: there are no such studies of the Camsell River area. K-Ar ages from the Hepburn Batholith (G.S.C., various) cluster around 1700-1760 m.y. and the Great Bear Batholith is of similar age.

The Upper Echo Bay Group gives a Rb-Sr age of  $1770 \pm 30$  m.y. (Robinson and Morton, 1972) and is intruded by granite giving a U-Pb age of  $1820 \pm 30$  m.y. (Jory, 1964). K-Ar ages of andesites, granodiorite and granite at Echo Bay (Robinson and Morton, op. cit.) give ages of 1570-1700 m.y. The model to be presented proposes the very close temporal relations of volcanic and intrusive events and the different ages obtained are presumed to represent differences in analytical methods used. Most of the Alpebian events in the Camsell River area

are presumed to have taken place in the 1850-1700 m.y. interval.

The diabase sheet and possibly associated veins have been dated at  $1400 \pm 75$  m.y. (K-Ar: G.S.C. 67-80) and  $1370 \pm 60$ - $1435 \pm 60$  m.y. (K-Ar: Robinson and Morton, 1972). Uranium from the Port Radium Mine has been dated frequently as being about 1450 m.y. old (Cumming et al., 1955; Eckelman and Kulp, 1957; Jory, 1964) but Thorpe (1971), using both Jory's and new data, indicates a model lead age of 1625 m.y. for the earliest stages of mineralisation and ascribes the 1400 m.y. ages to updating by the diabase sheets.

This geochronological data has been used in constructing Figure 5.

## 8. A DIGRESSION ON THE METACALCARGILLITE AT TERRA

The comprehension of this lithology is of crucial importance in understanding the controls of both vein and skarn mineralisation at the Terra Mine. This understanding has been hampered by the fact that the unit is only seen in the aureole of the Terra intrusion. Where it occurs in the albite-epidote facies, palimpsest features can be seen and the original rock is interpreted as having consisted of finely-banded limestone and tuff. Much of the tuff is fine-grained and of ash-fall origin, but some beds are coarser crystal tuffs, composed of fragments of quartz and feldspar. The nature of the banding is very variable and no regular or cyclic sequences can be seen. The calcargillite is interpreted as having been deposited in a calm environment where limestones were chemically precipitated, and into which distal tuffs fell spasmodically.

Most exposures of the unit are now on the border of the hornblende-hornfels and albite-epidote facies, between 150 and 300 m from the intrusive contact. The rock is still well-banded, but the present bands do not represent original bands; they are the product of diffusion reactions between bands. Minerals recognised are diopside, hornblende, hastingsite, tremolite, actinolite, andradite, grossularite, scapolite, idocrase, zoisite, clinozoisite, epidote (usually pistacite), albite, biotite, muscovite, apatite, sphene, magnetite, marcasite, pyrite, chalcopyrite, sphalerite, galena, quartz, dolomite, and celestine; i.e. the basic mineralogy is

quartz, carbonates and Ca-Al-Fe silicates.

The paragenesis of these minerals in the hornblende-hornfels facies (Fig. 26) shows the retrogression of the suite from the hornblende to the albite-epidote facies and, indeed, textures seen in thin section suggest that:

1. The garnets have altered to epidote, quartz, chlorite calcite assemblages.
2. The amphiboles are altering to chlorite and magnetite.
3. The diopside has altered to tremolite.

Each of these is a retrogression and no remnants of the prograde reactions are seen.

In the albite-epidote facies rocks, original impure carbonate can be seen, but in the higher grades only fresh calcite has been observed. Prograde reactions to form albite, tremolite and muscovite are indicated by textures in the albite-epidote facies rocks.

The mineralogy of the bands is now rather simple. Individual bands rarely contain more than three minerals and are often monomineralic. Groups of bands containing symmetrically-arranged simple bands are common and suggest diffusion reactions between original bands. Monomineralic bands include epidote, garnet, hastingsite, chlorite, albite, magnetite and sulphides.

In all cases the magnetite (apart from a little from degradation of the amphiboles) and the sulphides have been introduced subsequent to the peak of metamorphism.

The mineralogy of some of the symmetric bands is shown

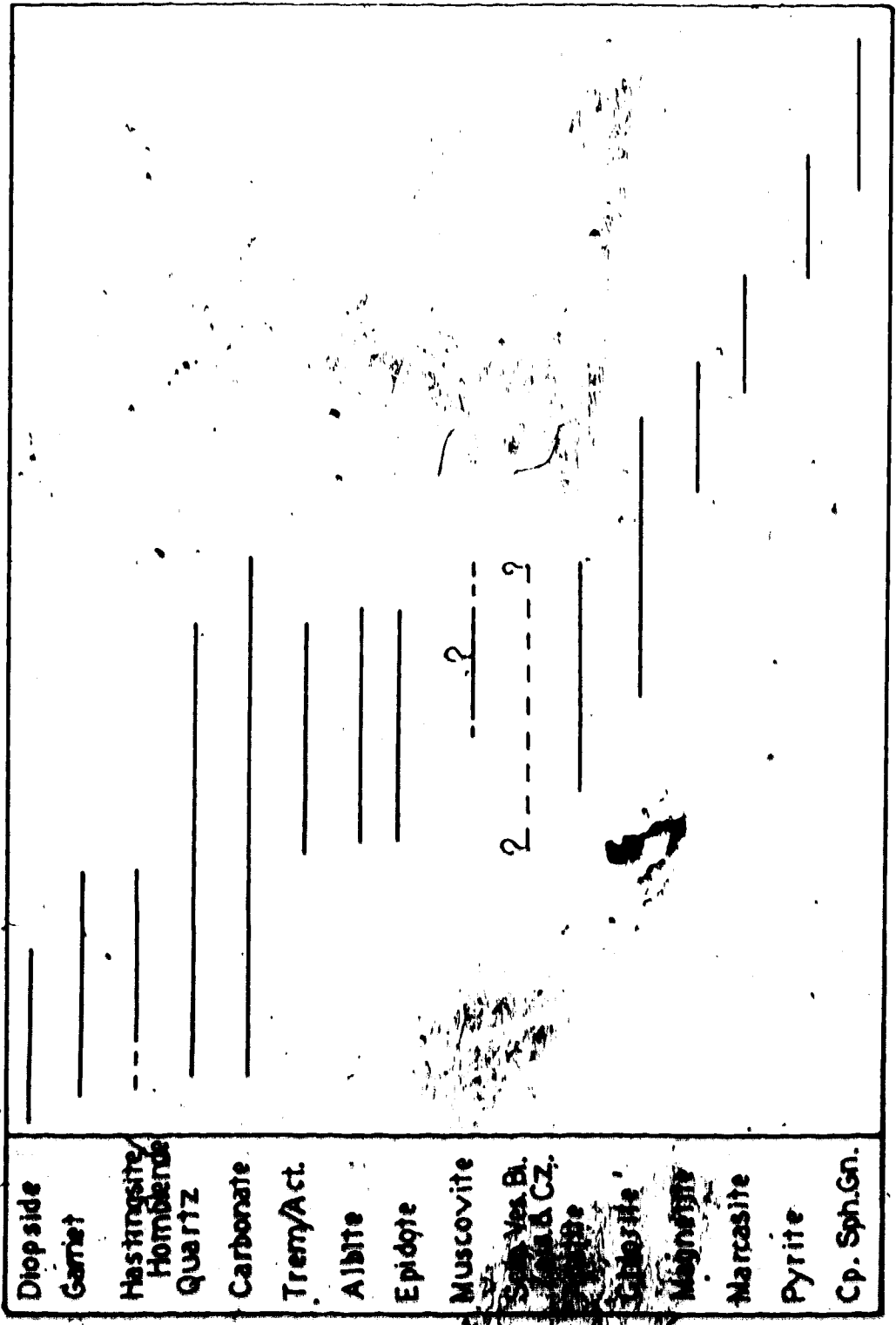


Figure 26. Paragenesis of the Meta-calcarellite at Terra.

schematically (Fig. 27). Individual bands are seldom thicker than a few hundred microns, but the symmetric groups of bands are often over 1 cm wide. The mineralogy and chemistry of all the bands that have been studied suggest three main band types:

1. Silicate; low Ca
2. Tuffaceous
3. Calcareous

From the evidence presented earlier concerning the pre-metamorphic nature of this rock, it is proposed that of these bands the 'tuffaceous' and calcareous are original and the 'siliceous' (which usually separate the former two) are the product of diffusion reactions between the two. In other words, this rock is predominantly a 'diffusion' skarn.

Sample SX 9.14 (Fig. 28) was investigated in some detail. The albite-epidote-quartz assemblage is presumed to represent the site of a tuff and the various central bands are thought to represent the diffusion reaction products between this and a (siliceous?) limestone band.

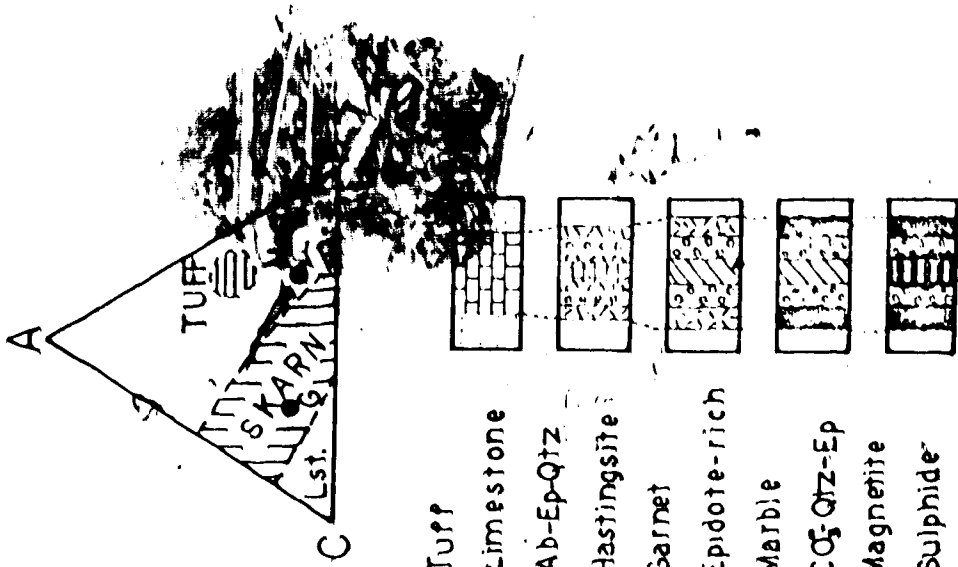
The hastingsite was analysed by C. R. Ramsay, using the electron microprobe at the University of Alberta (Table 3). It can be seen that the amphibole is a typical ferrohastingsite. The analysis is closely similar to that of a hastingsite from an amphibolite skarn in Russia (Leake, 1968: Analysis 916).

Optically the garnet is a green/yellow andradite/grossular with corroded cores and some corroded rings. Alteration is to an epidote, chlorite, quartz-carbonate assemblage (Plate 4.1). Under

A =  $Al_2O_3 - (Na_2O + K_2O)$

C = CaO

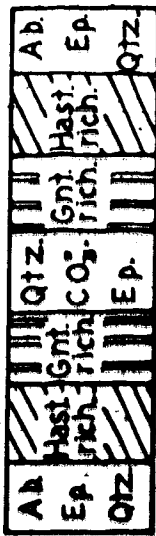
F =  $FeO + MgO + MnO$



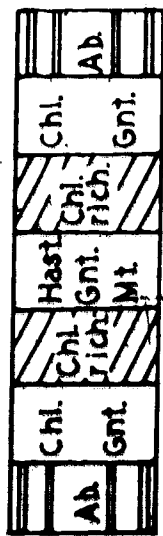
- Tuff
- limestone
- Ab-Ep-Qtz
- Hastingsite
- Garnet
- Epidote-rich
- Marble
- $CO_2$ -Qtz-Ep
- Magnetite
- Sulphide

Diffusion  
+ Fe?

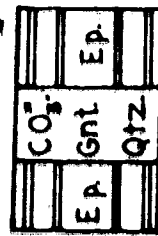
Infiltration



SX9.14



SU 8.4



TM18.5

Figure 27. Schematic Mineralogy of some metamorphic bands in the Meta-calcarellite: an ACF Diagram and proposed mechanisms for development of these bands.

Oxide	%	Structural Formula on the basis of 23 Oxygen Atoms.	
SiO <sub>2</sub>	40.12	Si	6.50
TiO <sub>2</sub>	0.598	Al <sup>4</sup>	1.50
Al <sub>2</sub> O <sub>3</sub>	9.819		8.00
FeO <sub>t</sub>	29.870	Al <sup>6</sup>	0.38
MnO	0.265	Ti	0.07
MgO	2.274	Fe	4.09
CaO	11.291	Mn	0.04
Na <sub>2</sub> O	0.722	Mg	0.55
K <sub>2</sub> O	3.213		5.09
Total	98.172	Ca	1.96
		Na	0.23
		K	0.66
			2.85

Table 3. Electron Microprobe Analysis of the Amphibole in sample SX9.15.



crossed nicols (Plate 4.2) the garnet can be seen to be strongly zoned and fairly strongly anisotropic - both common properties of skarn garnets, but rarely seen so clearly. One of these garnets was investigated by S.R. Winzer, using the electron microprobe, and from qualitative results and X-ray scanning photographs it was found that the zoning was caused simply by variations in the andradite:grossular ratio. Essentially, the core zones are grossular and the surrounding rings become successively enriched in Fe and depleted in Al until a thin outer rim is approximately 80% andradite, 20% grossular (a bulk composition is estimated to be about 50-50). There is virtually no titanium in the garnet.

Let us consider the reactions. Figure 28 shows comparisons of the analyses for the 'average andesite tuff' in the Camsell River area, the hastingsite, an average grossular/andradite garnet, and a slightly siliceous limestone. Each of these compositions is also shown on an ACF diagram (Fig. 27). Both these diagrams show quite clearly the feasibility of a limestone:tuff diffusion metasomatic reaction as a mechanism for the development of the banding. There is a problem, however, in the iron contents of both garnet and amphibole. The garnet is zoned essentially from aluminous at the centre, to iron-rich at the margins, indicating a progressive increase in the availability of iron over aluminium. In the model the availability of calcium is buffered by the presence of limestone and must be a constant. Consequently, it is proposed that towards the end of the main diffusion reactions, the first infiltrations of iron-rich solutions

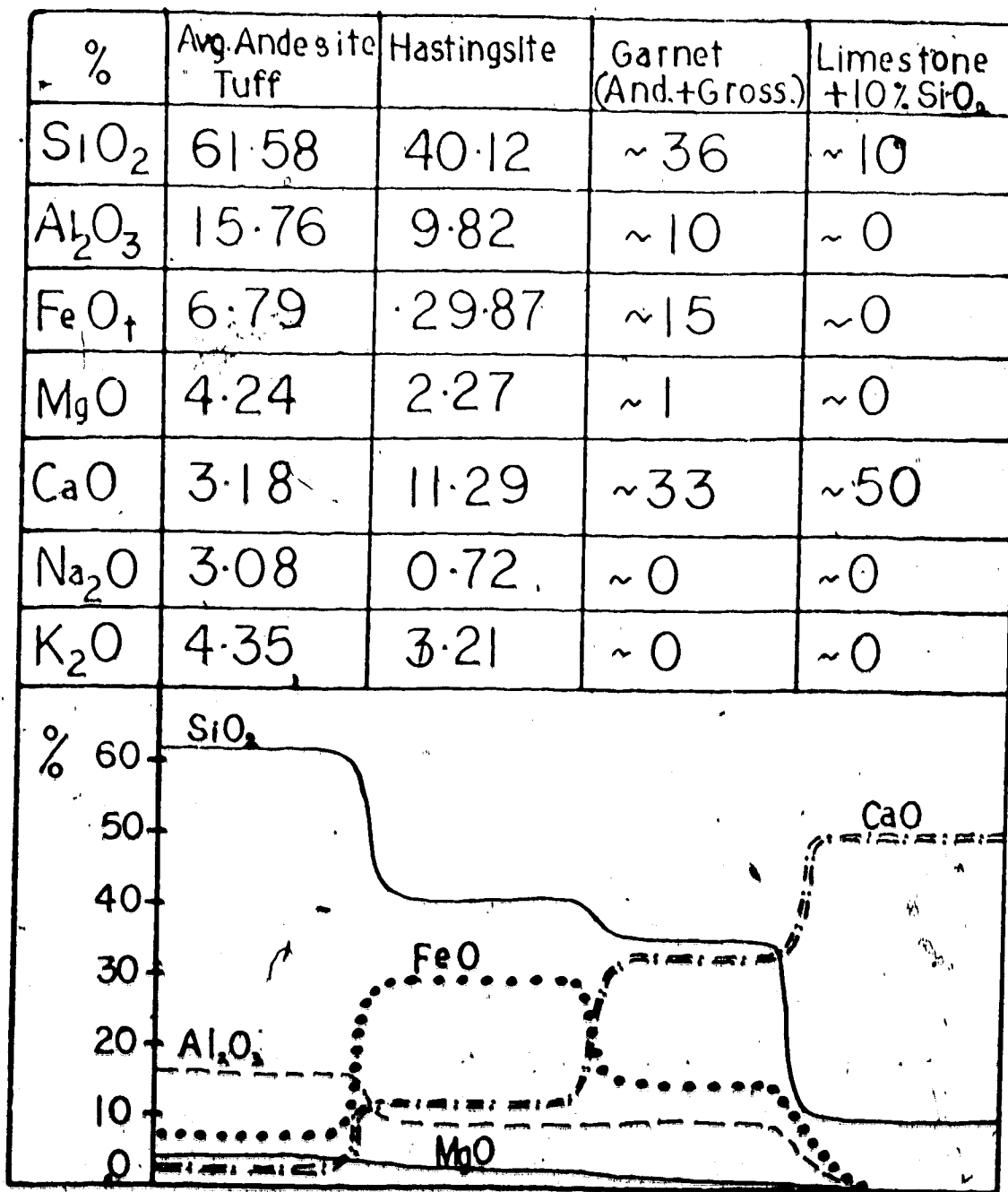


Figure 28. Analyses of Tuff, Siliceous Limestone, Hastingsite and Garnet, and a plot showing the variations of Major Element Oxides between these.

from the magma began to react with the earlier-formed minerals. Hastingsite, epidote and the rims of the garnets probably grew at this time. Continuing infiltration and cooling produced the retrograde effects in these bands.

At some late stage during the cooling of the magma, after all the silicate-forming diffusion and infiltration reactions were 'frozen', magnetite was introduced, preferentially replacing the chlorite and amphibole-rich bands. Small lenses and pods of banded magnetite, epidote, garnet, quartz, carbonate rock are common in the calcargillite horizon. Pegmatitic magnetite-apatite-amphibole bodies are also found in the aureoles of the intermediate plutons and may be related to this skarn phase (see Part II). Magnetite metacrysts in the banded rocks are often colour-zoned (Plate 14.1). Electron microprobe investigations showed that this zonation is not chemical.

Subsequent to the formation of magnetite, sulphides were introduced and preferentially replaced the carbonate-rich bands. Marcasite, followed by pyrite and then chalcopyrite with minor amounts of galena and sphalerite, form some economically interesting copper skarns; notably in the Terra Mine. The introduction of these sulphides seems to correspond with the late-stage hydrothermal effects of the cooling plutons: effects which also mineralised the margins of some of the plutons.

A schematic model for the development of the diffusion-infiltration skarn is shown in Figure 27. Skarn-generation models that involve only the reaction of magmatic silicate fluids and carbonate rock do

not apply in this situation for a number of reasons.

1. The original banding can be seen to be 'blanketed' by new mineral bands.

2. There is no sign of endoskarn (reaction of the displaced calcium from the limestone with the magma) in the nearby intrusions.

3. The zoning of garnets and the whole paragenesis indicates a progressive increase in the availability of iron.

4. The banding remains bed-parallel.

That the reaction between tuff and limestone can produce the observed mineral assemblage is demonstrated on the ACF diagram (Fig. 27).

Brock (1972) has shown that similar reactions have occurred to form skarns in banded limestone-pelite sequences close to an intrusive contact, and shows a remarkably similar evolution from diffusion to infiltration skarn with a progressive increase in the amount of iron in the formation of these bodies.

Vidale (1969) has demonstrated the viability of such reactions experimentally, and found that the critical control for the generation of monomineralic bands is the amount of pore-fluid: too little inhibited reaction and too much resulted in development of cavities. As a consequence, it is proposed that the infiltration skarns developed in the aureoles of the plutons where the pore-fluid was somehow concentrated to an amount required for reaction. However, similar results might be expected if the ratio of carbon-bearing species ( $\text{CO}_2$ ,  $\text{CH}_4$ , etc.) to pore-fluid varied. In other words,  $\text{CO}_2$  'sinks' could equally well have controlled skarn development. Where

the correct pore-fluid, etc. concentrations were not reached, the skarn reactions did not take place. Pore-fluid 'sinks' might be faults, breccias, beds capped by impermeable rock, etc. As yet mapping has not been detailed enough to show any obvious control for the location of skarns in this area.

It is of interest to note that remarkably similar calc-silicate skarns, which were progressively replaced first by magnetite and then by sulphides, are developed around the margins of the Fubilan stock in Papua (Bamford, 1972) - a stock which is the host of the Mount Fubilan porphyry copper deposit.

PART II

METALLOGENESIS

## 1 INTRODUCTION

The geological evolution of the Camsell River area has been documented in some detail. There are many types of potentially economic mineralisation in the area, including iron oxide-apatite bodies, sulphide skarns, potential porphyry copper bodies, and varied hydrothermal vein mineralisation.

In Part II each of these deposits is described and attempts are made to relate them to a unified concept of the total evolution of the area. As part of such studies analytical data have been obtained via optical, diffractometric and electron microprobe techniques. The details of the analytical procedures and corrections applied are given in Appendix II.

Oxygen and carbon isotopes were extracted from vein carbonates and were analysed at the University of Alberta. The corrected results are presented as  $\delta O^{18}$  and  $\delta C^{13}$  values where:

$$\delta C^{13} \text{ per mil} = \left( \frac{C^{13}/C^{12} \text{ sample}}{C^{13}/C^{12} \text{ standard}} - 1 \right) \times 10^3$$

$$\text{and } \delta O^{18} \text{ per mil} = \left( \frac{O^{18}/O^{16} \text{ sample}}{O^{18}/O^{16} \text{ standard}} - 1 \right) \times 10^3$$

$\delta C^{13}$  is reported against the PDB standard, and  $\delta O^{18}$  against the SMOW standard. Details of analytical procedures, corrections and errors are reported in Appendix III.

The sulphur from skarn and vein sulphides was originally extracted at the University of Alberta. A temporary lack of analytical facilities caused abandonment of the project until Dr. B.W. Robinson kindly analysed the samples at the D.S.I.R., Lower Hutt, New Zealand. The corrections, errors and analytical procedures are reported in Appendix IV. The results are presented in  $\delta S^{34}$  values where:

$$\delta S^{34} \text{ per mil} = \left( \frac{S^{34}/S^{32} \text{ sample}}{S^{34}/S^{32} \text{ standard}} - 1 \right) \times 10^3$$

and are quoted relative to the troilite phase of the Canon Diablo meteorite, which, by definition, has a  $\delta S^{34}$  value of 0 per mil.

Analyses for trace elements in the host-rocks are reported here, but details of analytical techniques are given in Appendix I.



## 2. MAGNETITE-APATITE-ACTINOLITE INTRUSIONS AND RELATED BODIES

Many authors who have worked in the Great Bear Batholith have recognised the metasomatic nature of the alteration around the early, intermediate plutons (see in particular, Furnival, 1939b). The elements involved include Fe (Al?) Si, P, B, F, (Cl?), Ti, S and base metals, and the metasomatism is manifested in the formation of tourmaline, scapolite, magnetite, apatite, actinolite and sulphides. These minerals are recognised replacing country rocks (Kidd, 1932) - often selectively along certain beds (Robinson, 1933) - as lenses (Kidd, 1936), as veins (Furnival, 1939a, b; Robinson, 1971) and as plugs (Badham, 1972). The metasomatic minerals were developed after the thermal peak of contact metamorphism, during the waning stages of cooling of the pluton, and a continuum of minerals and events documents this cooling.

Although small specks of tourmaline were noted in a number of contact aureoles, the best evidence of boron metasomatism comes from a vein at Balachey Lake. Here a 10 m wide NE-striking dyke consists of black tourmaline that has been brecciated by hydrothermal quartz-carbonate veining, with which considerable pyrite was introduced (Plate 3.6). The vein is emplaced in a fault whose dextral movement post-dates the tourmaline and is probably coeval with the quartz-carbonate veining. The composition of the tourmaline is not known, but is presumed to be schorlitic from its optical characteristics.

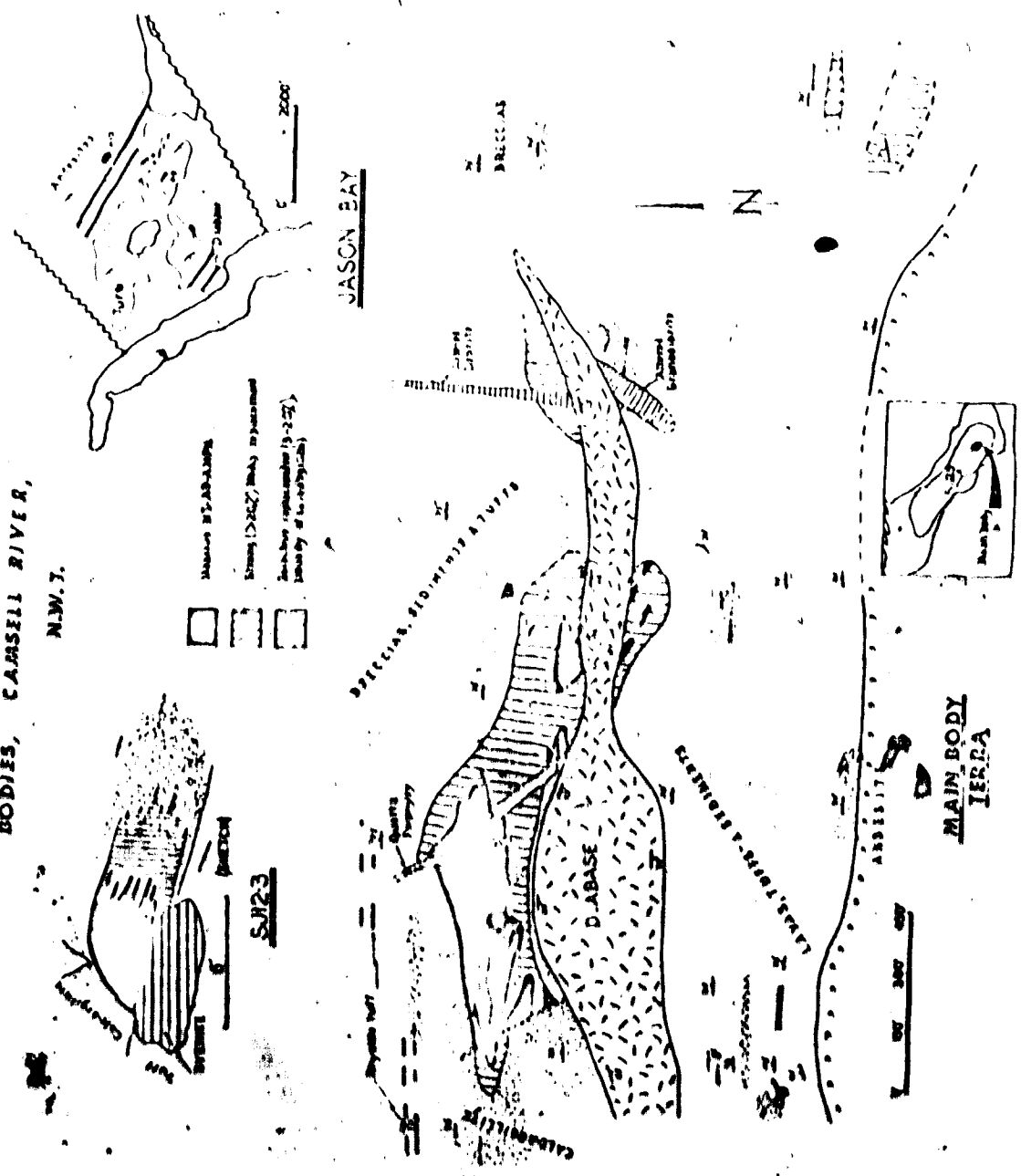
Scapolite is not common, but is ubiquitous in the contact aureoles.

Its composition is unknown, but may generally be taken to contain F and Cl (Shaw, 1960) and hence its presence may be taken to indicate metasomatic migration of these elements.

There is a plug and replacement zone of magnetite-apatite-actinolite close to the Terra Mine (Fig. 7). In the field both intrusive and replacive relations are clearly visible. It can be seen (Fig. 29) that the plug consists of a lensoid core which intrudes volcanic rocks at its western end, but which fades out into a long, replacive 'tail' to the east. Much of the plug consists of fine-grained intergrowths of magnetite (60-70%) and apatite. The contacts are sharp and slightly chilled and there are numerous angular xenoliths (Plate 12.5). Metamorphism at the contacts cannot be distinguished from the hornblende-hornfels facies aureole within which this plug outcrops. The plug is cut by veinlets of coarser, fractured magnetite and apatite (Plate 12.6), and by thin pegmatitic seams of magnetite, apatite and actinolite, which post-date the fractured veinlets (Plates 13.2 and 13.4). In places the plug is flow-banded, forming apparent sequential 'beds' of magnetite and apatite (Plate 13.1). The plug is cross-cut by a quartz-porphyrx dyke (Plate 3.3), by small faults (Fig. 29), and by small quartz-carbonate veins containing haematite. All these features are cut by a diabase dyke which is considerably younger. The age relations of the magnetite and altered dykes (Fig. 29) are equivocal.

The plug intrudes the calcargillite horizon, but this is split up and thin here, and by the western end of the plug's core, most of

Figure 29 MAGNETITE-APATITE-AMPHIBOLE BODIES, CARSELL RIVER, N.W.7.



Magnetite-apatite-amphibole  
 Bodies (see map) (see map)  
 Boundary of the study area

5000

MAIN BODY TERRA

the host-rocks are volcanic breccias and tuffs. The rocks are contorted into small, open folds by the intrusion.

Towards its replacive extremity, the magnetite is arbitrarily divided into zones of strong and weak replacement (Fig-29). The magnetite-apatite preferentially replaced first calcargillite fragments in a breccia, and then the breccia matrix. This matrix replacement may be so strong as to make unreplaced breccia fragments appear to be xenoliths. In zones of weak replacement there are magnetite-apatite veins cutting the rocks, with patches of nebulous replacement emanating from them. Even where the breccia matrix is scarcely replaced at all, if there is a calcargillite fragment in the breccia it will be at least partially replaced. At first it was thought that these fragments indicated early brecciation of the magnetite body, but careful studies always revealed minute veinlets connecting the replaced calcargillite fragment to a magnetite vein. Where pegmatitic magnetite-apatite-actinolite veins cut the replacement zones they are always younger than the main replacement phase. Where magnetite veining is quite intense, surrounded blocks of country rock appear to have 'floated' and have been slightly rotated; their edges are slightly deformed.

Thin and polished section studies confirm the existence of two generations of magnetite (Plates 13.2, 13.3, 13.5 and 13.6). Large phenocrysts of apatite and magnetite are badly fractured and contained in a matrix of fine-grained, intergrown magnetite and apatite. The phenocrysts make up some 60% of the rock and it is concluded that the rock was intruded to its present level as a crystal mush. The

remaining liquid crystallised as a matrix, and occasional pulses of this formed the pegmatitic lenses and veins.

Minerals identified in the intrusion include magnetite, apatite, actinolite, quartz, carbonates, haematite, goethite, chalcopyrite and chlorite. The haematite, chlorite and goethite are alteration products produced during or after post-crystallisation carbonate-quartz veining. These younger veins also contain sparse chalcopyrite. A paragenesis is shown in Figure 30.

Studies by undergraduate students of Dr. R.D. Morton have indicated that the magnetite has a very low content of Ti and V, and has an 'a'-cell parameter of 8.389Å compared with 8.396Å for a 'pure' magnetite. XRF and wet chemical work indicate an average V content of 0.12% ± 0.03% and an average Ti content of 0.55% ± 0.03%. The apatite has been shown, from X-ray diffraction studies, to be fluorine-rich with an average fluorine-to-chlorine ratio of 0.867 to 0.133 (R.D. Morton, Pers. Comm., 1972).

The magnetite and apatite were investigated qualitatively using the electron microprobe. It was found that the phenocryst and matrix minerals were chemically identical. The magnetites, as indicated by the preliminary studies, contain very low amounts of Ti, V and Mn, with no other elements detected. The apatites contain considerable amounts of F, little Cl, trace amounts of Y and Ce and even smaller traces of Rb, Ba, Th and Zr. Such results are analagous to those of Parák (1973), who noted that Y, Ce and La are common in apatites from the Kiruna deposits, and found that they are often concentrated in

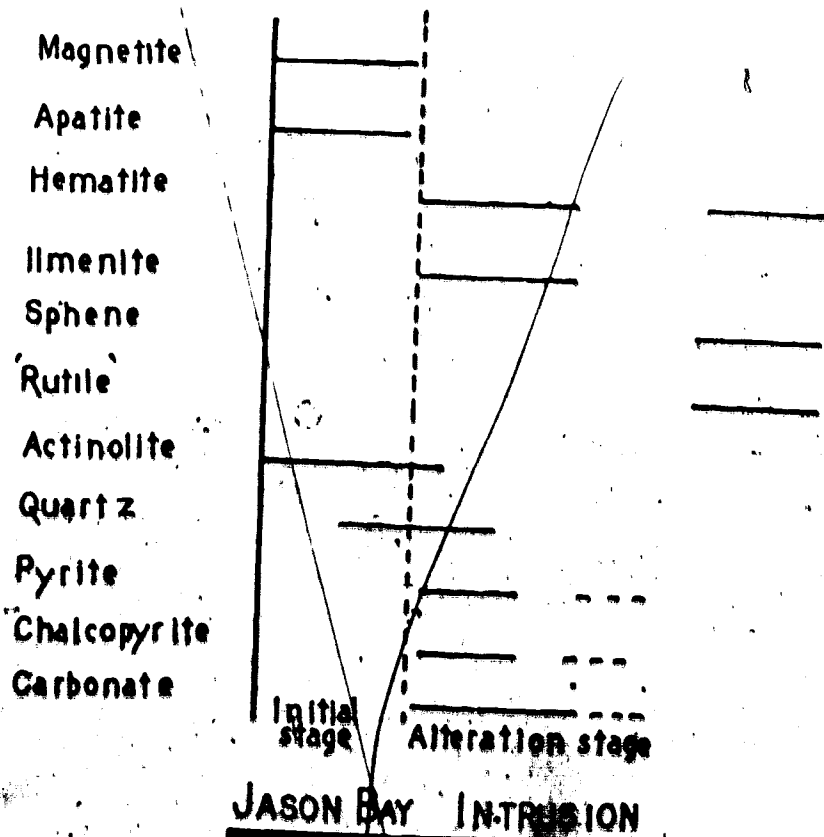
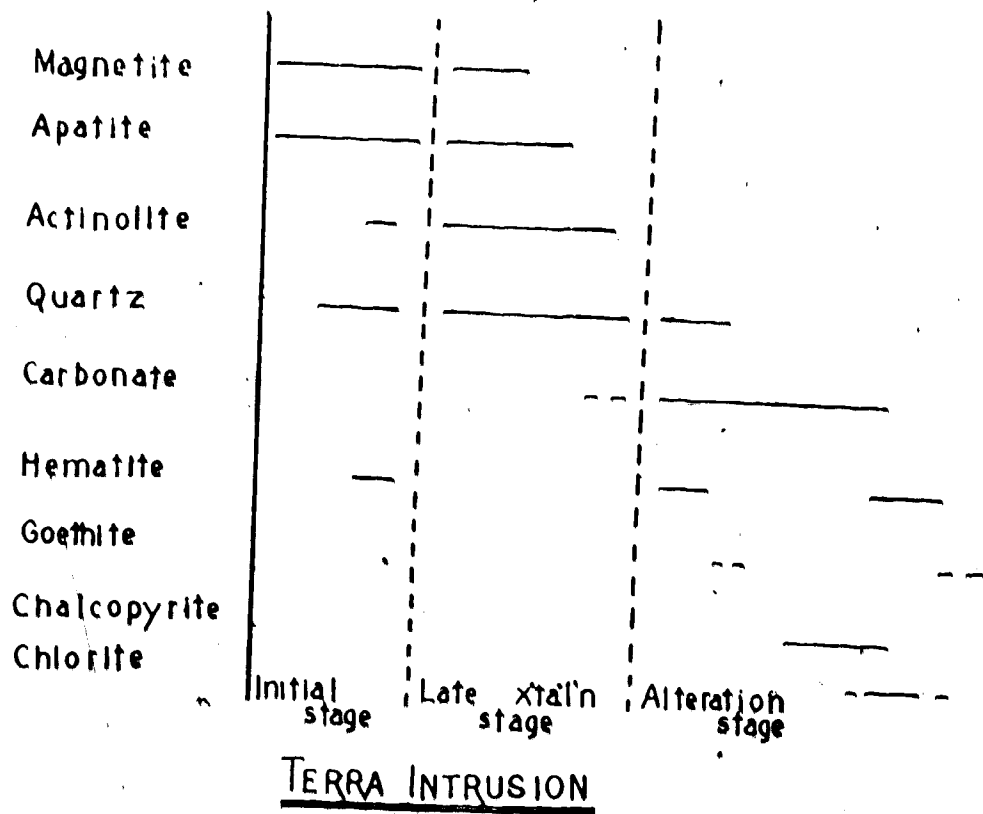


Figure 30. Paragenesis of the Magnetite Intrusions.

minute monazite inclusions. The actinolite was identified optically, and this was confirmed by XRD work.

The Ti and V contents of the magnetite indicate low temperatures of crystallisation (Buddington and Lindsley, 1964; Lister, 1966), but absolute estimates of this temperature are impossible to make.

The intrusion of the magnetite plug has had little effect on the country rocks and it must be concluded that these were at similar temperatures to the intrusion. In Part I it was estimated that the country rocks at this distance from the monzonite could have reached a maximum of 550° during metamorphism. It is assumed that the magnetite was intruded during or a little after this thermal peak and therefore must have been at a temperature of less than 600°C.

Evidence has been cited to show that the intrusion was 60% crystalline during emplacement. It is presumed, therefore, that the remaining liquid was rich in volatiles, allowing it to remain liquid at less than 600°C. The extent of replacement around the intrusive core is evidence of the high content of volatiles. The quartz-porphry dyke, intruded soon after the emplacement of the magnetite, is strongly chilled at the margins, indicating that the plug had cooled quickly before the waning effects of the crystallising monzonite were manifested.

Consequently there existed, very close in time and space, two radically different magmas - the magnetite-apatite-actinolite and the monzonite. It is of importance to remember the following points:

1. The Mt:Ap ratio is about 2:1 in the main plug.

2. The monzonite was the source for many of the elements in the skarn.
3. The monzonite is strongly altered near its margins, which are rich in apatite.
4. The Ap-Act pegmatite dykes are associated with the magnetite intrusion.
5. The monzonite is alkali-rich (Table 2: SX 2.1).

Phillpotts (1967) proposed that a 2:1 magnetite:apatite mixture forms a eutectic in the system magnetite-fluorapatite, and indicated that such a eutectic is immiscible with alkaline, intermediate igneous melts. He concluded that the magnetite-apatite fraction formed an immiscible liquid which separated from a differentiating parent magma, leaving an alkaline intermediate melt. Such an hypothesis explains the observed time relations at Terra, and it is proposed that such a mechanism operated. Indeed, Phillpotts notes that "mixtures of magnetite, diorite and apatite containing apatite in excess of 30% form three immiscible liquids on melting: an apatite-rich one, a magnetite-apatite melt and a silicate melt". Here then, is a possible source for the apatite in the margin of the Terra monzonite.

The magnetite-apatite-actinolite lenses at Jason Bay (Fig. 29) are a little different. There are essentially three lenses, but each is surrounded by a zone of haematitisation. Small lenses of pyrite are very common. The lenses are all parallel to the bedding and there are numerous amphibole veinlets near them, also conformable to bedding.



Lens 4.8 is 60 m by 4 m in size. Actinolite crystals up to 15 cm long grow perpendicularly in from a very sharp contact (Plate 12.4). The central zone is made up of pegmatitic magnetite, apatite and actinolite with interstitial patches of younger quartz, carbonate and pyrite. The magnetite is almost completely altered to haematite. The country rocks are in the upper albite-epidote facies, but the lens has had no noticeable effect on them. Lens 4.9 is similar but smaller (10 m x 1 m), and is surrounded by other much smaller lenses. The amphibole veinlets are all pegmatitic and have crystals grown at right angles to the walls.

Lens 4.12 is more complicated as it has been cut by a diabase dyke. There are a number of pods, veins and lenses of pegmatitic actinolite containing apatite and magnetite, and quartz, carbonate and sulphides. The affected zone is 200 m by 20 m in size. Adjacent to the diabase the pegmatitic material has been recrystallised making it appear, perhaps, as if the diabase were the parent.

Thin and polished section and electron microprobe studies of the Jason Bay lenses reveal a similar paragenesis to that at Terra, but the proportion of actinolite is much greater and the alteration much more intense. Again, the alteration is considered to be related to the quartz-carbonate-sulphide event (Fig. 30).

The magnetite is extremely altered everywhere. Usually it has formed haematite, but the large number of exsolved lamellae of ilmenite testify to an initially high Ti content (Plates 13.7, 13.8 and 14.4). In places this ilmenite:haematite:magnetite mixture has been further

altered by reaction with silica and lime to form highly complex intergrowths of rutile and sphene (Plates 14.2 and 14.3), and this appears to have been coeval with the introduction of pyrite and chalcopyrite.

The  $\delta S^{34}$  value for the sulphur in this chalcopyrite is 4.2 $\pm$ 0.1‰ (NK 4.12: Appendix IV) and may be compared with values of 2.1‰ and 2.2‰ for pyrite from similar amphibole:magnetite veins at Echo Bay (Robinson, 1971). The value is not distinguishable from those of the sulphur in the skarns and disseminations.

Other similar bodies not studied in detail include:

1. Bi-Mt-Act-Pyt 'skarn', half a kilometre to the east of the Silver Bay Mine.
2. Mt-Ap-Act veins on the south shore of the Camsell River, due north of the Norex Mine.
3. Mt-Act-Pyt-Cp disseminations in tuffs on the mainland, east of Trish Island.
4. Mt-Ap-Act veins and breccia cement (or matrix replacement), half a kilometre north of Seahorse Lake.

It is concluded that there is a continuum in these events from a purely magmatic (Terra) to infiltrative 'sweat' concentrations. The Jason Bay lenses may represent the top of an intrusion similar to that at Terra. Indeed, in the 'U' between the two lobes of plutons, and extending as far north as Pole Bay, there is a strong magnetic anomaly that is consistently greater than 3000  $\gamma$  and often greater than 5000  $\gamma$ , compared with an average background of 2800-3000  $\gamma$  over much of the

area (unpublished information from D.I.A.N.D., Yellowknife).

It is also concluded that these bodies are derived from the parent magma of the early plutons, and that the continuum above represents the range in derivative process, from immiscibility with, to infiltration from the magma. Kidd and Haycock (1935) and Furnival (1939a, b) have reached similar conclusions for similar bodies in other areas. Robinson (1971) also reached similar conclusions from the field relations for magnetite-actinolite veins near Echo Bay, but obtained K-Ar ages of 1435, 1370 and 1415 m.y. (all  $\pm 60$  m.y.) for the amphiboles in these. Consequently, he concluded that the veins were related to, and derived from the diabase sill at Echo Bay. Since the diabases caused updating (U-Pb) of the mineralised veins, it is presumed that the effects on the K-Ar system in the magnetite-actinolite veins may have been similar.

These magnetite bodies occur only in the western complexes and have not been observed anywhere to the east (Hoffman, Pers. Comm., 1973). Park (1972), in an excellent review, noted that magnetite-haematite bodies of various types were "distributed throughout the highly-deformed rocks bordering the Pacific Ocean basin". Included in these bodies are pyrometamorphic deposits and apatite-amphibole-magnetite intrusions, and descriptions of these are indistinguishable from those of the Camsell River bodies. Park emphasises the association of these bodies with intermediate, calcalkaline magmatic activity in continent-margin orogenic belts, and concludes that it is typical of this environment, and possibly even diagnostic. This data is thus considered further

strong evidence in support of the geotectonic evolution of the Great Bear Batholith, proposed in Part I.

### 3. SULPHIDE MINERALISATION

High-level, intermediate, porphyritic stocks in orogenic regions very commonly contain 'porphyry Cu-Mo' mineralisation. The model presented by Stanton (1972) for the development of porphyry mineralisation, presumes that the ore-minerals concentrate in the upper portions of an intrusive and in the adjacent host-rocks. When the ore-fluid is restricted to the intrusion, it forms deposits in hydrothermally altered and fractured, chilled rock. If the post-chilling fracturing is intense enough, the ore-bearing fluids may migrate completely into the adjacent host-rocks and replace suitable horizons. Such a model is used to explain the almost-ubiquitous presence of skarns around mineralised porphyry bodies (e.g. Bamford, 1972). The mineralisation in these systems consists of pyrite and chalcopyrite, with lesser amounts of bornite, sphalerite, galena and molybdenite. Mineralised country rocks may also contain magnetite, pyrrhotite and marcasite.

The early plutons of the Camseil River area fulfil all the requirements for porphyry-type mineralisation, i.e.:

1. They range in composition from diorite to granodiorite.
2. They were extremely hydrous, and were emplaced at shallow depths.
3. Porphyritic phases are common.
4. Late-stage fracturing and hydrothermal alteration were common.

5. Many contain veinlets rich in Fe and Cu sulphides.
6. They are closely associated with calcalkaline orogenic volcanic rocks.
7. They are not deeply eroded.

Similar features have been described from other parts of the Great Bear Batholith (see especially: Furnival, 1935, concerning alteration of, and quartz and sulphide veining in intrusive margins).

The best candidate for a 'porphyry-copper' body in the Camsell River area is a small, highly-complex porphyritic adamellite-granodiorite dyke, close to the Norex silver property. It contains pyrite and chalcopyrite, both as lenses at its contacts and in veinlets, and disseminated sphalerite and galena have been noted (Plate 11.1). The dimensions of the body are too small for economic interest. Other intrusions in the area contain sulphide-rich veinlets, or have chilled border-phases rich in sulphides. One of these, a mile to the southeast of the Terra Mine, has been drilled and was found to consist of pyrrhotite, pyrite and chalcopyrite in badly-sheared and hydrothermally-altered granodiorite. To date no even-remotely-economic porphyry-copper body has been found in the Great Bear Batholith, although prospecting interest is picking up and rumours of veinlets of molybdenite and chalcopyrite in porphyries have been heard. In the author's opinion, it is inevitable that a 'type' porphyry Cu-Mo body will be found in the area. Whether such a body would be mined cannot be foretold, but the dictates of economics at present make it unlikely.

Far more common than porphyry-mineralisation are the sulphide

skarns and impregnations, and all those investigated can be related directly to the waning stages of contact metamorphism around the smaller intermediate stocks. These have been described from the Echo Bay area (Kidd and Haycock, 1935; Robinson, 1971), and Kidd and Haycock intimate that:

1. The smaller intrusions are now exposed at a level very close to their original tops.
2. Fracturing was initiated during the post-metamorphic (sensu stricto) hydrothermal alteration.

Minerals of metasomatic origin have been recognised in many of these sulphide lodes, and include actinolite, scapolite, biotite, iron oxides, apatite and sphene, as well as the sulphides. In the Gamsell River area, sulphide lenses and impregnations outcrop to the west of Trish Island, on Nic Island, north of Slapdaw Lake, on the Terra peninsula, near Seahorse Lake, Black Bear Lake, at Noxex and Silver Bay, along the west side of Jason Bay and on the peninsula between Heath and Balachey Lakes. Where they occur in volcanic rocks, oxides, biotite and actinolite are predominant accessories. Scapolite and calcsilicates are more common in sedimentary rocks. All occur within at least the albite-epidote facies of the contact aureoles.

The sulphide skarn at Terra has been worked on in most detail. It is the host to much of the younger vein mineralisation, although this relationship is thought to be for structural and chemical, and not genetic reasons. The skarn sulphides are almost totally restricted to the metacalcargillite horizon, and small lenses of pyrite and

chalcopyrite occur in many places along the outcrop of this bed (Fig. 6). It is only in the Terra Mine, however, that the sulphides occur in economically interesting amounts.

The simplified geology of the mine is shown in Figure 31, and it can be seen that the sulphide-rich horizons occur mainly as two lenses replacing parts of metacalcargillite beds. The lenses are bed-parallel and consist of a core of chalcopyrite and, commonly, a rim of pyrite. The sulphides selectively replace certain horizons and the resulting ore-bands are bed-parallel. Bands vary from a few millimetres to a few centimetres thick. Where the sulphide zones are transected by younger quartz-carbonate veins, the sulphides are remobilised into massive bands lining the veins.

In polished section, the sulphides can be seen to replace the quartz-carbonate-rich beds of the metacalcargillite preferentially (Plate 5.3), although amphibole-bearing beds are often partially replaced. The mineralogy is simple and consists of marcasite, pyrite, chalcopyrite, sphalerite and galena. The paragenesis (Fig. 32) shows that the sulphides developed after the metasomatic silicates and oxides in the order: marcasite-pyrite-chalcopyrite and sphalerite-galena but there is some overlap. Marcasite first formed as large euhedral crystals, very commonly containing remnant lamellae of carbonate or amphibole, forming a 'fingerprint' texture (Plates 5.1 and 5.3). The crystals are best developed in carbonate beds, and finger out into amphibole-rich beds.

Pyrite, presumably formed from the marcasite, replaces the



AMPHIBOLE

GARNET

QUARTZ

CALCITE

DOLOMITE

MAGNETITE

HAEMATITE

CHLORITE

PYRROPHOSPHATE

MARCASITE

PYRITE

CHALCOPYRITE

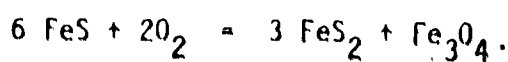
SPHALERITE

GALENA

Figure 32. Paragenesis of the Sulphide Skarn at Terra.

latter, and cross-cuts the fingerprints (Plates 5.1 and 5.3). Subsequent to this, chalcopyrite and sphalerite were introduced. The chalcopyrite replaced the earlier Fe-sulphides and often overlapped the original bands, replacing neighbouring silicate bands as well (Plate 5.2). The sphalerite, which is only a minor constituent, often replaced the 'fingerprints' in the marcasite, forming a marcasite-sphalerite net (Plate 5.1). Sphalerite also replaced silicate minerals on the margins between chalcopyrite and silicate bands (Plate 5.2). Exsolution blebs of chalcopyrite are common in the sphalerite. Galena is found only as very small specks on the margins of the silicate bands.

Randohr (1969) describes this 'fingerprint' texture in detail and notes many cases (p. 597) where it occurs from the degradation of pyrrhotite to marcasite, pyrite and magnetite, thus:



No remnant pyrrhotite has been seen in Terra samples, but it is certainly common enough in the other skarn sulphide bodies. It is concluded that pyrrhotite was probably the first sulphide to form in the skarn.

It was proposed earlier that the sulphides originated by infiltration from the cooling monzonite, and that the first element to be expelled from the intrusion in significant amounts was iron, forming the Fe-rich silicates and, later, the oxides. As the Fe/S

ratio decreased, so pyrrhotite, followed by more S-rich sulphides would be expected to form. By the time the intrusion had cooled sufficiently to leave only hydrothermal solutions as the terminal fraction, copper and sulphur were the main constituents of these solutions, and the supply of iron was nearly exhausted.

An interesting sequence of remobilisation can be seen in the copper zones around the younger silver veins. The first noticeable effect is the recrystallisation of marcasite to form metablasts and cross-cutting veinlets, and this may occur up to some 5 m from the vein. At about  $\frac{1}{2}$  m, marcasite, pyrite and chalcopyrite veinlets form, cross-cutting the original bands and filling in the silicate-rich interstices. The chalcopyrite blebs in the sphalerite grow and join to form large crystals in the corroded host. By about 20 cm, the sulphide zone has become massive and all the sulphides are recrystallised. Veinlets of one, or up to all five sulphides are common, but in the polymineralic examples each individual sulphide is in a single band (Plate 5.5). Impregnations of quartz and carbonate from the vein are intergrown with the sulphide veinlets. The sulphides are, nevertheless, sharply cross-cut by the veins, whose margins are always sheared.

The sulphur isotope values for the skarn at Terra, and for other sulphide impregnations in the area, are remarkably consistent (Table 4) and range between values of  $\delta S^{34}$  of 0.9‰ to 5.1‰, with the grouping at Terra even tighter. These values compare closely with host-rock sulphide values for the Echo Bay area (Table 4), and it is

Table 4. Sulphur Isotope values for the Terra skarn Sulphides and comparisons with those of Sulphide Impregnations from other parts of the Camsell River Area, and from the Echo Bay Area.

Sample	Location	Mineral	$\delta S^{34}\text{‰}$ (CDT).
TJ3.3A	Terra	Primary skarn; Marcasite.	4.0±0.2
TJ5.1D	Terra	Primary skarn; Marcasite.	3.7±0.1
		Recrystallised marcasite 1m from vein	2.8±0.1
		" chalcopyrite " "	3.4±0.1
		Chalcopyrite on edge of vein	3.9±0.1
TJ10.2B	Terra	Recrystallised chalcopyrite	3.1±0.2
		" marcasite	3.4±0.2
TX3.1	Terra	Primary skarn; Chalcopyrite.	3.7±0.1
		" " Marcasite.	0.9±0.1
TX7.2	Terra	Chalcopyrite on vein margin.	3.2±0.1
A1.1	Terra	Chalcopyrite on vein margin.	1.0±0.1
		Marcasite " " "	2.7±0.1
A1.5	Terra	Chalcopyrite 1m from vein	3.2±0.1
TM24.2	Terra	Pyrite in banded tuffs.	5.1±0.1
TJ11.2D	Terra	Chalcopyrite in silicified tuff	4.0±0.1
TX24.7	Terra	Pyrite in banded tuffs.	3.5±0.1
NK18.17B	Balachev L	Pyrite in andesite.	4.2±0.2
NK4.12	Jason Bay	Chalcopyrite in Mt-Ap-Act pegmatite	4.2±0.1
S1	Echo Bay	Pyrite in tuff	4.8
S2	Echo Bay	Pyrite in andesite	3.0
S3	Echo Bay	Pyrite in tuff	2.4
S4	Echo Bay	Pyrite in tuff	4.2
S7	Echo Bay	Pyrite in breccia	4.2
S8	Echo Bay	Pyrite in agglomerate	6.2
S9	Echo Bay	Pyrite in tuff	5.1
S11	Echo Bay	Pyrite in Mt-Amphibole veins	2.1
S12	Echo Bay	Pyrite in Mt-Amphibole veins	2.2
S56	Terra	Primary skarn; Galena	5.2
S57	Terra	Primary skarn; Chalcopyrite	5.8
S60	Terra	Primary skarn; Pyrite	5.1
S61	Terra	Primary skarn; Chalcopyrite	5.2

All 'S' samples are from Robinson (1971).

suggested that this is primary magmatic sulphur. Ideally, magmatic sulphurs should have values close to zero per mil, but Thode and Gross (1968) quote values of  $\delta S^{34}$  around +4‰ for ores associated with orogenic plutons, and Schneider (1970) proposes a model whereby increasingly positive sulphur isotope values might be expected with increasing oxidation potential (and  $PH_2O$ ) and increasing alkalinity of the magma. Thus, as the Camell River plutons were wet, sub-alkaline and orogenic, it is concluded that the above isotope values indicate a primary magmatic origin for the sulphur. Such an origin is compatible with the suggestion that the components of the skarns were derived from the plutons. ○

It is of interest to note that the sulphur isotope values remain unchanged even where the sulphides have been remobilised by younger veins. The isotopic values show that neither the primary nor the recrystallised sulphides are in equilibrium with each other. Consequently, attempts to estimate temperatures of crystallisation from mineral pairs are futile.

Further attempts to note differences between the primary and recrystallised sulphides were made with the electron microprobe. It might be expected that, during recrystallisation, sulphides could be 'flushed' clean of trace elements and would become more 'ideally stoichiometric'.

Primary and remobilised chalcopyrite, pyrite and marcasite were analysed for Zn, Co, Ni, As, Ag and Se, and sphalerite was analysed for Fe and Cu in addition. Zinc was found in measurable quantities

in the chalcopyrites (Table 5) but no differences between the two types were seen. The Fe-content of the sphalerites is high (Table 6) but again does not vary. The Cu-content of sphalerites was found to be patchy and to vary sympathetically with iron and antipathetically with zinc. Since the sphalerites contain visible exsolution blebs of chalcopyrite, it is concluded that these small Cu-Fe-rich patches are sub-microscopic exsolution blebs, also of chalcopyrite. According to Park and McDiarmid (1970), such exsolution indicates temperatures of formation in excess of 350°C. The total free Fe-content of the sphalerites was calculated after removing enough iron to balance the 1.70 mole % of copper. It was found to be 6.64% of FeS and this appears to be uniformly distributed in the sphalerite. Application of the sphalerite geothermometer (Barton and Skinner, 1967) is impracticable because of the lack of data on the absolute sulphur fugacity during the formation of the sphalerite.

None of the other trace elements mentioned was detected in any of the sulphides. In conclusion, there appears to be no chemical change accompanying the recrystallisation of the primary sulphides.

Estimates made by the author in 1970 predicted a total tonnage of 64,000 short tons of mineralisation at 2% Cu to the base of the second level. Mining has now continued to a third level, but it is not known if the copper zones have been found at that depth. The controls of the mineralisation are not certain, other than that the calcargillite acts as a host. Presumably pore-fluid concentrations at the time of the first skarn formation are important, as was discussed in Part I:8.

Table 5 ZINC CONTENTS OF PRIMARY AND RECRYSTALLISED SULPHIDES

Sample	Mineral	No. Analyses	Pk-Bg Counts/Sec.
TM24.2	Primary Marcasite	5	0
	" Chalcopyrite	5	61.0
TM20.9	" Marcasite	5	0
	" Pyrite	5	3.1
	" Chalcopyrite	5	67.6
TM24.1	" Pyrite	5	0
	" Chalcopyrite	5	56.7
TM10.1B	Recrystallised Chalcopyrite	5	69.5
TUX02.1	"	5	35.0

The concentrations are so low that corrections for Atomic Number, Fluorescence and Absorption were not made.

Apparent Zn concentration Primary Chalcopyrite = 0.134 wt.%.  
 Apparent Zn concentration in recrystallised Chalcopyrite = 0.113 wt.%.

Table 6 ANALYSES OF SPHALERITES

Samples TM20.9, TU15.1, TU24.2

The values are closely similar and are fully corrected using Probedata (Smith and Tomlinson, 1970).

Totals are corrected to 100%.

Cu = 2.26 wt.%. Zn = 58.30 wt.%. Fe = 5.52 wt.%. S = 33.92 wt.%.

#### 4. A MODEL OF THE COOLING PLUTONS

The porphyry dykes, magnetite-apatite bodies, tourmaline veins, and oxide and sulphide skarns are thus seen as part of a continuum in response to the intrusion of the plutons (Fig. 33). The plutons were sub-alkaline and wet, and were emplaced at high levels in the crust during orogeny. As such they may have been the sources of immiscible fractions, which separated at depth and formed individual intrusions - such as the magnetite-apatite-amphibolite bodies. During their final emplacement, the plutons began to de-gas. Misfit elements, such as P, B, Cl and F, were then fixed in apatite, tourmaline and scapolite, both in the intrusive margins and in the recrystallising country rocks. Excess iron was expelled from the intrusions. This was taken up first by the silicates, forming Fe-rich rims and phases, but, as temperatures declined, the silicate reactions were arrested and Fe-oxides were formed. These were precipitated either as replacements of suitable hosts, or in magnetite-apatite-actionite pegmatites. As the cooling continued, the sulphur and base-metal concentration rose in the remnant fluids. At first sulphur combined with the remnant iron, forming first pyrrhotite and, as [Fe] decreased, pyrite. Finally the Fe-sulphides were replaced by chalcopyrite, sphalerite and galena. These processes were taking place around the early plutons and, while the time involved can only be guessed at, it is probable that the sulphides were emplaced prior to, or during the period of intrusion of the late granite batholiths.



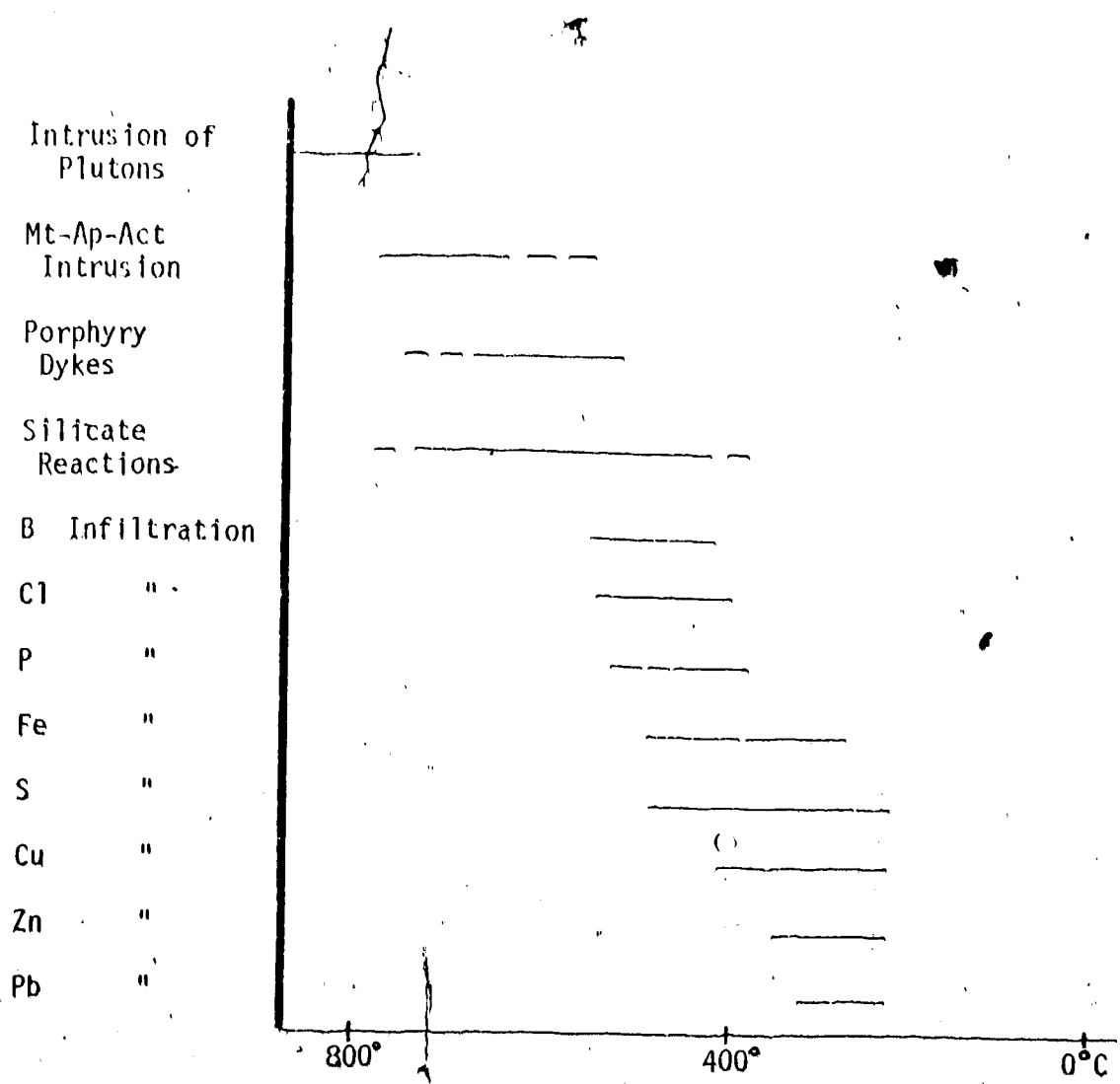


Figure 33. Paragenesis of events forming skarns around the Early Plutons, with estimated Temperatures.

## 5. HYDROTHERMAL VEIN DEPOSITS

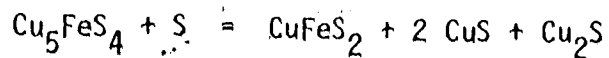
### a) Giant Quartz Veins and Associated Mineralisation

The nature of the Giant Quartz Veins has been discussed extensively by Furnival (1935) and also in Part I. Mineralisation was found in three of these veins - at Echo Lake, Jason Bay and Uranium Point.

At Echo Lake a 10-20 m wide quartz stockwork cuts the contact between granite and metamorphosed felsic volcanic rocks. The veins show three phases of quartz introduction separated by periods of fault-movement. The sense of movement on the fault has not been documented, but from the geometrical considerations outlined earlier (Fig. 18), it is probably dextral. A small lens of uranium mineralisation was found in this vein in 1969. The lens was so small that subsequent trenching destroyed it. However, samples collected from the blastings showed that the third phase of quartz (clear and vuggy) contained interstitial rosettes of haematite, which in turn contained low amounts of a radioactive element - presumably uranium. No primary uranium minerals were seen, but a few grains of a yellow 'uranium bloom' (bequelierite?) were noted. Polished sections have not been made, due to a lack of suitable samples.

A 5-10 m wide massive quartz vein outcrops in a NE-trending fault on both shores of Jason Bay. Two phases of quartz intrusion are recognised. The first is banded and milky, and the second coarse and vuggy. This second generation was deposited in thick bands parallel

to the vein margins, and in places is interbanded with Fe-rich dolomite and ankerite. Both quartz and carbonates get coarser towards the centre of the vein, and locally lenses of copper minerals and haematite are developed. The copper minerals are confined to the carbonates, which they replace, but are usually located at contacts with quartz. The copper mineral was originally bornite, but this has been strongly altered to chalcopyrite, which occurs both as rims around, and as exsolution lamellae in the bornite (Plate 5.7). Small veinlets of chalcocite and, rarely, covellite are seen in the chalcopyrite and occasionally cross-cut into the bornite. These textures are typical of the degradation of bornite, thus:



Haematite, occurring as rosettes in the quartz and bands of plates and needles in the carbonates, cuts all these copper minerals. No radioactive minerals were detected.

East of Uranium Point a 30 m wide quartz stockwork contains massive quartz that was brecciated and cemented by banded, milky quartz, and this in turn is locally replaced by blebs of pyrite and chalcopyrite. A thin branch of this vein runs NW through Uranium Point, where it is occupied by a younger diabase dyke, and the edges of this vein are full of haematite. The diorite which it cuts is extremely altered up to 20 m from the vein. Heavy impregnations of haematite in the diorite contain radioactive elements in small lenses,

( ) No uranium minerals were recognised.

Near Njc Island the Bloom Fault is occupied by a 50-100 m wide Giant Quartz Vein that contains all three phases of quartz. Chalcopyrite and pyrite were found in the third phase as blebs, but no haematite, carbonates or uranium minerals were seen.

Consequently, a detailed paragenesis of the Giant Quartz Veins is as follows:

Phase 1. Growth of massive, white, quartz veins in dilatancies in the regional NE-trending faults.

Phase 2. Brecciation of these veins and introduction of more quartz. Cementing of fragments by new quartz (banded and milky). Stockworks of quartz veinlets around the main vein. Silicic and other alteration in the veined country rocks. Introduction of some iron and copper sulphides.

Phase 3. Further dilatancy developed in the veins. Fillings of clear, vuggy quartz. Iron-rich carbonates in later stages. Copper and uranium minerals and haematite introduced with the quartz.

These descriptions are closely similar to those of other Giant Quartz Veins throughout the Bear Province (Kidd, 1932; Furnival, 1935; Smith, 1953). It is important to note that the veins cut all the Aphebian rocks of the Bear Province, but that the initial vein fillings were developed relatively soon after the end of the Aphebian era.

b) Barren Quartz-Carbonate Veins

Podiform, banded veins of coarse amethystine quartz and pink and brown carbonates (calcite, dolomite and ankerite) are common throughout the area. They commonly fill NW- and NE-striking joints and microfaults, splaying from the larger faults. They also occupy the E-trending tension-fractures. They cut all rock types, but their thickness is lithologically controlled - they are thin and sinuous in plutonic and massive volcanic rocks, but podiform in the tuffs and sedimentary rocks. The quartz and carbonates form thick bands with large crystals of quartz growing perpendicular to the vein margins. The carbonates are fine-grained and banded on the outside and become coarser towards the centre. The vein-centres are often vuggy. Flakes and specks of haematite and chalcopyrite are locally common. The edges of the veins are chloritised, and the surrounding rocks are altered for a few centimetres on either side. These veins are cross-cut by the youngest diabases and are probably related to the youngest phase of quartz-filling in the Giant Quartz Veins. No fault movement has taken place since their formation.

One rather unusual vein that appears to belong to this group fills an E-striking tension-fracture in tuffs near the outlet of Balachey Lake. It contains, in addition to the typical quartz and carbonate assemblage, pods of barite, which in turn contain bornite and chalcopyrite.

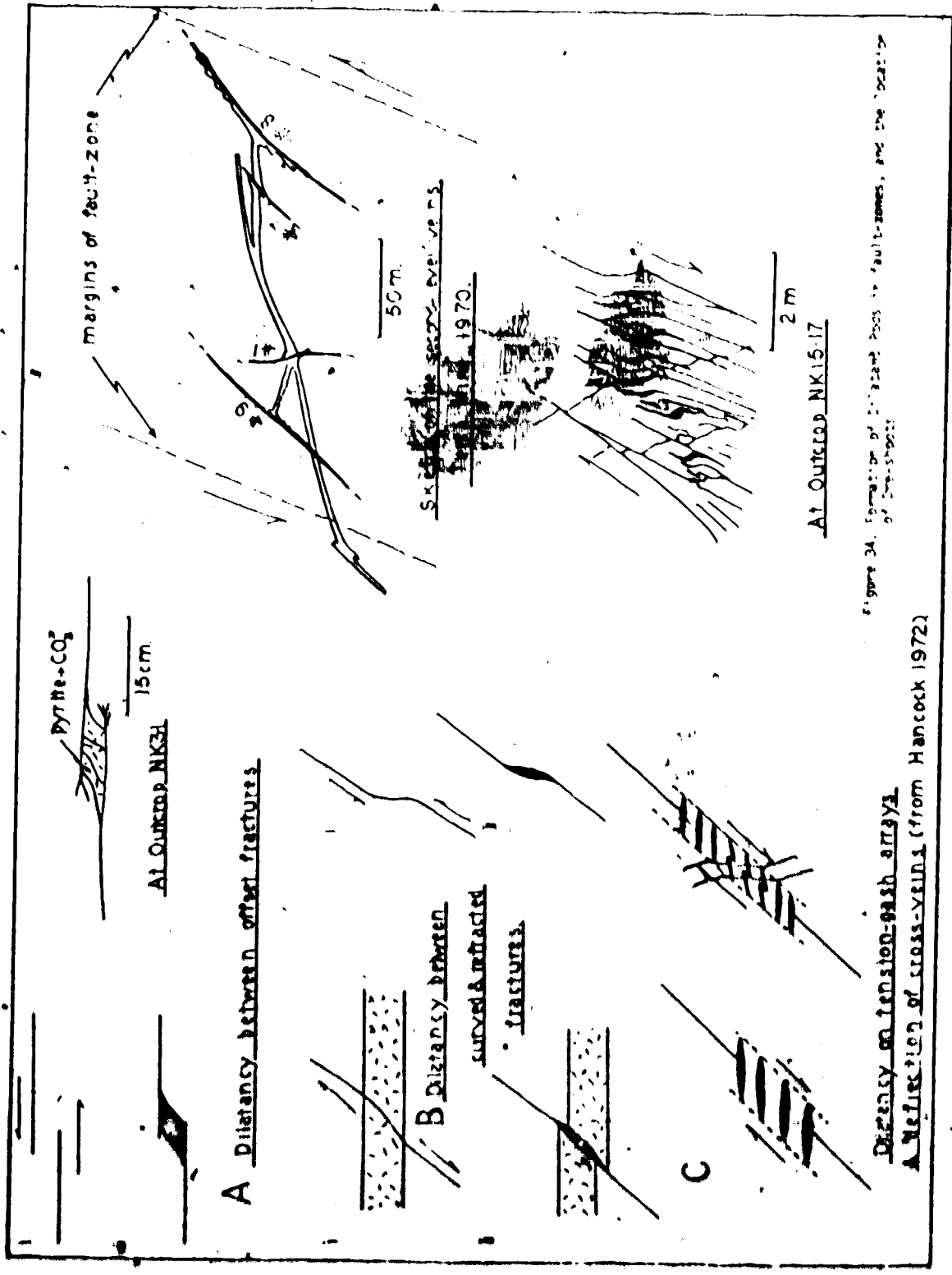
c) Quartz-Carbonate Veins Containing Silver, Bismuth and/or Arsenides

These veins occupy second and third-order faults splaying from the major NE-trending faults. Occasionally, however, they are emplaced in E-striking tension-fractures between the NE-trending faults. These splay-faults are usually vertical, but their orientations are extremely variable. In plutonic and massive volcanic rocks they are single-plane shears, and veins in them are seldom more than 5 cm wide. These veins are filled with finely-banded carbonates and granular quartz, with rare patches of chalcopyrite, fluorite, haematite, arsenopyrite and cobalt arsenides. The wall-rocks are haematitised and chloritised for a few centimetres on either side. In bedded volcanic rocks the shears splay and horsetail, and their trends vary. Movements were taken up on a number of planes, and as a consequence dilatant zones were developed. These dilatancies occur on all scales, but their mode of formation is best seen on the microscale.

Figure 34 shows three ways in which dilatancies may occur and these ideal cases are compared with examples. The principal modes of generation of dilatancy are:

1. Between offset fractures.
2. Between curved and refracted fractures.
3. As tension gashes.
4. At cross-fractures.

The first of these requires that faulting be taken up on more than one plane - a condition that develops where the faults cut bedded volcanic rocks, plutonic contacts and sulphide-impregnated rocks.



Pyrite-CO<sub>2</sub>

15cm

At Outcrop NK15-17

A Dilatancy between offset fractures

B Dilatancy between successively fractured fractures

C

Dilatancy on tension-parallel strata  
A Reflection of cross-veins (from Hancock 1972)

Figure 34. Formation of dilatancy zones in fault-zones, and the location of the study area

At Outcrop NK15-17

2m

50m

Sketch of the section at the top of the page  
Hancock 1970

margins of fault-zone

The second and third require inhomogeneities in the faulted rocks - i.e. bedding, cross-faults or intrusive contacts. The first two require more than one period of movement on the faults. All these conditions can be seen to apply in the Camsell River area on outcrop scale and can be deduced as applicable to the veins in the three mines.

The 'silver' showings usually consist of one such dilatant pod in a thin carbonate vein and the structural controls of these are easily seen (Fig. 35). These mineralised pods seldom exceed 10 m in length and vary between 10 and 50 cm in width.

The mineralised lenses are distinct from those in the barren veins in containing numerous brecciated fragments of wall-rock and in showing signs of more than one period of fault-movement. In the pods the carbonates become coarser and vugs may develop. The ore-minerals develop as thin sheets and replacement zones on brecciated wall-rock fragments, as blebs in the carbonates, and interstitially in rare, thin bands of 'sugary' quartz.

The mines are developed where there are a number of veins, each with a number of mineralised pods close together. Again the pods contain most of the mineralisation, together with numerous fragments of wall-rock and earlier vein material. At least two, and often more periods of fault-movement can be proven. The area between main veins is extensively fractured and contains numerous carbonate 'stringers'. Between pods the veins are narrow (1-10 cm) and rarely mineralised. The pods may be as wide as 5 m, although 10-50 cm is more common. In



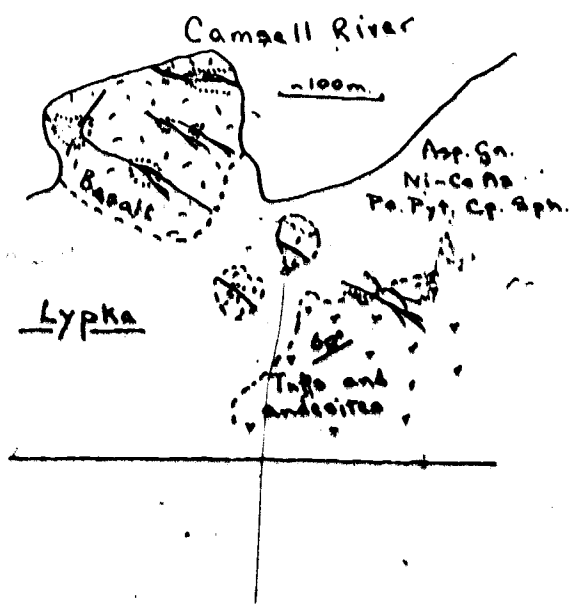
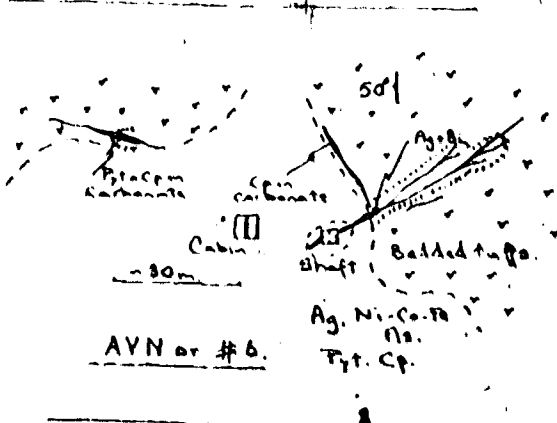
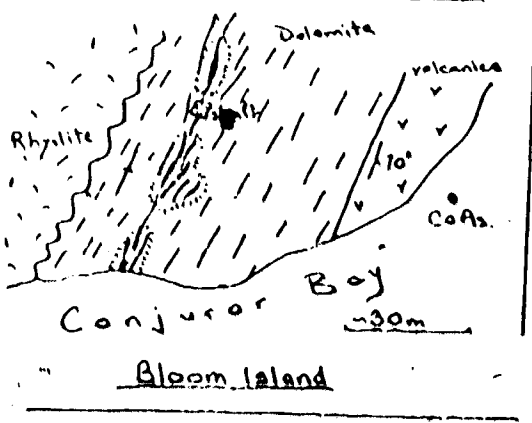
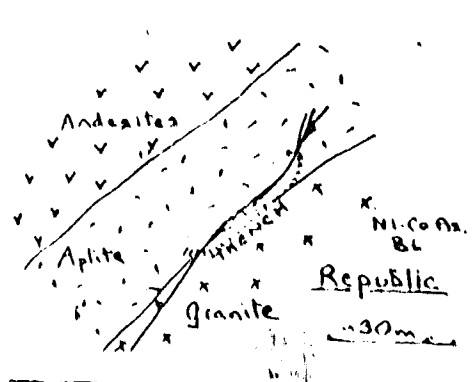
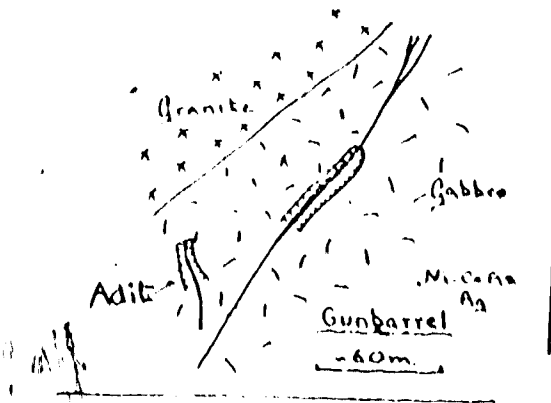


Figure 35. Sketch maps of some of the Ag, Ni-CoAs showings

J. P. N. B. 1972



general the E-trending tension-fractures have become the most dilatant and the NE-trending faults and shears remain thinner, but more richly mineralised.

The gangue minerals are usually quartz and carbonates, with fluorite common locally. The vein minerals consist of native metals and complex salts, mainly of the following elements: U, Ag, Bi, Ni, Co, Fe, Cu, Zn, Pb, As, Sb and S.

It is clear that mineralised veins are localised by:

1. Intrusive contacts - since the intrusives are demonstrably older, this must be a structural control.
2. The host-rock. Competency is certainly important, but rock-chemistry may also be a controlling factor.
3. The secondary and tertiary NE-striking faults and their related E-striking tension-fractures.

The ore-shoots within the veins are contained in dilatant zones and these are localised by:

1. The presence of pre-existing sulphides in the host-rocks. This is certainly a competence control and may also be a chemical control.
2. Curves, refractions and bends in, and offsets between faults that have moved more than once, causing dilatancy.
3. Areas where the veins cut contacts or other faults.
4. The rock-type. Ore-shoots are most common in bedded volcanic rocks and are never seen in the volcanoclastic sediments.

The nature and controls of the mineralised veins will be discussed further after the mines and showings have been described in detail.

## 6. THE TERRA MINE

### a) History

The property was investigated by Eldorado's Exploration Division in 1960 and a few holes were drilled to test the copper zone at depth. The silver veins were thought to be too small for exploitation and the ground was dropped. Terra Mining and Exploration acquired the property late in 1966. They drilled 39 holes in 1967 and then began a programme of underground development and drilling in 1968.

A mill was constructed early in 1969 and the mine was officially opened in September of that year. Production has since been sporadic with both economic and physical factors causing problems. Since the spring of 1972, when both the third level and the Number 9 vein were developed, good ore has been mined and production has been continuous.

### b) General

The mine geology and the location of the most important mineralised veins have been described in the section on sulphide skarns (Fig. 31). Details of the fracture pattern (Fig. 36) show the complex nature of the faulting in the mine. The mine is localised where a small second-order fault, splaying from the Bull Fault, cuts banded andesite tuffs and the sulphide skarn. The fault can be seen as a single plane in plutonic rocks to the south, and as a 5 m wide set of shears in the andesites and volcanoclastic sediments to the north. In the mine area the fracture zone widens to about 100 m and is bounded by two main

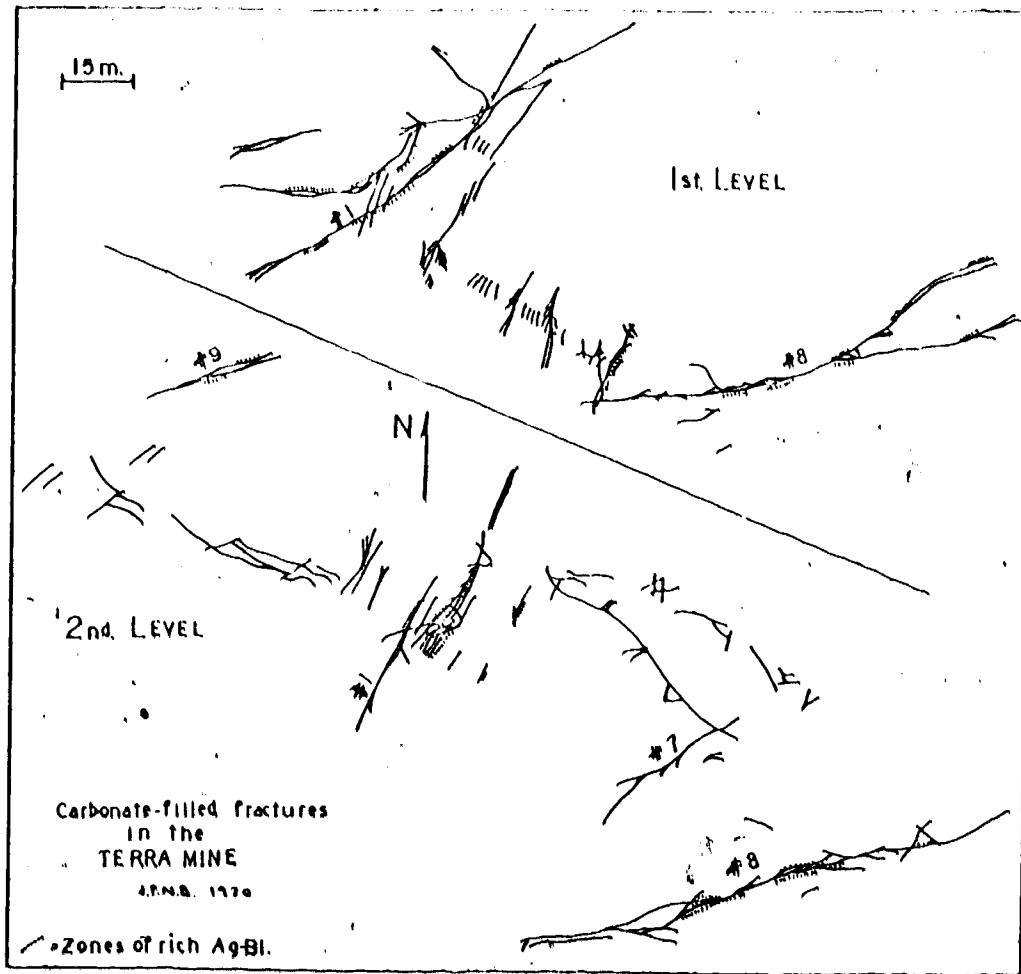


Figure 36. Carbonate-filled fractures and the location of Ore-shoots in the Terra Mine.

veins, the Numbers 8 and 9 (Fig. 34). These two veins are, however, sinuous and do not always remain parallel to the direction of faulting. The main veins are composite and highly complex. Between them are numerous sub-parallel veins and stringers (e.g. Numbers 1 and 7), and even more numerous cross-fractures. The complexity of the mine is greatly simplified by showing only the carbonate-filled fractures in Figure 36. In reality, chlorite-covered shears and joints, which developed before, during and after mineralisation, outnumber the veins and stringers by an order of magnitude. When it is also considered that many of the host-rocks were originally breccias (e.g. metacalcargillite), show extreme lateral facies variation, and are differently metamorphosed and skarn-mineralised, the problems of correlation between, and prediction of veins and ore-shoots are more than this writer could deal with, except in the most general manner.

It is clear that the mine is localised by the host-rocks, which permitted development of a wide fracture-zone on the fault. Similar conditions exist elsewhere on the Terra peninsula (see Fig. 7) and each of the fault-zones widens as it transects the andesite tuff and calcargillite horizon. Carbonate veins were found in all of these faults and were investigated where they cut the andesite flow on the shores of the Camsell River. They were found, predictably, to be thin and barren. They are not well-exposed where they cut favourable horizons for ore-mineralisation and recommendations that the veins be drilled in these areas were not followed. It has been rumoured, however, that one of these veins was finally drilled in 1973 and

yielded a 'significant' intersection containing arsenides. The author has been unable to substantiate this rumour.

c) Wall-Rock Alteration

The veins in the mine evidence at least three periods of movement. Each is shown by the brecciation of pre-existing vein material and by the introduction of fresh mineralising fluids. The faults must have existed prior to the first phase of mineralisation, for this mineralisation fills the faults, and associated siliceous and haematitic alteration are widely developed in the wall-rocks. The massive volcanic rocks are especially affected and altered to a deep red 'chert'. Fragments of this are common in all the veins (Plates 9.4 and 9.5).

These red fragments are healed by carbonates, and the wall-rocks were altered again at this time. This alteration extends for about twice the vein thickness on each side and is best developed in the tuffs and calcargillite. In these rocks an outer zone of white mica and carbonate replaces much of the host-rock and gives way inwards to a zone of chlorite and carbonate with or without haematite, and then to a zone of almost-complete carbonatisation on the edge of the vein (Plate 4.8). In the siliceous volcanic rocks this alteration is seen only as black and green (chloritic) stringers along fractures.

A further period of fault-movement caused brecciation of all pre-existing vein and wall-rock material, and permitted the introduction of quartz and carbonates. Alteration around these veins was not

observed, but the margins are plated with chlorite and white mica (Plate 9.4), and slippage has occurred on these again and again (Plate 3.7).

d) Location of Ore-Lenses

The location of rich silver-bismuth ore-lenses is shown in Figure 36. It can be seen that the ore occurs sporadically and irregularly in the veins, but most frequently at areas of splaying and coalescence of the veins, and particularly where the veins intersect the 'copper zone' (compare with Figure 31).

Figure 37 shows the assay results of sampling along the Number 8 vein on the first level. Firstly, the podiform nature of the silver-rich lenses can be seen. Secondly, the location of these lenses just before and in the pods of 'copper zone' is well shown. The silver lenses always occur on the southern side of the copper pods - i.e. closer to the monzonite. This may imply that the silver-bearing fluids were migrating along the veins away from the intrusion, and that the silver was precipitated in dilatancies where the fault began to splay on the margins of a copper pod. The lack of silver right through the copper pod suggests that the chemical effect of the copper sulphides was not the dominant factor in precipitating the silver.

These conclusions are substantiated by similar data from the 201 area (Fig. 38) which shows the considerable enrichment of silver on and in the edges of the main copper zone - notably in the edge

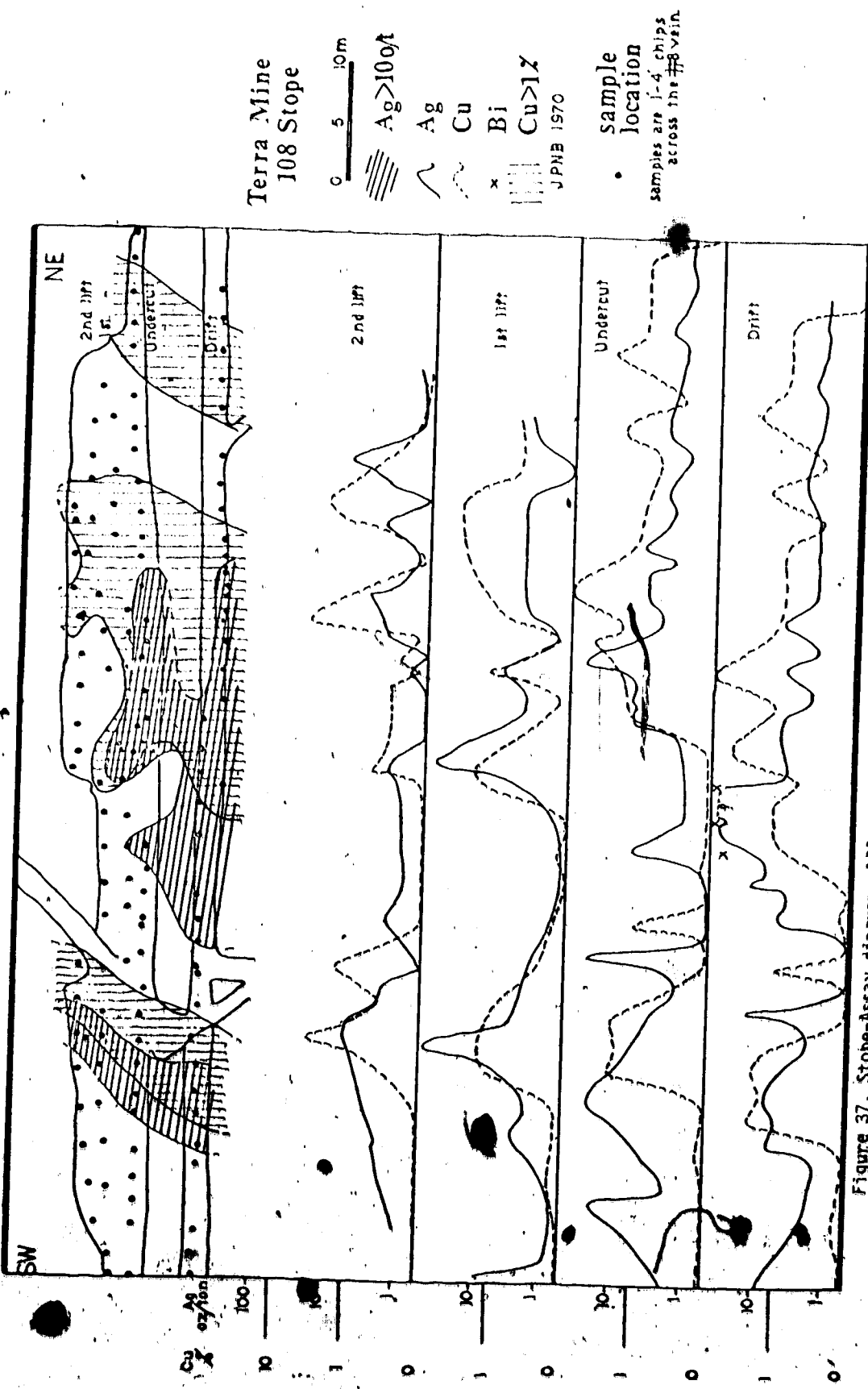


Figure 37. Stope-Assay diagram, 108 stope, Terra Mine.



# Terra Mine 201 area

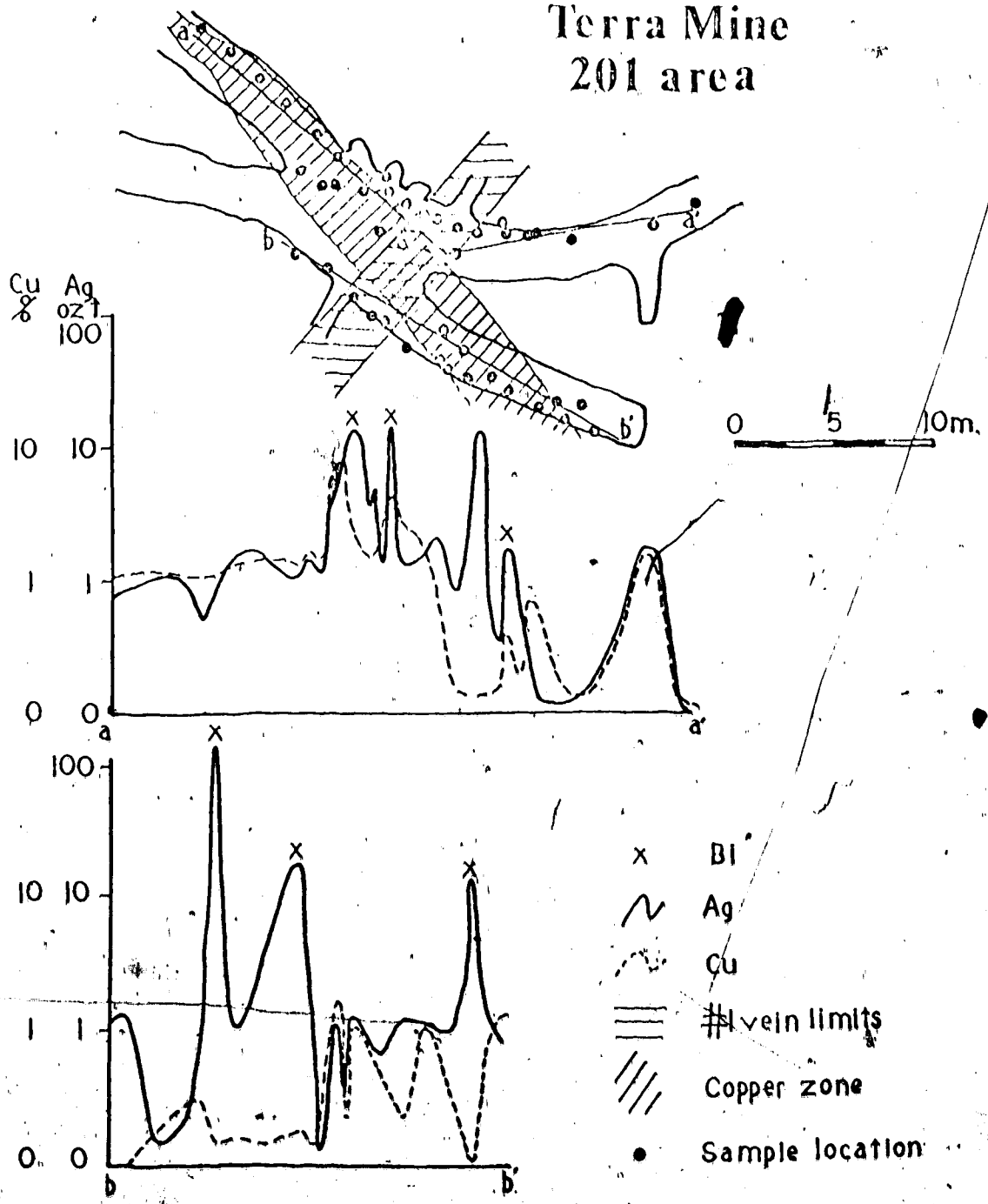


Figure 38. Stope-Assay diagram, 201 area, Terra Mine.

closest to the monzonite. Furthermore, the recrystallisation and consequent enrichment of the copper sulphides close to the veins is well demonstrated in the data from the traverse a-a'.

The ore-lenses in the main veins consist dominantly of uranium minerals, arsenides and silver or bismuth. However, in the cross-veins, most of the ore is of the younger silver-bismuth sulphosalt and sulphide variety. It is interesting that both types and ages of mineralisation show the same relation to the copper zones, again suggesting that the control is structural. The coincidence of the rich copper zone and the remarkably complex and well-mineralised portion of the Number 1 vein is no accident.

These data were assembled from results of sampling to determine grades and tonnages in the mine. Further data on the more recent developments are not available to the author. However, from brief visits to the mine in 1971 and 1972, it is apparent that the two features (splaying of faults and intersection of faults and copper zones) control much of the important mineralisation in the mine.

The data concerning a possible direction of travel of the mineralising fluids is interesting. It was originally proposed that the location of silver lenses on one side of the copper zones indicated that solutions travelling through the copper zones leached the sulphides of trace contents of Ag, Ni, Co, etc. during their recrystallisation, and deposited these elements beyond the copper zone. However, it was noted earlier that the primary sulphides contained virtually none of the elements common in the younger veins

and that there was no difference in the trace element contents of primary and recrystallised sulphides (see Table 5). Consequently, the hypothesis of fluid-transport away from the monzonite is preferred.

It must be stressed here that there can be no genetic connection between the monzonite itself and the veins - the intrusion was one of the earlier ones in the area, and was certainly cooled and, possibly, even unroofed at the time of mineralisation. The genetic significance of this proposed direction of fluid migration will be discussed later.

#### e) Details of the Vein Mineralisation

When describing complexly-mineralised veins, there is a problem in deciding whether to describe first the separate minerals and their textures, and then a paragenesis, or vice versa. The cart is always being put before the horse, however it is done. In this section the groups of minerals that typify the various stages of the paragenesis are described and their textural relationships with other groups documented. A detailed summary of the paragenesis follows.

#### Carbonates

The carbonates can be divided into five groups on the basis of both morphology and age-relations. The first phase is seen only as brecciated fragments in younger veins, always associated with the red-altered fragments. The fragments consist of fine-grained calcite and dolomite which are badly haematitised. Since the red fragments are not veined by this material, it is thought that the red-alteration

may be younger. These carbonate fragments may have been the first hydrothermal vein material in the faults.

The second group of carbonates consists of granular, fine-grained dolomite, with small admixtures of calcite. This cements the red fragments and is often banded. Occasionally it contains small patches of quartz, magnetite, haematite and pyrite. The bands are often separated by smears of chlorite, and moss-like botryoids of chlorite have grown from these. The dolomite contains much of the more massive silver and arsenide mineralisation. Faulting then sheared, and occasionally brecciated this dolomite, and a coarse white dolomite was emplaced, forming thick veins which cement both red and green altered fragments. This dolomite contains smears of chlorite and coatings of a fine haematite dust. It is replaced by much of the dendritic and botryoidal arsenide mineralisation.

The fourth group cuts the third, which was not brecciated. It is a coarse white dolomite, containing chlorite and haematite in places. Patches of coarse, clear quartz are common, and thin veins of quartz lie in this dolomite. These veins are usually of clear, euhedral quartz, but one was seen to be fine-grained and granular, and to contain specks of native silver. The dolomite also contains patches of fluorite, green muscovite, pink feldspar, bismuth and many sulphides and sulphosalts. Quartz-feldspar-fluorite-muscovite veins both cut and are cut by the dolomite veins. The dolomite was the last main filling of the veins, and there are large vugs in it, most especially in the cross-veins. These vugs are often lined with pyrite and

haematite, and fine needles of pavonite were found in one. The last carbonate in the veins is calcite, which forms elongate scalenohedra in the vugs and is often intergrown with pyrite and haematite.

The results of analysis of isotopes of oxygen and carbon are shown in Figure 39. All the dolomites plot in a very tight group and there is no evidence of fluid evolution, although the averages of nine Stage 2 and 15 Stage 3 dolomites are separate, with the same trend as that shown by equivalent stage dolomites in the Echo Bay deposit (Robinson, 1971). However, the values are close to those of dolomite in the metacalcargillite and it is suspected that all the dolomites have equilibrated (Badham et al., 1972).

The calcites show a considerable spread and it has been suggested that they represent a continuous trend from the equilibrated dolomite value to equilibration with a late influx of meteoric water (Badham et al., 1972). However, scatter is really too large to be interpreted simply. In addition, many of the Stage 3 calcites were so intimately intergrown with dolomite as to be physically inseparable, and the analyses were made on the gasses produced after only two hours of acid digestion (see Appendix III). The analysed carbonates were all identified using X-ray diffraction methods: only Ca and Mg carbonates were identified at Terra.

#### Quartz

No quartz was seen in association with the red alteration of

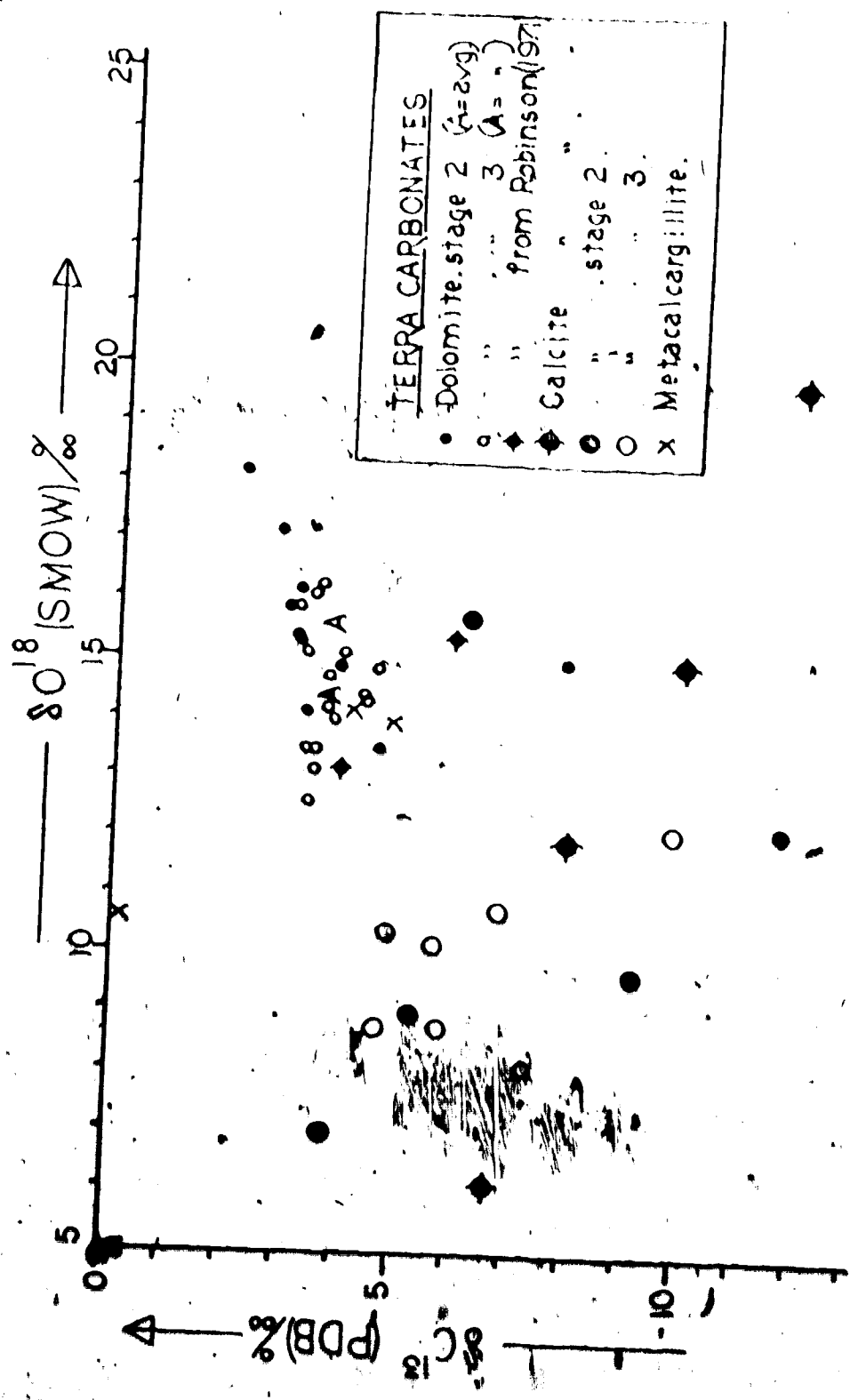


Figure 39. C & O Isotope data for Terra Mine Carbonates.

Terra, but its presence is implied by the extensive silicic alteration. Quartz is first seen as patches in the second phase carbonates, where it is clear and euhedral and often dusted with haematite. No quartz was seen in the third phase carbonate veins, but it becomes common in the coarse, white dolomites, both as veins of coarse, clear euhedral crystals and as 'dogstooth' vug linings. In the latter it is commonly coated with haematite or pyrite. Small crystals of quartz very occasionally overgrow the late calcite scalenohedra.

The quartz crystals contain numerous fluid inclusions, and are eminently suitable for fluid inclusion work, which is planned for the future.

#### Uranium Minerals

Uranium minerals are commonly associated with the silver- and arsenide-rich lenses in the main veins. Studies with a scintillometer in the mine and on hand specimens reveal that much of the uranium is associated with the early red-alteration (haematitic and silicic). The uranium minerals are present in black streaks in the altered rocks, but no uranium mineral could be identified in polished sections of this material. However, it seems that later influxes of silver and arsenides recrystallised the uranium, sometimes in place, but more often with mobilisation as well. The uranium minerals were flushed to the margins of the red-altered fragments, and recrystallised with the silver. The autoradiographs (Plates 9.1 and 9.2) show the concentration of uranium minerals on the edges of, and in cracks in

the red-altered fragments, and their further concentration as thin coronas around silver and arsenide growths. There is evidence, however, that some of these coronas of uranium minerals grew before the other minerals and acted as a nucleation centre for precipitation of the latter. For instance, in Plate 8.2 a corona of banded uraninite in carbonate was cored by silver and rimmed by diarsenide rosettes. These thin bands of uraninite probably correspond to the early uraninite dendrite stage at Echo Bay (Robinson, 1971).

Uraninite also occurs as zoned spherules between 5 and 10 microns in diameter. Some of these appear to have preceded silver and arsenide minerals (Plate 8.3), but some crystallised with or after these minerals (Plate 8.1). The zoning consists of a darker annulus near the core (Plate 8.3) and a pale outer ring. Electron microprobe investigations showed this annulus to be enriched in lead over the outer ring. Galena itself is common in the cracks in and around the edges of the spherules, and was presumably formed from radiogenic lead.

Although the uranium mineral in the spherules was identified optically as uraninite (this is confirmed by the presence of uraninite lines in an X-ray diffraction powder photograph of a heavy concentrate of Sample A 2.7 - Plate 9.3), the uranium minerals, detected both by scintillometer and by autoradiograph, could not be identified with certainty.

It is concluded that uranium was introduced into the veins at the same time as the silicic and haematitic alteration. Subsequent



brecciation and the introduction of new minerals served to recrystallise, and sometimes remobilise the uranium minerals. This conclusion agrees with isotopic data on the leads, from which Thorpe (1971) has concluded that pitchblende at Port Radium was deposited at 1625 m.y. and remobilised at 1450 m.y. Whether or not these ages are correct is arguable, but the conclusion of importance is that two ages are indicated.

### Native Silver

Native silver is economically the most important mineral in the veins. Silver is most commonly associated with the arsenides, but does occur away from arsenide mineralisation, as leaves and wires in carbonates, as interstitial blebs in quartz, and intergrown with sulphides.

Native silver has been seen veining and replacing an early generation of granular, yellow dolomite in a number of polished sections. The silver first surrounds grains or areas of dolomite with thin rims, and then gradually replaces the surrounded carbonate (Plate 6.1). The resulting silver often forms coarse dendrites in the carbonate. Thin dendrites are also common, and these have a cubic symmetry and cut indiscriminately through the carbonates. Individual silver crystals within the dendrites often retain the pseudomorphic shape of replaced carbonate (Plate 6.1).

Dendritic textures are commonly reported in the literature, but few attempts are made to explain them. The author has studied the

growth of ice dendrites on windshields for the last three years and the following generalisations can be made.

1. The dendrites always have a hexagonal symmetry, although interferences between two dendrite sets in differing orientations may obscure this symmetry.

2. The dendrites are longest, thinnest and least-branched when the air-temperature has been lowest.

3. The dendrites are short, fat and many-branched, and often join to form massive ice-sheets, when the temperature is barely below freezing and the humidity is high.

4. Rosettes are equally as common as dendrites and show similar relations to temperature and humidity.

5. The dendrites obey only their own symmetry. Dendrites may cross patches of dirt or pre-existing lumps of ice with no deflection or perturbation of their regularity.

6. The point of nucleation and initiation of a dendrite appears to be random. They do not necessarily nucleate from pre-existing ice patches.

It is concluded that the ice dendrites form best when the temperature contrast between the mineralising 'fluid' (in this case the atmosphere) and the area of deposition is greatest, and when the concentration of 'mineral' (water) in the 'fluid' is not high. Ice dendrites were observed to grow with great rapidity, and it is generally accepted that dendritic textures are indicative of fast growth (Phillips, 1963).

All the silver dendrites and many of the arsenide dendrites in the Terra ores are cubic. They may be short and fat, with massive interstitial patches, but are predominantly long and thin. They show the same features as ice dendrites, and it is concluded that a mineralising fluid containing silver was intruded into carbonate-bearing veins: the physical (temperature) and chemical ( $f[\text{Ag}]$ ) parameters between carbonate and fluid so contrasted that silver was immediately precipitated and grew through the veins as dendrites. Elsewhere, the silver can be seen to have nucleated on uranium minerals or wall-rock fragments in the veins, or on the colloform chlorite growths in the early carbonates. It often completely replaces these chlorites, but retains the colloform texture.

Many of these early silver dendrites were rimmed by successive bands of arsenides, which vary from generally nickel-rich near the silver, to cobalt-rich near the margins (Plate 6.2). However, there is clear evidence to show that much of the silver in the cores of arsenide roses and dendrites was introduced after the arsenides and replaced carbonates left in the cores (Plate 6.3). Both these types of silver were later recrystallised to cubes (from pseudomorphous rhombs) with the simultaneous formation of maucherite at the expense of less Ni-rich arsenides next to the silver. The recrystallised core silver can be seen to cut the arsenides (Plate 6.5). At this time some new silver may have been introduced, as veinlets filling cracks in the arsenides (Plate 6.4). These arsenide-core silvers are often replaced by later carbonate (which grows as pseudomorphous cubes

now!), quartz, fluorite and, less commonly, sulphides (Plate 6.5).

Silver was again introduced during the sulphide and sulphosalt phase, and although most is present in the sulphosalts, small specks of native silver were sometimes exsolved from galena-tetrahedrite mixes, and the metal was once observed in a granular quartz vein.

Consequently, we have at least three phases of silver mineralisation. The pre- and post-arsenide silvers may have been deposited essentially synchronously, but the 'vein' and 'exsolved' silvers are different.

Silver from hydrothermal veins frequently contains small amounts of antimony and mercury in solid solution (Boyle, 1968), and the concentrations of these usually decrease with time and falling temperature (e.g. Petruk, 1971). In 1971 four silver samples (two pre-arsenide, two recrystallised post-arsenide) were analysed for their Hg, Cd, Sb and Ni contents, using an electron microprobe. Antimony and cadmium were found to be below detection limits, and nickel was detected rarely, and only in patches (found later to be blebs of nickel arsenides in the silver). The mercury contents, however, showed a perfect bimodal distribution from greater than 1.5 wt % in the 'earlier' silver, to less than 1% in the 'younger' silver (Table 7).

This bimodality was tested in 1973 with samples from all three mines. A number of the samples selected contained silver of both earlier generations. The results (Table 7), show that there is still a bimodality in mercury contents, but that this does not correspond

Table 7. Mercury contents of Native Silver from Terra, Norex and Silver Bay.

Sample	App. wt.% Ag	App. wt.% Hg	App. total %	No. Grains Analysed.
<b>TERRA</b>				
<u>Run 1</u>				
TM19.3A	-	1.63(1.83)	-	5
TM30.6A	-	2.67(3.00)	-	5
TUX08.1	-	0.31(0.34)	-	5
TM19.3C	-	0.62(0.70)	-	3
<u>Run 2</u>				
A2.5 (0)	98.87	0.599	99.47	10
TX16.11 (0-C2)	95.05	1.82	96.87	3
A2.12 (0)	94.62	2.08	96.76	3
A2.7 (0)	98.43	0.306	98.74	10
<u>Run 3</u>				
TJ1.5A (F/C1-6)	98.67	1.36	100.03	9
TJ1.8A3 (C1)	99.05	0.60	99.65	5
TJ1.8B (C5-6)	97.11	1.25	98.36	10
A2.8 (0)	95.62	2.47	98.09	5
NK20.1A (-Q1)	94.75	1.96	96.71	5
MJ24.3A (C5-8)	93.15	2.02	95.17	10
MJ24.3B (C3-4)	93.35	3.28	96.63	5
MJ24.7 (0-A1)	94.72	2.03	96.75	9
MJ24.3C (C9-10)	86.65-96.9	2.30-3.40	-	3
TJ1.8A2 (F3-4)	88.89-94.4	3.06-5.90	-	10
<b>NOREX</b>				
<u>Run 3</u>				
NX11.5H	90.03	2.47	92.50	8
<b>SILVER BAY</b>				
<u>Run 2</u>				
SBX10.10 (0)	88.76	0.98	89.74	2
SBX10.30 (0)	87.62	6.45	94.07	2
SBX10.8B (0)	96.03	1.77	97.80	5

to the optically-defined generations of silver. In addition, some of the apparent totals are alarmingly far from 100%, indicating the presence of other components. (Only background corrections were made on the results of the second and third sets of data; atomic number, fluorescence and absorption corrections, applied to the first set of data, were apparently so small as to make no statistical difference to the results). The bimodality still defined the same two groups as had the first analyses. It was concluded that the difference between the two groups (ignoring, for a moment, the anomalous Silver Bay sample) was in the degree of replacement of the silver by later carbonate, quartz or fluorite.

Consequently, 11 samples from the Terra Mine, and one from Nore, were selected, after arbitrary degrees of replacement had been designated from optical work. The same criteria were applied to the samples analysed previously. These criteria are denoted in Table 7 on the following system:

A, F, C, Q	=	Replacing mineral: argentite, fluorite, carbonate or quartz
1 - 10	=	Degree of replacement
0	=	No replacement.

From the results of these analyses, it can be seen that the hypothesis is not valid. Detailed correlations of all the results with the optical data show that the mercury content drops in the

post-arsenide silvers as they develop in the arsenides. The mercury content reaches a minimum as the silver starts to be replaced by other minerals, but does not change with continuing replacement. The silver need not develop as fully euhedral crystals in the arsenide, but continued to be precipitated until its supply was exhausted. The later minerals replace partially or fully-developed silver crystals with equal facility. The silver in the anomalous sample from Silver Bay occurs as tiny spocks exsolved from tetrahedrite, and is clearly not part of the main group of silvers.

The recrystallisation of silver in the arsenides apparently had no effect on the mercury content - at least none was indicated by the analyses. However, during the third analysis, two samples were found to be zoned (the analyses were carried out in such a way that inhomogeneities would have been detected earlier had they existed). The ranges of this zonation are considerable (Fig. 40), and further investigation showed that the mercury was enriched in a thin outer band and depleted in the core of the silver dendrites in these two samples. This is clearly shown by scanning photographs for silver and mercury (Plate 6.6). This particular silver dendrite is the core of a thick dendrite of niccolite with skutterudite rims. There is some maucherite next to the silver, which is being replaced by fluorite. Since the mercury content of the adjoining niccolite is very low, this zonation cannot represent a diffusion from silver to niccolite or vice versa. It may represent a flushing-out of mercury from the silver during a recrystallisation, or it may be a depositional feature.

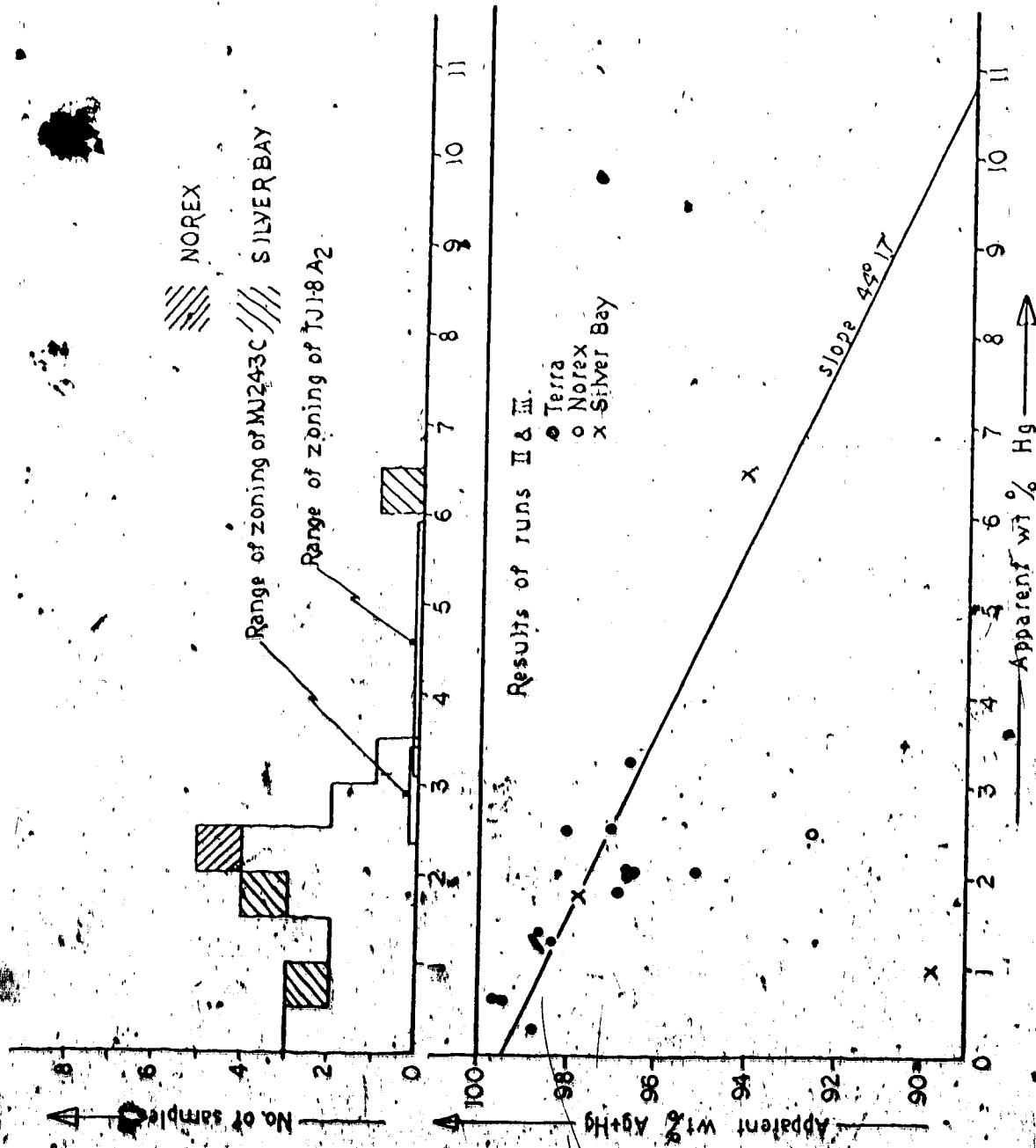


Figure 40. Hg-Ag diagrams for the Terra, Norex and Silver Bay Mines.

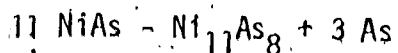


Many of the totals of the first two sets of analyses were reasonably close to 100% (apparent wt % Ag + apparent wt % Hg). However, when all the analyses are plotted (Fig. 40) it can be seen that there is a regular deficiency in the apparent total, and that this deficiency almost exactly equals the apparent concentration of mercury in the sample (exact equality would produce a best-fit line with a gradient of 45°).

Earlier results had indicated that there were only low concentrations of nickel and antimony and no cadmium in the samples; later qualitative investigations showed no detectable sulphur or uranium. Full-range scans were made of the most deficient samples from each of the mines, and it was found that Si, Bi, Sb and Ni were present in low amounts and that arsenic was present in the two most deficient Silver Bay samples and the Norex sample. This work is reported as it stands at present, and further analyses of the silvers are planned, especially to test whether the third component(s) is (are) real, or merely a function of analysis that will not appear when full corrections are applied.

Other data that have come out of this project are interesting. Throughout most of the analyses the third channel of the electron microprobe was tuned to nickel (L $\alpha$ ), to detect microblebs of arsenides in the silver and avoid them during analysis. Qualitative tests continually showed that the arsenides surrounding the silver cores of dendrites and rosettes are Ni-rich. Furthermore, maucherite was nearly always found only in contact with the silver. The Ni-content

of niccolite was found to be higher in a thin band up against the silver. However, where the silver cores are recrystallised and veinlets of silver transect the arsenides, there is no enrichment in nickel against the silver. Consequently, it was deduced that the arsenides originally contained more Ni-rich central zones, and that this represents the depositional evolution of the arsenides, which is independent of the silver. The silver may have replaced the most Ni-rich parts, or the Ni-rich parts may have precipitated around the silver - later recrystallisation has destroyed the original texture relationships. However, it does seem that the maucherite has formed from niccolite by loss of arsenic, thus



and that this occurred during recrystallisation of the silvers. The arsenic released may have migrated into other arsenides (arsenides are commonly stoichiometric).

Secondly, the cross-analyses of the silver and cinnabar standards enabled analyses for mercury and silver in these to be made. It was found that the cinnabar standard contains, between 0.0088 and 0.013 wt % Ag (88-130 ppm).

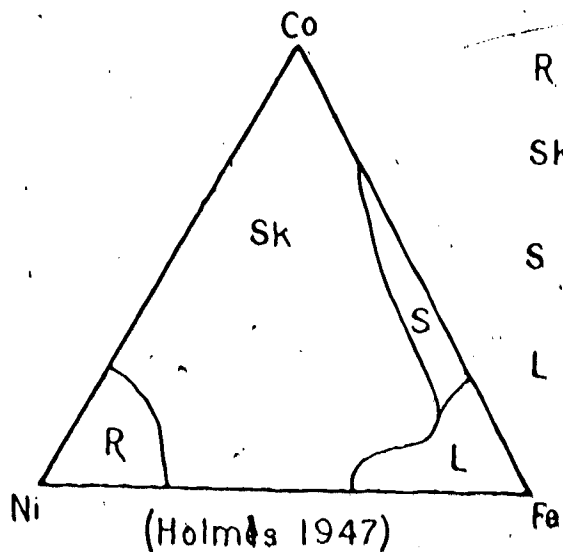
Thirdly, a number of bismuth grains were (accidentally!) analysed for their silver and mercury contents, and these data are reported below (Table 8):

It is concluded finally, that silver was introduced before, during

and after the main phase of arsenide deposition, but that all were deposited from the same (evolving) fluid, and are geochemically similar. Later silver, deposited with the sulphides, may be remobilised from earlier silver, or may represent a fresh introduction. The earlier silvers replace, and are replaced by arsenides, gangue minerals and sulphides. Frequent recrystallisation and common pseudomorphous textures complicate interpretation of the paragenesis.

### Arsenides

Studies of the arsenide minerals, especially the di- and tri-arsenides, have been hampered for many years by a profusion of structural and chemical data that not only failed to be consistent, but were frequently obviously in error. The cause of this confusion is that most arsenide minerals occur in highly complex intergrowths, and that analyses and X-ray diffraction studies were made on mixtures, rather than on single phases. Although a most detailed paper by Holmes (1947) and excellent subsequent work by Roseboom (1962, 1963) sorted out much of the confusion, errors were still common, even in the sixties. A history of the evolution of ideas on arsenides is given by Holmes, and the essence of his classification is adopted here (Fig. 41). The higher arsenides consist of two series. The first - an isometric triarsenide series - is grouped under the general name of 'skutterudite'. There appears to be complete solid solution between Ni-, Co- and Fe-end members, but triarsenides with only a single element in the metal sites are confined, apparently, to the cobaltian member. In Ni- and



- R Rammelsbergite  
(orthorhombic diarsenide)
- Sk Skutterudites  
(isometric triarsenides)
- S Safflorites  
(monoclinic diarsenides)
- L Lollingites  
(orthorhombic diarsenides)

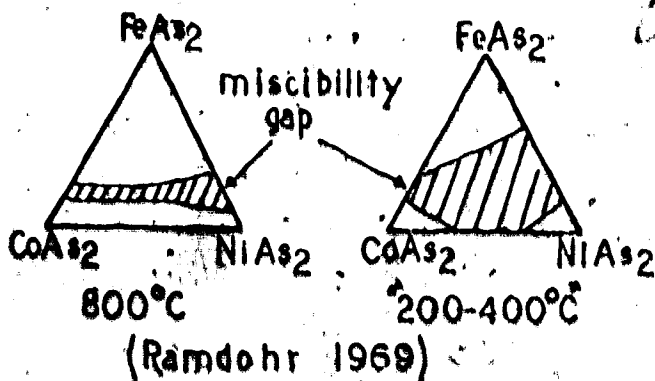
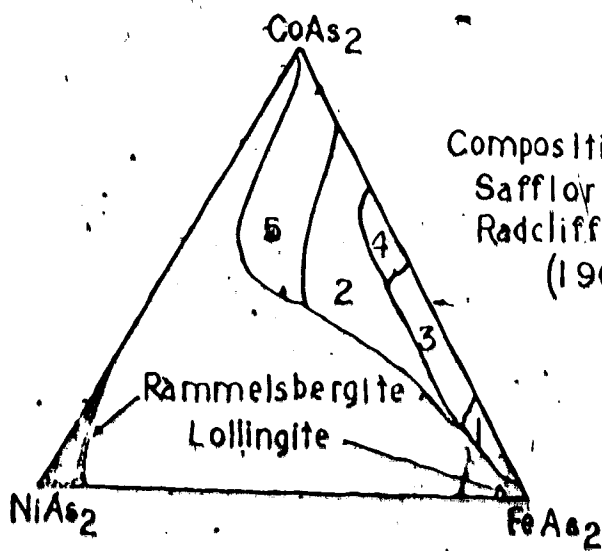


Figure 41. Stability fields and compositional ranges of Di- and Tri-Arsenides.

Fe-rich members the triarsenide structure breaks down to that of the second series - a group of monoclinic or orthorhombic diarsenides. This series can be subdivided further into three mineral groups - the safflorites, monoclinic Co-Fe diarsenides; lollingite, an orthorhombic Fe-rich diarsenide; and rammelsbergite, and its polymorph pararammelsbergite (Radcliffe, 1966), a Ni-rich orthorhombic diarsenide. At high temperatures, experimental data (Ramdohr, 1969) indicate complete solid solution between cobalt and nickel in the diarsenides, and the skutterudite field is small. At lower temperatures this solid solution breaks down, and two separate diarsenides result (Fig. 41). However, presence of a pure cobalt diarsenide has not been documented in the literature, and was not found in this study.

It was not until the advent of the electron microprobe that small enough areas could be analysed to prove the validity of Holmes' work in the cryptically zoned and banded samples: studies by Radcliffe (1966, 1968) and Radcliffe and Berry (1968) have been especially important. It was found that the diarsenides are essentially stoichiometric and that previous postulates of metal- or arsenic-deficient members are erroneous. There is no documented substitution for the nickel, cobalt and iron, and only sulphur has been shown to replace the arsenic up to a maximum of about 5 wt %. Radcliffe and Berry (op. cit.) proposed slightly different limits to the Fe-Co diarsenide field (Fig. 41), and distinguished five different safflorites which, because of differing Fe:Co ratios, have slightly different X-ray diffraction patterns. Radcliffe and Berry also note

that the safflorites are predominantly orthorhombic, although monoclinic examples have been recorded since (Petruk, 1971). Skutterudites have frequently been reported as being arsenic-deficient, and this is well-documented by Petruk (1971) who gives an average Fe:As ratio of 1:2.8.

Electron microprobe analyses on samples from the Cobalt area, Ontario, have substantiated the proposals presented above (Petruk, 1971). Consequently, it was not considered worthwhile to examine the exact chemical nature of the mineral phases. Rather, it is the relations between coexisting phases and the trends in mineral zoning that are of interest, and it is these that were investigated using the electron microprobe.

In this study, the higher arsenides were identified optically and separated into isometric and non-isometric groups. X-ray diffraction studies on rare samples that were large enough to permit extraction confirmed the isometric series as skutterudites, and the second series as either rammelsbergite or 'safflorites'. Further optical data, including the use of microhardness and reflectance measurements, allowed clear separation of the rammelsbergite and 'safflorite' groups. Safflorite (*sensu stricto*) could not be distinguished optically from lollingite.

Two lower arsenides were encountered during the investigation, namely, niccolite and maucherite. Pararammelsbergite was not observed.

The arsenides occur as single crystals in the wall-rock or gangue, as dendrites, rosettes and tubercules, and as massive patches formed

by the coalescence of finer structures. The rosettes are not the cross-sections of dendrites, but are clearly spherical. The tubercles are morphologically similar to the dendrites, but are straight-stemmed and unbranched.

All three structures are made up of very finely-banded, mixed arsenides. Relationships in the banded areas are variable, but the following generalisations can be made.

1. Cores are more coarsely crystalline, and rims most finely-banded (Plates 6.2, 6.3 and 6.4).
2. Banding may parallel and reflect the shape of the outer walls of the structure, may parallel inclusions in the core, or may be highly variable (Plates 6.3 and 6.4).
3. Niccolite and maucherite generally occur in the centre of structures.
4. Rammelsbergite is most common near the centre of structures, but thin bands occur in many of the diarsenide-rich areas.
5. Maucherite appears to have formed at the expense of niccolite and was not deposited initially (Plates 6.3 and 6.5).
6. Many of the structures examined in hand specimen show that niccolite with rammelsbergite rims formed initially, and that this recrystallised later and was rimmed further by other arsenides.
7. In banded di- and triarsenide sequences, the triarsenide bands are often preferentially replaced - e.g. by bismuth, fluorite, quartz, carbonate or sulphosalts (Plate 10: 1-5).
8. In polished sections containing niccolite, diarsenides,

skutterudites and silver, silver was seen only in niccolite in 14 and on the edge of rammelsbergite bands in the other five.

9. In 23 polished sections containing all the arsenides and bismuth, bismuth was seen only in the triarsenides in 18, and in carbonate gangue in the remaining five. Silver in three of these samples was confined to the niccolite.

10. There are Ni-As-rich areas in the ore-lenses, and silver is generally associated with them. Co- and Fe-As-rich areas are more widespread, generally occur on either side of the Ni-rich areas, and have bismuth closely associated.

11. No zoning of arsenides along the veins or with depth was noted by the author, but the mine was really too small in 1970 for such details to be observed consistently. The presence of different assemblages probably indicates that such zoning will be found now that more of the veins are available for study (see especially, Petruk, 1971, for comparable data from the Cobalt area, Ontario).

Electron microprobe data substantiate many of these generalisations and permit further ones:

1. There is no Co-rich (Co > 80%) diarsenide; but all the skutterudites are Co-rich (Co > 80% of metal).

2. The Ni-content of safflorites is much lower where these are in contact with bismuth than in Bi-free areas.

3. The Ni-content of arsenides is much higher adjacent to silver in arsenide cores. However, it is not enriched where silver veins transect banded arsenides (Plate 7.1).



4. Fe-rich diarsenides are only seen in thin, discontinuous bands in diarsenide sequences (Plate 7.2), or as thin skins on the outer margins of dendrites (Plate 7.1).

5. Co- and Fe-rich arsenides are more common in the outer margins of structures (Plate 7.1).

6. Co- and Fe-rich diarsenide sequences are often intimately interbanded with triarsenides. Ni-rich arsenides are never seen in association with triarsenides.

The investigations of Sample TM 16.1, (Plates 6.3 and 6.4) show the typical zonation of diarsenides around a silver core. The silver has replaced carbonates and has been slightly remobilised to fill thin cracks in the arsenides. Close to the silver, the arsenides are niccolite, maucherite and rammelsbergite, and these occur as a well-crystallised aggregate. Around these are botryoidal bands of diarsenides. X-ray scanning photographs (Plate 7.1) show the complexity of these bands. Compositional bands do not necessarily coincide with colour bands. To determine the variances in the three metals, a step-scan was made. The path of this scan is shown on both Plates 6.3 and 7.1. Peak counts on standards were made for Ni, Co, Fe and As, and the approximate compositions of points on the step-scans were estimated from these. No corrections are made, but then it is not detailed analyses that are required. The sample was counted in 23 spots (40 $\mu$ ) at 9  $\mu$  intervals. The results are shown in Figure 42. Spot analyses probably integrate a number of cryptic compositional bands, but the variations between Ni, Co and Fe are of interest. It

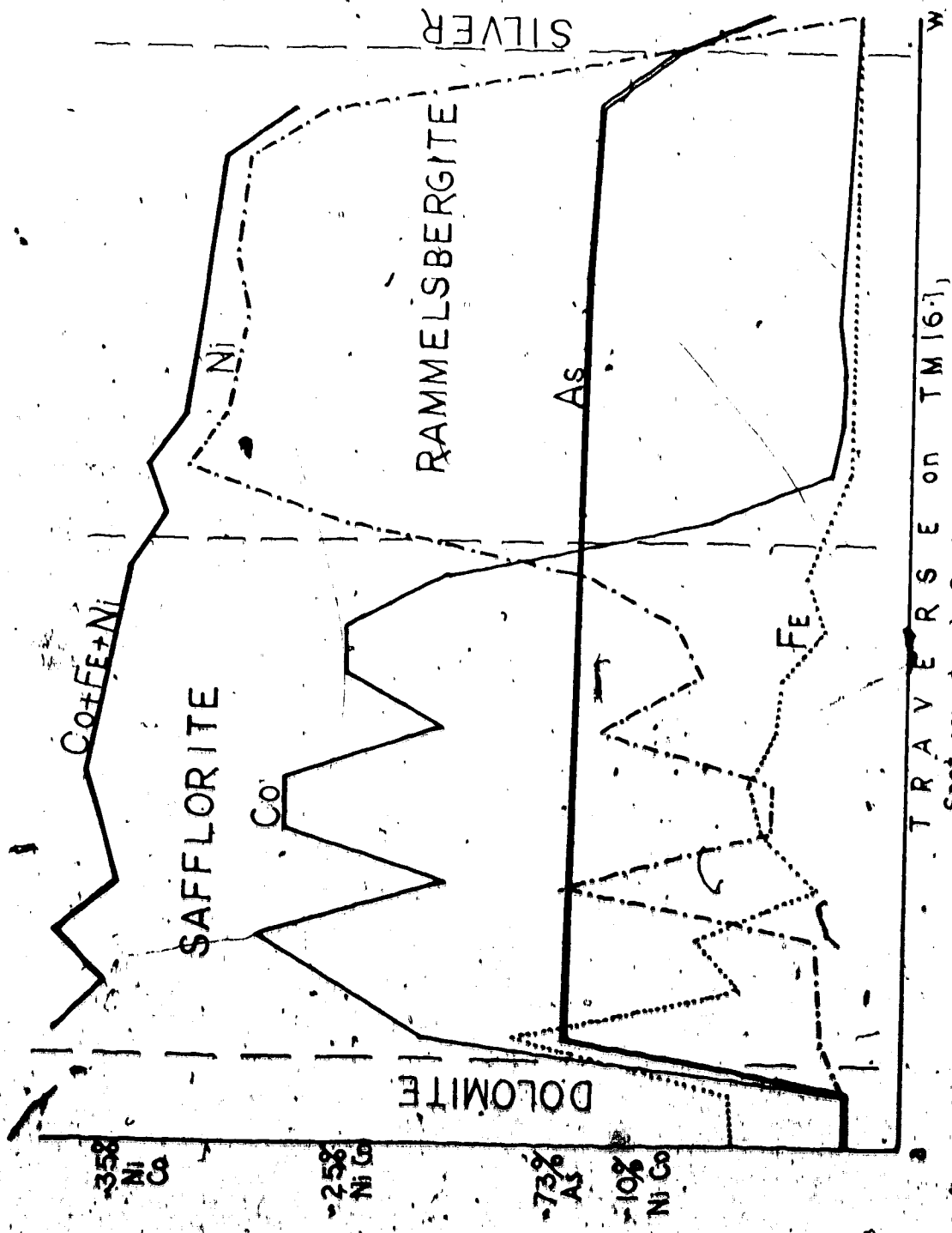


Figure 42. Variation in Ni-Co-Fe across a zoned arsenide. The traverse is located on Plate 7.1.

can be seen from the constancy of the As and total Co + Fe + Ni that all the minerals are diarsenides. Nickel and cobalt, however, vary antipathetically. Iron shows some sympathetic variations with cobalt but generally decreases from the margin inwards. The transition zone between rammelsbergite and safflorite is real and is about 20  $\mu$  wide.

X-ray scanning photographs of Sample TJ 11.2A<sub>4</sub> (Plate 7.2) show similar features, although here the original silver core has been completely replaced by fluorite. The band immediately around the fluorite is a skutterudite, and seems to contain approximately equal amounts of the three metals. The remaining bands are all diarsenides. It is interesting to note the thin broken band of almost-pure lollingite. Other examples of mixed skutterudite cores with banded diarsenides around them were investigated. In general they only occur away from Ag- and Ni-rich lenses, and many examples were seen where sulphosalts and bismuth replaced these skutterudites, but not the diarsenides.

One of the most intriguing facets of the arsenides is the banding. How does it form? Many authors have dismissed the problem with generalities, such as that they are colloidal, or that they are growth bands. From the descriptions above, however, it is clear that many of the bands, and certainly the well-crystallised cores, are not original, but are post-depositional features. Another problem lies in knowing which was deposited first: the outside or the inside? It has been shown earlier that some dendrites can grow by rim replacement and gradual infilling. Others have clearly grown outwards. How can

rosettes, for instance, have grown inwards, for they would cut off their own supply? A number of hypotheses have appeared in the literature, although some are less plausible than others. Oelsner (1961) proposed that native metals (Ag, Bi) formed skeletons in an arsenide gel which then coagulated into the arsenide assemblages in successive bands. This, however, fails to account for the common relict cores of carbonate. Kidd and Haycock (1936) and Stanton (1972) assume that the arsenides accreted in successive bands around silver, bismuth, or carbonate cores. Both mention the possibility of colloidal precipitation. Robinson (1971) proposes the accretion hypothesis for the Echo Bay samples.

In general it can be seen that a paragenesis of Ni-Co+Fe is developed in the arsenides at Terra. Since Ni-rich minerals generally form at cores, it is assumed that the Co- and Fe-rich arsenides grew around them. However, the exact mechanism of banding is not known. That successive incredibly thin bands were able to replace the carbonates with equal facility is unlikely. It is proposed that the bands developed from a single phase, or at the most two separate phases. The bands may have developed with their present chemistry by direct precipitation from a gel; or a mixed arsenide, stable at higher temperatures, may have formed first and broken down into the banded di- and triarsenide sequences as it became unstable. This second mechanism is preferred.

Phase relation studies of the arsenide minerals are not common, perhaps the best being that of Yund (1961) on the Ni-As system. Yund

implies that rammelsbergite is unstable and reverts to pararammelsbergite at  $590 \pm 10^\circ\text{C}$  under the vapour pressure of the assemblage. Petruk (1971, 1972) used this data to propose a high temperature of formation for the veins in the Cobalt district. Other evidence from fluid inclusion and isotope work (Robinson, 1971) and from the preservation of pre-arsenide assemblages, indicates that temperatures cannot have been in excess of  $300^\circ\text{C}$ . Yund, himself, doubts that the inversion occurs at such high temperatures in natural examples, and indicates that iron, cobalt and sulphur may all lower the inversion temperature, so that "it is not possible to set a lower temperature limit for the formation of rammelsbergite in nature."

The sequence of arsenides is most likely to represent deposition from a cooling and chemically-evolving fluid. The data indicate that skutterudites were apparently unable to crystallise until the Ni-content of the fluid was severely depleted, and the same is true of the safflorites. It is proposed that an original fluid, containing nickel, cobalt, iron and arsenic, was injected into the veins. As it cooled, so Ni-rich minerals precipitated until the temperature and Ni-contents were low enough for Co-Fe arsenides to form. These either exsolved from the breakdown of an original complex mineral, or were deposited sequentially. Probably, at the same time as they started to crystallise, the Ni-rich core minerals recrystallised and maucherite was formed from niccolite. Later fluid injections failed to crystallise the arsenides, but often selectively replaced them.

### Sulpharsenides

Sulpharsenides are not common in the Terra Mine. Arsenopyrite was identified in hand specimen, cobaltite and glaucodot in polished section, and gersdorffite, tentatively, from an X-ray diffraction pattern. They all occur as small euhedral crystals, either in carbonates or in areas where sulphides have overgrown earlier-formed arsenides. Cobaltite was also tentatively identified in two examples, intergrown with skutterudite in rosettes.

### Bismuth

Native bismuth is one of the most abundant ore-minerals in the veins of the Terra Mine. Massive pods of bismuth frequently replace gangue minerals in some of the cross-fractures, forming a most spectacular ore. The bismuth was introduced in Stages 3a and 3b and can be seen intergrown with carbonates, quartz, fluorite, muscovite, sulphides and sulphosalts. The metal occurs in four separate settings. Firstly, bismuth commonly replaces Co-rich arsenides. In these situations, bismuth and silver never coexist. Initial replacements occur as 'speck zones' of bismuth along bands in the arsenides. These later fill out and join, forming massive patches (Plate 10.5). In other cases, bismuth forms skeletal growths in arsenides. These have an unusual morphology, resembling the figures on Haida totem poles in British Columbia. Rather poor examples of these 'totem structures' are shown in Plates 10.1 and 10.2. In all cases the bismuth has clearly replaced the arsenides. It is, in turn, frequently overgrown by quartz.

sulphides, sulphosalts or fluorite (Plate 10.1). Elsewhere, bismuth overgrows sulphosalts that have replaced the Co-rich arsenides, and here the totem structures are beautifully developed (Fig. 43).

Secondly, bismuth is common as veinlets and blebs in the Stage 3 dolomites. Sometimes these are replacive, and sometimes they have grown interstitially. They are intergrown with sulphides and fluorite. Where there is some quartz in the carbonate, the bismuth grows all around it, forming a massive ore with 'quartz eyes'. There are commonly thin reaction zones where bismuth is in contact with sulphides, and one in particular can be well documented. Here, bismuth and chalcopyrite have reacted to form emplectite, with the excess iron apparently forming pyrite and pyrrhotite, perhaps thus:



Thirdly, bismuth replaces chloritised wall-rocks, especially around Bi-bearing veins. This replacement is often extensive, forming a rich ore. The bismuth occurs as nebulous to massive patches and as complex micro-vein stockworks. Later shear planes are often coated with smears of the metal.

Fourthly, minute specks of bismuth are often exsolved from sulphosalts - especially tetrahedrite and galena (Plate 11.8). These specks were mistaken for similar ones of silver at first, but were later identified as bismuth during the electron microprobe analyses.

Bismuth is very commonly replaced by bismuthinite (Plate 10.5).

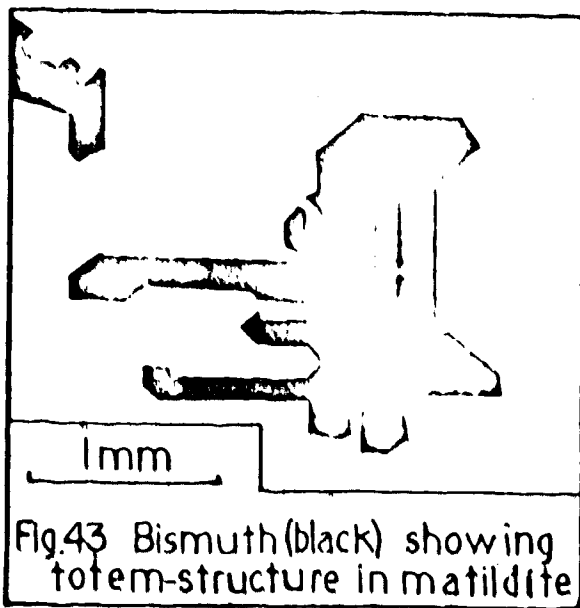


Fig.43 Bismuth (black) showing totem-structure in matildite

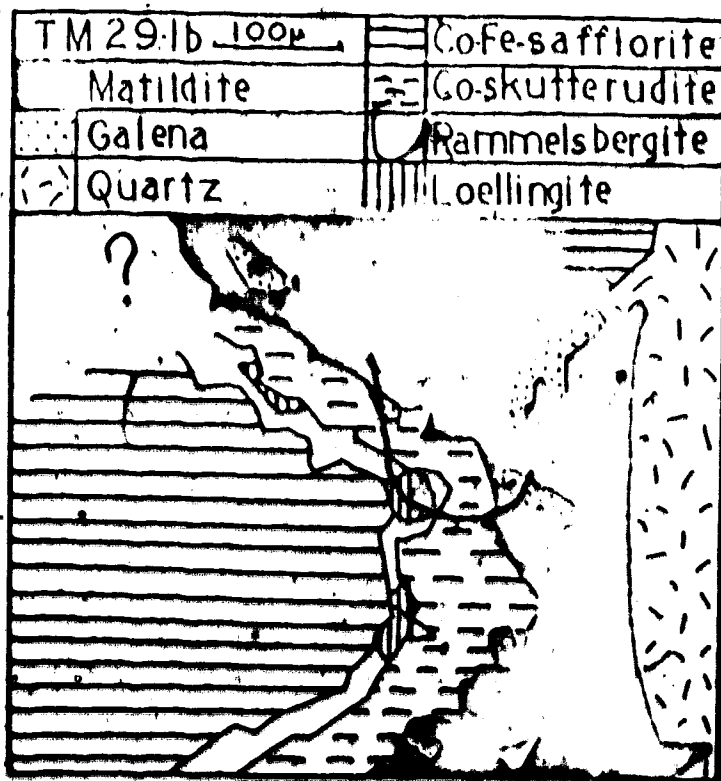


Figure 44. Compilation of Electron microprobe data showing Sulphosalts replacing zoned arsenides. See also Plate 10.7.



In many cases it seems that the metal and sulphide were growing simultaneously from an ore-fluid, either with a limited sulphur content, or whose sulphur was preferentially taken up by other minerals. However, as deposition progressed, so sulphur apparently became more available to the bismuth; consequently, the bismuthinite started to overgrow the earlier-formed bismuth.

The mercury and silver contents of some arsenide-replacing and some exsolved bismuths were measured using the electron microprobe, during the silver analyses. The results are reported in Table 8 (along with values for a Silver Bay sample). No conclusions can be drawn, other than that the mercury content is of the same order as that in the silver.

Sample	Ag app wt %	Hg app wt %	No. grains counted
TM 30.7 <sub>2</sub>	0.175	1.46	6
TJ 11.2D <sub>2</sub>	0.09	1.44	5
SBX 10.3A	0.01	1.08	2

Table 8: Operating Conditions as for Ryn 2, Table 6

From the replacement textures it is evident that bismuth was introduced during much of Stage 3 and that it replaces, is replaced by, and grows with the other minerals of this stage. There is no evidence of a pre-arsenide bismuth - the replacement textures are always obvious, which contrasts with the ambiguous textures of silver in the arsenides.

### Sulphides

Small amounts of pyrite are associated with every stage of mineralisation. However, sulphides are only common in the veins at the beginning of Stage 3. Sulphides identified are: pyrite, chalcopyrite, galena, sphalerite, acanthite, bismuthinite, stibnite, chalcocite, pyrrhotite, pentlandite, and millerite. The last three are very scarce. Pyrrhotite and pentlandite were seen only as thin slivers at contacts between bismuth- and iron-bearing sulphides and are presumed to be reaction products. Specks of millerite were seen replacing niccolite in the core of a rosette in one specimen only.

Stibnite was not observed in polished section, but crystals over 2 cm long, intergrown with dolomite, fluorite and pyrite, were found in two vugs. The only example of chalcocite was observed in one of these vugs as a thin layer intergrown with Stage 4 pyrite.

Bismuthinite is extremely common in the sulphide- and sulphosalt-rich lenses. It commonly replaces (Plate 10.5), but is also intergrown with bismuth, as well as tetrahedrite, galena and matildite. These five minerals commonly make up a massive rich ore. Indeed, areas in the 201 stope commonly contained solid pods of them over 50 cm wide and 2 m long and high. The bismuthinite commonly occurs as coarse-grained laths, intergrown with these other minerals. However, it also often replaces the base-metal sulphides in fine 'net-like' zones along cracks (Plate 5.4). X-ray diffraction data for six bismuthinite samples show no variation and are typical of pure  $\text{Bi}_2\text{S}_3$  with no antimony substitution.

Acanthite is common in the upper levels of the mine, where it occurs patchily in Stage 3 carbonates. It is commonly smeared-out by late fault-movements. In the second-level samples it is not common and occurs only as local replacements of massive silver in arsenide cores (Plate 6.5). Acanthite is often seen in thin films on fractures and working faces in the mine a few months after they were blasted. Such 'silver glance' is common in silver mines (Boyle, 1968).

Pyrite and the base-metal sulphides are common in the veins, but are not volumetrically important. They occur as isolated euhedral crystals and monomineralic bands in the Stage 3 carbonates, although galena and chalcopyrite are also common as blebs and lenses in the sulphosalts. Galena has often been smeared-out by later movements on the faults (Plate 9.4). Galena, chalcopyrite and tetrahedrite are commonly intergrown in blebs in the Stage 3 dolomites. Pyrite and, very rarely, chalcopyrite overgrow the Stage 4 calcite scalenohedra in a thin layer of fine crystals.

Many of the base-metal sulphides are clearly remobilised from the skarn by the veins. However, there is a volume problem in that galena, which is the least common in the skarn, is the most abundant in the veins. Consequently, there must have been an introduction of base metals in Stage 3, along with the bismuth, silver and sulphosalts.

Sulphur isotope data from the vein sulphides are shown in Table 9. It proved possible to sample only one coexisting pair of sulphides whose  $\delta S^{34}$  fractionation is experimentally documented - the chalcopyrite and galena in TM 25-10. The fractionation of +5.0% (Cp-Gn) indicates

Table 9. Sulphur Isotope Values of Vein Sulphides and Sulphosalts in the Terra Mine.

Sample	Mineral	Paragenetic Stage	$\delta S^{34}\%$ (CDT)
TM21.4C	a. Chalcopyrite in coarse Dolomite	3a	2.6±0.1
	b. " overgrowing a.	3b/4?	5.9±0.1
TM24.1	Fine Galena impregnating chloritised wall-rock	3a	4.2±0.1
TM25.8	Massive Matildite on edge of Dolomite vein	3b	4.2±0.1
TM25.10	a. Galena in Sulphide band	3a	1.4±0.1
	b. Chalcopyrite in a.	3a	6.4±0.1
TM30.1A	Chalcopyrite in Dolomite	3b	8.8±0.1*
TJ3.1A	Chalcopyrite on late Calcite in Vug	4	4.3±0.1
TJ11.2A	Chalcopyrite (With Tetrahedrite) in Fluorite and Dolomite.	3b	4.0±0.1*
TJ19.1	Pyrite on Calcite in Vug	4	-26.0±0.1 <sup>†</sup>
TX3.3	a. Chalcopyrite in Dolomite	3a	3.7±0.1
	b. Tetrahedrite in a.	3a	3.7±0.1
A2.1	Bismuthinite with Bismuth	3b	2.7±0.1
A2.18	Matildite in Dolomite	3b	1.4±0.1

\* Samples with more than 20% CO<sub>2</sub> in the extracted gasses.

<sup>†</sup> Analysis repeated and confirmed.

that if the minerals are in isotopic equilibrium, then they formed at something less than 50°C (Kajiwara and Krouse, 1971). This is considered unreasonably low, and the conclusion is that the sulphides are not in isotopic equilibrium. There is no available data of fractionations between the other base-metal sulphides, acanthite, bismuthinite or sulphosalts.

The results do indicate, however, the small spread of the isotopic values and the very close similarity to those of the skarn sulphides. These low values and the small spread are typical of magmatic hydrothermal deposits (e.g. Jensen, 1967). The only disparate value is for the very late-stage pyrite (TJ 19.1) - the datum was checked by resampling and analysing, and the first result was duplicated to within the limits of error. Such highly negative values are not common and are usually taken to represent biogenic fractionations or sulphate-sulphide reductions at low temperatures (Sakai, 1969). This pyrite was formed after the main mineralisation and represents a fundamentally different source of sulphur from that of the other sulphides in the area.

One sample of bismuthinite was analysed using the electron microprobe. The results are shown in Table 11. Problems with the analyses are described in the following section on sulphosalts. Essentially, the mineral contains only about 2% Pb, and small amounts of Ag, Zn, As and Sb.

### Sulphosalts

The sulphosalts occur as massive and mixed ore, as complex replacements of arsenides, or as intergrowths with sulphides. In polished section and hand specimen they are all closely similar, and different phases are recognised only by subtle nuances of colour in polished section. The complexity of intergrowths often makes X-ray diffraction work impossible, and certain identification can only be made after microprobe analysis.

Pyrargyrite ( $\text{Ag}_3\text{SbS}_3$ ) was seen in a number of hand specimens as small flakes on shear planes, along with acanthite. It is considered to be a late-stage alteration product of other silver sulphosalts.

Pavonite ( $\text{AgBi}_3\text{S}_5$ ) occurs rarely as rosettes of tiny fibres growing between large dolomite crystals at vug centres. Again, it is presumed to be the product of alteration of other sulphosalts. Pavonite has been recorded previously only from Bolivia (Ramdohr, 1969), where its paragenetic position is not documented.

Stephanite ( $\text{Ag}_5\text{SbS}_4$ ) was identified from X-ray diffraction data only, in a mixture with matildite. The two occur as blebs with fluorite and chalcopyrite in Stage 3 dolomite. Stephanite could not be distinguished from matildite in polished section - Ramdohr admits that the two can be "dangerously similar".

Polybasite ( $\text{Ag}_{16}\text{Sb}_2\text{S}_{11}$ ) was identified from an X-ray diffraction pattern only. The sample was taken from a bleb of sulphosalts in Stage 3 dolomite. Tetrahedrite and argentite were the only minerals positively identified from polished section alone, although small

grains of other sulphosalt phases were noted.

Matildite and tetrahedrite are the two most common sulphosalts at Terra. Matildite ( $\text{AgBiS}_2$ ) forms the end member of a solid solution series with miargyrite ( $\text{AgSbS}_2$ ) and intermediate members are generally known as 'aramaoite'. The X-ray diffraction pattern changes with the substitution, and a progressive change is shown by the (002) line. Powder photographs were prepared for 10 matildites and the data are shown in Table 10, where they are compared with published values for the members of the solid solution series. It is clear that the Terra samples are mostly pure matildite end members.

Matildite forms in massive patches: as intergrowths with bismuth, tetrahedrite, bismuthinite and galena (contrary to data in Harris and Thorpe, 1969); as replacements of arsenides (Plates 10.2, 10.3 and 10.4); or as minute exsolved blebs in tetrahedrite. It is especially common replacing Co-rich arsenides, often selectively, in certain zones. In these zones it has grown with, or is replaced by fluorite (Plate 10.3). The matildite shown in Plate 10.2, and another occurring as exsolved blebs in tetrahedrite, were analysed using the electron microprobe, and the results are reported in Table 11. It can be seen that they are very similar and are pure matildites with no antimony or arsenic substitution in the bismuth site, thus confirming the X-ray diffraction data. These data agree well with earlier observations on matildite from the surface outcrop of the Number 8 vein (Harris and Thorpe, 1969).

Although galena and matildite commonly occur together, the

Table 10. d-Spacings of the Principal Diffraction lines of ten Matildite samples from the Terra Mine, compared with data from Ramdohr (1969)\* and the A.S.T.M. Index (1972)†.

Sample	dÅ(002)	dÅ(011)	dÅ(020)	dÅ(200)
1	2.80	3.30	2.04	1.96
2	2.80	3.28	2.02	1.97
3	2.80	3.26	2.02	1.97
4	2.81	3.30	2.03	1.98
5	2.81	3.30	2.03	1.96
6	2.81	3.29	2.03	1.96
7	2.82	3.30	2.04	1.97
8	2.83	3.30	2.04	1.97
9	2.83	3.31	2.04	1.97
10	2.84	3.29	2.02	1.97
Matildite*	2.83	3.32	2.03	1.963
Aramaoite*	2.84	3.24	-	-
Margyrite*	2.88	3.42	-	-
Matildite†	2.84	3.33	2.03	1.96
Aramaoite†	2.82	3.22	2.02	1.94
Margyrite†	2.88	3.44	2.75	1.96

Operating conditions for samples 1-10:

Radiation: CuK $\alpha$  .Filter: Ni. Exposure: 3 hours at 35 K.volts and 15m.amps.



Sample wt.-%	TUX02.1dk.	TUX02.11t.	TJ10.1B	TJ11.2D
Ag	12.8 (15.69)	23.1	23.6	0.46
Cu	28.9 (26.73)	0.95	0.15	0.41
Pb	0.39 (0.46)	0.25	0.20	2.33
Zn	1.93 (1.83)	0.54	0.50	0.69
Fe	4.48	0.18	0	0
As	0.1 (0.16)	0.4	0.1	0.1
Sb	23.8 (26.15)	0	0	0.2
Bi	0.6	46.7	47.6	71.6
S	24.6 (23.1)	20.7	20.9	23.8
Total	97.60 (94.38)	92.82	93.15	99.59

Table 11. Electron microprobe analyses of Tetrahedrite, Matildite and Bismuthinite. Background corrections have been made on all the results. Results for sample TUX02.1dk. were further corrected using Probedata (Smith and Tomlinson, 1970), and are shown in parentheses. Complete scans were made on all the samples and no other elements were detected. Analytical conditions are shown in Appendix 2.

TUX02.1dk	Tetrahedrite
TUX02.11t	Matildite
TJ10.1B	Matildite
TJ11.2D	Bismuthinite

presence of the galena wherever matildite occurs is not a pre-requisite, as appears to be the case in many other occurrences, and the common Widmanstätten-texture intergrowths were not seen in Terra samples. However, specks of galena were found in one sample during electron microprobe studies. X-ray scanning photographs (Plate 10.6) show matildite replacing Co-rich arsenides, and containing minute exsolution blebs of galena (Fig. 44). Matildite and galena form a complete solid solution above 215° (Craig, 1967), but break down into exsolution intergrowths below this temperature. If the mineralising fluid is below 215°C initially, then galena-free matildite may form - as appears to be the case in most of the Terra samples.

Tetrahedrite is common, intergrown with sulphides and sulphosalts. It has not been observed replacing any of the earlier phases of mineralisation. In more massive patches it commonly contains exsolution blebs of silver, bismuth, galena, matildite and chalcopyrite.

X-ray diffraction data for five tetrahedrites from different associations showed little variation. Electron microprobe analyses of one tetrahedrite (Table 12) (containing exsolved chalcopyrite and matildite) show it to contain considerable amounts of silver with a little iron, lead and zinc substituted for copper, but no bismuth and little arsenic substitution in the antimony site. Calculations of the structural formula (Table 13) show the tetrahedrite to be fairly stoichiometric. It compares closely with argentiferous tetrahedrites from the Cobalt area (Petruk, 1971), but does not contain enough silver to be classified as a true argentiferous tetrahedrite.

TUX02.1dk.

Atomic %	Atomic proportions on the basis of 13 Sulphur atoms.
Ag 9.42	2.59
Cu 27.31	7.51
Pb 0.14	0.04
Zn 1.82	0.50
	<hr/> 10.54 <hr/>
Fe -	
As 1.41	0.39
Sb 13.94	3.84
Bi 0	0
	<hr/> 4.23 <hr/>
S 47.21	13.0

This corresponds closely to the ideal Tetrahedrite formula of  $M_{12}N_4S_{13}$ . The deficiency in the M site can be accounted for by Iron, which was analysed later, and for which corrections were not made.

Table 12. Atomic percentages of elements in the Tetrahedrite sample.

The data in Table 11 have not been corrected and it is pertinent at this juncture to explain why. Considerable problems arose with the microprobe analysis of the sulphosalts, and it is as well to trace some of the problems and their solutions here, so that other workers may avoid the same pitfalls.

In 1970, tetrahedrite and an exsolved phase, thought to be galena, were identified optically in Sample TUX 02.1. A short electron microprobe investigation showed that the tetrahedrite contained Sb, S, Cu and Ag, with traces of Zn, As, Pb and Bi. The 'galena' was found to contain Ag, Bi, S and traces of Cu, Zn, Pb and As. Bi and Pb were analysed using M-lines, for which the correction programme 'Probedata' (Smith and Tomlinson, 1970) has no data. The results were consequently not corrected for atomic number fluorescence and absorption effects. Apparent concentrations, however, indicated that these were complex sulphosalts, and a complete analysis was proposed.

In 1972, during examination of over 200 polished sections, two sulphosalts which could not be positively identified were often found. Samples (TJ 10.1B and TJ 11.2D) containing these were selected for analysis.

Early in 1973, complete X-ray scans were made of all four minerals and only Ag, Cu, Pb, Zn, As, Sb, Bi, S and (in one) Fe were detected. Analyses using K- and L-lines only were carried out, and apparent totals in excess of 100% were found (Table 13). Subsequent corrections using Probedata only increased this excess!

The analyses had been set up with some care (perhaps not enough,

Sample # Analysis # App. wt. %	TUX02.1dk.			TUX02.11t.			TJ10.1B.			TJ11.2D		
	1	2	3	1	2	3	1	2	3	1	2	3
Ag	12.8	-	-	23.1	-	-	23.6	-	-	0.46	-	-
C	29.0	-	28.9	12.0	-	0.95	4.0	-	0.15	9.0	-	0.41
Pb	0	0.39	-	2.10	0.25	-	2.0	0.2	-	3.0	2.33	-
Zn	1.93	-	-	0.54	-	-	0.50	-	-	0.69	-	-
Fe	-	-	4.48	-	-	0.18	-	-	0	-	-	0
As	0.1	-	-	0.4	-	-	0.1	-	-	0.1	-	-
Sb	23.8	-	-	0	-	-	0	-	-	0.2	-	-
Bi	2.0	0.6	-	40.5	46.7	-	50	47.6	-	75	71.6	-
S	24.6	-	-	20.7	-	-	20.9	-	-	23.8	-	-
Total	94	93	97.6	108	104	92.82	101	97	93.15	112	108	99.59

Table 13. Apparent analyses of the Sulphosalts after each of the three Electron Microprobe investigations. Refer to the text for details of the corrections applied to each set of data.

as it happened) to avoid especially fluorescence effects and inaccuracies from 'tail-effects' of overlapping peaks. Counting procedures were arranged in such a way that any sample inhomogeneities would be detected. The only inhomogeneities were in the bismuth content of the tetrahedrite (< 0.1%) and in the bismuth and lead contents of TUX 02.1 Lt. In the latter case, the apparent variation was between grains, but not within single grains.

Results of this first analysis indicated that the apparent percentage of lead varied proportionately with the apparent percentage of bismuth. It was immediately suspected that there had been an error in setting and that the effects of overlap of the  $\text{BiLa}$  and  $\text{PbLa}$  peaks had not been fully avoided. Consequently, a scan was made over the peaks for standards and samples and it was found that there was far less lead in the samples than the original analyses had indicated. The samples were re-analysed for bismuth and lead. Background measurements were taken below the  $\text{PbLa}$  and above the  $\text{BiLa}$  peaks, and corrections from the peaks were made using a graphical extrapolation. The results of this analysis show very little lead in the samples (Table 11). It was also now found that all grains in TUX 02.1 Lt were the same, and that the inhomogeneities had been apparent. However, the apparent totals were still in excess of 100% and the minerals were still not identifiable. It was thought at this time that there might be new minerals, and the results were corrected again using Probedata. The correction factors were impressive mainly due to the great range in atomic numbers of the analysed elements, but the totals increased

once more. It was noted, however, that the fluorescence correction for sulphur was small. It was known that bismuth fluoresced sulphur, and because of the amounts of bismuth in the samples it was thought that this correction should be larger. It was finally realised that the fluorescing line was BiMa, and that the correction programme was not 'aware' that this line existed, and could not, therefore, make the correction. Consequently, the results were corrected again, this time assuming the percentage of sulphur by difference. These data showed Sample TUX 02.1D<sub>1</sub> to be a reasonable stoichiometric tetrahedrite. The remaining samples were still not identifiable (although the data were not much changed), and were thought to be new minerals. There were, however, still some doubts. It was apparent that the amount of excess in the analyses was approximately proportional to the percentages of copper and bismuth. In addition, Samples TUX 02.1Lt and TJ 10.1B were remarkably similar in all respects, except for the percentage of copper. To clear all suspicion and confirm three new minerals, the samples were checked for their copper content - complete scans over the copper peak showed only trace contents in all the samples! From where had the original apparent copper counts come? The immediate suspect was bismuth. Close investigation, however, revealed no bismuth line of any sort in the CuK $\alpha$  region. Consequently, re-analysis for copper was proposed, and on this run iron was also analysed, to see if its presence accounted for the apparent metal deficiency in the tetrahedrite.

The results were alarming (Table 13). The iron content of the

tetrahedrite in order to fill the deficiency, and there the analysis of tetrahedrite rests. The apparent copper content of the tetrahedrite was changed only in the second decimal place by this analysis, which indicated that there could be no setting-up error in the first run. However, the copper contents of the remaining three samples were reduced to less than 1% and the resultant apparent totals to less than 100%. The counts for copper on the standard before and after the sample analyses were almost identical. It would be an incredible coincidence if some electronic malfunction were to operate to give spurious copper counts during the exact extent of the last three analyses. There is at present, therefore, no apparent explanation for this anomaly, and none is offered.

Subsequent processing of the final results indicates that two of the samples are matildite and one bismuthinite. Scrapings of the sulphosalt-arsenide intergrowths were taken, and X-ray diffraction patterns of this material revealed that lines of matildite or bismuthinite respectively were present. Consequently, since these were not, after all, new minerals, the results were not corrected - it was thought that the corrected data were not worth the cost of computation.

New sources of error in microprobe analysis have been found and mistakes that might have been avoided with a little more care were made. The tale is told as a warning to future analysts of complex sulphosalts.



### Fluorite, Green Mica and Feldspar-Mica Veins

Fluorite is abundant in the Stage 3 carbonates, intergrown with sulphides, sulphosalts and green mica. It is usually coarse and well crystallised, but in places occurs as thin growth-bands in dolomite. It may be pale blue, green or deep purple. Often the three are intergrown. Simple heating experiments did not alter the colour of the fluorites, at least up to the temperature of a bunsen burner ( $\sim 800^{\circ}\text{C}$ ). It is concluded that the colour is simply a function of structure or trace-element content.

Fluorite commonly replaces silver, bismuth and arsenides (Plates 10.1, 10.3 and 7.2), and where it does, so it is invariably purple. There appears to be no mineralogical control on the occurrence of blue and green fluorite, and purple fluorite is also common away from areas of silver, bismuth or arsenide mineralisation. In places, the wall-rocks are impregnated with the mineral and, beyond the limit of mineralisation, the thin-banded carbonate veins often contain streaks of it.

Veinlets and pods of a pale green mica are also common in Stage 3 carbonates and in the wall-rocks nearby. Veinlets are thin and fibrous, with the fibres oriented normal to the vein walls. Pods are made up of masses of veinlets and bunches of thin sinuous sheets. The morphology and colour of the mica are such that it was initially identified in hand specimen as a serpentine mineral. However, thin section and X-ray diffraction studies showed it to be a muscovite. In thin section the fibrous nature of the mica is well seen and 'flames' of

mica extend into the surrounding dolomite (Plate 5.8). Very rarely, massive, dense, fine-grained patches are found.

The mica veinlets cross-cut bismuth mineralisation (and all preceding stages) but are coeval with the sulphosalts, sulphides and fluorite. The veins themselves are unmineralised, but are most commonly associated with blebs of chalcopyrite. The mica contains no Cr.

An electron microprobe analysis of the mica shown in Plate 5.8 was kindly performed by C.R. Ramsay, and the results are shown in Table 14. On an AKF diagram (Fig. 45) it can be seen that the mica is a typical phengitic muscovite. The colour and morphology remain unexplained.

Three pegmatitic veins containing seams and pods of this mica have been found in the mine. They consist mainly of coarse pink K-feldspar with interstitial quartz, fluorite and chalcopyrite. The veins are not long and the largest is just over 25 cm wide. The centres are vuggy and filled with large quartz crystals. The veins cut arsenide, silver and bismuth mineralisation, and are clearly coeval with the sulphosalts, sulphides, dolomite, quartz and fluorite of late Stage 3. The green mica veins and pods were clearly derived from the same source as the pegmatitic veinlets. Neither type of vein has been observed elsewhere by the author, and there are no reports of similar veins in the mines in the Echo Bay area. Their origin is not known.

### Haematite

Haematite is the most ubiquitous of the vein minerals, being present in one form or another in every stage. Usually it is manifested

Oxide	%
SiO <sub>2</sub>	48.97
TiO <sub>2</sub>	0.02
Al <sub>2</sub> O <sub>3</sub>	28.91
FeO <sub>t</sub>	4.03*
MnO	0.11
MgO	0.89 <sup>†</sup>
CaO	0.04
Na <sub>2</sub> O	0.10
K <sub>2</sub> O	10.77
H <sub>2</sub> O	~4.50
Total	98.33

\* Average value. Grain variation from 1.97- 4.96%.

<sup>†</sup> Average value. Grain variation from 0.35- 1.98%.

Table 14. Analysis of the Green Muscovite in sample TX24.4.

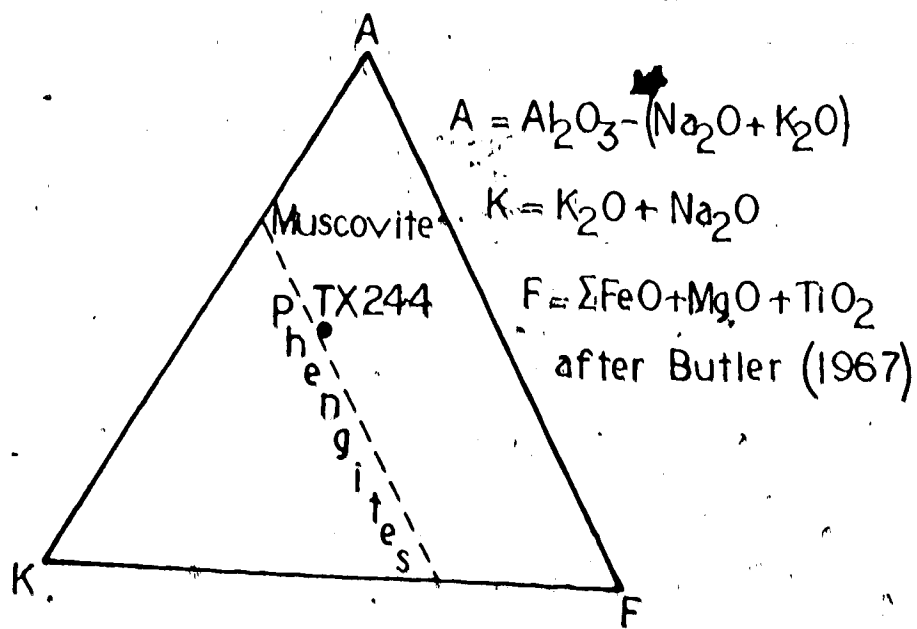


Figure 45. AKF diagram for the Green Muscovite.

by a red dusting of carbonates, especially in the arsenide stage. This redness is more extensive in the earliest vein material. Coatings of haematite appear on quartz and carbonate crystals in Stage 3 and again on the youngest carbonates. Needles in rosettes are common in vugs, between dolomite crystals, and strongly resemble those of pavonite.

#### Alteration Minerals

Annabergite, erythrite, malachite, azurite, goethite, hydrozincite and wad were all identified in surface outcrops of the Number 8 vein, which is extensively weathered. Annabergite and erythrite form in a matter of weeks on massive arsenides left in ore-piles on surface, and were noted a number of times underground. The veins are not oxidised below about 2 m beneath surface.

#### f) Paragenetic Sequence and Depositional Conditions

The paragenesis is shown schematically on Figure 46. Each period of mineralisation was preceded by movement on the faults which cracked open the veins that had been sealed by the previous phase, and permitted an influx of further ore-fluids which again sealed the veins. Although it has been proposed that the main faults were active during the time of batholith emplacement, the mineralised faults were not generated until after this event. First movements on the Terra fault offset the contact and aureole of the stock, as well as the skarn sulphides. The morphology of the veins that filled dilatancies caused



by this first movement is not known, for only brecciated remnants are found. However, uraninite, haematite, quartz and dolomite were introduced soon after, and this phase is probably correlatable with the initial introduction of uranium into the Giant Quartz Veins throughout the Bear Province. Data from Clayton and Epstein (1958) indicate temperatures (from  $O^{18}$  fractionation data) of  $140^{\circ}\text{C}$  and  $150^{\circ}\text{C}$  for this stage of mineralisation in the Eldorado Mine, and Robinson (1971) reports a temperature of  $150^{\circ}\text{C}$  (from fluid inclusion data) for this stage at the Echo Bay Mine.

The first phase of vein mineralisation is different in character from the others, and substantial fault-movements preceded the following stages. Subsequently, a series of multi-element ore-fluids were introduced into dilatancies during small repetitive movements on the faults. The constancy of oxygen and carbon, and sulphur isotopes from dolomites and sulphides, respectively, indicates that all these fluids had the same source. However, the metal content of the veins changes progressively (a fact which may indicate a changing source). This paradox can be explained in four ways:

1. The parent-fluid acted as an infinite source for carbon, oxygen and sulphur, but had such low metal contents as to be depleted in each metal as its salts were precipitated in the veins.
2. The parent-fluid remained unchanged, but the physical and chemical character of the areas of deposition altered, such that different metals were deposited, but sulphur, oxygen and carbon remained in equilibrium with the parent-fluid.

3. Each period of vein-filling may represent a different ore-fluid, but one whose carbon, oxygen and sulphur were derived from a similar source.

4. The ore-fluid was evolving, but the sulphur, oxygen and carbon continually attained equilibrium with the host rocks.

In order to see which explanations are the more probable, it is important to know the depositional temperatures of each stage.

In Stage 2a, silver and arsenides were both formed, but there is a general sequence from Ni-rich to Co- and Fe-rich in the arsenides. This probably represents a cooling, and it seems to be general that in Ni-Co deposits nickel minerals were the first to precipitate. Chlorite was introduced prior to the arsenides and remained unaffected by any later mineralisation. Chlorite breaks down at 600°C (Fawcett and Yoder, 1966) and so the temperature can never have exceeded this. Rammelsbergite ideally inverts to pararammelsbergite at 590°C±10° (Yund, 1961). Although others have used this as a minimum for deposition of rammelsbergite alone (Petruk, 1971, 1972), it is likely that in a mixed, complex system the inversion occurs at much lower temperatures, if at all (Yund, 1961). Pararammelsbergite was not found in the Terra veins. Robinson (1971) quotes temperatures of around 200°C for the arsenide stage in the Echo Bay Mine.

The temperature of deposition throughout Stage 3 can be well documented from the various assemblages present. For example, pyrite coexists with silver at the start of Stage 3, and the two should react to form pyrrhotite and argentite at 235°±25°C (Barton and Skinner, 1967);



this reaction was not observed. For the latter part of Stage 3a and all of Stage 3b, the temperature can never have exceeded 271.5°C, the melting point of bismuth. In Stage 3b, galena was exsolved from matildite in only one example. In all other cases the two were deposited individually. Experimental evidence shows that the two form complete solid solution above  $215 \pm 15^\circ\text{C}$  (Craig, 1967). It is presumed that the depositional temperature was on the order of  $210^\circ\text{C}$  at the start of Stage 3b. At the end of this stage stephanite was deposited, and this is unstable above  $197^\circ\text{C}$  (Keighin and Honea, 1969).

Fluid inclusion and sulphur isotope data from similar stages of mineralisation at Echo Bay show a temperature range from about  $230^\circ\text{C}$  at the start of Stage 3, to about  $100^\circ\text{C}$  by the end (Robinson, 1971).

The physical nature of minerals in Stage 4 indicates low temperatures of deposition, and pavonite, though stable at higher temperatures, is typical in the late stages of silver veins, deposited at temperatures around  $100^\circ\text{C}$  (Ramdohr, 1969).

From this data a time-temperature curve can be constructed (Fig. 47). The availability of various elements in the ore-fluid is assumed to be equivalent to the amount of each element precipitated at the various stages, and is also represented in Figure 47. From this it is apparent that the ore-fluid for Stage 2a was geochemically quite different from the later multi-element fluids. Stage 2b to 3b could have been deposited from a single ore-fluid, or from two separate ones. The single fluid hypothesis is preferred because of the presence of a number of elements common to all the stages.

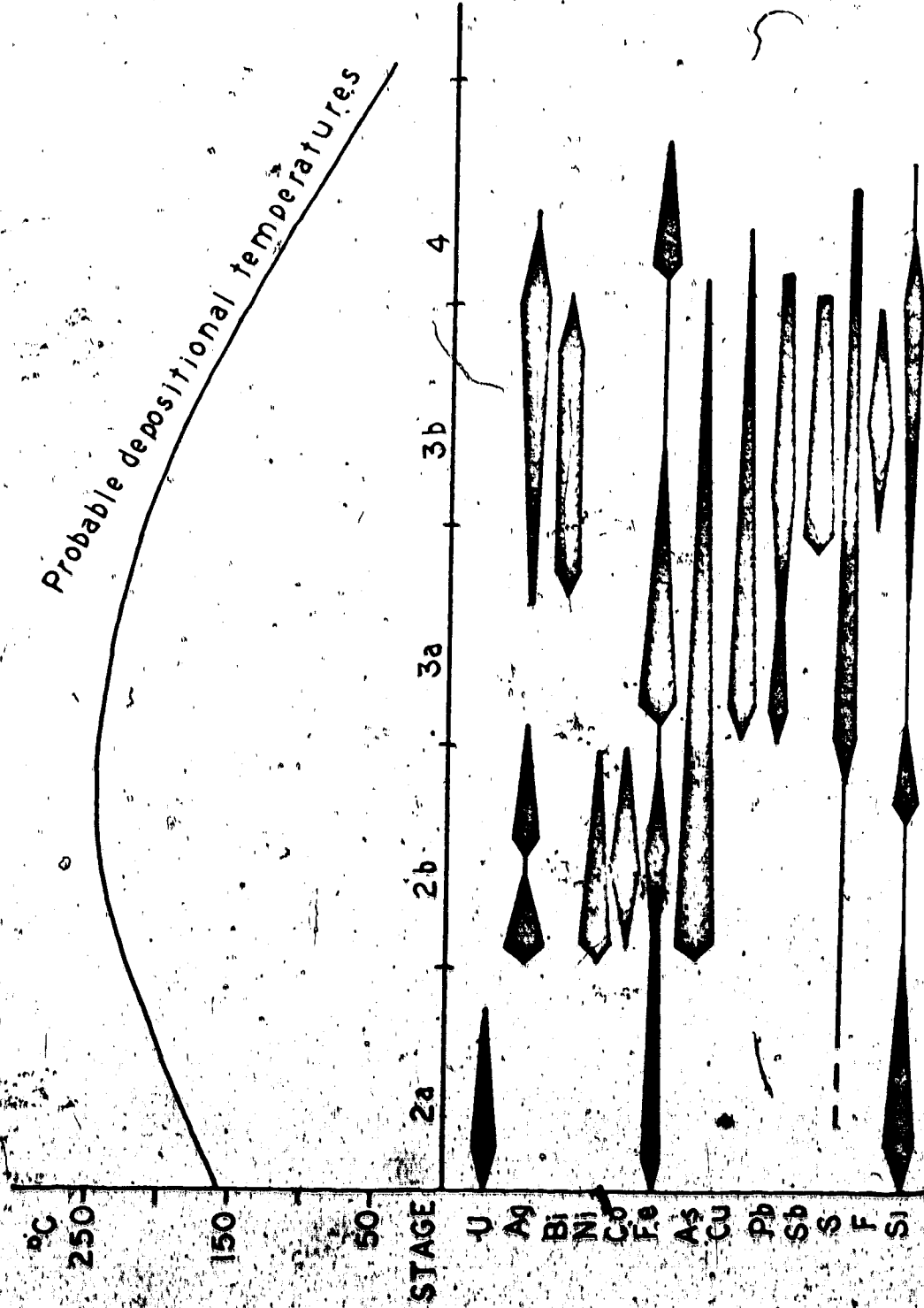


Figure 47. Depositional temperatures and availability of elements during deposition, Terra Mine.

Did this single fluid evolve, from being Ni-Co-Ag-As-rich to being Ag-Bi-base metal-rich, or did it contain all the elements but only precipitate each under certain conditions? In one case we require a changing source condition, and in the other, changing depositional conditions. Since it has already been shown that the depositional temperatures vary, it is likely that it is these that control precipitation, and that the ore-fluid remained fairly constant throughout. It is unlikely that the paragenesis represents a single sequence of crystallisation because of the time and complexity of events involved in a number of depositional stages.

A discussion of the source and evolution of the ores follows the description of the other deposits.

#### g) Ore Potential

The controls of mineralisation outlined above make it unlikely that ore will be found in these veins beyond the confines of the skarned tuff and calcargillite horizon. On the Terra peninsula there are a few other secondary faults (albeit smaller than that on which the mine is situated) cutting this horizon, and they are sites for potential reserves. The limited horizontal extent of mineralisation and the high costs of mining will make exploitation impracticable below a depth of 200 m unless the ore at depth proves considerably richer. The Echo Bay Mine cannot operate profitably with silver values of much less than 100 oz/ton and the mineralisation continues far further there than in the Terna Mine. Recent figures published by Terra for

the six months ending in February, 1973, show that 1.76 million oz. silver were recovered. At the milling rate of 175 tons/day, this is equivalent to a mill head value of just under 70 oz/ton, and realised a net profit of a little over \$500,000. This ore was recovered from the third level, which was considerably richer than much of the first and second levels. Should these grades continue at depth, much of the net profit will be taken with increased mining costs. Consequently, it is important that the mine discover new reserves at shallower levels.

Since this thesis was first written the prices of silver and copper have jumped from \$1.50 to \$2.50 and 45 cents to 70 cents respectively. Price fluctuations of this nature substantially affect the economics of this mine and if the new prices hold, mining over the next few years should realise good profits.

## PLATE 5

1. Marcasite crystals with fingerprint texture, being cut by pyrite (white). Sphalerite (dull grey) replaces the 'fingerprints', giving a net texture. Chalcopyrite (pale grey) and sphalerite surround the grains. Terra: Stage 1. P.P.L.
2. Tremolite being replaced by sphalerite (grey) on margins of a chalcopyrite band. Terra: Stage 1. P.P.L.
3. Marcasite with 'fingerprints' of silicate, overgrown by pyrite (white). Terra: Stage 1. P.P.L.
4. Cataclastic pyrite being replaced by bismuthinite (grey) especially in cracks. Terra: Stage 3A. P.P.L.
5. Carbonate (black) cut by pyrite (white), galena (scratched), chalcopyrite (pale, in galena), sphalerite (dull grey) and quartz (on right) vein. Terra: Stage 3. P.P.L.
6. Fractured arsenopyrite annealed by dolomite. Lypka Vein. P.P.L.
7. Bornite (grey) exsolving chalcopyrite (white) and later chalcocite and some covellite (dark). Jason Vein. P.P.L.
8. Green muscovite (pale) overgrowing carbonate (dark) on edge of muscovite vein. Terra: Stage 3. P.P.L.



PLATE 5

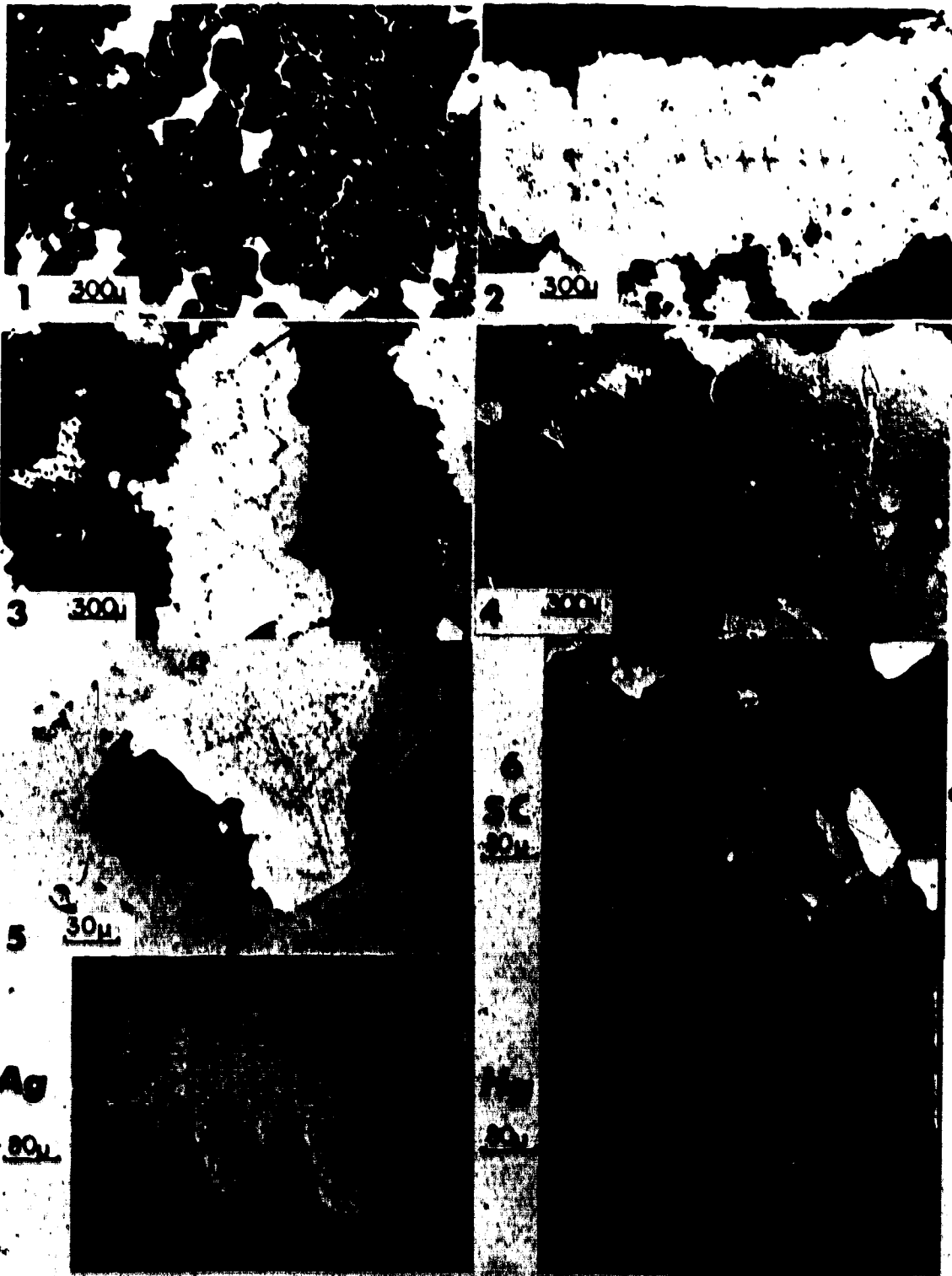
## PLATE 6

1. Silver replacing dolomite and quartz. Note the rim-replacement followed by infilling. Terra: Stage 2. P.P.L.
2. Tarnished Marienberg crosses of silver in the core of a zoned niccolite dendrite, with thin skutterudite rims. Terra: Stage 2. P.P.L.
3. Rhombs of silver that have replaced dolomite in the core of a zoned niccolite + safflorite dendrite. Dark arsenide around the silver is maucherite. Note remnants of carbonate in silver, and silver growing in interstitial dolomite. Terra: Stage 2. P.P.L. Line indicates microprobe traverse (Plate 7.1).
4. Cryptic zoning in safflorites around rammelsbergite, round silver at the end of the dendrite in 3. Note cross-cutting nature of silver. Terra: Stage 2. Normarski phase interference optics.
5. Silver (white) in zoned skutterudite (pale grey) and niccolite (medium grey), being replaced by acanthite. Terra. P.P.L. Green filter.
6. Sample current and silver and mercury scanning X-ray photographs to show zoning of mercury in silver dendrite. Dendrite surround is niccolite (grey) and fluorite (white). Terra.

SC 3 sweeps 15 KV

Ag  $10^5$  counts F 16

Hg  $8 \times 10^4$  counts x 1



1 300μ

2 300μ

3 300μ

4 300μ

5 30μ

Ag

80μ

SC  
30μ

10μ  
20μ

SLATES



## PLATE 7

1. Sample current and Fe, Ni and Co X-ray scanning photographs for the zoned arsenide dendrite in Plate 6.3. Terra.

SC 3 sweeps F 16

Fe  $7 \times 10^4$  counts x 2

Co, Ni  $8 \times 10^4$  counts 15 KV

2. Sample current and Fe, Ni and Co X-ray scanning photographs for a zoned safflorite whose core has been replaced by fluorite (F). Terra.

SC 3 sweeps F 16 x 2

Co, Ni, Fe  $8 \times 10^4$  counts 15 KV

1

40 $\mu$

SC

Co

2

10 $\mu$

SC

Co

Co

Ni

PLATE 7

## PLATE 8

1. Spherules of uraninite (grey) around quartz (black) and silver (white) on margins of a niccolite (pale) rosette.

Terra: Stage 2. P.P.L.

X-ray scanning photograph of uraninite spherules around quartz for U, showing weak concentration of U in quartz.

U  $8 \times 10^4$  counts F16 x 4 29 KV

2. Uraninite rim around silver (white) surrounded by safflorite rosettes (grey). Terra: Stage 2. P.P.L.

Sample current and U, Ag and Pb X-ray scanning photographs of a similar feature show the uraninite rimming silver that contains uranium, and the concentrations of radiogenic lead, some of which has recrystallised as galena

U  $5 \times 10^4$  counts 29 KV

Pb  $8 \times 10^4$  counts F 16

Ag  $8 \times 10^4$  counts x 1

SC 3 sweeps

3. Remnant zoned spherules of uraninite in dolomite being replaced by silver. The darker patches in the uraninite are richer in lead. Terra. P.P.L. Oil immersion.



1 30μ

U  
20μ

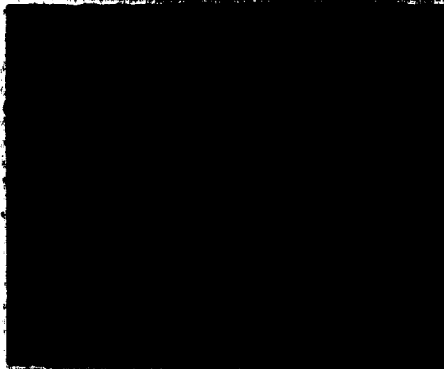


2 30μ

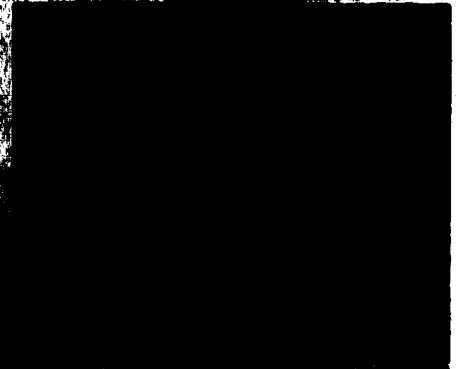
SC  
90μ



U



Ag



Pb



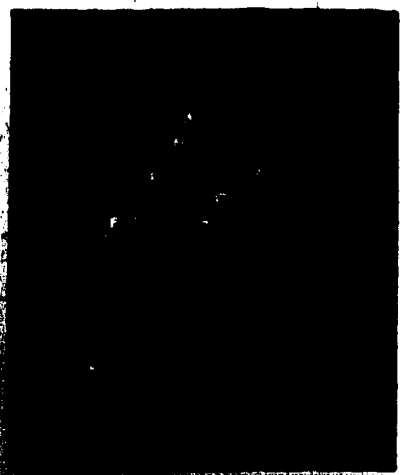
**PLATE 8**

## PLATE 9

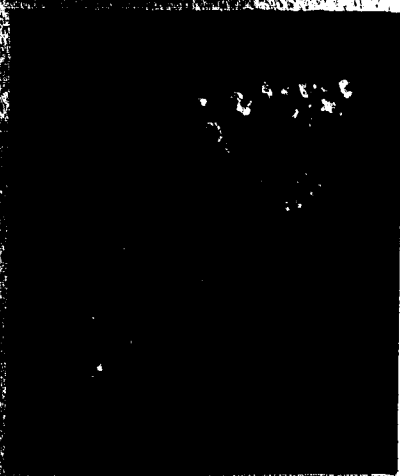
1. Hand specimen (x 1) and autoradiograph pictures showing the concentration of uranium minerals in fragments and streaks in the Stage 2B white dolomite. Terra.
2. Hand specimen (x 1) and autoradiograph pictures showing concentration of uranium minerals on the margins of silver and arsenid mineralisation in Stage 2B dolomite. Terra.
3. Hand specimen (x ½) and autoradiograph pictures showing close correlation of uranium and silver in Stage 2 dolomite. Terra.
4. Hand specimen (x ¼) of Sample TX 7.6, representing half of a symmetric part of the #8 vein at Terra.
  - a) Fragments of haematite-quartz-uranium rich rock in Stage 2 dolomite.
  - b) Dendritic arsenides and silver in Stage 2 dolomite.
  - c) Stage 3 dolomite with chlorite, haematite and bismuth.
  - d) Faulted margin of vein containing gouge, rock fragments and veinlets of galena and matildite.
5. Close-up of silver dendrites in Stage 2B dolomite over Stage 2A dolomite, with chlorite streaks, cementing red fragments. Terra. x ½.



1



2



A27



a

b

c

d

3



5

27A

PLATE 9

## PLATE 10

1. Bismuth (scratched) overgrowing skutterudite (pale) in dolomite (grey-black). Fluorite (black) overgrows the bismuth with 'teardrop' texture. Terra: Stage 3. P.P.L.
2. Matildite (grey) selectively overgrowing zoned skutterudite (white), around remnant quartz. Terra: Stage 3. P.P.L.
3. Matildite and other sulphosalts (grey) overgrowing zoned safflorite-skutterudite rosettes (white). The original carbonate matrix has been replaced by fluorite (black) which has also grown with the sulphosalts on the margins of the rosettes. Terra: Stage 3. Etched by 1 minute rough polishing on card. P.P.L.
4. Matildite (grey) and fluorite (black) overgrowing zoned arsenides, selectively replacing them. Terra: Stage 3. P.P.L.
5. 'Speck zones' and massive bismuth replacing cobalt skutterudite in dolomite. Bismuth is in turn replaced by bismuthinite (grey). Terra: Stage 3. P.P.L.
6. Ag, Bi and S X-ray scanning photographs of matildite around a safflorite rosette, which is being replaced (dark, on left). Black inclusions in the matildite (Ag, Bi deficient) are exsolved galena. Dark on right is quartz. Terra: Stage 3.

Ag, Bi, S 8 x 10<sup>4</sup> counts 29 KV F 16

1 grid square = 60 μ



1 300μ

2 80μ

3 300μ

5 80μ

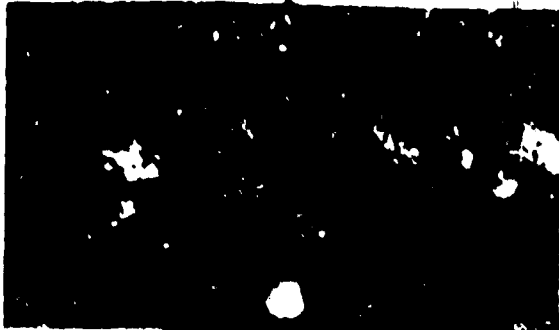
BI

PLATE 10



## PLATE 11

1. Specks of sphalerite and galena (white) in 'porphyry'.  
Norex: Stage 1. P.P.L.
2. Cubes and 'Marienberg crosses' of silver in niccolite. The silver overgrows the arsenide into remnant, interstitial dolomite. Norex: Stage 2. P.P.L.
3. Silver stringers cutting intergrown safflorite (darker) and rammelsbergite in an arsenide dendrite. Norex: Stage 2. Normarski phase interference optics.
4. Zoned, twinned safflorite rosette in dolomite. Note the mimetic star-shaped twin (upper left). Norex: Stage 2. Half crossed nicols.
5. Salt and pepper ore. Silver in quartz. Norex: Stage 3. P.P.L.
6. Cataclastic pyrite (white: Stage 1) with sphalerite (grey) filling cracks and overgrown by sphalerite and chalcopyrite and galena (similar-medium grey). Silver Bay. P.P.L.
7. Quartz (black) overgrown by chalcopyrite, sphalerite, galena, tetrahedrite and bismuth. Possibly emplectite as a reaction zone between bismuth and chalcopyrite. Silver Bay: Stage 3. P.P.L.
8. Intergrown chalcopyrite and galena with exsolved specks of tetrahedrite and bismuth. Silver Bay: Stage 3. P.P.L.



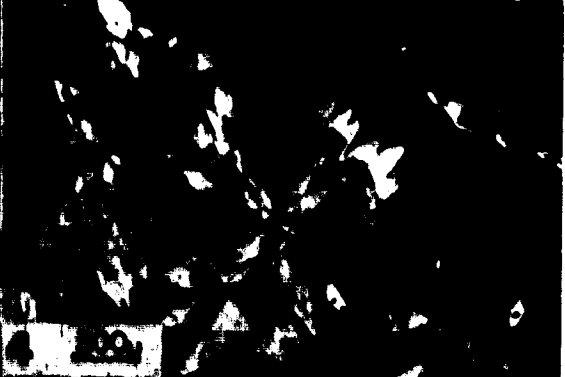
1 300μ



2 300μ



3 30μ



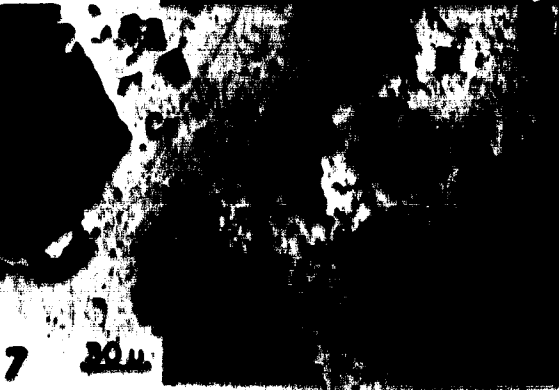
4 30μ



5 300μ



6 30μ



7 30μ



8 30μ

PLATE II

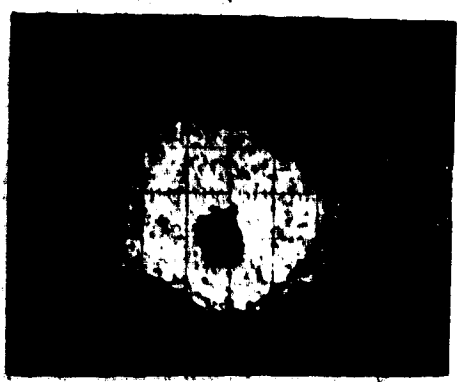
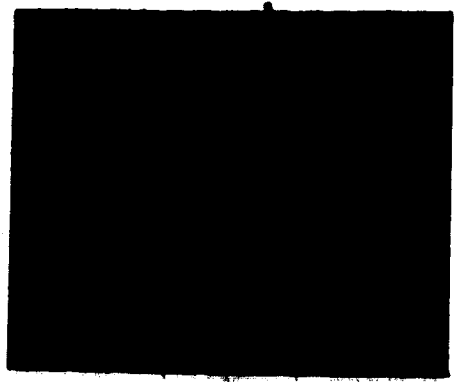
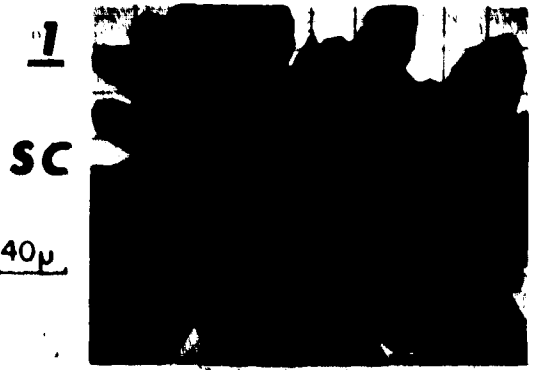
## PLATE 12

1. Sample current and Ni, Co and Fe X-ray scanning photographs of a safflorite rosette with silver in the core, in dolomite.  
Norex; Stage 2.

Ni, Co, Fe 8 x 10<sup>4</sup> counts 17 KV x 2 F 16

SC 3 sweeps

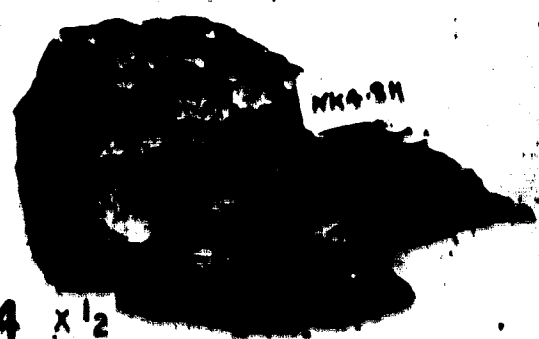
2. Xenoliths of altered tuff in massive magnetite-apatite.  
Terra.
3. Pegmatitic apatite with interstitial magnetite-apatite.  
Terra.
4. Pegmatitic actinolite growing normal to vein margin (on left).  
Jason Bay.
5. Cataclastic apatite, in a mesh of magnetite. Terra.



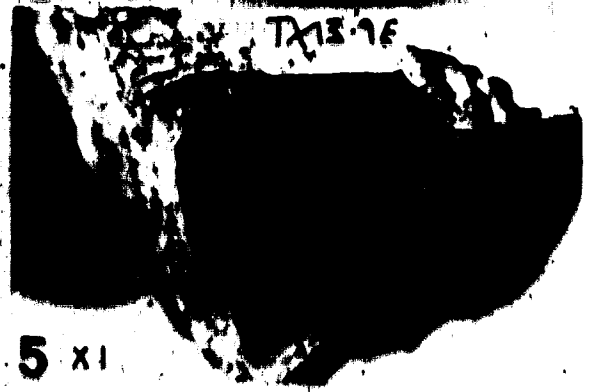
2 x 1/4



3 x 1/2



4 x 1/2



5 x 1

PLATE 12

## PLATE 13

1. Flow banded magnetite-apatite. Terra.
2. Crushed apatite and actinolite veinlet cutting coarse apatite (above) and intergrown apatite and actinolite (below). Terra. P.P.L. Transmitted.
3. Fractured apatite crystals with interstitial actinolite and magnetite. Terra. P.P.L. Transmitted.
4. Pegmatitic apatite and amphibole with interstitial quartz and late haematite. Terra. P.P.L. Transmitted.
5. Fractured magnetite-apatite band in a 'crystal-mush' of magnetite and apatite. Terra. P.P.L. Reflected.
6. Magnetite (white) and quartz (dull grey) filling cracks in pegmatitic apatite (dull grey). Terra. P.P.L. Reflected.
7. Magnetite (dull) replaced by haematite (pale) with spindles of ilmenite and intergrown oxides exsolved on three crystallographic planes. Jason Bay. P.P.L. Reflected.
8. Close-up of a complex exsolved spindle in haematite (pale) replacing magnetite (dull). Spindle consists of intergrown magnetite, haematite and ilmenite. Jason Bay. P.P.L. Reflected.

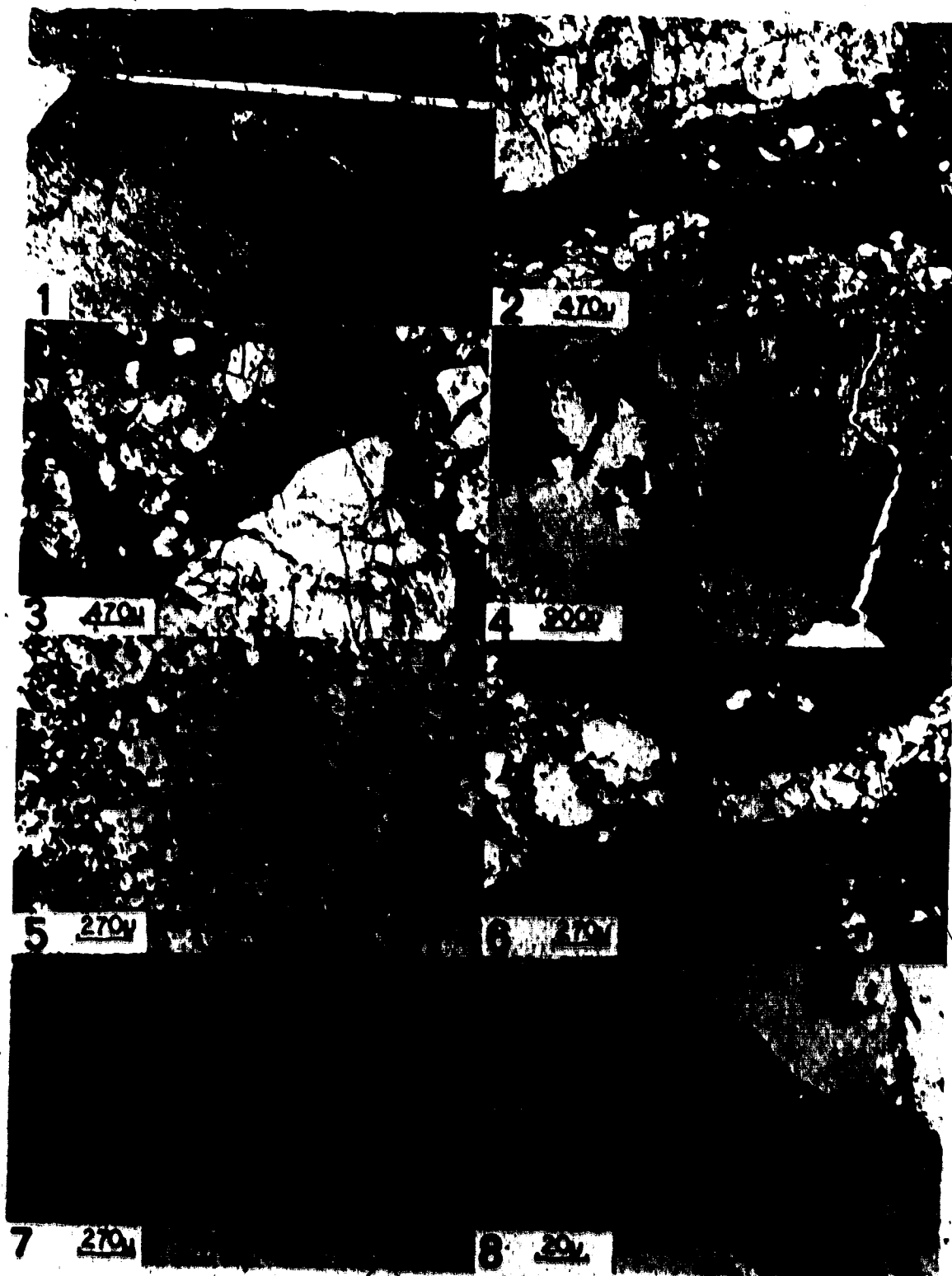


PLATE 13

## PLATE 14

1. Zoned magnetite in hastingsite skarn. Terra. P.P.L. Reflected.
2. Sphene (medium grey) and ilmenite (light grey) exsolved from and replacing magnetite/haematite. Surrounded by pyrite (white) and quartz. Jason Bay. P.P.L. Reflected.
3. Fe, Ti, Ca, and Si scanning X-ray photographs of intergrowths shown in 2.

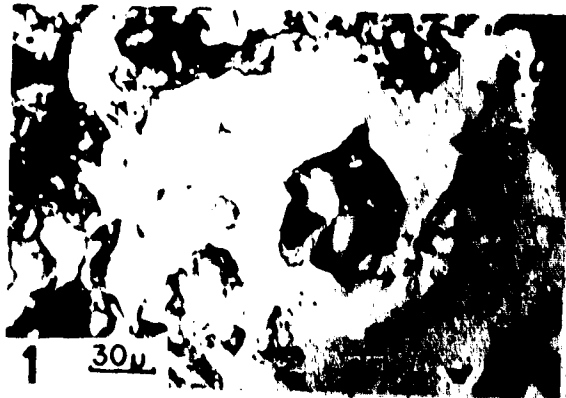
Fe  $5 \times 10^4$  counts

Cu, Ti, Si  $10^4$  counts F 16 x 1 15 KV

4. X-ray scanning photographs for Fe and Ti of ilmenite exsolution lamellae in haematite after magnetite (as in Plate 13.8).

Fe  $156 \times 10^3$  counts Ti  $4 \times 10^4$  counts

15 KV F 16 x 1



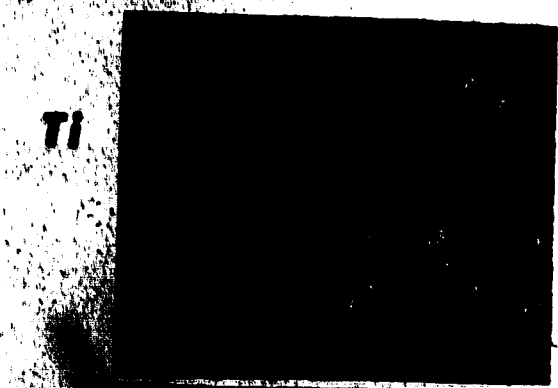
1 30μ



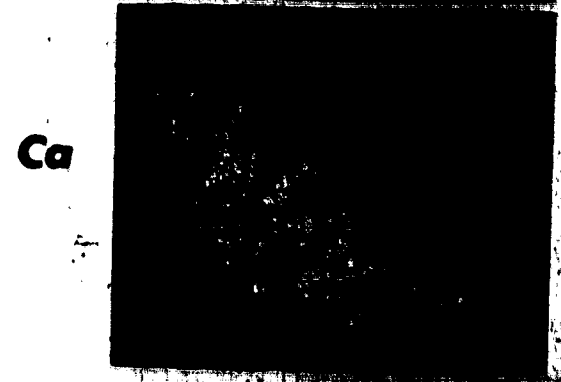
2 40μ



3  
Fe  
80μ



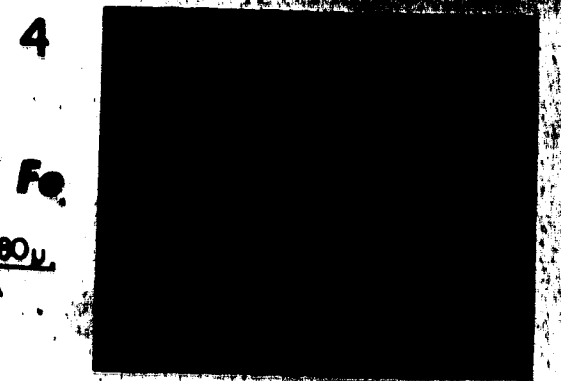
Ti



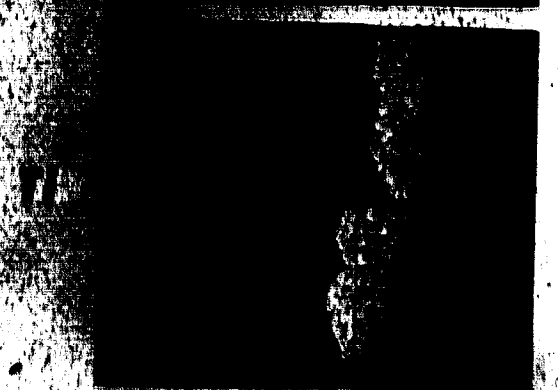
Ca



Si



4  
Fe  
80μ



Ti

PLATE 14



## 7. THE SILVER BAY MINE

### a) History

The surface outcrops of the Numbers 1 and 6 veins (Fig. 48) were first worked in 1932 as the Camsell River Silver Mine and the AVN shaft (Fig. 35), respectively. In these early days the price of silver was low and, although rich silver ore was mined, it was gold that the disillusioned Klondikers wanted. With the first rumours from Yellowknife in 1934, they left and the mine was closed. In 1943 considerable drilling and trenching were performed, and the three main veins (Numbers 1, 4 and 6) outlined under the aegis of White Eagle Silver Mines Limited. It was not until 1968, however, that the rich ore-shoot on the Number 1 vein was stoped out by Silver Bay Mines Limited. The property was taken over by Federated Mining Corporation in July, 1970; a mill was installed, and mining continued until all of the ore on the first level of the Number 1 vein had been bagged. The high initial expenditure and high cost of exploration work caused a temporary cessation in 1972, but new financing is apparently arranged for further mining in 1973.

### b) Geology

The mine is located in a series of massive hornblende-plagioclase porphyritic basalts with tuffaceous horizons that form the core of the Camsell River syncline (Fig. 48). These basalts are metamorphosed to the albite-epidote facies by a granodiorite which outcrops a little

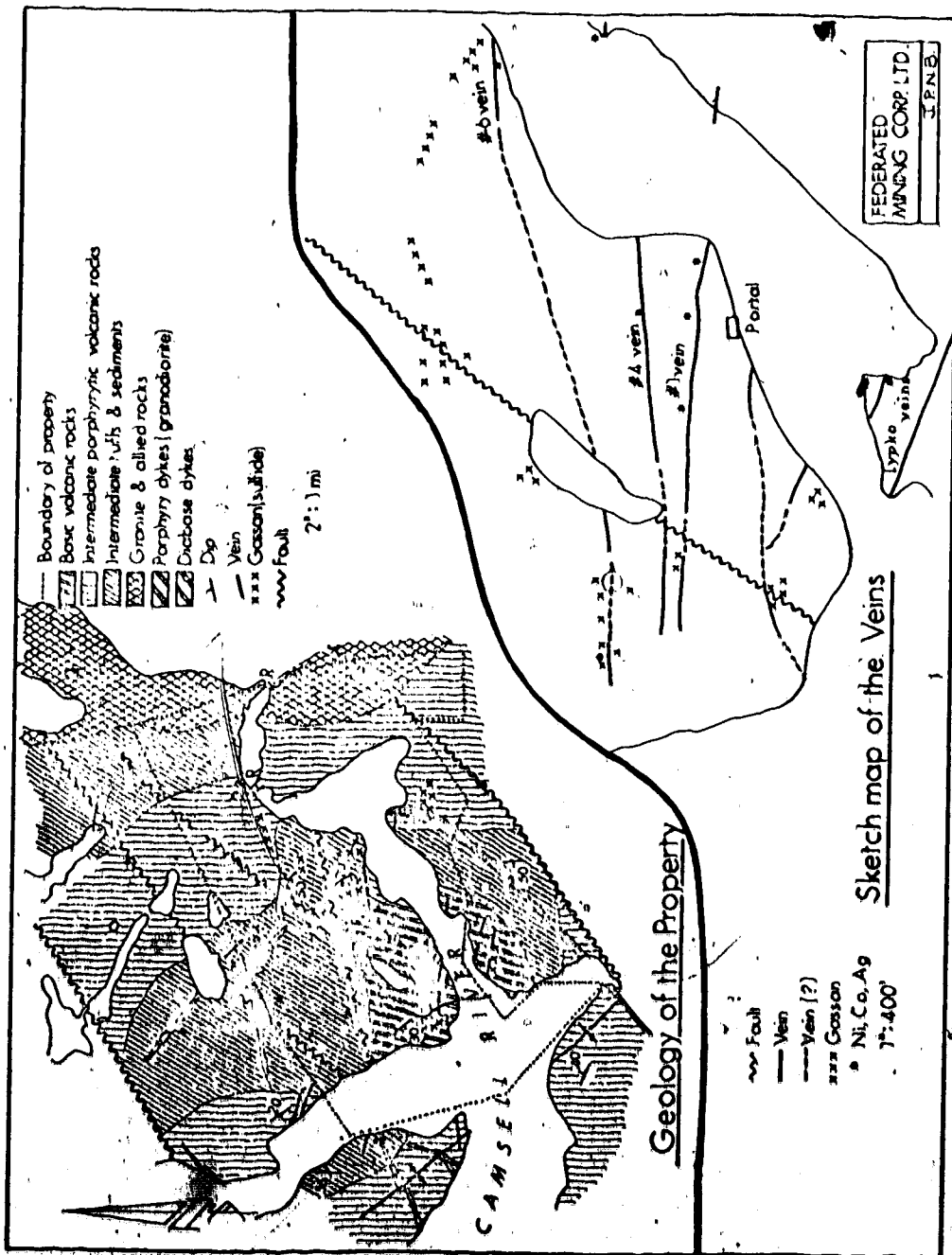


Figure 48. Geology of the Silver Bay Mine.

over a mile to the east, but whose contact probably dips quite gently to the west. The host rocks are often impregnated with pyrite and chalcopyrite skarns, or magnetite-actinolite pods and veinlets, all of which are cut by a thin porphyritic granodiorite dyke.

The ore-veins fill E-W striking, dilatant tension-fractures between major NE-trending faults. There are no offsets on the fractures and they appear to cross a third-order NE-trending splay fault which contains a barren quartz-carbonate vein. The veins die out to the west, but pass beneath the river to the east, and outcrop on the south shore before being covered by overburden.

The veins are sinuous and highly podiform. On surface the Numbers 1 and 4 veins seldom exceed 20 cm in width, but widths of over 3 m were noted 10 m below surface. The outcrop is virtually unweathered, and even though erythrite, annaberqite and malachite stain the vein carbonates, primary minerals are little altered. Tiny patches of radioactive material were detected with a scintillometer in the richest pod on the Number 1 vein, but no uranium mineral has yet been identified.

The veins are relatively simple and do not splay very much. The rocks between the main veins are full of thin carbonate stringers, but these are barren and discontinuous.

### c) Wall-rock Alteration

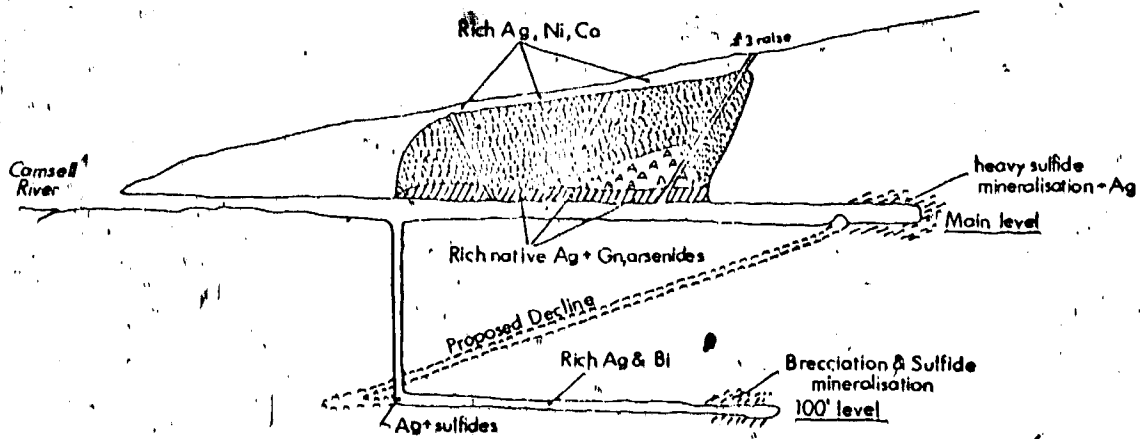
Some of the brecciated rock fragments in the veins are reddened with haematite, but are not silicified. They appear far less altered

than the 'red chert' at Terra. The host rocks are impregnated with carbonate for a few centimetres, and carbonate and epidote replace the feldspars in particular for a distance about equal to the vein thickness on either side of the veins. Chlorite is common on shear-planes in, and near the veins, and also replaces mafic minerals in the host-rock. Nearly all the rock fragments in the veins are chloritised and epidotised, and are interpreted as having been torn from the walls of earlier veins during development of the major dilatancies on the tension-gashes. The wall-rocks around ore-lenses are often rich in pyrite and chalcopyrite.

d) Location of Ore-lenses

The main silver ore occurs in shoots in areas where the vein is more than 10 cm wide. Where the veins exceed 1 m in width, only a few sulphides are found. The two ore-shoots in the Number 1 vein occur at the eastern ends of an area where the vein widens enormously - i.e. on the side closest to the intrusive contact. The location of other ore-shoots is imperfectly known, for they have only been studied in small surface pits. The outline of the main ore-lens is shown on Figure 49.

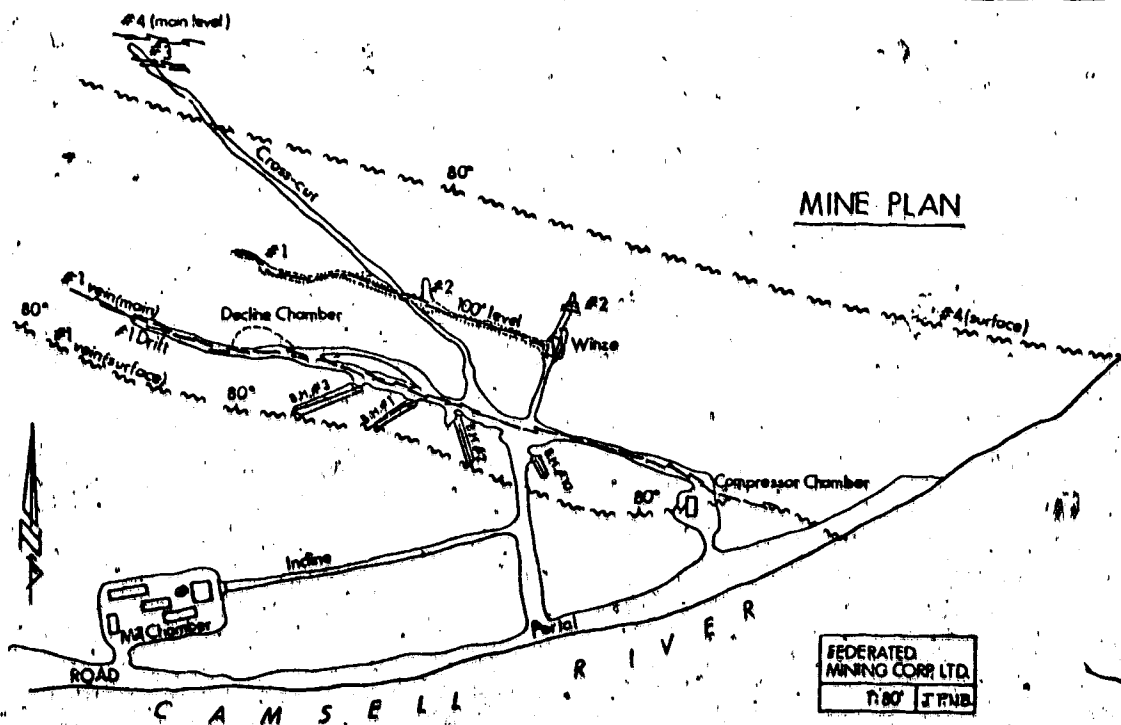
Ore-lenses can usually be predicted underground by an increase in the number of 'stringers' close to the vein, and the presence of a nebulous sulphide halo in the wall-rocks.



Stopped out  
 Broken ore (100 tons)  
 Unbroken ore (250 tons)

**Cross-section of the Mine Workings on the #1 Vein.**

FEDERATED MINING CORP. LTD.  
 1" = 80' JPNB



FEDERATED MINING CORP. LTD.  
 1" = 80' JPNB

Figure 49. Map and Section of the Silver Bay Veins.

e) Details of the Vein Mineralisation

Details of the Silver Bay veins are limited by the fact that only one ore-lens has been sampled, and that much of this had been mined before the property was examined. Since the minerals are similar to those at Terra, descriptions here will be briefer, and will concentrate on the relationships between phases. The paragenesis is shown in Figure 51 and will be documented after the following descriptions.

Most of the carbonates are dolomite, but calcite is intergrown with dolomite in some parts of the sequence. Pink and brown carbonates in banded sequences were thought to be rhodochrosite and ankerite, respectively, but X-ray diffraction data identified them as having a dolomite structure.

Dolomite in Stage 2 (Fig. 51) is fine-grained and yellow. It occurs in very thin stringers, cutting the wall-rocks, and a few fragments have been found in the veins. The dolomite deposited in Stage 3a is coarse and white, and a number of sulphides grow in it and replace it. It was deposited on the outer walls of the veins, and was overlain by the rhythmically-banded, fine-grained, vari-coloured dolomites of Stage 3b, which contain up to 20% calcite. These latter dolomites became slightly coarser towards the vein centre and are overgrown by quartz. Where the veins widen to over 1 m, much of the carbonate filling is coarse, white dolomite, similar to that of Stage 3a. It is, however, probably equivalent to all the Stage 3 carbonate, for it is overgrown by quartz. The Stage 3a dolomite contains numerous angular fragments of altered wall-rock, whereas the

banded dolomites do not. The bands were deposited sequentially in an open space, and reflect beautifully the shape of the vein walls at the time.

Analyses of the oxygen and carbon isotopes in the dolomites reveal a remarkably similar pattern to that at Terra (Fig. 50), but there is not yet enough data on the calcites. Samples taken from sequential bands in the banded dolomites show no regular differences or trend.

Quartz occurs in three distinct forms in the veins. Firstly, as fine granules in the Stage 2 stringers, and usually barren of minerals. Secondly, it occurs as coarse, white-to-purple crystals, and overgrows the banded carbonates: the crystals have grown at right-angles to the vein walls and often form dogtooth growths into vugs. Thirdly, a fine-grained, white, granular quartz occurs in veinlets up to 10 cm wide, cutting the banded carbonates and the coarser quartz. This invariably contains interstitial silver in a very rich ore, known by the miners as 'salt-and-pepper' ore (Plate 11.5).

Chlorite occurs as thin streaks and veinlets on the margins of veins, and in the Stage 2 stringers. Small patches of botryoidal growths, similar to those at Terra, were observed infrequently in the coarse, white dolomite.

Base-metal and iron sulphides are common in the wall-rocks at Silver Bay. In part these were formed by the contact metamorphism and related events, but the common mantle of sulphides round silver ore-lenses indicated that some were derived from the veins. Initially, pyrite and chalcopyrite formed, replacing mafic minerals in the basalts, and

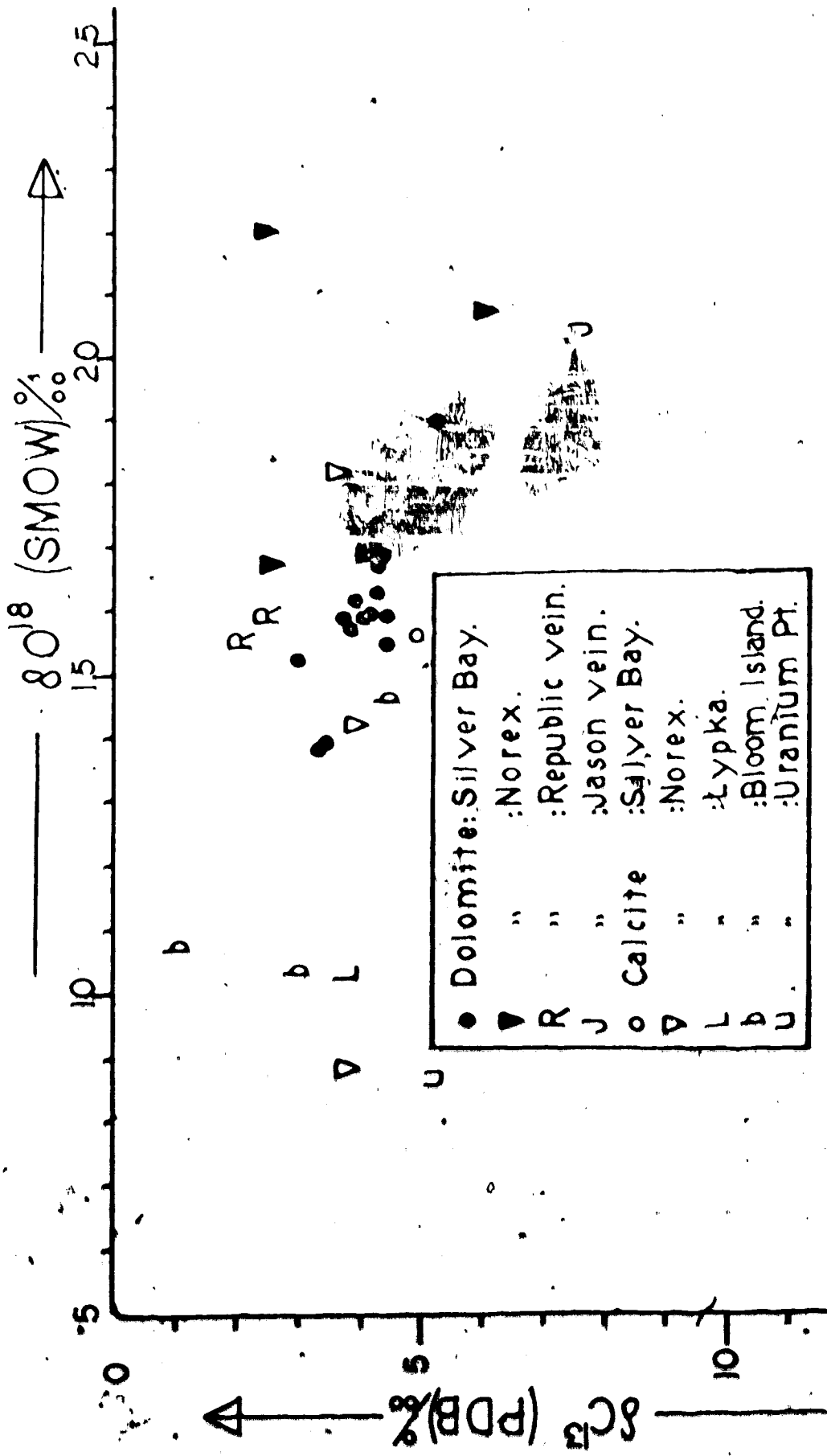


Figure 50. C & O isotope data for the Silver Bay and Norex Mines and the small showings.



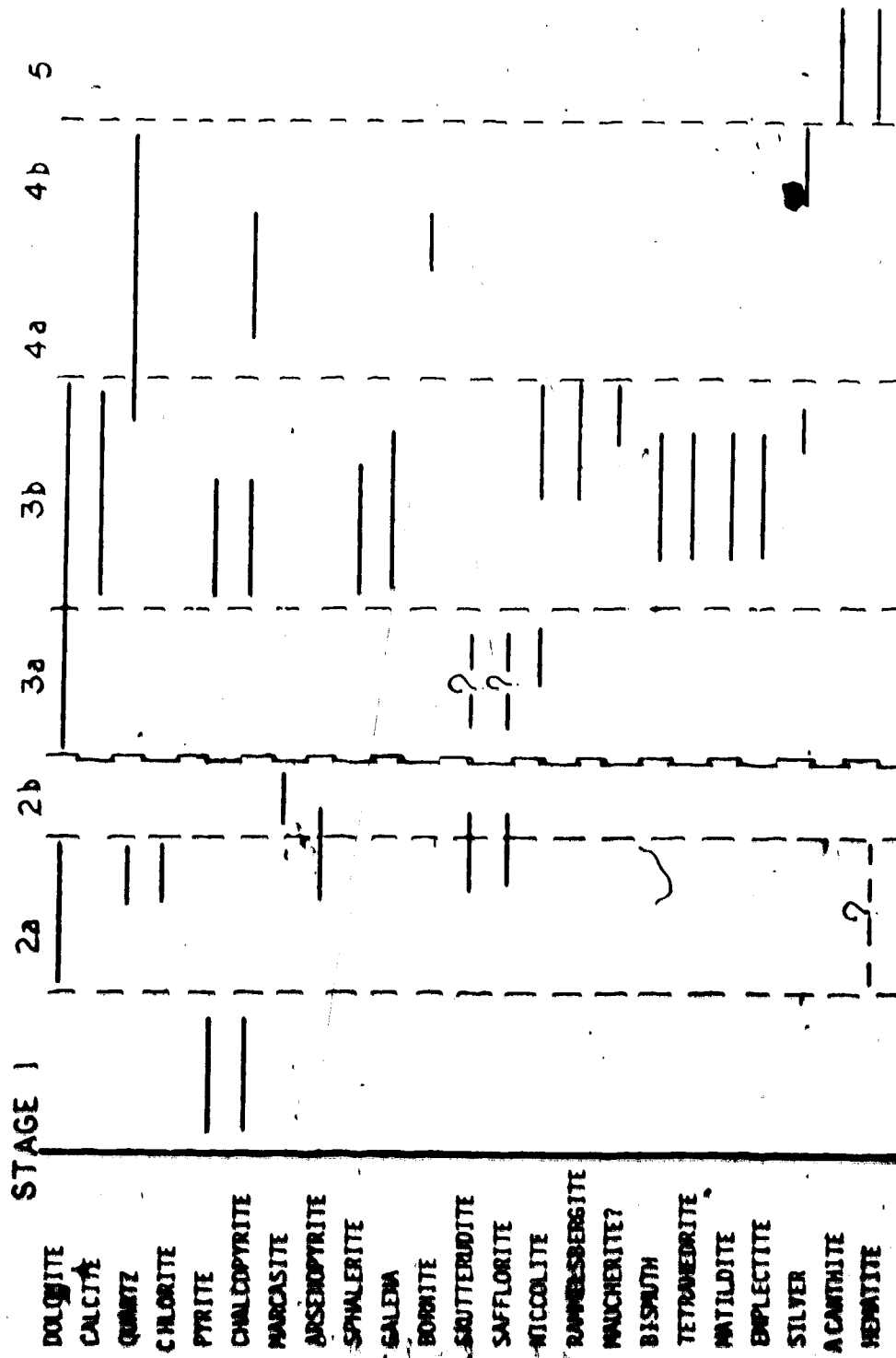


Figure 81. Paragenetic sequence of the Silver Bay mine. Double line represents the main period of dilation.

it is assumed that these are equivalent to the Stage 1 skarn sulphides at Terra. The Stage 2 carbonate veins effected some recrystallisation and concentration of these sulphides, and large patches of marcasite replace pyrite. Arsenopyrite was formed at this time, commonly replacing wall-rocks on the edge of the veinlets.

Following a period of brecciation which sheared arsenopyrite and the pyrite/marcasite, sphalerite and galena were introduced and overgrow the earlier sulphides, often healing fractures in them (Plate 11.6). Base-metal sulphides continued to be deposited in the banded carbonates, along with bismuth and silver, and reactions between these minerals produced emplectite and, perhaps, tetrahedrite (Plate 11.7). During the latter phases of Stage 3, bismuth, silver, tetrahedrite and matildite were apparently exsolved from massive galena. (Plate 11.8).

Chalcopyrite and, rarely, bornite were deposited with the Stage 4 quartz, and acanthite can be seen replacing the 'salt-and-pepper' silver in places. Smears and coatings of acanthite are common on fractures in the veins and wall-rocks close to the silver-rich lenses.

Sulphur isotope ratios for the vein sulphides are shown in Table 15. They are significantly different from those of any other sulphides in the area, both in their absolute values and in their greater total range. The similarity of the isotopic values of wall-rock sulphides (SBX 10.6) and those in the veins, and their difference from the skarn sulphide values elsewhere (Table 4) suggests that these sulphides are derived from the same fluid that deposited the veins.

Sample	Mineral	Mode of occurrence	Stage	$\delta S^{34}$ ‰ (CDI)
SILVER BAY				
SBX10.1B	Cp	Massive sulphides in Quartz-Dolomite Veins.	3b	-3.9±0.2
	Gn	As above.	3b	-8.0±0.1
SBX10.1C	Cp	Massive sulphides in Dolomite.	3b	-4.2±0.1
	Gn	As above.	3b	-6.5±0.1
	Gn	Late Gn. overgrowing above.	4?	-1.5±0.1
SBX10.3F	Pyt	Massive sulphides replacing rock-fragments in vein.	3a/b	-1.2±0.1
	Gn	As above.	3a/b	+2.8±0.1
SBX10.4A	Cp	Massive Cp in Dolomite vein.	3b	-1.0±0.1
SBX10.6	Pyt	Massive Sulphides on edge of Ag Ore-shoot.	2	-8.4±0.2
	Cp	As above.	2	-10.2±0.1
	Gn	Smear on joint-plane in above.	?	-9.6±0.2
NOREX				
NX20.1C	Gn	Massive sulphides in Dolomite vein.	3b	+0.5±0.1
	Cp	As above.	3b	+1.4±0.1
NX20.1J	Gn	Disseminated in rock fragments in Dolomite vein.	3b	-2.0±0.2
NX11.4A	Cp	In dolomite on edge of Ag-Quartz vein.	3b	+2.1±0.1
LYPKA VEINS				
NJ30.2	Asp	Brecciated fragments in Dolomite.	?	+2.7±0.2
NK1.1A	Pyt	In Dolomite vein.	?	+3.8±0.1

Table 15. Sulphur Isotope values for vein sulphides from the Silver Bay and Norex Mines, and from the Lypka Veins.

Coexisting sulphide pairs give fractionations of:  
 $\delta S^{34}$  Cp-Gn =  $4.1 \pm 0.3\%$ ,  $\delta S^{34}$  Cp-Gn =  $+2.3 \pm 0.2\%$  and  $\delta S^{34}$  Pyt-Cp =  
 $1.8 \pm 0.3\%$ . Using the calibration curves of Kajiwara and Krouse (1971)  
 these fractionations indicate formation temperatures of 120°C, 255°C  
 and 230°C, respectively. Since the first two temperatures are  
 derived from coexisting sulphides in samples taken 1 m apart, from  
 the same stage in the same vein, it is unlikely that these derived  
 temperatures are meaningful: the minerals may not have been in  
 isotopic equilibrium, or may have been differentially altered later.  
 The pyrite-galena pair in SBX 10.3 is clearly not in equilibrium.

Niccolite, rammelsbergite, safflorite and skutterudite are the  
 only arsenides that have been recognised. Safflorite and skutterudite  
 grow as rosettes in the wall-rocks in Stage 3a, and locally as  
 vermiform growths in the coarse, white dolomites. Where they occur in  
 carbonates they are strongly overgrown by sulphides and sulphosalts.  
 Niccolite grew as botryoids, always with thin rammelsbergite skins.  
 These grow into the banded carbonates, and often overgrow base-metal  
 sulphides and tetrahedrite. Very occasionally the niccolite contains  
 grains of a mineral, tentatively identified as maucherite. In places  
 there is a little niccolite in the centres of skutterudite masses.  
 This double period of arsenide deposition differs substantially from  
 the paragenesis at Terra.

Silver was found in four different situations. Firstly, minute  
 grains are exsolved from tetrahedrite-galena-matildite mixtures.

Secondly, dendrites of pure silver very occasionally cut the banded

carbonates, but only in areas where the carbonates are cut by granular quartz veins with the interstitial 'salt-and-pepper' silver. Acanthite commonly replaces small amounts of silver of the latter two types. The fourth occurrence is as small specks in the niccolite that lies in the cores of skutterudite.

The apparent mercury content of the unreplaced salt-and-pepper silver is 0.98 wt %, which is lower than that for similar silver that is partly replaced by acanthite (1.77 wt %). In addition, the apparent silver content becomes appreciably greater (Table 7). It would appear therefore, that the silver is enriched by the replacement. Specks of silver of the fourth type have a relatively low silver content and a very high mercury content (6.45 wt %) that is apparently different from that in any other analysed silver from the area (Fig. 40).

Bismuth occurs in three situations. Firstly, as exsolution blebs from tetrahedrite and galena (Plate 11.8). Secondly, as intergrowths with sulphides and sulphosalts of Stage 3b (Plate 11.7), and thirdly, as replacement of wall-rocks in the immediate proximity of the veins containing bismuth. Bismuth is not a common mineral in the first level of the Silver Bay Mine, but reports (W. Dollery-Pardy, Pers. Comm., 1971) and samples from the now-flooded second level indicate that bismuth is more common there (Fig. 49).

Matildite and tetrahedrite occur rarely in patches of massive sulphides of Stage 3b, and the X-ray diffraction data show that they are structurally identical with their counterparts at Terra; no electron microprobe analyses have been performed.

Haematite, as staining, is common in the Stage 2 carbonates and quartz, but is absent from Stage 3. Thin layers of haematite sometimes coat the Stage 4 quartz, and vugs often contain small rosettes of haematite needles.

f) Paragenetic Sequences and Depositional Conditions

The paragenesis (Fig. 51) differs in some important aspects from that at Terra (Fig. 46), although the mineralogy is very similar. Five stages of mineralisation are proposed and numbered to correspond as nearly as possible to the Terra Sequence.

The most important differences between the ores at Silver Bay and those at Terra are the development of arsenides and silver after the sulphides and bismuth, and the different sulphur isotope values. Clearly, the same elements were present in the ore-fluids, but the conditions at the site of deposition must have been different. These different conditions are clearly the single-stage development of dilatancy at Silver Bay and the very wide opening at this time, and are reflected in the crustification textures of the gangue minerals. Further discussion follows after the other veins have been described.

g) Potential

The Silver Bay Mine has perhaps the greatest potential of any mine in the Camsell River area, but has produced the least ore to date. It is inevitable that there are other rich ore-lenses on the Number 1 vein, and the surface outcrop of one is seen in the Number 4 vein

(Fig. 48). Old workings on the Number 6 vein indicate pods of high-grade silver, but these could not be reached by the author because of flooding in the shaft. The length of these three main veins is considerable, especially if the extrapolations beneath the river are valid. It is proposed, from a study of the three Camsell River mines, and data from the Echo Bay area mines, that ore-lenses occupy between 1 and 10% of the vein lengths. The Numbers 1, 4 and 6 veins are 230 m, 430 m and, possibly, 2000 m long, respectively, although extrapolations on the Number 6 vein are tenuous. Taking the average ore-lens as about 30 m long, it is statistically probable that there be between one and two ore-lenses in veins Number 1 and 4, on the present working-level.

The ore-lens on the Number 1 vein yielded about 1,000 tons of ore, averaging about 200 oz Ag/ton - although more careful mining would have decreased dilution considerably. At a price of \$2/oz for silver, this lens produced about  $\$4 \times 10^5$  gross value. The total cost of the operation to mine the lens worked out at around \$50/ton (Terra's costs are about \$40/ton) and the resulting net profit was some \$35,000.

Assuming the next ore-lens to be 30 m long, it will most probably be between 170 m and 330 m away at the same level. Costs for a 3 m x 2 m drift are around \$20/foot; thus between 10,000 and 20,000 dollars will probably be needed to find the next ore-lens. Add to this the costs of operating the camp while no ore is being produced, the cost of diamond-drilling, and the costs of other exploration, and it can be seen that mining these veins is, at best,

a marginal business.

These calculations have considered only horizontal exploitation, over a height of perhaps 20 m. It is the possibility of rich ore in the third dimension that makes the mines attractive.



## 8. THE NOREX MINE

### a) History

The original surface showing of the Norex vein was discovered in 1932, but until 1968 only minor surface exploration work was performed. In that year a number of short diamond-drill holes confirmed the presence of a vein some 200 m long, of variable width, to a depth of 20 m. Within this, an extremely rich silver ore-lens was found to be about 30 m long and 20 m deep. A small shaft was sunk in the vein to test this zone. The samples from this shaft were 'salt-and-pepper' silver ore, and so rich that mining was started immediately from an open-cut trench. High-grade ore was hand-picked, and the resulting profits were used to construct a road to the Camsell River and an airstrip at Smallwood Lake (Fig. 6). Unfortunately, no other ore was found and the main lens was almost worked out by this time. Terra acquired a 50% interest in, and the right to mine the claims in 1972, but there has been no further work of significance.

### b) Geology

The vein is vertical and varies between 20 cm and 5 m wide. It strikes to the east and is about 200 m long. It lies close to the contact between bedded andesite tuffs and massive porphyritic andesite flows, which are sometimes separated by a thin screen of felsic tuffs (Fig. 52). All these rocks are cut by a plagioclase-porphyritic granodiorite dyke that strikes to the northeast. The vein apparently

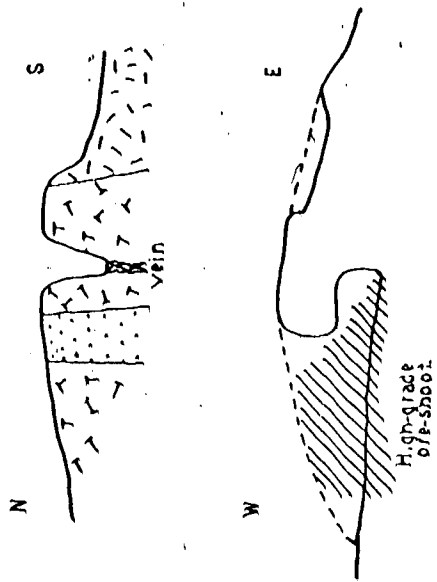
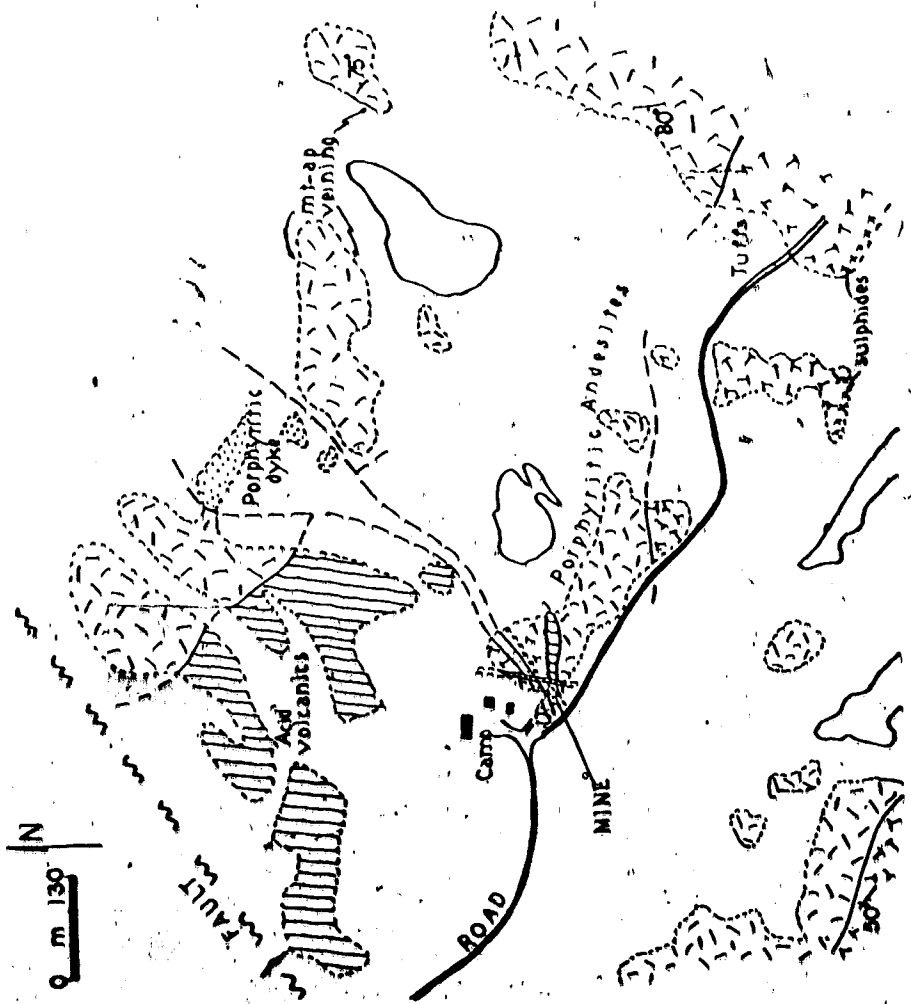


Figure 52.

Sketch map and sections  
of the

**NOREX MINE**

J.R.N.B. 1971.

cuts this dyke, although exposure at the contact is poor. Both dyke and vein are cut by a 2 m wide NNE-trending diabase dyke which contains very thin stringers containing specks of galena, sphalerite, chalcopyrite and pyrite.

The rocks are in the upper albite-epidote and lower hornblende-hornfels facies in the aureole of a granodiorite that outcrops some 2 km to the east, but whose contact dips shallowly to the west. The rocks are folded in small drag-folds that seem to be related to the axis of the main syncline in the area. The structure is complicated in that small jostling movements have occurred on a number of faults and joints, and bed-by-bed correlation is difficult.

Veinlets of carbonates, epidote, quartz and magnetite-actinolite-apatite are common (Fig. 52), and appear to be a product of the contact metamorphism. Sulphide gossan zones are very common, especially in the tuffs and on the edges of the porphyry dyke. Trenching has revealed fresh minerals, pyrite, pyrrhotite and chalcopyrite are the most common, and the mineralisation appears to be metamorphogenic and similar to other skarns throughout the area. Both the porphyry dyke and the porphyritic andesite flows contain specks of base-metal sulphides that appear to be original and not introduced (Plate 11.1).

### c) Vein Mineralisation

Since only the one ore-lens has been found in the vein, it can only be said that the ore-lens occurs in the most dilatant part of the vein. The edges of the vein are chloritised and epidotised, but

no red alteration has been observed.

The country rocks around the vein are impregnated with sulphides and contain thin dolomite stringers containing specks of sulphide. Close to the vein these strike to the east and are thought to represent a period of veining prior to the main period of dilation. The main vein is filled with dolomite and quartz. The dolomite veins are composite, and often contain lenses and 'streams' of wall-rock fragments. The dolomite is usually white, and varies from fairly massive at the margins, to coarse-grained and well-crystalline further in. Occasionally weakly-banded dolomite overgrows the coarse, white dolomite. Carbon and oxygen isotope data for the dolomite (Fig. 50) show a wider spread than, but grossly similar values to those from the other mines. No evolutionary trend is apparent.

The host-rocks, and occasionally the dolomite veins, are cut by thin stringers of bright red calcite - red because of fine haematite dusting. The isotopic values for these are similar to the values for dolomites from all the other mines (Fig. 50).

Quartz overgrows the dolomite and is at first massive, and then coarse-grained, and often vuggy. Often vugs are lined with the later stages of dolomite and the initial stages of quartz deposition. The quartz veins are not cut by the red calcite stringers. Frequently the quartz veins become fine-grained and sugary, and tongues and stringers of this sugary quartz cut the dolomite, and commonly contain the 'salt-and-pepper' ore - some of these silver-carrying veins are over 25 cm wide.

Sulphides common in the veins are chalcopyrite, sphalerite and galena. They usually occur in the dolomite and quartz of Stage 3b as massive patches. In addition, galena often replaces wall-rock fragments. Massive intergrowths of galena and chalcopyrite occasionally contain small amounts of tetrahedrite. Matildite was identified in one polished section.

The sulphur isotope ratios (Table 15) were only measured on these coarse-grained sulphides, and show values that overlap the Silver Bay and Terra ranges, but whose mean lies between those of the other two mines. A coexisting pair of chalcopyrite and galena gives a fractionation of  $\delta\Delta S^{34} = 0.9 \pm 0.2\%$ , which indicates a temperature of about 600°C - somewhat unlikely because the rock contains older bismuth and coeval tetrahedrite, both of which would not survive such temperature. It is concluded, once again, that the sulphides are not in isotopic equilibrium.

Acanthite occurs quite commonly as minor replacements of silver in the salt-and-pepper ore, and as smears on joint planes near silver-rich lenses.

Skutterudite, safflorite, rammelsbergite and niccolite are the only arsenides that have been identified at Norex. The first three occur as complex zoned rosettes and dendrites in dolomite, with rammelsbergite invariably present in the cores. Niccolite is present as coarse crystals in the cores of some dendrites, and sometimes appears to have overgrown more complex arsenides almost to the rim of the dendrite (Plate 11.2).

The rosettes show the mimetic twinning common to safflorites (Plate 11.4), and exhibit a beautiful chemical zonation from a nickel-rich core to a cobalt-iron-rich outer band, which may contain thin nickel-rich bands (Plate 12.1).

Niccolite also grows as tiny botryoids at the contacts between the dolomite and quartz. These overgrow silver in the dendrites, but not the salt-and-pepper ore. Most of the samples examined were badly weathered, but thin skins of rammelsbergite were tentatively identified on the botryoids.

Silver occurs in two completely separate environs. Firstly, it replaces the cores of arsenide dendrites (Plate 11.2) and rosettes (Plate 12.1). The dendrite cores are made up of strings of cubes of silver, which frequently overgrow the arsenides into the surrounding dolomite. Cracks in the arsenides are filled with silver (Plate 11.3), which is clearly younger. Dendrites of silver alone are also very common in the Stage 3 dolomites, and form some of the richest ore in the mine. Thin section studies of these show that the surrounding dolomite was recrystallised and flushed clear of impurities and inclusions during the growth of the dendrite. In every case these dendrites are cubic.

The apparent mercury content of silver in a rosette core is 2.47 wt %, with only 90 wt % of silver apparently present (Table 6). This considerable deficiency is in part due to the presence of arsenic and is in part unknown.

Silver also occurs plentifully in the salt-and-pepper ore (Plate

all.5), where it is indistinguishable from that at Silver Bay.

Bismuth was found in one sample only, replacing fragments of wall-rocks in a dolomite vein containing galena and chalcopyrite with intergrowths of tetrahedrite and matildite. Contacts between bismuth and the sulphides were not seen, but the minerals are presumed to be coeval.

Vugs in the quartz veins contain specks of chalcopyrite, and this and the quartz are overgrown by thin dustings of haematite.

d) Paragenetic Sequence and Depositional Conditions

The Norex Mine contains parts of the paragenesis that resemble that of Silver Bay and parts that resemble that of Terra (Fig. 53). For example, the arsenide and silver dendrites are indistinguishable from those at Terra, and the 'salt-and-pepper' ore and massive sulphides with late niccolite are identical to those at Silver Bay. (The numbering of stages attempts to keep the same number for the same type of deposition in all the mines).

At first it was thought (Badham et al., 1972) that all the mines were mineralised with different parts of the same paragenesis - i.e. that much of the available material had been deposited at Terra, and that lesser portions had been deposited in the other mines. The reason offered for this was that the Norex and Silver Bay veins had only opened once and could only receive whatever ore-fluid was available at the time of dilatation: the Terra veins had opened many times, and were thus able to garner a greater part of the 'spectrum'

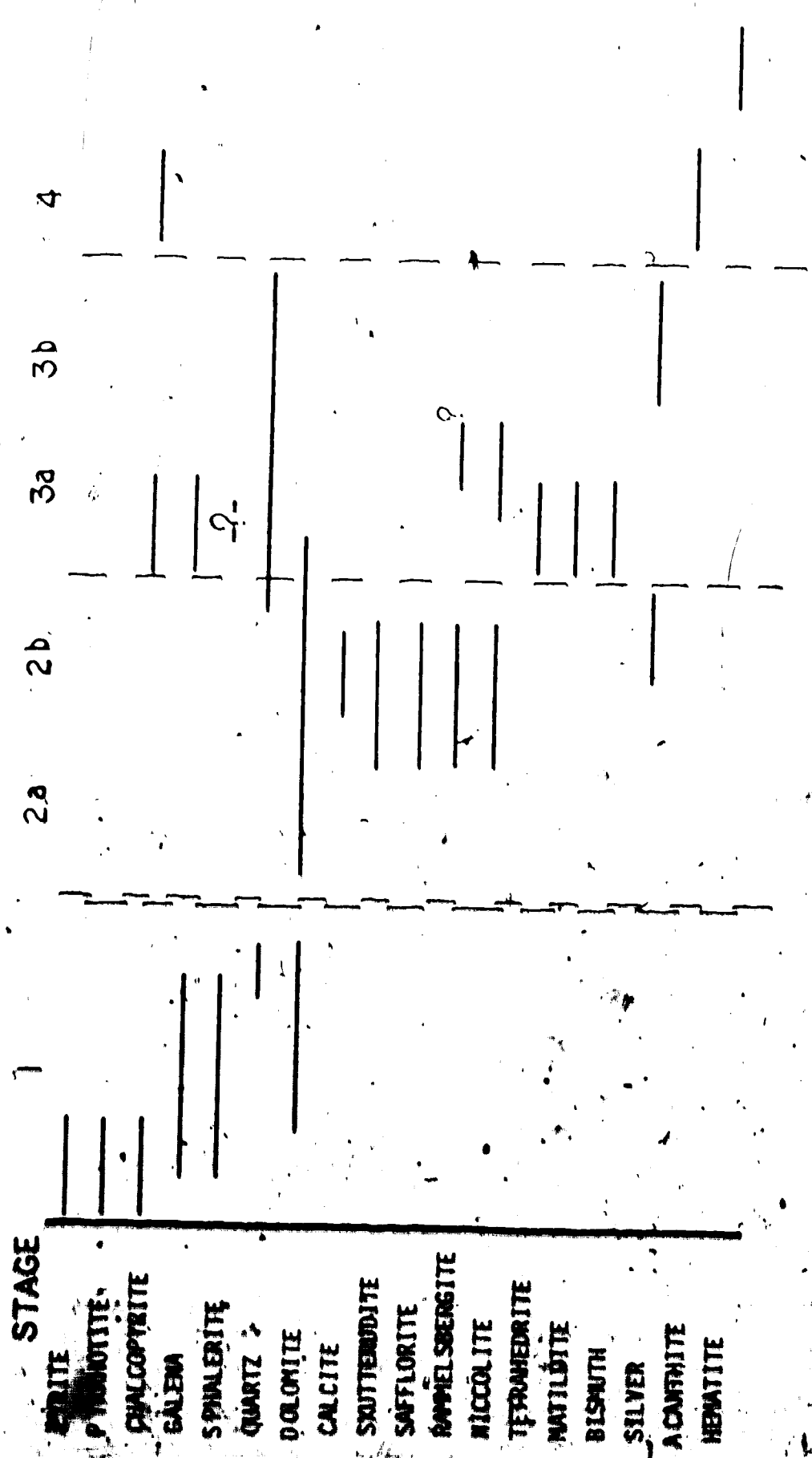


Figure 53. Paragenesis of the Norex Vein.



of the ore-fluid. This hypothesis is now thought to be only partly correct: discussion continues below, in the section on the origin of the veins.

Temperatures of deposition in both Norex and Silver Bay Mines are less easy to delimit than those for Terra because of the smaller assemblages. The melting point of bismuth ( $271.5^{\circ}\text{C}$ ) defines an upper limit for Stage 3 in both mines. Matildite is so uncommon that its relationships with galena are uncertain: although the two are often in close association, neither was seen exsolving from the other and may therefore have been deposited below  $215^{\circ}\text{C}$ .

In general it is thought that similar temperatures of deposition prevailed in all three mines: i.e. that the curve for Terra (Fig. 47) applies equally to the other mines.

#### e) Potential

The potential for the Norex vein is not great. The vein is not long and the main ore-lens is all but stoped out. Drilling to 20 m depths in the vein revealed no other mineralised pods. Unless ore is found at greater depth it would appear that the only potential the mine has is in the remaining ore in the main lens.

## 9. OTHER SILVER-, ARSENIDE-BEARING VEINS

The Lypka veins outcrop on the south shore of the Camsell River, opposite Silver Bay (Fig. 48). They are vertical and sinuous, and transect porphyritic basalts. They splay out and stop to the east, where they run into andesite tuffs (Fig. 35). There are essentially only two important veins, but also numerous stringers with small dilatant pods. The north vein contains arsenide minerals and sulphides and numerous brecciated wall-rock fragments, all cemented by two generations of dolomite. It is only well-exposed in one large trench where it widens from 5 cm to 70 cm in a 1 m vertical section. The following sequence of events is observed:

1. Brecciation of wall-rocks on the margins of a tension-fracture. Deposition of fine-grained, white dolomite.

2. Replacement of dolomite and wall-rock fragments by arsenopyrite and some skutterudite. This arsenopyrite has a sulphur isotope value of  $\delta S^{34} +2.7 \pm 0.2\%$ . (Table 15).

3. Further brecciation of wall and vein rocks, and deposition of dolomite, followed by galena and a little pyrite. Only thin quartz bands were found in the vein, and no silver was found in these (Fig. 54).

The southernmost vein can be traced into the banded tuffs and for about 200 m in the basalts. It consists of mostly banded dolomite, with no rock fragments, and contains two zones where small NE-trending fractures cross it. The veins themselves do not widen particularly at these intersections, but pyrite and chalcopyrite replace both dolomite

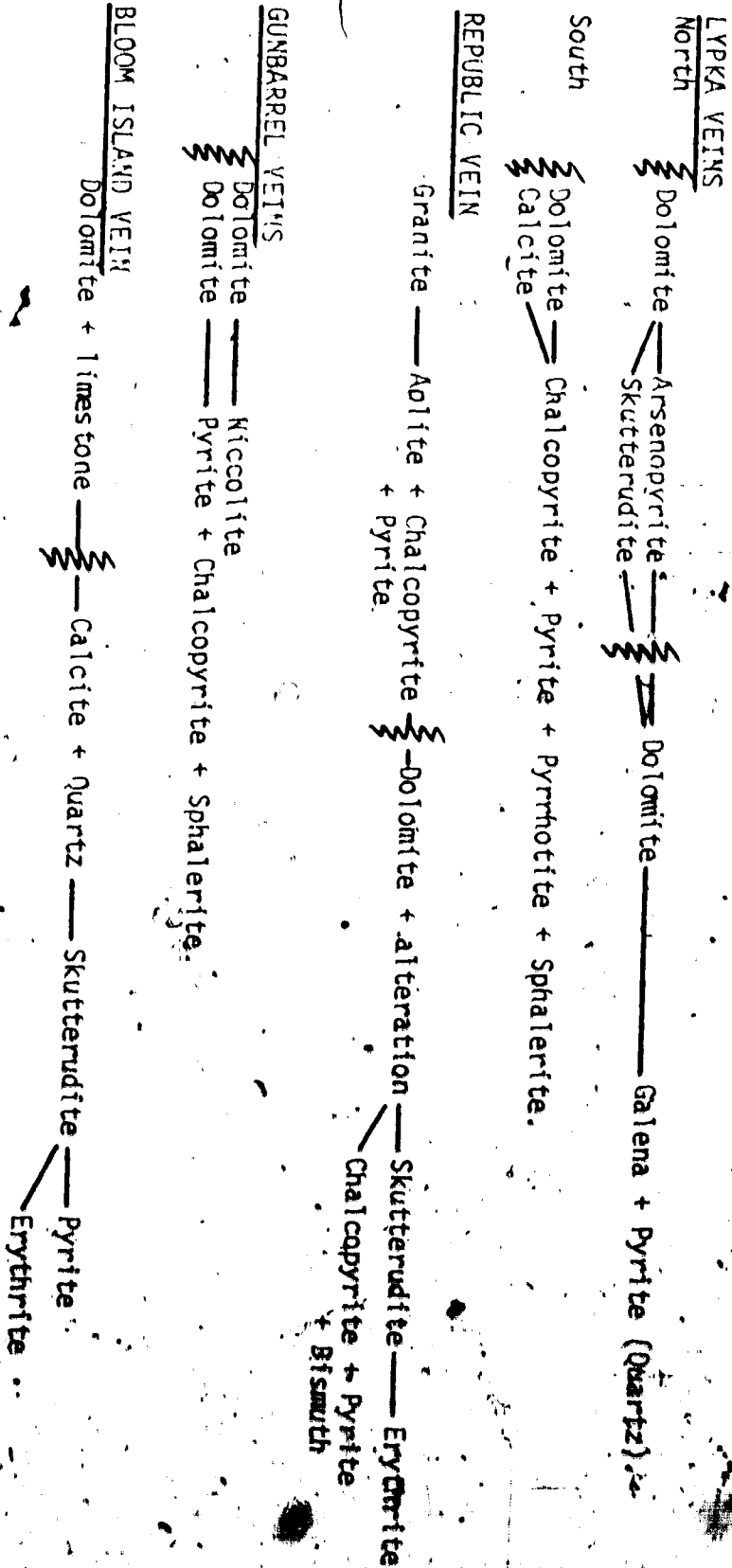


Figure 54. Deduced Parageneses for the four mineralised Veins.

and wall-rock extensively. A sample of pyrite from the westernmost trench (Fig. 35) has a sulphur isotope value of  $\delta S^{34} = 3.8 \pm 0.1\%$  (Table 15). Small grains of sphalerite and pyrrhotite were also seen. Where this vein intersects the tuffs it carries predominantly calcite. A carbon and oxygen isotope analysis (Fig. 50) shows this to be similar to late-stage calcites in other veins.

The potential of the Lypka veins, especially the northern one, is as great as that for the Silver Bay veins to which they are closely similar. The southern vein is thought to be equivalent in age to the Stage 1 of the Silver Bay Mine; but its age relations are not clear at present.

The Republic vein is again short and sinuous, and lies on the contact of a granite and a thin aplite screen that separates the granite from metamorphosed intermediate and felsic volcanic rocks (Fig. 35). The aplite is locally impregnated with blebs of chalcopyrite, but these have not been recrystallised or concentrated by the vein. The vein is about 100 m long and strikes to the northeast. The south end tails out in the granite, and the north end splays into numerous thin stringers before exposure ends. Much of the vein is only some 5 cm wide, but this increases up to 2 m for a 30 m length which contains the mineralisation.

The vein is filled with dolomite, much of which is replacing granite rather than filling a dilation in a fault. There is no demonstrable offset across the vein. The dolomite is intermixed with remnant quartz, epidotised feldspar and some calcisilicate minerals.

Oxygen and carbon isotope data for the dolomite show it to be closely similar to the vein dolomites from all the other mines.

Small patches of pyrite and chalcopyrite replace this dolomite, along with rare masses of skutterudite. Erythrite coats all the joint planes. One speck of native bismuth was seen, close to skutterudite. No effective paragenesis can be worked out for this vein because of the paucity of exposure and mineralisation. Likewise the economic potential is not known.

The two Gunbarrel veins are 40 m and 180 m long, respectively, and cut a coarse gabbro sheet close to its contact with the Richardson Island granite. The west vein (Fig. 35) strikes northerly and consists of a 5-10 cm wide dolomite stringer containing specks of chalcopyrite, sphalerite and galena. The east vein strikes to the northeast and is the longer of the two. It varies between 5 and 20 cm in width and is filled with banded, coarse, yellowish dolomite. The old adit is collapsed and the rocks are badly weathered, but annabergite is common, and erythrite was seen in places. Some fresh vein samples were obtained and were seen to contain patches of massive to botryoidal niccolite, replacing the dolomite. No other minerals were identified, but silver values were reported from the vein when it was worked in 1932, and Furnival (1934) identified silver and "a cobalt mineral". Again, the paragenesis is not known in detail, and the showing cannot be said to have much economic potential.

The Bloom Island vein was discovered in 1932, and extensive exploration on the showing has not only failed to reveal any significant

mineralisation, but has destroyed or covered much of the interesting exposure. The vein is well-exposed for about 100 m, striking NE, parallel to the strike of steeply-dipping metamorphosed siliceous dolomites and limestones. Calcite veins have recrystallised in the host-rocks and the calcite is isotopically similar to that in the Lypka veins (Fig. 50). The vein is not continuous, but is a series of splaying stringers, up to 10 cm wide, of calcite and dolomite. Occasionally thin quartz stringers cut the dolomite, but are coeval with the calcite. Erythrite is ubiquitous on joint planes and two pieces of skutterudite were seen in the quartz. Small pyrite crystals grow over quartz, calcite and dolomite. Furnival (1934) reports leaf silver, bismuth and 'cobalt' from the first trench opened in the vein.

A paragenesis of dolomite, followed by calcite and quartz, skutterudite, and lastly pyrite is proposed. The vein has no economic significance.

In general the mineralisation in the veins is closely similar to parts of the sequence in the mines. Clearly they were small and 'once-only' events compared with the mines, and have only sampled part of the paragenetic spectrum. The approximate sequence of events in each of these veins, as far as is known, is shown in Figure 54.

## 10. GENESIS OF THE VEIN MINERALISATION

### a) Nature of the Ore-fluid

From the descriptions of the mines and showings, it is concluded that an ore-fluid was available over much of Camsell River area in post-Aphebian time. Whether each mineralised vein originated from the same fluid, or whether each formed from different fluids, which were derived by so similar a process that there was no difference between their deposits, cannot be told. However, all the mineralised veins were deposited from an identical fluid. Furthermore, it is clear that this fluid was extremely complex and carried at least the following elements: U, Fe, Si, Q, Ag, Ni, Co, As, Sb, Bi, S, Cu, Pb, Zn, Hg, C, Mg, F, Al, K, Ca and Mn. In addition, fluid inclusion studies (Robinson, 1971) indicate that the fluids were rich in Na and Cl.

Isotopic data from the Camsell River area show the close similarity of the mineralising fluid at each mine and showing. Certainly carbon and oxygen isotope data indicate that either these elements were in infinite supply to the ore-fluid, or that all dolomites were continually equilibrated after deposition. Calcites show considerable scatter, but generally indicate a trend of decreasing  $\delta^{13}C$  with time. It has been proposed that the late calcites were in equilibrium with an influx of meteoric water, and that the trend represents stages in the equilibration of older calcites with this late fluid (Badham et al., 1972). The dolomites, being more resistant to re-equilibration, were

not affected. These data lead to the conclusion that the main mass of isotopic values for the dolomites are original, and that the source had an infinite supply of carbon and oxygen, with a constant isotopic value. Since there is no sign of isotopic change with time, there can have been no essential change in the parent-fluid or in the depositional conditions. The average values for  $\delta O^{18}$  and  $\delta C^{13}$  in dolomites in all the samples analyses are:

Average  $\delta O^{18} = +15.5\%$       Range 12.6 - 22.0%.

Average  $\delta C^{13} = -3.97\%$       Range -2.1 - -7.9%.

Carbon and oxygen isotope data from the Echo Bay area show a regular evolutionary trend in the dolomites from values of  $\delta O^{18} = +22\%$  to  $\delta O^{18} = +12\%$  (Robinson, 1971). It is concluded that there must be an essential difference in the two areas. This is discussed below.

The sulphur isotope data also indicate a homogeneous source, both for the skarn and metamorphogenic sulphides, and for the vein sulphides. In each case the low values and the low spread are typical of magmatic hydrothermal solutions, but the differences in value are important. Again there is no sign of an evolution in the sulphide system during vein mineralisation. Furthermore, the data from the Terra Mine are closely similar to those from the Echo Bay Mine (Robinson, 1971). Differences must again be due to the mode of deposition in each vein and will be discussed below.

Since the mineralising fluids have an homogeneous source with respect to carbon, oxygen and sulphur, it is likely that the ore-elements were either derived from, or at least passed through this



source, and that all existed in the ore-fluid at once. Consequently, the paragenetic sequences are the result of the stability of the depositing mineral phases, firstly with respect to the remaining phases in the ore-fluid, and secondly with respect to the depositional conditions.

b) Mode of Deposition

In all the mines it is obvious that the principle control of ore-deposition was dilation on faults. Areas with more faults and greater numbers of dilatant zones have a greater potential for mineralisation. The evident host-rock control is dominantly structural - bedded rocks in contact metamorphic aureoles are the preferred units for splaying and dilation of faults. Dilation alone is not enough, and it appears that second or third-order faults on the NE-trending system were preferentially mineralised over the E-trending tension-fractures, even though the latter may have opened far wider.

It is also clear that the amount and type of deposition depend on the number of times a vein system has been 'cracked open' to allow an influx of new mineralising fluid. Finally, there appears to be a chemical control on the location of ore-shoots within dilatant zones. Evidence has been adduced, because of these controls, to show that the ore-fluids generally seemed to have migrated away from areas of granitic intrusion, and towards the thicker parts of the volcano-sedimentary complexes.

The ore-minerals were deposited in a relatively constant order,

but there are significant differences, illustrated thus:

Terra

U → arsenides (Ni → Co, Fe) → Bi, sulphides, sulphosalts  
Ag

Norex

arsenides (Ni → Co, Fe) → Bi, sulphides → Ni arsenides → Ag  
Ag sulphosalts

Silver Bay

Co, Fe arsenides → Bi, sulphides → Ni arsenides → Ag  
sulphosalts

There seems to be a continuum from the Terra to Silver Bay Sequences, with the Norex Sequence intermediate. This is not caused by the fact that at Terra we are seeing the first part of a paragenesis whose latter part is shown at Silver Bay, because the final stages (i.e. 4 at Terra and Norex, and 5 at Silver Bay) are similar in each mine, and represent the closure of the mineralisation. Clearly there is a progressive change in the mode of deposition.

Such a change is also shown by the sulphur isotope data for sulphides from the veins, i.e.:

Terra	Average	$\delta S^{34} + 3.5\%$	range 5.0%
Norex	Average	$\delta S^{34} \approx 0.5\%$	range 4.1%
Silver Bay	Average	$\delta S^{34} - 5.0\%$	range 11.7%

Such a change may be the result of different temperature or pressure on the fluid, or a different distance of deposition from the source of the ore-fluid. It has already been shown that the temperatures of deposition were similar in all three mines. The pressure at the site of deposition is dependent both on the depth, and perhaps partially on the amount of dilation. A fluid rushing through a newly-opened fault may deposit when it reaches a dilatant zone, and the release of pressure on the fluid is presumably proportional, in part, to the size of the dilatant zone. It has been shown that the width of the dilatant zones at Silver Bay and Norex are far greater than those at Terra. However, Norex and Silver Bay are similar in their mode and amount of dilation. It would seem unreasonable, from these considerations, to expect a trend in the paragenesis at the three mines, and more reasonable to expect a bimodal distribution.

It is concluded, therefore, that the predominant control on the paragenesis may be the distance the fluid has travelled from the source. This is substantiated by the sulphur isotope data. If the fluids were travelling outwards from a source along faults, and precipitating sulphides on the way, then, if there is a limited amount of sulphur, the precipitated sulphides will be isotopically heavier than the fluid - i.e. a typical reservoir effect will operate. Consequently, deposits further from the source might be expected to have progressively lighter isotopic values. It is proposed that the trend in isotopic values from Terra to Silver Bay represents an increasing distance from a source with a limited amount of sulphur. Whether the source

was the same one, or a number of chemically identical ones from different locations, is irrelevant. The problem remaining is to determine what and where this source was.

The mode of deposition in the actual ore-lenses is also important. In the Silver Bay and Norox Mines the textures indicate that the carbonates and quartz essentially grew by gradual infilling of the dilation zones. As soon as the zones were filled they were effectively sealed and, apart from very minor cracks that allowed the late quartz and silver veins in, they were not reopened. At Terra, on the other hand, there is evidence of frequent movement on the faults. The first influx of minerals sealed the faults, but these were cracked open by later movements which allowed fluids to enter each time. The structure control of the dilation zones is well demonstrated by the fact that dilation developed in the same places each time.

There is evidence at Terra that some of the lenses were sealed off from the main vein by the first minerals to crystallise from an introduced fluid, and that the later minerals gradually filled in the pod, crystallising from a static medium. This is especially true of the latter stages of mineralisation in the cross-veins. In each stage of filling, the carbonates appear to have grown first, and it is they that seal off a pod of mineral-rich fluid (Fig. 55). As minerals start to precipitate the carbonates and wall-rocks may be replaced, or the minerals may encrust the carbonates. Other lenses were not sealed off and remained in contact via thin cracks. Nevertheless, the vein system probably became closed to supply of further liquid because of

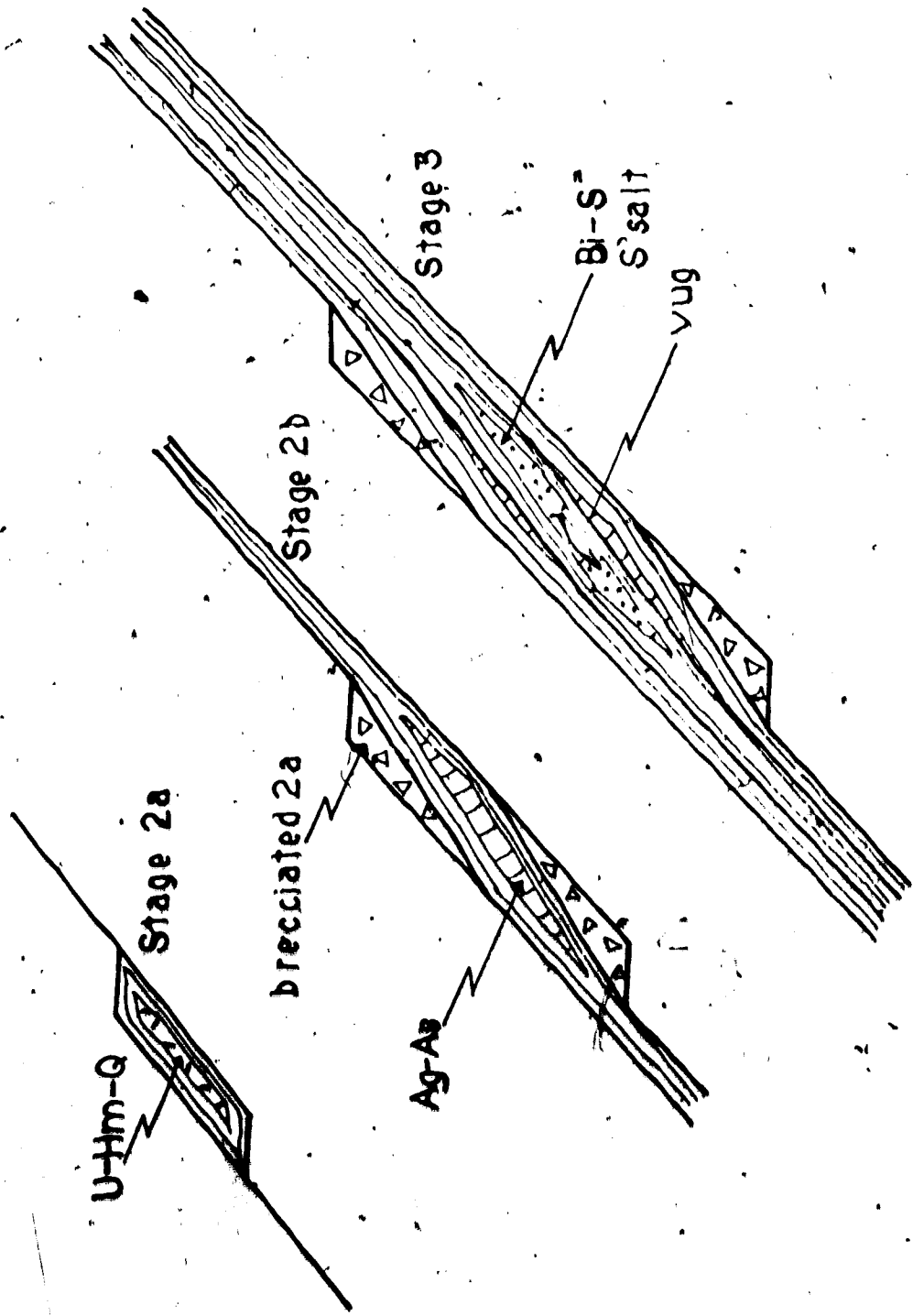


Figure 55. Idealised development of mineralised lenses in the Terra Veins.

local sealing.

Similar isolation of ore-lenses has not been observed at Echo Bay, where the fault-systems are far larger. It is thought that the minerals were deposited by fairly continuously-flowing fluids. This may explain why there is a trend in the isotopic values of the dolomites and why the sulphur isotope values, although averaging  $\delta S^{34} = 6.56\%$ , vary from  $\delta S^{34} = 26.9\%$  to  $-21.5\%$ ; these variations are most pronounced between early and late stages (Robinson, 1971). However, other explanations are possible and the limited data are not definitive.

c) Source of the Ore-fluid

It has been shown that there existed a multi-element ore-solution, or a number of identical solutions, that had an unlimited supply of carbon and oxygen, and a homogenised but limited supply of sulphur. In addition, it has been adduced that many of the metals were in limited supply, and that the deposition of one was enough to deplete the ore-fluid in that metal. The resultant change in fluid chemistry permitted deposition of other phases. Deposition occurred mainly in the  $150^{\circ}$ - $250^{\circ}$ C range and had virtually ceased by the time the temperature had dropped to  $100^{\circ}$ C.

The deposits themselves are typical of magmatic hydrothermal veins, as are their sulphur isotope values and the ranges of depositional temperatures. Most of the elements in the ore-solutions are typical of the 'felsic' association (e.g. Stanton, 1972), but

nickel and cobalt are perhaps more typical of basic rocks. One of the main problems in discussing, in general terms, the source of the U-Ni-Co-As-Ag-Bi ore-solution is this apparent mixture of associations. Consequently, there has been a mixture of hypotheses concerning the source.

Robinson (1971) showed that tuffs and andesites near the Echo Bay Mine were strongly enriched in all the elements found in the ore-bodies. He concluded that burial metamorphism in an area of high heat-flow had caused saline brines to scavenge metals from the host-rocks, and to deposit them in veins. Such an hypothesis is attractive, but should be viewed with caution for a number of reasons:

1. All Robinson's samples were taken within 1400 m of the veins, in an area where it might be argued that outward migration of ore-elements had occurred.

2. Robinson's samples were collected within the contact aureole of intrusions in which infiltration skarns are developed and which might, therefore, be expected to be enriched in many of the ore-elements.

3. The model would be far more reasonable if every small joint and fissure contained ore-veins (c.f. the rücken in the Kupferschiefer). The fact that only a specific fault-system was mineralised militates against such a widespread origin.

4. The typical homogenised sulphur isotope values and the reservoir effects observed in the Camsell River area would not be expected were the fluids derived by the above hypothesis.

Thirty-eight rock samples were analysed for a number of the

ore-elements in order to test the applicability of Robinson's hypothesis to the Camsell River area. The results are shown in Table 16. Analytical techniques and sample locations are reported in Appendix I. Some of the data are repeated from Table 2, because of their relevance here.

The results are fairly consistent, and anomalous values, that indicate that the sample contained some sulphide mineral (usually metamorphogenic), are distinct. There is a fairly good correlation between copper and zinc, probably indicating the presence of metamorphogenic sulphides. Most of the elements behave as might be expected in progressively more differentiated rocks (see Fig. 23). The plutonic rocks are quite distinct in their higher gold and uranium contents, but not in copper contents. This is taken as evidence that much of the copper escaped the confines of the plutons and formed skarns, which explains why skarns predominate over 'porphyry-type' mineralisation in this area. However, the one late granite sample analysed (NK 14.2A) is distinctly enriched in copper, manganese and gold over the earlier more basic intrusions. (The granite sample RJ 17.4 was collected about 1 m from the edge of the Republic vein. The results indicate the extent to which the ore-elements can pervade the country rocks around a mineralised vein).

The normal 'basic' affinities of nickel and cobalt are clearly demonstrated by the higher values in both basalts and diabases. No single rock-type is enriched over others, either in all, or in a significant number of the ore-elements. The values for the volcano-



sample	p.p.m. Ni	Co	Cu	Zn	Mn	Ag	Au	U
Basalt SJ29.8	43	45	190	758	3100	1.6	5	n.d.
NK1.1b	28	32	<20	74	745	1.6	5	n.d.
NK4.1a	53	40	133	151	1040	1.6	<5	n.d.
NJ29.14	20	22	31	<10	590	0.8	5	2.0
NK8.25	<20	<30	232	1250	>4500	-	-	-
Andesite lava								
SX3.9a	26	18	<20	41	1140	1.0	5	2.0
SX7.1f	7	5	33	<10	>5000	0.9	5	n.d.
NK7.13	8	16	-	-	1200	1.0	5	0.2
NK15.8	25	19	28	117	1380	0.9	5	2.0
Andesite tuff								
SJ3.3	6	12	<20	155	875	0.9	10	1.0
SJ5.1	20	26	-	-	-	0.9	10	0.8
SJ10.1	16	37	<20	80	1165	1.0	<5	0.8
NK18.8	12	18	18	125	875	0.8	<5	2.0
NK19.6	16	13	25	121	1645	1.1	-	1.0
SX14.3	-	-	<20	<10	580	-	-	-
TM24.2a	<20	<30	(1053)	(470)	>3200	-	-	-
TU-06	<20	88	37	121	3200	-	-	-
Rhyolite								
SX7.2f	8	13	31	85	305	0.9	5	-
NK12.2	10	6	<20	125	687	0.6	<5	0.8
NK16.30f	23	<30	(171)	37	385	-	-	-
SX24.1b	<20	<30	<20	135	230	-	-	-
SX16.1	<20	<30	37	<10	560	-	-	-
TU-07	8	10	18	133	177	0.6	<5	2.5
Plutonic rocks								
SX2.1	8	13	39	63	1470	0.8	15	2.0
SX14.18b	7	7	<20	107	950	0.7	<5	2.0
NK14.2a	8	14	115	85	1790	1.0	25	3.0
NK19.7	10	42	<20	<10	420	0.6	10	3.0
NK19.10	20	20	-	-	-	0.9	10	5.0
SX3.13b	4	1	<20	13	450	0.4	10	6.0
RJ17.4	(57)	(830)	(92)	(438)	(1090)	(1.0)	(25)	(3.5)
Volcanoclastic sed's.								
SJ27.1f	23	28	49	89	810	1.0	5	0.8
SX2.2	28	20	(125)	48	580	0.8	5	1.0
NK18.18	22	28	<20	106	1090	1.8	10	1.0
T-12	-	-	37	36	445	-	-	-
NK9.11	35	32	26	70	1090	1.3	5	-
Diabase								
SX3.1c	51	44	38	(2000)	>4000	1.6	<5	n.d.
NK21.1a	23	18	<20	95	1020	0.5	10	0.5
NK15.2a	20	26	-	-	-	0.6	<5	0.6

\*p.p.b.

Table 16. Whole rock trace element analyses from the Camell River Area. Figures in parentheses were not used in the averages.

clastic sediments are, predictably, close to those of the andesites.

The average trace element contents of the various lithological groups in the area are compared with data from elsewhere in the Great Bear Batholith, and with data for other calcalkaline rock suites (Table 17). The values for manganese (as not being particularly relevant) and for gold (for which there is no data from other sources) are omitted.

Robinson sampled within 1400 m of known veins, the extent and amount of mineralisation of which is considerably greater than the veins in the Camsell River area. Mursky (1963) analysed 284 samples collected on a grid basis from representative lithologies over the whole of the Hunter Bay area (120 km x 100 km, with Echo Bay in the SW corner) and used his results to demonstrate the comagmatic nature of all the volcanic, hypabyssal and plutonic rocks. The only silver mineralisation in the area he sampled was in the immediate environs of Echo Bay. Thus we can compare areas both with and without silver mineralisation.

It is apparent from Table 17 that the Echo Bay area samples are enriched over both the Hunter Bay area and the Camsell River area samples. It is also obvious that the Hunter Bay and Camsell River areas are generally similar, and it is concluded that these values are typical of the calcalkaline magmas of the area. Of particular interest, however, are the continually high zinc values in the Hunter Bay area - especially in the light of recent data (Allan et al., 1972) showing a 3000 sq mile zinc anomaly around the whole length of the

	p.p.m.	Ni	Co	Cu	Zn	Ag	U
<u>BASALT</u>							
Camsell River	31	29	119	448	1.4	0	
Lassen Peak*	63	38	80	-	-	-	-
High Alumina	25	40	35	-	-	0.2	-
<u>ANDESITE</u>							
Camsell River	14	20	20	65	0.95	1.2	
Echo Bay'	55	100	27	135	0.8	0.9	
Hunter Bay"	24	30	35	230	-	-	
High-K <sup>†</sup>	3	13	40	-	-	0.45	2.2
<u>TRYPHOLITE</u>							
Camsell River	10	12	21	87	0.7	1.7	
Hunter Bay"	10	10	20	-	-	-	
<u>PLUTONIC ROCKS</u>							
Camsell River	10	16	37	55	0.7	3.5	
Echo Bay'	56	35	117	108	0.6	5.3	
Hunter Bay"	27	32	29	188	-	-	
<u>VOLCANOCLASTIC SEDIMENT</u>							
Camsell River	27	27	30	70	1.2	0.9	
<u>DIABASE</u>							
Camsell River	31	29	24	95	0.9	0.6	
Echo Bay'	68	73	65	3950	1.2	0.6	
Hunter Bay"	90	43	122	325	-	-	

Table 17.

Comparisons of Trace Element data from the Camsell River Area with that from other parts of the Great Bear Batholith, and with Calcalkaline averages. Data from Mursky (1963)", Prinz (1967)\*, Taylor (1968)<sup>†</sup>, and Robinson (1971)<sup>†</sup>.

Wopmay Fault.

It is also apparent from the comparisons with other calcalkaline suites, that the andesites are enriched in silver, nickel and cobalt. Taylor (1968) noted that low nickel and cobalt values, and a Ni/Co ratio of less than one were definitive of calcalkaline suites. The ratios in the Camsell River and Hunter Bay areas are less than, or very close to unity for all lithologies. The ratios for the Echo Bay area are highly variable, especially between the andesites and the plutonic rocks, and this is taken as further evidence that the host-rocks have been 'mineralised' by the veins.

In discussion of the anomalies of the Echo Bay region, Robinson (Pers. Comm., 1973) has pointed out that the andesite tuffs especially may be preferentially mineralised, and that the values of nickel, arsenic, silver and uranium increase in samples taken closer to mineralised veins.

It is concluded that, although the Echo Bay area is anomalous, the magmatic rocks of the Great Bear Batholith are typically enriched in nickel, cobalt and silver. The hypothesis that the ores are derived by leaching of the volcanic rocks is not supported by the data, for the following reasons:

1. Copper and zinc are far more abundant in the host-rocks than nickel, cobalt or silver, and any scavenging process would garner these with equal or greater proficiency. This does not appear to have been the case.

2. Arsenic and sulphur are not abundant in the volcanic rocks

(Mursky, 1963; Robinson, 1971), except where sulphide skarns are developed, and therefore are unlikely to have been derived from the host-rocks.

3. The obvious ease with which host-rocks close to the veins are enriched in the ore-minerals, and the lack of depletion haloes suggests that the leaching hypothesis is invalid.

4. Metallogenic provinces may evolve for a number of reasons. They are characterised by deposits of certain elements and higher than normal contents of these elements in all lithologies. This reflects a high general content of these elements throughout the province, and hence in the source. Redistribution of elements from 'normal rocks' does not cause similar features, unless the redistribution were due to a depletion at depth and a concentration at the presently-exposed level. The Great Bear Batholith is a metallogenic province, typified by deposits of Ag-Ni, CoAs-Bi-U and by high contents of some of these elements in the host-rocks. Since almost all of the rocks in the batholith are magmatic, it is further implied that the original magmas were derived from an enriched source, or were contaminated by enriched material.

The geology, chemistry and isotope data continually point towards a magmatic origin for the ore-fluids. Furthermore, it has been shown that the three mines may lie progressively further away from the source. This distance cannot be purely vertical for the three mines are at closely similar structural levels now, and have been so since before the mineralisation. Furthermore, the temperatures of

deposition are closely similar. Consequently, there must have been a horizontal component to the direction of movement of the ore-fluids, and it has been shown that the fluids were apparently migrating away from the plutonic complexes. It is unlikely that the whole Great Bear Batholith was underlain by a potential ore-fluid, but far more probable that a similar derivative process operated in a number of areas. What was this process?

The carbon and oxygen isotope data have been interpreted as showing an infinite source for these elements. The model often postulated to explain mineralisation associated with high-level intrusions, be it of the porphyry, skarn or hydrothermal variety, involves a large cooling pluton which initiates migration of water from the rocks alongside it, into the intrusion, and eventually out through the top. Wodzicki (1971) has shown that certain elements may migrate into intrusions from the country rocks, and Shieh and Taylor (1969) have demonstrated, from oxygen isotope data, the feasibility of migration of water into intrusions. If the country rocks contain a (relatively) infinite supply of carbon and oxygen in the water, then the circulation through the intrusion will produce water with perfectly homogeneous carbon and oxygen isotope values. If these values are retained in hydrothermal fluids expelled from the intrusion, and if these fluids deposit carbonates at constant conditions, then all the carbonates will have the same isotopic values.

Continuing this model, one may conclude that because the sulphur and the metals show reservoir effects, then they must be in limited

supply to the hydrothermal fluids. Both sulphur and the metals may be supplied by the intrusion, or may be brought in by the circulating water. Since they are in limited supply, for the latter to have operated, either the rocks being leached were not rich in these elements, or the leaching process was not effective under the prevailing conditions.

Considering the processes around the upper parts of this model intrusion, a continuum of events can be predicted of the general type: metamorphism to metasomatism to progressively lower temperature hydrothermal events. This is a continuum both in time and space (i.e. in distance from the contact). The earlier parts of such a continuum have been documented around the Terra monzonite, but the veins at Terra are clearly much younger than this intrusion. Furnival (1939b) has documented a continuum from metamorphism to alteration to quartz-veining and sulphide-skarning at Contact Lake.

A time-distance plot of a single pluton (Fig. 56)<sup>1</sup> allows predictions concerning vein mineralisation to be made. At any distance (D) from an intrusive contact a certain sequence of events will occur - represented by the vertical line through D-1. Some of these events may be unable to occur until a certain time - e.g. hydrothermal veins cannot develop until fractures have opened (the fractures may be opened by an increasing hydrostatic head or by external mechanisms such as isostatic adjustments of the intrusion). Thus there may be no hydrothermal veins until time T<sub>1</sub>, even though a hydrothermal fluid existed prior to this time. From time T<sub>1</sub> onwards, a regular paragenesis

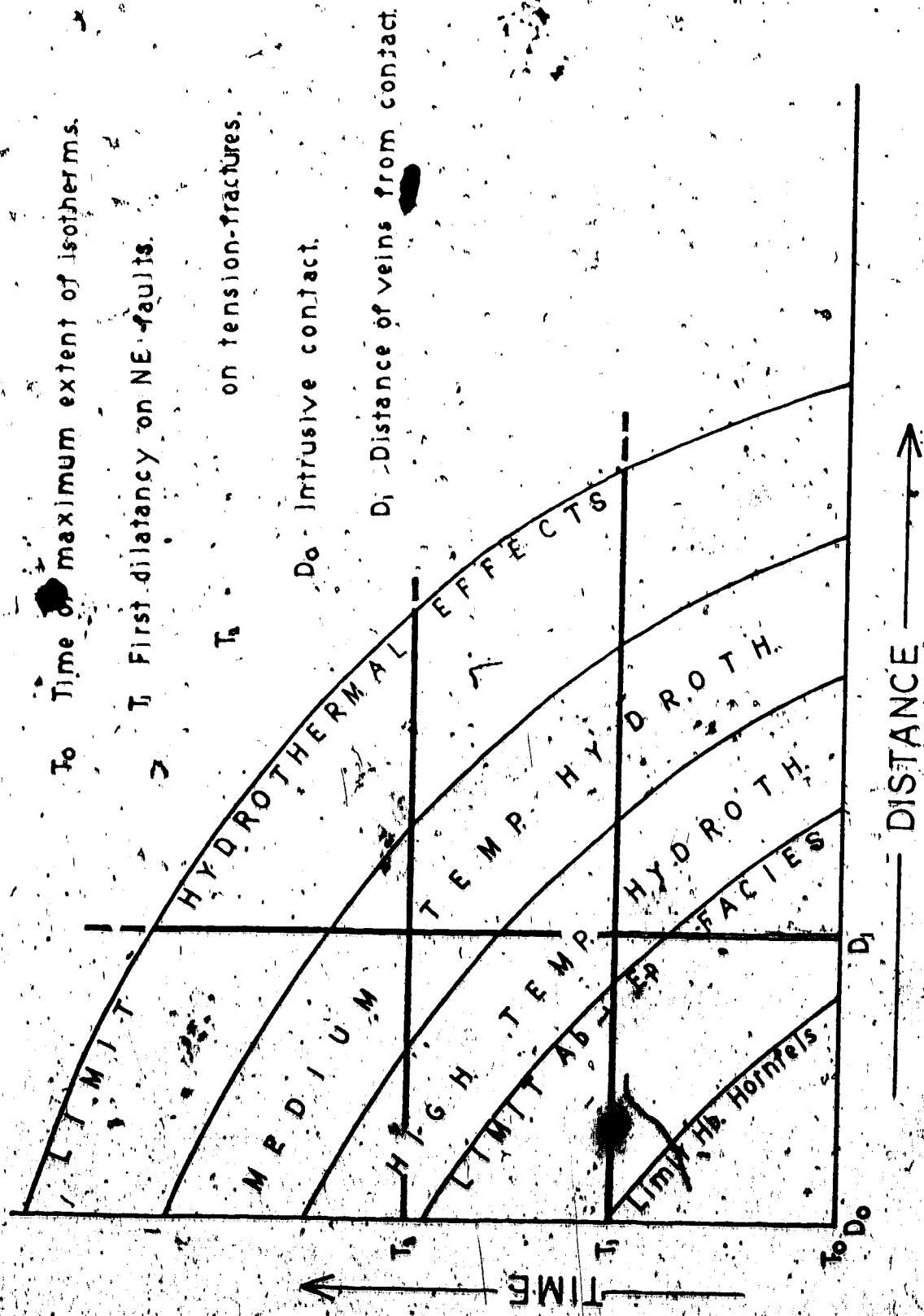


Figure 56. Idealised Time-Distance plot for development of veins around a cooling pluton.



of hydrothermal events occurs in the fracture until they become sealed. Thus, close to Terra, there are quartz veins (high temperature hydrothermal) which post-date the metamorphism, and pre-date the medium-temperature hydrothermal-mineralised veins.

Now if we consider another area where an identical intrusion has cut identical rocks, but here no fracture opens until time  $T_2$ , the conditions at time  $T_2$  may be changed enough for the same elements to deposit in a different order in the medium-temperature hydrothermal veins. Here then, is another explanation for the differences between the Terra, Norex and Silver Bay parageneses - i.e. there is a difference in the time of deposition from an identical ore-fluid.

This is obviously an extremely naïve model with respect to the Camell River area, because the deposits are not related to a simple intrusion. Nevertheless, viewing the area as a whole, a broad spectrum of events can be distinguished - from metasomatic deposits, to aplite dykes, to high-temperature quartz veins, to lower-temperature quartz and carbonate veins, to mineralised veins, and so on. It is concluded that the ores are an intimate part of this association and not the product of an exotic event.

#### d) Time and Duration of Mineralisation

If the continuum above is applicable, the relative ages of each event should fit in predictable stages, notwithstanding the added complexities of polyphase plutonism. Figure 57 shows that the relative ages of all the events fit with a typical evolutionary

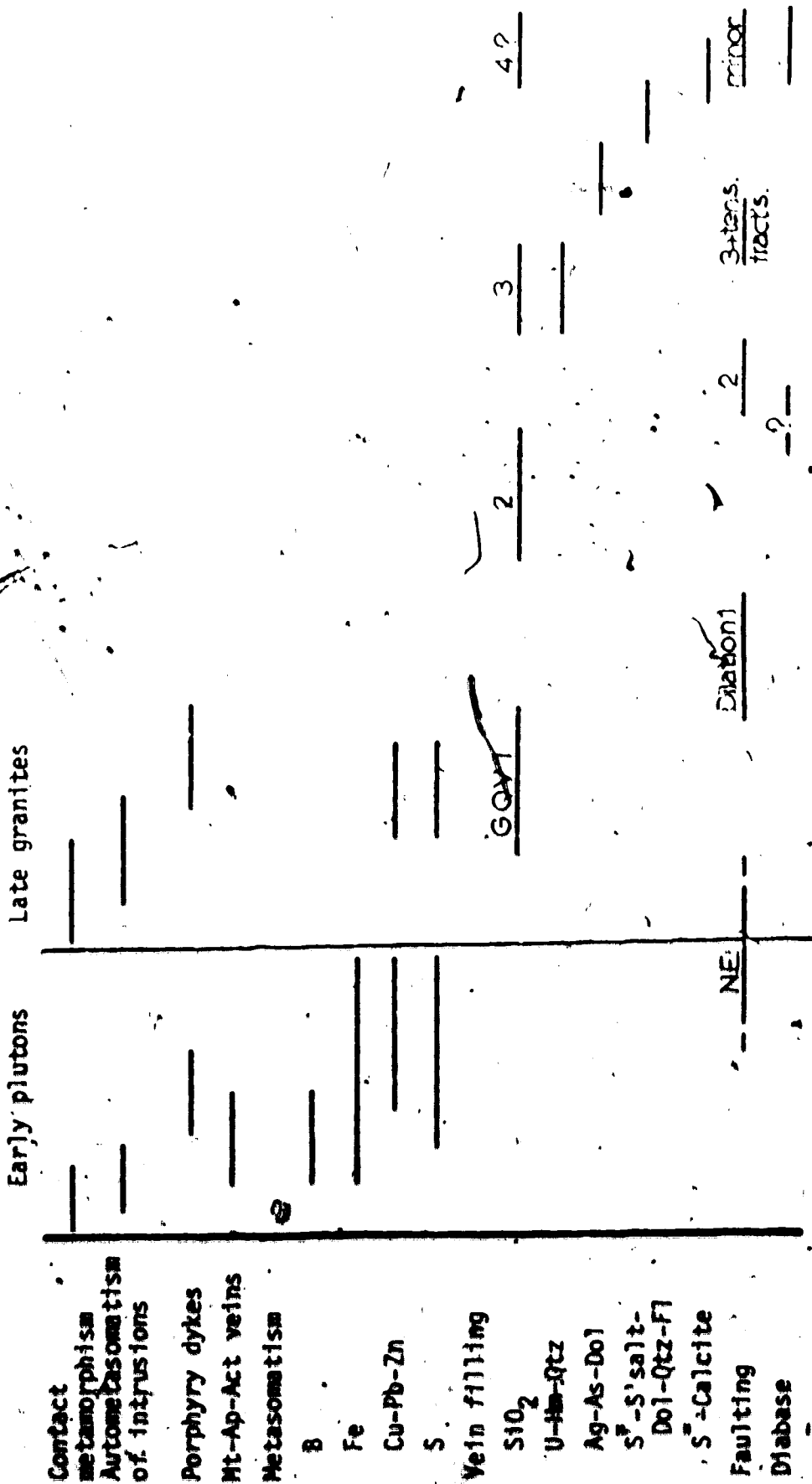


Figure 57. Paragenesis of events around the cooling plutons in the Camseil River Area.

sequence around cooling plutons. The mineralised veins fit at the latter part of a sequence that is continuous from the intrusion of the late granites, and it is proposed that the ore-fluids were derived via these late granites. There is clearly no genetic relation between the early plutons and the mineralised veins.

Although it has been proposed that the last intrusions were emplaced by 1700 m.y. ago, K-Ar cooling ages regularly range down to 1650 m.y. (Wanless et al., 1968) with some as low as 1570 m.y. (Robinson and Morton, 1972). In other words, hydrothermal activity might be expected around these granite intrusions for at least 100 m.y. after their final emplacement.

Thorpe (1972) has shown that the initial phases of the hydrothermal mineralisation occurred at 1625 m.y., and about 1400 m.y. old diabases post-date the main mineralisation: these data indicate that hydrothermal events took place for some 200 m.y. after the final granitic intrusions.

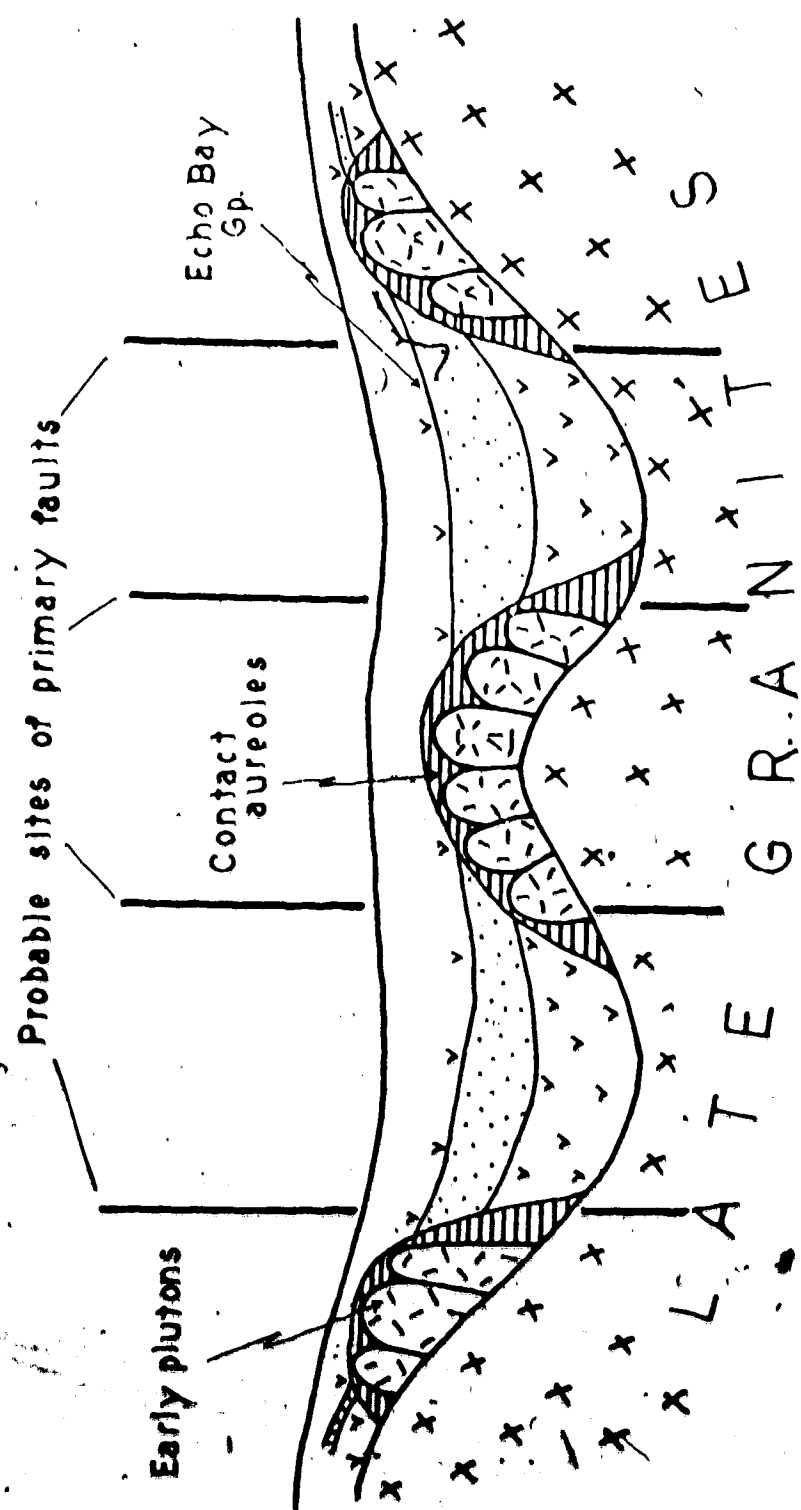
#### e) Summary

A model is proposed, therefore, where late granites intrude earlier volcanic and plutonic complexes at the close of an orogenic cycle. The granites assimilated waters from surrounding rocks at depth and homogenised them. These waters were then expelled as hydrothermal fluids into fissures developed above the granites. At some stage the waters picked up sulphur and a number of metals. In the final analysis it is unlikely that the metals were leached from the host rocks because the distinct Ni-Co-As-Ag-U-Bi association occurs in many different

geological settings throughout the world. Consequently, it is considered that the metals were present in the magmas themselves.

The expelled hydrothermal solutions migrated away from the granites and deposited sequentially lower temperature facies at different times or distances from the contacts. The initial filling of the Giant Quartz Veins is presumed to be the result of the highest temperature stage of the hydrothermal deposition. The mineralised veins were deposited in a fairly restricted zone, and at fairly restricted temperatures. In other words, for their deposition, a coincidence of the right structural, chemical and physical conditions was required. This is demonstrated in Figure 58, a schematic model of the Camsell River area. It has already been shown that the late granites intrude 'highs', marked by the older satellite plutons and surrounding 'lows' of volcanic rocks. Thus, hydrothermal solutions migrated out from these 'highs' into the interstitial keels of volcanic rock and deposited minerals in veins. The coincidence of the correct physical, chemical and structural conditions for deposition occurs where the suitable temperature and pressure zone meets the fractured and sulphide-rich rocks in the contact aureoles of the early plutons, and it is in these locations that all the mineralisation is found.

The foregoing model explains the observed geologic relations, the parageneses of hydrothermal events, and the isotopic data. There is only one fact that jibes with the model - that the niccolite-bearing vein at Gunbarrel Inlet is in gabbro that apparently post-dates



Maximum and minimum extent of areas physically and chemically suitable for hydrothermal mineralisation:

Figure 58. Schematic Cross-section of the Camell River Area showing probable sites for development of hydrothermal veins derived from the late granites.

the main hydrothermal events. It can only be concluded that the gabbro remobilised a pre-existing vein during its intrusion.

How reasonable is this model? Earlier workers have proposed a gamut of origins for the veins, from a source in the granites (Kidd and Haycock, 1935), and a source in the volcanic rocks (Robinson, 1971) to a source in the diabases (Furnival, 1934). It is interesting to note the temporal sequence of these ideas, and its similarity to the sequence of ideas explaining the dissimilar Cobalt deposits. The main objection voiced by many critics of the granite-origin hypothesis is the time involved. "Veins are observed cutting the granites and therefore cannot be related to them" is a criticism voiced at the International Geological Congress in 1972. "How can any hydrothermal system last for 200 m.y.?" is another. Yet when the deposits are considered as part of a continuum of events, their relation to the granites is quite obvious. It is strange that workers will go to extraordinary lengths to justify exotic origins for this ore-association, and yet will accept that other major batholiths acted as a source for hydrothermal veins of other metallic associations. For example, it has been shown that the granite in SW England produced a continuum of events as follows:

skarns and pegmatites, followed by porphyry dykes, followed by hydrothermal mineralisation (Sn - Cu-As-W - Pb-Zn-Ag - Fe-Mn-Sb)  
(Park and McDiamid, 1964)

Hosking (1964) has shown that mineralisation continued from the Permian-Carboniferous to the Eocene (an interval of 230 m.y.), and that

chloride-rich hot springs are active in some of the mines at present.

The comparison with the granite in SW England is, in fact, far closer. This batholith is typical of the Hercynian orogenic intrusions and is morphologically very similar to the Great Bear Batholith. The ores lie in similarly controlled structural sites. The principal difference is that the ores are zoned with successively younger and lower temperature ores lying further from the contact. This presumably indicates that suitable sites for deposition were present at all distances from the contact, and contrasts with the limited distribution of such sites in the Camsell River area. If the total assemblage of Stages 5 and 6 (Fig. 59) of the English granite is combined, the mineralogy is indistinguishable from that of the Camsell River mines, except in the lack of native silver. Certainly all the elements are present, and the paragenesis is the same. The metallography of the two examples does differ in that the English granites contain tin, wolfram and molybdenum, and that the proportions of nickel, cobalt, silver, bismuth, arsenic and uranium are much lower.

Consequently, it is proposed that the multi-element Great Bear Lake assemblage is the result of the constriction or telescoping of separate stages of an evolving hydrothermal system into one depositional location. The assemblage is retained in the source (i.e. the granite) until all the elements are contained in a complex polymetallic ore-fluid. Where there has been no such retention, a complex fluid will not develop - as each metal or group of metals becomes able to be precipitated, it is so, and the elements are lost to, and therefore





cannot affect, the remaining fluids.

If the assemblage is the product of 'telescoping' in this manner, then it might be reasonable to expect gradations from completely telescoped situations to completely untelescoped examples. For example, the almost identical deposits at Jachymov are preceded by a period of molybdenum, wolfram, tin, arsenopyrite mineralisation as in the SW England case, but at Jachymov, the products of each stage coincide in space. Similarly, the deposits at Kongsberg are preceded by veins containing pyrite, pyrrhotite, sphalerite, galena and molybdenite. At the lower temperature end deposits of silver, copper and sulphosalts are typical of many of the mining provinces in Mexico and the Andes. In many of these, the early stages of pre-vein volcanogenic sulphides contain concentrations of arsenides, bismuth, silver and antimony (Goossens, 1972). In particular, the deposits at Sorpresa, in Bolivia, and Cusco, in Peru, show the typical Ni-Co etc. assemblage in areas otherwise characterised by the later-evolved Ag-Bi-sulphosalt veins (Ramdohr, 1969). Gillerman (1968) has shown that silver and sulphosalt mineralisation gives way to older uranium and arsenide mineralisation at depth in the Bullard Peak veins in New Mexico. Consequently, there is a progressive sequence in the amount of telescoping.

#### f) Comparisons with Other Deposits

The deposits at Jachymov and in the Erzgebirge are remarkably similar to those at Great Bear Lake (Boyle, 1968; Pavlu, 1970; Naumov

et al., 1971), and Pavlu ascribes their origin to late Variscan granites. They are similar in mineralogy, in paragenesis, in the amount of telescoping, in the controls and mode of deposition, and in their zoning. Most especially, the distinct antipathy of bismuth and silver, and the association of silver with the nickel-rich arsenides, and bismuth with copper-iron-rich arsenides was noted by Pavlu (op. cit.).

The deposits of the Kongsberg district of Norway show a similar paragenesis and mineralogy, but they are localised where veins cross pre-existing sulphide-rich fahlbands (Vokes, 1967). In addition, they lack uranium and bismuth, and it has been proposed that they originated by leaching of metals from the sulphides.

Kroutov (1972), in describing the veins of the Khouvu-Axy district relates them to hydrothermal solutions percolating from the 'foyer abyssal' up regional faults. The paragenesis, mineralogy and morphology of the veins is identical to that of the Great Bear Lake veins, and the minerals were emplaced after a period of skarning and metasomatism around intermediate intrusions. However, details of the geology are not available, and the time relations are not clear.

Gillerman (1968) relates the very similar New Mexican veins to Early Tertiary monzonite intrusions, and Ramdohr (1969) has noted the supraplutonic-subvolcanic nature of the Sorpresa and Cusco deposits.

The deposits in the Chalanches, France, area post-date sulphide-carbonate veins, and show the same mineralogy and paragenesis as the Great Bear Lake deposits. Ypma (1972) implies that these veins may have their source in diabase, in which they lie, and compares them

with the Cobalt deposits. He notes that depositional temperatures range between 280° C and 150° C.

The deposits in Ontario are, again, mineralogically and paragenetically similar to others, and the structural controls and mode of deposition are similar to those at Great Bear Lake. Jambor and Petruk (1971) continually stress the relationships of the ores and the Nipissing diabase, and suggest that the diabase is the parent magma for deposits. Halls and Stumpf (1969) and Boyle and Dass (1971) equally firmly stress the relationships of Archean sulphides and ore-veins, and propose a leaching model. The Ontario deposits differ in that there appears to be no granite intrusion nearby. The validity of leaching hypotheses is evident in the Mansfeld district, where nickel, cobalt, arsenic and silver, in particular, have been leached from the Kupferschiefer and deposited in joints and fractures (rücken). However, these rücken remain just that - they are in no way similar to the hydrothermal vein deposits.

It is shown that many of the Ni-Co etc. deposits have been, and most may be related to hydrothermal activity around large intrusions. Unless other evidence comes to light, the deposits at Cobalt must remain a unique and special case. Furthermore, the deposits generally occur in a restricted structural site, and many periods of mineralisation may coincide in space, indicating that the association is the product of a telescoped hydrothermal sequence, whose elements have been unable to separate in space and time.

## 11. SUMMARY AND THE ORIGIN OF THE NICKEL-COBALT ARSENIDE SILVER ORE TYPE

Nickel-cobalt arsenide deposits throughout the world occur typically in podiform hydrothermal veins. The ore-association is complex, both because of polymetallic assemblages, and also because of extended sequences of deposition and a resultant host of accretionary and replacement textures. It has been shown in Part II that the Great Bear Lake deposits are part of a continuum of events around calcalkaline batholiths, and in Part I it was argued that these batholiths are the product of continent-margin tectonics and partial melting beneath the edge of this continent. It was further argued that the metals in the ore-veins were derived from the batholith magmas, and hence are themselves the product of continent-margin tectonics. The validity of this hypothesis may be tested by comparison of the Great Bear Lake deposits with other similar deposits in the world.

Table 18 shows various features of all the deposits known to the author, and demonstrates a number of factors common to these deposits. Firstly, it is clear that the Ni-Co-Ag deposits of the world fall into three distinct age groups:

1. 1700-1400 m.y. Associated with Aphebian orogenic events.
2. 400-250 m.y. Associated with Hercynian orogenic events.
3. 100-10 m.y. Associated with Alpine/Andean/Laramide orogenic events.

Age and Deposit	Main elements other than Ni-Co-Fe-As-Ag.	Host Rock	Associated Intrusions	Theories of Origin	Reference
1700-1400 m.y. Great Bear Lake, Canada.	Cu-Pb-Zn-Bi-Sb-U-S	Intermediate volcanics	Calcaline plutons	Hydrothermal from intrusions.	This work.
Great Slave Lake, Canada.		Gneisses and limestone	Intermediate dykes and laccoliths	As above	Work by author in 1971.
Thunder Bay, Canada.	Cu-Pb-Zn-Sb-S-C	Clastic sed.	'Granite'	As above	Bastin, 1939.
Cobalt-Gowanda, Canada.	Mg-Cu-Pb-Zn-Sb-S	" "	Nipissing Diabase	i From diabase. ii From hidden Granite.	Jambo, 1971 Bastin, 1939
400-250 m.y. Kongsberg and Modum, Norway.	Pb-Sb-S-Tl	S-rich schists ? and gneisses.	Minor Amphibolite	iii From leaching of Sulphides.	Boyle and Dass 1971.
Erzegebirge, Germany.	Cu-Pb-Zn-Sb-Bi-S- Sn-U.	Mica schists	Calcaline plutons	i From parent magma of amphibolite. ii From sulphide Fahbands.	Gammon, 1966 Vokes, 1967.
Jachymov, C.S.S.R. Lahmjaure, Sweden.	As above No Ag	As above ?	'Granitoids'	Hydrothermal from intrusions	Stanton, 1972
Down N.Y., U.S.S.R.	Bi-S	Sediments & volcanics	Intermediate plutons and basic sills.	As above ?	Pavlu, 1971 Ramdohr, 1955.
Cornwall, U.K.	Sn-W-Cu-Pb-Zn-U-S	Clastic sed.	Calcaline Batholiths	Hydrothermal up faults from "Foyer abyssal".	Kroutov, 1972.
Boj Azzer, Morocco Age uncertain.	Au-Cu-U	?	?	Hydrothermal from batholiths	Park & McDiarmid, 1970 Stanton, 1972.
					Ramdohr, 1969

Table 18. Age, Chemistry, Host-rock and possible sources of Ni-Co-As-Ag Deposits in the World. C'nt'd overleaf.

Age and Deposit	Main elements other than Ni-Co-Fe-As-Ag	Host Rock	Associated Intrusions	Theories of Origin	Reference
400-250 m.y. c'nt'd. Pozoblanco, Spain	Pb-Zn-Bi-Sb-S	?	?	?	Ramdohr, 1969
Sarrabus, Sardinia	Cu-Pb-Zn-Bi-Sb-S-Ba	Black Schists	Granite/Aplite/Porphyr.	Hydrothermal from intrusions	Stanton, 1972
Dobschau, Hungary	Cu-S-B	Diorite	Diorite	As above	Stanton, 1972
100-10 m.y. Chalanches, France	Cu-Pb-Zn-Bi-Sb-S-Au-Hg	Diabase	? Diabase	From diabase magma?	Ypma, 1972
Kalterberg and Val d'Anniviers, Switzerland	Cu-Pb-Zn-Sb-S	?	?	?	Ramdohr, 1969
Schladming, Austria	No Ag	?	?	?	Ramdohr, 1969
Tajmesti, Iran	Cu-S	?	?	?	Ramdohr, 1969
Chanarcillo and Japonesa, Chile	Cu-Bi-Sb-S-C	?	Calcalcaline Intrns.	Hydrothermal from intrusions	Ramdohr, 1969
Cusco, Peru	No Ag	?	As above	As above	Ramdohr, 1969
Sopressa, Bolivia	Cu-Pb-Zn-Bi-S-C	?	As above	As above	Ramdohr, 1969
Bullard Peak, New Mexico	Cu-Pb-Zn-Bi-Sb-S-U-CI	Gneisses	Monzonite	As above	Gillerman, 1968.
Mickenberg, Arizona	As above	As above	Granitic Pegmatites	As above	Stanton, 1972
Batipolias, Mexico	Pb-Zn-Sb-S-Ba	Andesite/Diorite	Granite	As above	Stanton, 1972
Sabinal, Mexico	Cu-Pb-Zn-Sb-Bi-S	Limestone	Aiskaita	As above	Stanton, 1972
Age Unknown Shashani, Rhodesia	None	?	?	?	Ramdohr, 1969

Table 18. Continued from previous page. Age, Chemistry, Host Rock and possible sources of Ni-Co-Fe-As-Ag deposits in the World.

Consequently, it is proposed that the deposits form an intimate part of each of these orogenic events, regardless of their apparent origin. Furthermore, each of these orogens, apart from the Alpine, is of a continent-margin (Andean) type, and in each case the ore-deposits are emplaced in the orogenic hinterland.

Secondly, the ore-deposits are usually part of a polymetallic association that typically includes: Cu, Pb, Zn, S, Bi, Sb, As, U, and, less commonly, Hg, Mo, Sn, W, as well as Ni, Co, Fe, Ag and Au. In almost every case, for which adequate documentation could be found in the literature, the veins are telescoped, and are pre-dated by Sn, Mo, W, U mineralisation, and post-dated by sulphide and sulphosalt mineralisation. This implies not only a common source for the ore-fluids, but also a common environment of deposition that demands at least some telescoping of the deposition. This environment must relate in some way to the history of continent-margin orogens.

Thirdly, the environment of deposition is totally independent of the host rock lithology, but in 14 of the 17 cases that are accurately documented, the veins have been ascribed to deposition from hydrothermal fluids that originated in various types of intermediate-to-acidic igneous rocks. The environment of deposition is controlled by the structures caused by intrusion of these igneous rocks. It is of interest to note that wherever the igneous rocks have been analysed, they are calcalkaline to alkaline - i.e. typical of the inner parts of continent-margin orogens.

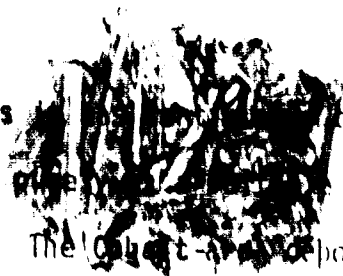
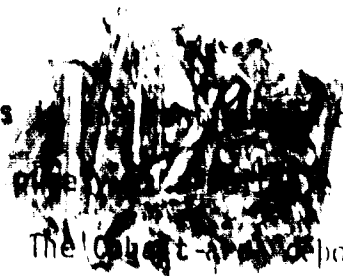
In addition, lateral secretion from pre-existing sulphide bodies

has been proposed for two of the best-documented deposits, and an origin from diabase magma has been proposed for three others.

Consequently, it is proposed that the Ni, Co, As-Ag deposits are part of a continuum of ores that results from hydrothermal activity around late orogenic calcalkaline-to-alkaline intrusions in the inner parts of continent-margin orogens. The association is best developed where deposition is condensed into one structural site, and is poorly developed, and consequently often not recognised, where an abundance of depositional sites has allowed uncondensed mineral zoning to develop (c.f. Cornwall).

In conclusion, although the Great Bear Lake, Cobalt, or Erzegebirge areas appear to be metallogenic provinces, and although the Aphebian, Hercynian, etc. periods appear to be metallogenic eras for these deposits, it is argued that this is due, not to an anomalous metal content in these areas and at these times, but to the coincidence of a number of geotectonic processes. There is but one thorn in the side of this argument - and a rather large one at that: the Cobalt-Gowganda deposits. It is of interest, however, that for all the deposits that have, at some time or other, been ascribed to a source in diabase (Cobalt, Kongsberg and Chalanchoy), other theories of origin have also been advanced (see Table 18), whereas in the other deposits only the one (magmatic hydrothermal) origin has been proposed. These 'other theories' include an origin in hidden or distant granitic rocks, or by lateral secretion from older massive sulphide concentrations. Support for the lateral secretion hypothesis



has dwindled, as  been demonstrated that the sulphides acted  structural site for deposition (Gammon, 1966). The Cobalt-area deposits are anomalous in a number of ways. Firstly, the ore-province is orders of magnitude larger than others. Secondly, bismuth is rare, and uranium is absent in these veins. Thirdly, there is no temporal relationship between the deposits and any form of orogenic event, and there are no granites exposed in the area. Bastin (1939) has pointed out the association of granites and identical ore-veins in the Thunder Bay district, but unless the granites in the Cobalt area are well-hidden, there is no such association there.

Consequently, until new data comes to light, it can only be said (and many authors have similarly shrugged their shoulders and given this conclusion) that the Cobalt-area deposits are anomalous, but that the origin of the remaining deposits is similar and distinct.



## REFERENCES

- ALLAN, R.J., Cameron, E.M. and Durham, C.C., 1972: Bear-Slave Operation. Geol. Surv. Canada, Paper 73-1A, 50+52.
- A.S.T.M., 1972: X-ray powder diffraction file.
- BADHAM, J.P.N., 1972: The Camsell River-Conjuror Bay area, Great Bear Lake, N.W.T. Can. Jour. Earth Sci. 9, 1460-1468.
- \_\_\_\_\_, 1973: Calcalkaline volcanism and plutonism from the Great Bear Batholith, N.W.T. Can. Jour. Earth Sci. (in press).
- \_\_\_\_\_, Robinson, B.W. and Morton, R.D., 1972: Geology and genesis of the Great Bear Lake silver deposits. 24th Intern. Geol. Congr., Montreal, Sect. 4, 541-547.
- BAMFORD, R.W., 1972: The Mount Fubian porphyry copper deposit, Territory of Papua and New Guinea. Econ. Geol. 67, 1019.
- BARAGAR, W.R.A., 1966: Geochemistry of the Yellowknife volcanic rocks. Can. Jour. Earth Sci. 3, 9-30.
- BARTON, P.B. Jr. and Skinner, B.J., 1967: Sulphide mineral stabilities. In Geochemistry of Hydrothermal Ore Deposits, ed. H.L. Barnes. Holt, Reinhardt and Winston, New York, 665 pp.
- BASTIN, E.S., 1939: The nickel-cobalt - native silver ore-type. Econ. Geol. 34, 1-40.
- BELL, J.M., 1900: Topography and geology of Great Bear Lake. Geol. Surv. Canada, Ann. Rept. XIIIIC, 5-28.
- BOYLE, R.W., 1968: The geochemistry of silver and its deposits. Geol. Surv. Canada, Bull. 160, 264 pp.

- BOYLE, R.W. and Dass, A.S., 1971: Origin of the native silver veins at Cobalt, Ontario. *Can. Mineral.* 11, 414-417.
- BROCK, K.J., 1972: Genesis of Garnet Hill skarn, Calaveras Co., California. *Bull. Geol. Soc. Amer.* 83, 3391-3404
- BUDDINGTON, A.F. and Lindsley, D.H., 1964: Iron-titanium oxide minerals and synthetic equivalents. *Jour. Petrol.* 5, 310-357.
- BYERS, F.M. Jr., 1961: Petrology of three volcanic suites, Umnak and Bogolosof Islands, Aleutian Islands, Alaska. *Bull. Geol. Soc. Amer.* 72, 93-128.
- CAMPBELL, D.D., 1955: Geology of the pitchblende deposit of Port Radium, Great Bear Lake, N.W.T. Unpubl. Ph.D. Thesis, Calif. Inst. Tech.
- CHINNERY, M.A., 1966: Secondary Faulting. 1. Theoretical aspects; 2. Geological aspects. *Can. Jour. Earth Sci.* 3, 163-190.
- CLAYTON, R.N. and Epstein, S., 1958: The relationship between  $O^{18}/O^{16}$  ratios in coexisting quartz, carbonate and iron oxides from various geological deposits. *Jour. Geol.* 66, 352-373.
- CRAIG, H., 1957: Isotopic standards for carbon and oxygen and correction factors for mass-spectrographic analysis of carbon dioxide. *Geochim. Cosmochim. Acta* 12, 133.
- CRAIG, J.R., 1967: Phase relations and mineral assemblages in the Ag-Pb-Bi-S system. *Mineral. Dep.* 1, 278-306.
- CUMMING, G.L., Wilson, J.T., Farquhar, R.M. and Russell, R.D., 1955. Some dates and subdivisions of the Canadian Shield. *Proc. Geol. Assoc. Canada* 7, 27-29.

- DEWEY, J.F. and Bird, J.M., 1970: Lithosphere plate-continental margin tectonics and the evolution of the Appalachian Orogen. Bull. Geol. Soc. Amer. 81, 1031.
- \_\_\_\_\_ and Horsfield, B., 1970: Plate tectonics, orogeny and continental growth. Nature 225, 521-525.
- DICKINSON, W.R., 1970: Relations of andesites, granites, and derivative sandstones to arc-trench tectonics. Rev. Geophys. 8, 813-860.
- DOUGLAS, B.J.W. and Price, R.A., 1972: Variations in tectonic styles in Canada. Geol. Assoc. Canada, Spec. Paper 11, 688.
- ECKELMANN, W.R. and Kulp, J.L., 1957: Uranium-lead method of age determination. Part II. N. American localities. Bull. Geol. Soc. Amer. 68, 1117-1140.
- ENGEL, C.G., 1959: Igneous rocks and constituent hornblendes of the Henry Mountains, Utah. Bull. Geol. Soc. Amer. 70, 951-980.
- EWART, A., Taylor, S.R. and Capp, A.C., 1968: Trace and minor element geochemistry of the rhyolitic volcanic rocks, Central North Island, N.Z. Contr. Mineral. Petrol. 18, 76-104.
- FAWCETT, J.J. and Yoder, H.S. Jr., 1966: Phase relationships of chlorites in the system  $MgO-Al_2O_3-SiO_2-H_2O$ . Amer. Mineral. 51, 353-380.
- FAHRIG, W.H. and Wanless, R.K., 1963: Age and significance of diabase dyke swarms of the Canadian Shield. Nature 200, 934-937.
- FENIAK, M., 1947: The geology of Dowdell Peninsula, Great Bear Lake, N.W.T. Geol. Surv. Canada, Spec. Rept., 14 pp.

- FENIAK, M., 1949: McAlpine Channel map-area. Geol. Surv. Canada, Paper 49-19.
- FISHER, R.V., 1961: Proposed classification of volcanoclastic sediments and rocks. Bull. Geol. Soc. Amer. 72, 1409-1414.
- FLANAGAN, F.J., 1969: U. S. Geological Survey Standards. II. First compilation of data for the new U.S.G.S. rocks. Geochim. Cosmochim. Acta 33, 81-120.
- FLEISCHER, M. and Stevens, R.E., 1962: U. S. Geological Survey Standards. I. Summary of new data on rock samples G1 and W1. Geochim. Cosmochim. Acta 26, 515-543.
- FRASER, J.A., Hoffman, P.F., Irvine, T.N. and Muirsky, G., 1972: The Bear Province, In Variations in Tectonic Styles in Canada, eds. R.J.W. Douglas and R.A. Price. Geol. Assoc. Canada, Spec. Paper 11, 454-503.
- FURNIVAL, G.M., 1934: Silver mineralisation at Great Bear Lake. Can. Min. Jour. 1, 5.
- \_\_\_\_\_, 1935: The large quartz veins of Great Bear Lake. Econ. Geol. 30, 843-850.
- \_\_\_\_\_, 1939a: A silver-pitchblende deposit at Contact Lake, Great Bear Lake area, Canada. Econ. Geol. 34, 739-776.
- \_\_\_\_\_, 1939b: Geology of the area north of Contact Lake, N.W.T. Amer. Jour. Sci. 237, 476.
- GABRIELSE, H., 1972: Younger pre-Cambrian of the Canadian Cordillera. Amer. Jour. Sci. 272, 521-586.

- GAMMON, J.B., 1966: Fahlbands in the Precambrian of southern Norway.  
Econ. Geol. 61, 174-188.
- GILLERMAN, E., 1968: Uranium mineralisation in the Burro Mountains,  
New Mexico. Econ. Geol. 63, 239-246.
- GOOSSENS, P.J., 1972: Metallogeny in the Ecuadorian Andes.  
Econ. Geol. 67, 458-468.
- GREEN, D.C. and Baadsgaard, H., 1971: Temporal evolution and  
petrogenesis of an Archean crustal segment at Yellowknife, N.W.T.,  
Canada. Contr. Mineral. Petrol. 12, 177.
- GEOLOGICAL SURVEY OF CANADA: Maps 1014A, 997A, 1224A, A9-19
- GULSON, B.L., Lovering, J.F., Taylor, S.R. and White, A.J.R., 1972:  
High K-diorites, their place in the calcalkaline association,  
and relation to andesites. Lithos 5, 269-279.
- HALLS, C., and Stumpf, E.F., 1969: Geology and ore deposition,  
western Kerr Lake Arch, Cobalt, Ontario. 9th Common. Min.  
and Met. Cong., Paper 18, 44 pp.
- HAMILTON, W., 1969: Mesozoic California and the underflow of the  
Pacific Mantle. Bull. Geol. Soc. Amer. 80, 2409-2430.
- \_\_\_\_\_ and Myers, W.B., 1967: The nature of batholiths.  
U.S. Geol. Surv., Prof. Paper 554-C, 30 pp.
- HARRIS, D.C. and Thorpe, R.I., 1969: New observations on matildite.  
Can. Mineral. 9, 655-662.
- HEITANEN, A., 1963: Idaho batholith near Pierce and Bungalow.  
U.S. Geol. Surv., Prof. Paper 344-D, 33 pp.
- HOFFMAN, P.F. 1969: Proterozoic paleocurrents and depositional history  
of the East Arm Fold Belt, Great Slave Lake. Can. Jour. Earth  
Sci. 6, 441.

- HOFFMAN, P.F., 1972: Cross-section of the Coronation Geosyncline (Aphebian), Tree River to Great Bear Lake, District of Mackenzie. Geol. Surv. Canada, Paper 72-1A, 119-125.
- \_\_\_\_\_, 1973: Evolution of an early Proterozoic continental margin: the Coronation Geosyncline and associated aulacogens of the NW Canadian Shield, In Evolution of the Pre-Cambrian Crust. Phil. Trans. Roy. Soc. London 1
- \_\_\_\_\_, Fraser, J.A. and McGlynn, J.C., 1970: The Coronation Geosyncline of Aphebian age, In Basins and Geosynclines of the Canadian Shield, ed. Baer. Geol. Surv. Canada, Paper 70-40, 201-212.
- HOLLAND, J.G., and Brindle, D.W., 1966: A self-consistent mass absorption correction for silicate analysis by X-ray fluorescence. Spectrochim. Acta 22, 2083-2093.
- HOLMES, R.J., 1947: Higher mineral arsenides of cobalt, nickel and iron. Bull. Geol. Soc. Amer. 55, 299-292.
- IRVINE, T.N. and Baragar, W.R.A., 1971: A guide to the chemical classification of the common volcanic rocks. Can. Jour. Earth Sci. 8, 523-548.
- IRVING, E., Donaldson, J.A. and Park, J.K., 1972: Palaeomagnetism of the Western Channel diabase and associated rocks, N.W.T. Can. Jour. Earth Sci. 9, 960.
- JAKES, P. and Smith, I.E., 1970: High K-calcalkaline rocks from Cape Nelson, E. Papua. Contr. Mineral. Petrol. 28, 259-271.



- JAKES, P. and White, A.J.R., 1972: Hornblendes from calcalkaline volcanic rocks of island arcs and continental margins. *Amer. Mineral.* 57, 887-902.
- JAMBOR, J.L., 1971: Origin of the silver veins of the Cobalt-Gowganda region. *Can. Mineral.* 11, 402-412.
- JENSEN, M.L., 1967: Sulphur isotopes and mineral genesis, In *Geochemistry of Hydrothermal Ore Deposits*, ed. H.L. Barnes. Holt, Reinhardt and Winston, New York, 143-165.
- JOLLIFFE, A.W., 1948: The NW part of the Canadian Shield. *Intern. Geol. Congr., Sess. 18, Part 3*, 141-149.
- JOPLIN, G.A., 1968: The Shoshonite Association - a review. *Jour. Geol. Soc. Australia* 15, 275-294.
- JORY, L.T., 1964: Mineralogical and isotopic relations in the Port Radium deposit. Unpubl. Ph.D. Thesis, Calif. Inst. Tech., Pasadena.
- KAJIWARA, Y. and Krouse, H.R., 1971: Sulphur isotope partitioning in metallic sulphide systems. *Can. Jour. Earth Sci.* 8, 1392-1409.
- KEIGHIN, A. and Honea, J., 1969: The system Ag-Sb-S from 600°C to 200°C. *Mineral. Dep.* 4, 123.
- KIDD, D.F., 1932: A pitchblende-silver deposit, Great Bear Lake. *Econ. Geol.* 27, 145.
- \_\_\_\_\_, 1933: Great Bear Lake area, N.W.T. *Geol. Surv. Canada, Summ. Rept.*, C 1-36.
- \_\_\_\_\_, 1934: Rae-Great Bear Lake area, north sheet. *Geol. Surv. Canada, Map 333A.*

- KIDD, D.F., 1936: From Rae to Great Bear Lake, Mackenzie District, N.W.T. Geol. Surv. Canada, Mem. 187.
- \_\_\_\_\_ and Haycock, M.H., 1935: Mineragraphy of the ores of Great Bear Lake. Bull. Geol. Soc. Amer. 46, 881-905.
- KROUTOV, G.A., 1972: Le Gisement des mineraux As-Ni-Co au Khouvu-Axy. 24th Intern. Geol. Congr., Montreal, Sect. 4, 527.
- LEAKE, B.E., 1968: A catalogue of analysed calciferous and sub-calciferous amphiboles, together with their nomenclature and associated minerals. Geol. Soc. Amer., Spec. Paper 98.
- LISTER, G.F., 1966: The composition and origin of selected Fe-Ti deposits. Econ. Geol. 61, 275.
- MacDONALD, G.A., 1953: Pahaehoe, aa and block lava. Amer. Jour. Sci. 251, 169-191.
- MANSON, V., 1967: Geochemistry of basaltic rocks - major elements, In Basalt, eds. H.H. Hess and A. Poldervaart. John Wiley and Sons, New York, 215-270.
- McBIRNEY, A.R., 1969: Compositional variations in Cenozoic calc-alkaline suites of central America, In Proc. Andesite Conf., ed. A.J. McBirney. Oregon Dept. Mines, Bu 1 65, 185-190.
- McREATH, I., 1973: Petrogenesis in Island Arcs. Unpubl. Ph.D. Thesis, University of Leeds, England.
- \_\_\_\_\_, 1973: Ti-Zr fractionation in island arcs. In preparation.
- MITCHELL, A.H. and Reading, H.G., 1971: Evolution of island arcs. Jour. Geol. 79, 253.

- MONGER, J.W.H., Souther, J.G. and Gabrielse, H., 1972: Evolution of the Canadian Cordillera: a plate tectonic model. *Amér. Jour. Sci.* 272, 577-602.
- MURSKY, G., 1963: Mineralogy, petrology and geochemistry of the Hunter Bay area, Great Bear Lake, N.W.T. Unpubl. Ph.D. Thesis, Stanford University.
- NAUMOV, G.B., Motorina, Z.M. and Naumov, V.B., 1971: Conditions of formation of carbonates in veins of the Pb-Co-Ni-Ag-U type. *Geokhimiya* 8, 938-948.
- OELSNER, O., 1961: Atlas of the most important ore-parageneses under the microscope.
- PAPEZIK, V.S., 1972: Late Pre-Cambrian ignimbrites in Eastern Newfoundland and their tectonic significance. 24th Intern. Geol. Congr., Montreal, Sect. 1, 147.
- PARÁK, T., 1973: Rare earths in the apatite iron ores of Lapland, together with some data about the Sr, Th and U content of these ores. *Econ. Geol.* 68, 210-221.
- PARK, C.F., 1972: The iron ore deposits of the Pacific Basin. *Econ. Geol.* 67, 339-349.
- \_\_\_\_\_ and McDiarmid, R.A., 1970: *Ore Deposits*. W.H. Freeman and Co., San Francisco, 522 pp.
- PARSONS, W.H., 1948: Camell River map area. *Geol. Surv. Canada, Paper* 48-19.
- \_\_\_\_\_, 1968: Criteria for the recognition of volcanic breccias: review. *Geol. Soc. Amer., Mem* 115, 263-304.

- PARSONS, W.H. and Lord, C.S., 1947: The Camsell River map-area. Geol. Surv. Canada, Map 1014A.
- PAVLU, D., 1972: Ag-As-Bi-Co-Ni association in the Jáchymov ore district, Krusné Hory Mountains. 24th Intern. Geol. Congr., Sect. 4, 526.
- PETRUK, W., 1971: Mineralogical characteristics of the deposits and textures of the ore minerals. Can. Mineral. 11, 108-136.
- \_\_\_\_\_, 1972: Depositional conditions for the ore minerals in the silver-arsenide deposits in the Cobalt and Gowganda areas. 24th Intern. Geol. Congr., Montreal, Sect. 4, 539.
- PHILLIPS, F.C., 1963: An introduction to crystallography. Longmans, Green and Co. Ltd., London, 329 pp.
- PHILPOTTS, A.R., 1967: Origin of certain iron-titanium oxide and apatite rocks. Econ. Geol. 62, 303-315.
- PITCHER, W.S., 1972: The Coastal Batholith of Peru: some structural aspects. 24th Intern. Geol. Congr., Montreal, Sect. 2, 156.
- PRINZ, M., 1967: Geochemistry of basaltic rocks; trace elements, In Basalt, eds. H.H. Hess and A. Poldervaart. John Wiley and Sons, New York, 271-324.
- RADCLIFFE, D., 1966: Some properties of rammelsbergite and pararammelsbergite. Can. Mineral. 7.
- \_\_\_\_\_, 1968b: Structural formulae and composition of skutterudite. Can. Mineral. 9, 559-563.
- \_\_\_\_\_ and Berry, L.G., 1968: The safflorite-loellingite solid solution series. Amer. Mineral. 53, 1856-1881.

- RAMDOHR, P., 1969: The ore minerals and their intergrowths. Pergamon Press, Oxford, 1174 pp.
- REINHARDT, E.W., 1969: Wilson Island-Petitot Islands area, East Arm Great Slave Lake. Geol. Surv. Canada, Paper 69-1A, 177-181.
- ROBINSON, B.W., 1971: Studies on the Echo Bay silver deposit, N.W.T. Unpubl. Ph.D. Thesis, University of Alberta, 256 pp.
- \_\_\_\_\_ and Morton, R.D., 1972: The geology and geochronology of the Echo Bay area, N.W.T., Canada. Can. Jour. Earth Sci. 9, 158-172.
- ROBINSON, H.S., 1933: Notes on the Echo Bay District, Great Bear Lake, N.W.T. Can. Inst. Min. Metall., 609-629.
- ROSEBOOM, E.H., 1962: Skutterudites (Co,Ni,Fe) As<sub>3-x</sub>: compositions and cell dimensions. Amer. Mineral. 47, 310-327.
- \_\_\_\_\_ 1963: CoFeNi diarsenides, compositions and cell dimensions. Amer. Mineral. 48, 271-299.
- ROSS, C.S. and Smith, R.L., 1961: Ash flow tuffs: their origin, geologic relations and identification. U.S. Geol. Surv. Prof. Paper 366.
- SASSANO, G.P., Baadsgaard, H. and Morton, R.D., 1972: Rb-Sr isotopic systematics of the Foot Bay gneiss, Donaldson Lake gneiss and pegmatite dikes from the Fay Mine, N.W. Saskatchewan. Can. Jour. Earth Sci. 9, 1368.
- SCHNEIDER, A., 1970: The sulphur isotope composition of basaltic rocks. Contr. Mineral. Petrol. 25, 92-124.

- SHAW, D.M., 1960: The geochemistry of scapolite. I: Mineralogy.  
II: Geochemistry, Petrology. Jour. Petrol. 1, 218-285.
- SHIEH, Y.N. and Taylor, H.P. Jr., 1969: Oxygen and hydrogen isotope studies of contact metamorphism in the Santa Rosa Range, Nevada, and other areas. Contr. Mineral. Petrol. 20, 306-356.
- SIEGERS, A., Pichler, H. and Ziel, W., 1969: Trace element abundances in the "Andesite" formation of Northern Chile. Geochim. Cosmochim. Acta 33, 882-887.
- SMITH, D.G.W. and Tomlinson, M.C., 1970: An APL language computer programme for use in electron microprobe analysis. Comp. Contrib. 45, State Geol. Surv., University of Kansas.
- SMITH, F.G., 1953: Report on the Hottah lake uranium showing. Dept. Ind. Aff. and North. Develop., Private Report.
- \_\_\_\_\_, 1963: Physical Geochemistry. Addison-Wesley Publ. Corp. 320 pp.
- SMITH, I.E., 1972: High-K intrusives from southeastern Papua. Contr. Mineral. Petrol. 34, 167-176.
- SNYDER, G.L. and Fraser, G.D., 1963: Pillowed lavas. 1. Intrusive layered lava pods and pillowed lavas, Unalaska Island, Alaska. 2. A review of selected recent literature. U.S. Geol. Surv., Prof. Paper 454-B 1-23, C 1-7.
- STANTON, R.L., 1972: Ore Petrology. McGraw-Hill Ltd., New York, 713 pp.
- TAYLOR, S.R., 1968: Geochemistry of the andesites, In Origin and distribution of the elements, ed. L.H. Ahrens.

- TAYLOR, S.R., 1969: Trace element chemistry of andesites and associated calc-alkaline rocks. Oregon Dept. Geol. Min. Industries, Bull 65: Proc. Andesite Conf., 43-65.
- \_\_\_\_\_, Ewart, A. and Capp, A.C., 1968: Leucogranites and rhyolites: trace element evidence for fractional crystallisation and partial melting. *Lithos* 1, 179-186.
- \_\_\_\_\_, and Kolbe, P., 1964: Geochemical standards. *Geochim. Cosmochim. Acta* 28, 447-454.
- TAXIEFF, H., 1970: Mechanisms of ignimbrite eruption, *In* Mechanisms of igneous intrusion, eds. G. Newall and N. Rast. Seel House Press, 157-164.
- THODE, H.G. and Gross, W.H., 1968: Ore and the source of acid intrusives using sulfur isotopes. *Econ. Geol.* 58, 1370.
- THORPE, R.I., 1971: Lead isotopic evidence on the age of mineralisation, Great Bear Lake. *Geol. Surv. Canada, Paper* 71-1B.
- TURNER, F.J., 1968: *Metamorphic Petrology*. McGraw-Hill Ltd., New York, 404 pp.
- \_\_\_\_\_, and Verhoogen, J., 1960: *Igneous and Metamorphic Petrology*. McGraw-Hill Ltd., New York, 694 pp.
- VERGARA, M.M., 1972: Note on the palaeovolcanism in the Andean Geosyncline from the central part of Chile. 24th Intern. Geol. Congr., Montreal, Sect. 2, 222.
- VIDALE, R., 1969: Metasomatism in chemical gradient and the formation of calc-silicate bands. *Amer. Jour. Sci.* 267, 857-874.

- VITALIANO, C.J. and D.B., 1972: Cenozoic volcanic rocks in the southern Shoshone Mountains and Paradise Range, Nevada. Bull. Geol. Soc. Amer. 83, 3269-3280.
- VOKES, F.M., 1967: The Cobalt mining district. Rapport fra Studierlese; Private Rept. to Min. Assoc. Canada.
- WANLESS, R.K., Stevens, R.D., Lachance, G.R. and Edmonds, C.M., 1968: Age determinations and geological studies. K-Ar isotopic ages. Geol. Surv. Canada, Paper 67-2A, Rept. 8.
- \_\_\_\_\_, Stevens, R.D., Lachance, G.R. and Delabi, R.N., 1970: Age determinations and geological studies. Geol. Surv. Canada, Paper 69-2A.
- W  
W  
WISE, W.S., 1969: Geology and petrology of the Mount Hood area: a study of high Cascade volcanism. Bull. Geol. Soc. Amer. 80, 969-1006.
- WODZICKI, A., 1971: Migration of trace elements during contact metamorphism in the Santa Rosa Range, Nevada, and its bearing on the origin of ore deposits associated with granitic intrusions. Mineral. Dep. 6, 49-64.
- YUND, R.A., 1961: Phase relations in the system NiAs. Econ. Geol. 56, 1273-1296.
- YPMA, P.J.M., 1972: The multi-stage emplacement of the Chalanches (France) Ni-Co-Bi-As-Sb-Ag deposits and the nature of the mineralising solutions. 24th Intern. Geol. Congr., Montreal, Sect. 4, 525.



## APPENDIX I

Analytical Methods and Sample Descriptions and Locations

Analyses for the elements expressed as oxides and for Ba, Rb, Sr, Zr, Nb and Y were performed on compacted powder by Dr. G. Holland at the University of Durham, England, using a Phillips 1212 X-ray fluorescence spectrometer. The results were corrected by him using a computer technique (Holland and Brindle, 1966). Ni, Co, Ag, Au and U were analysed by Bondar Clegg and Company Limited. All analyses were carried out using atomic absorption spectroscopy. Ni, Co and Ag were extracted from the samples with  $\text{HNO}_3$  and  $\text{HCl}$ . U was extracted with  $\text{HNO}_3$ . Au was concentrated by fire-assay. Ni, Co, Cu, Zn and Mn were analysed at the University of Alberta using a Perkin Elmer 303 atomic absorption spectrophotometer. The method has been described in the text. There follow petrographic descriptions of the samples upon which whole-rock analysis was performed. Locations of all samples analysed are shown on Figure 60.

SJ 29.8 Trachybasalt. 20% aligned laths of oligoclase and andesine; moderately sericitised. 10% phenocrysts of hornblende partially altered to chlorite and carbonate. 60-70% matrix of very fine-grained plagioclase laths intergrown with chlorite and opaque oxides. 10% late 'metablasts' of opaque oxides.

- NK 1.1B Altered trachybasalt. 20% sericitised plagioclase phenocrysts. 20% subhedral pseudomorphs of chlorite and carbonate after amphibole. 60% fine-grained matrix of chlorite and opaque oxides.
- NK 4.1A Vesicular trachybasalt. 50% small, badly corroded laths of oligoclase and andesine showing flow textures around 20% large phenocrysts, that are now all chlorite and haematite, and around 10% aspherical vesicles with strained quartz and carbonate infillings. Chlorite-rich matrix.
- SX 3.9A Porphyritic andesite. 50% large, altered oligoclase and andesine laths. 10% large, subhedral amphibole phenocrysts, partially replaced by chlorite and magnetite. 40% matrix of fine-grained plagioclase laths, quartz, chlorite, haematite and rarely, apatite.
- SX 7.16, Porphyritic andesite. 40% large, dusty plagioclase laths cored with blebs of chlorite after original glass: compositions range from  $An_{20-60}$ , but average  $An_{25}$ . Scattered large phenocrysts of hornblende, partially altered to chlorite. 50% matrix of very fine-grained plagioclase, quartz, chlorite and haematite.
- NK 7.13 Andesite or micro-diorite. 80% interlocking mesh of altered andesine, with interstitial quartz and chlorite. Plagioclase has altered to epidote and carbonate. 20% large pseudomorphs of chlorite and magnetite after amphibole.

- SJ 3.3 Banded andesite tuff. Fine-grained plagioclase with sparse, interstitial quartz, carbonate and chlorite in pale bands. Chlorite, haematite and epidote constitute 90% of the dark bands and have been overgrown by pyrite and chalcopyrite (5%).
- SJ 5.1 Meta-andesite tuff. 60% small, unoriented laths of oligoclase which has partially altered to chlorite, carbonate, epidote and sericite. Rare interstitial patches of quartz and albite. 30% matrix of interlocking carbonate, chlorite, epidote and apatite. Albite-epidote facies.
- SJ 10.1 Lithic-crystal andesite tuff. Angular unsorted clasts of oligoclase (30%), andesine (10%), K-feldspar (5%), quartz (30%), fine-grained andesite tuff (as in Sample SJ 3.3) (5%) and unidentifiable volcanic rock (10%), and clasts now completely made up of chlorite, haematite and pyrite (15%). The clasts constitute 60% of the rock and occur in a matrix of fine-grained chlorite and quartz.
- NK 19.6 Lithic-crystal andesite tuff. 10% small clasts of fine-grained crystal tuff. 30% fractured clasts of oligoclase and andesine. 10% clasts of fractured, altered amphibole. 50% fine-grained matrix of quartz, chlorite, haematite and carbonate.
- NK 18.8 Vitric-crystal andesite tuff. 40% laths of sericitised plagioclase and fractured subhedral hornblende (partially altered to chlorite and magnetite); in a fine-grained, dusty devitrified matrix with flow-textures around the clasts.  
 Very sparse clasts of crystal tuff.

- NK 13.2 Rhyolite ignimbrite. 40% devitrified, red matrix with preserved flow-textures, but now mostly very fine-grained quartz, feldspar and haematite. 10% pseudomorphed shards. Clasts of devitrified glass, resorbed quartz, altered and broken oligoclase, K-feldspar and tuff. Perlitic devitrification textures are common. The shards and vitric fragments are welded and often bent around each other and around the clasts.
- SX 7.2F Rhyolite tuff. Pink and green banded. Very fine-grained with quartz and feldspar predominant in the pink bands, and with intergrown quartz, feldspar and chlorite in the green bands. The leucocratic minerals are often too fine-grained to identify. These rocks were frequently mapped as 'cherts' by earlier workers.
- SJ 27.1F Volcanoclastic arkose. Poorly-sorted, well-bedded sediment with angular to sub-rounded clasts of quartz, rhyolite tuff, oligoclase, trachybasalt. Oligoclase-porphyrific andesite, fine andesite tuff and, rarely, altered hornblende. 20% interstitial matrix of chlorite and haematite.
- SX 2.2 Volcanoclastic siltstone. Well-bedded, graded purple siltstone, with rounded volcanic fragments recognisable in the coarser beds. The finer portions are too fine-grained to identify individual minerals. They are frequently cut by water-escape structures from the coarser beds.

- SX 2.1 Monzonite. 60% large, altered laths of andesine and 20% large subhedral plates of dusty K-feldspar with a matrix of quartz, chlorite and fine-grained sericitised feldspar. Rare phenocrysts of hornblende, partially replaced along cleavage planes by magnetite.
- SX 14.18B Granodiorite. 50% laths of oligoclase and andesine, with overgrown rims of K-feldspar, 10% interstitial lobate intergrowths of albite and K-feldspar. 30% euhedral phenocrysts of hornblende, partially altered to green biotite and chlorite. 10% interstitial quartz, epidote and apatite.
- NK 14.2A Granite. 30% large, subhedral plates of orthoclase with rare perthite and some patches of granophyric quartz and K-feldspar. 15% large sericitised laths of oligoclase. 40% interstitial anhedral quartz. 10-15% badly contorted biotite. Rare apatite and zircon.
- NK 19.7 Granodiorite. 30% laths of altered andesine. 20% subhedral plates of microcline. 35% interstitial anhedral quartz. 10% laths of biotite. Sparse epidote, apatite, carbonate and zircon.
- NK 19.10 Meta-diorite. Intruded by NK 19.7. 20% badly altered laths of (?) sodic plagioclase. 30% euhedral albite that has overgrown the plagioclase. 20% interstitial, recrystallised quartz. 30% chlorite, magnetite and haematite.

- SX 3.13B Felsic dyke. Sample taken two feet from the contact, in a slightly chilled zone. 35% euhedral phenocrysts of quartz, 20% laths of oligoclase and andesine and 10% of shredded biotite laths in a groundmass of very fine-grained quartz, feldspar and biotite.
- SX 3.1C Quartz diabase. Ophitic texture. 40% subhedral augite with rims of green biotite, magnetite and hornblende, and with some replacement along cleavage planes. 35% euhedral andesine-labradorite. 5% interstitial granophyric quartz and K-feldspar. 10% interstitial magnetite, ilmenite and haematite. Rare epidote, carbonate and sphene.
- NK 21.1A Quartz gabbro. Ophitic texture. 50-60% unaltered laths of andesine-labradorite. 40% subhedral augite that has partly altered to hornblende, biotite, chlorite and magnetite. 10% interstitial granophyric quartz and feldspar.
- NK 15.2A Coarse diabase. Ophitic texture. 40% subhedral titaniferous augite. 30% unaltered laths of labradorite. 10-20% interstitial granophyric quartz and feldspar. 10% late skeletons and cubes of pyrite. Rare interstitial albite, chlorite and opaque oxides.

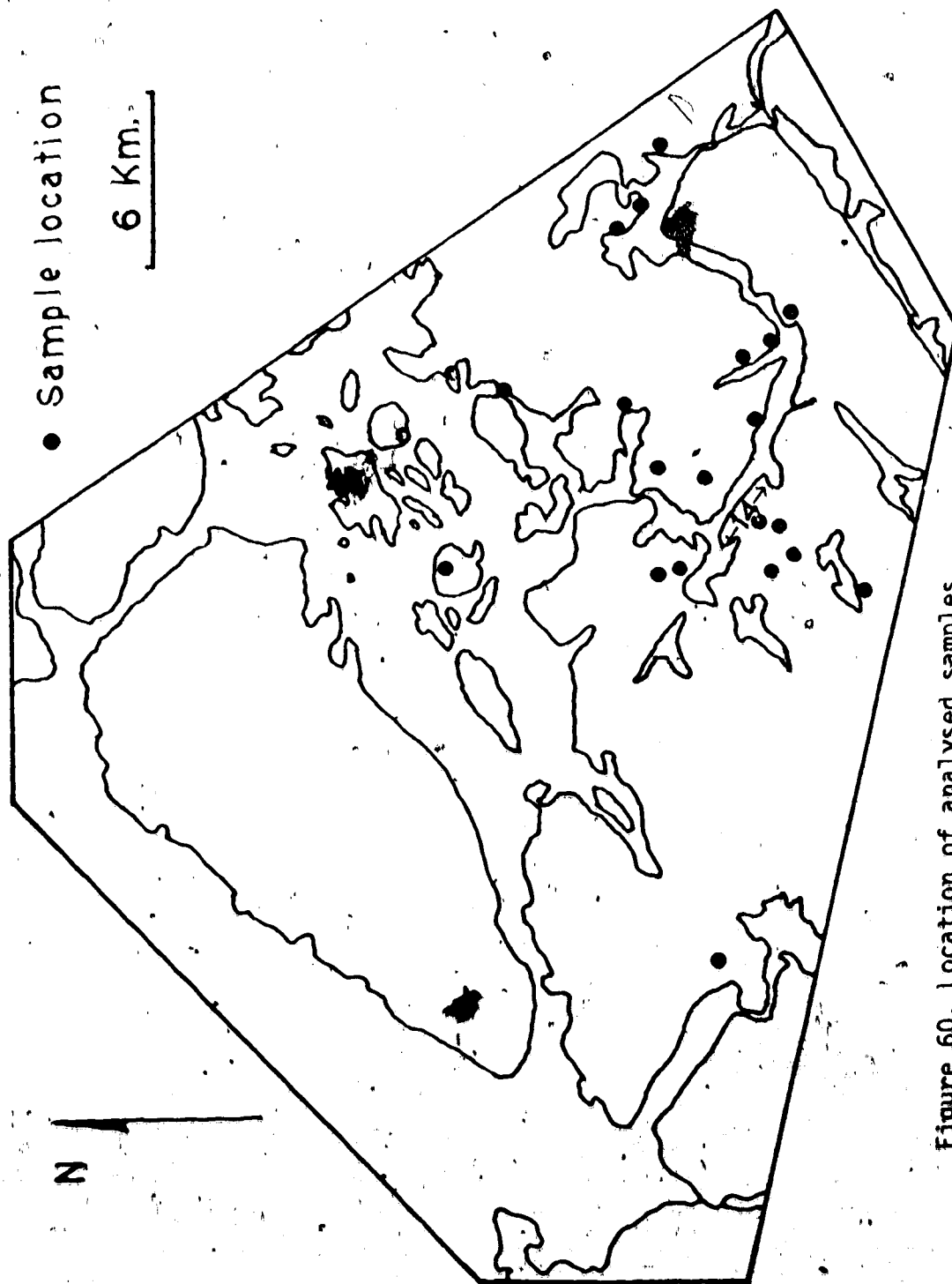


Figure 60. Location of analysed samples.

## APPENDIX II

Summary of Electron Microprobe Data and Operating Conditions

Electron microprobe: ARL Model EMX

Take-off angle:  $52\frac{1}{2}^\circ$

a) Ferrohastingsite. Table 3

Standards. EPS 12-1 Biotite: for Fe, Ti

EPS 12-2 Biotite: for Si, Al, K, Na

Kakanui Kaersutite: for Mg, Ca

A-6 Cummingtonite: for Mn

Operating voltage = 15 KV. All elements analysed on  $K\alpha$  with pulse height analysis. Analyst: C.R. Ramsay.

b) Phengitic muscovite. Table 14

Standards. EPS 12-1 Biotite: for Fe, Ti

Kakanui Kaersutite: for Ca, Na

EPS 12-2 Biotite: for Si, Mg, K, Mn

Hohenfels sanidine: for Al

Operating voltage = 15 KV. All elements analysed on  $K\alpha$  with pulse height analysis. Analyst: C.R. Ramsay.

c) Mercury contents of silver. Table 7, 8

Run I. Operating voltage = 15 KV. Line =  $HgLa$ .

Beam current = 200 ma. ZAF corrections, assuming Ag by difference, in brackets.

Background corrections made. Pulse height analysed.



Run II and Run III. Ag and Hg analysed ( $AgL\alpha$   $HgL\alpha$ ).

Background corrections only made.

Operating voltage = 29.1 KV. Beam current = 200 ma.

Pulse height analysed.

Standards. Ag. Electrolytic silver wire. Ag = 100%

Hg. Cinnabar. Assumed stoichiometric. Hg = 85.2%

d) Zinc contents of sulphides, Table 5

Operating voltage = 15 KV. Beam current = 200 ma.

Line analysed:  $ZnK\alpha$ , using pulse height analysis.

Standard. EPS 22-6 Sphalerite (Geochim. Cosmochim. Acta, pp. 1667-1676 [1967]).

e) Analysis of sphalerites. Table 6

Operating voltage = 15 KV. Beam Current = 200 ma.

Lines analysed:  $CuK\alpha$ ,  $ZnK\alpha$ ,  $FeK\alpha$ ,  $SK\alpha$ .

Standards. EPS 20-8 Synthetic chalcocopyrite. Cu, Fe, S

EPS 22-6 Sphalerite. As above.

f) Analysis of sulphosalts. Tables 11, 12, 13

Probe current = 200 ma. Using pulse height analysis.

Element	Line	Operating Voltage
Ag	$L\alpha$	15 KV
S	$K\alpha$	15 KV
As	$L\alpha$	15 KV
Sb	$L\alpha$	20 KV
Zn	$K\alpha$	20 KV
Bi	$L\alpha$	29 KV
Pb	$L\alpha$	29 KV
Cu	$K\alpha$	20 KV
Fe	$K\alpha$	20 KV

Standards. EPS 20-8 Synthetic chalcopyrite. Cu, Fe, S  
EPS 20-10 Arsenopyrite. As. Assumed stoichiometric  
EPS 20-2 Silver. Ag. Spec. pure metal  
EPS 20-9 Stibnite. Sb. Analysis in Dana #3, p. 273  
EPS 22-7 Galena. Pb. Assumed stoichiometric  
EPS 20-3 Bismuth. Bi. Spec. pure metal  
EPS 22-6 Sphalerite. Zn. As above

## APPENDIX III

Oxygen and Carbon Isotope Analyses (see Figures 39 and 50)

Sixty-six carbonates from the three mines and some of the veins were analysed for their carbon and oxygen isotopic compositions. Carbonate samples were identified using an X-ray diffraction procedure. They were then reacted with 100% phosphoric acid at 25°C for one day for pure calcite and 10 days for dolomite. In the case of mixed samples the gas produced after two hours of reaction was extracted and assumed to represent the decomposition of at least 90% of the calcite (Fritz, Pers. Comm., 1971). In some cases this was analysed, but more often was discarded.

The CO<sub>2</sub> produced was analysed using a 12", 90° mass spectrometer at the University of Alberta. Corrections were made following Craig (1957). Samples prefixed SBX come from the Silver Bay Mine, and those prefixed R come from the Republic Vein. D = dolomite and C = calcite. The stages refer to Figures 46, 51 and 53. The isotopic compositions are presented as per mil deviation from SMOW for oxygen and PDB for carbon and are reported below.

Sample Number	Mineral	Description	$\delta^{18}\text{O}_{\text{SNOW}}$ (‰)	$\delta^{13}\text{C}_{\text{PDB}}$ (‰)
TM 26.3	D	Dolomite in metacalcareous rock. Stage 1	+13.9	-4.9
TJ 5.1A	D	Dolomite from metacalpelite. Stage 1	+14.1	-4.2
TJ 8.10a	D	Dolomite from vein. Stage 2a	+16.2	-3.2
TJ 11.2Aa	D	Dolomite from vein. Stage 2a	+17.2	-2.8
TX 8.6Bb	D	Dolomite breccia fragments of Stage 2a	+15.9	-3.0
TJ 29.1	D	Dolomite and calcite from vein. Stage 2a	+15.3	-3.2
TJ 29.1	C	Dolomite and calcite from vein. Stage 2a	+9.0	-5.3
A 2.9a	C	Calcite from vein. Stage 2a	+9.7	-9.2
TX 8.6C	C	Calcite from vein. Stage 2a	+7.0	-3.8
TJ 5.2Ba	D	Dolomite from vein. Stage 2a-b	+15.0	-7.9
TM 28.2Da	D	Dolomite from vein. Stage 2a-b	+18.2	-2.1
TM 26.3a	D	Dolomite from vein. Stage 2a-b	+13.5	-4.6
TM 30.1Aa	D	Dolomite from vein. Stage 2b	+14.1	-3.3
TJ 10.1A	D	Dolomite from vein. Stage 2b-3a	+14.9	-3.9
TX 24.6	D	Dolomite from vein. Stage 3a	+16.1	-3.4
TX 8.6Ba	D	Banded dolomite. Stage 3a	+16.3	-3.5
TX 8.6b	D	Dolomite from vein. Stage 3a	+14.7	-3.7
TJ 11.2Ab	D	Pinkish dolomite from vein. Stage 3a	+12.6	-3.4
TM 26.3b	D	Dolomite from vein. Stage 3a	+14.8	-4.6
TM 30.1Ab	D	Dolomite overgrowing 2b dolomite. Stage 3a	+14.0	-3.9
TJ 5.2Bb	D	Dolomite overgrowing 2a-b dolomite. Stage 3a	+14.2	-3.7
TX 8.6Bc	D	Dolomite from vein. Stage 3a-b	+15.9	-3.1
TX 8.6Bd	D	Dolomite from vein. Stage 3a-b	+14.3	-4.4
TX 18.2	D	Dolomite from vein. Stage 3b	+13.5	-3.3

Sample Number	Mineral	Description	$\delta^{18}\text{O}_{\text{SMOW}}$ (‰)	$\delta^{13}\text{C}_{\text{PDB}}$ (‰)
TX 8.6a	D	Dolomite from vein. Stage 3b	+14.4	-4.3
TJ 25.1B	D	Dolomite from vein. Stage 3b	+13.5	-3.5
TJ 3.1Aa	D	Dolomite from vein. Stage 3b	+15.1	-3.3
TJ 3.1a	D	Dolomite from vein. Stage 3b	+15.1	-4.0
TM 26.3c	D	Dolomite with fluorite and chalcopyrite. Stage 3b	+13.1	-3.5
TM 25.1D	C	Calcite in vug centre. Stage 3b-4	+12.2	-9.8
TM 26.3d	C	Late calcite with pyrite. Stage 4	+7.8	-4.7
TJ 3.1	C	Late calcite with haematite and quartz. Stage 4	+7.8	-5.8
TJ 3.1Ab	C	Late calcite scalenohedra. Stage 4	+10.2	-5.7
TJ 8.1Db	C	Late calcite scalenohedra. Stage 4	+10.8	-6.8
TJ 19.1	C	Late calcite with pyrite. Stage 4	+8.1	-7.3
TJ 25.1Ba	C	Calcite with dolomite. Stage 3b-4	+10.37	-4.82
A 2.9b	C	Calcite overgrowing Stage 2a	+15.7	-6.17
NK 2.2	C	Calcite from calcargillite. Stage 1: Terra	+10.8	-
NK 20.1J	D	Red dolomite vein in porphyry. Norex	+20.7	-6.1
NX 11.3B	D	Dolomite from Norex vein. Stage 2a	+15.8	-4.4
NX 11.5Cb	D	Dolomite from Norex vein. Stage 2b	+16.7	-2.6
NX 11.5L	D	Dolomite with silver, Norex vein. Stage 2b	+16.9	-4.2
NX 11.3B	C	Calcite from Norex vein. Stage 2b-3a	+8.8	-3.8
NX 11.3Bb	C	Calcite from Norex vein. Stage 2b	+14.2	-4.0
NX 11.5C	C	Calcite with sulphides from Norex vein. Stage 2b	+18.2	-3.7
NX 11.5C	D	Dolomite with sulphides from Norex vein. Stage 3a	+22.0	-2.5

Sample Number	Mineral	Description	$\delta^{18}\text{O}_{\text{SHOM}}$ (‰)	$\delta^{13}\text{C}_{\text{PDB}}$ (‰)
RJ 17.1	D	Republic vein; early dolomite	+15.5	-2.1
RJ 17.2	D	Republic vein; early dolomite	+15.9	-2.5
NK 19.8	C	Jason vein calcite with sulphides	+20.5	-7.7
NJ 30.2	C	Lypka south vein; calcite with late galena	+10.3	-3.9
NK 20.3A	C	Lypka south vein; barren bluish calcite	+9.6	-
SBX 10.2I	D	Banded dolomite and quartz. Stage 2a-b	+15.9	-4.1
SBX 10.2Ja	D	Banded carbonate. Stage 2a	+15.9	-3.8
SBX 10.2Jb	D	Dolomite with silver. Stage 2a	+16.7	-4.3
SBX 10.2Jc	D	Pinkish dolomite. Stage 2a	+15.7	-4.0
SBX 10.2Jd	D	Dolomite from vein. Stage 2a	+15.9	-4.5
SBX 10.2Ca	D	Banded quartz and dolomite. Stage 3a-b	+15.9	-4.2
SBX 10.2Cb	D	Banded quartz and dolomite. Stage 3a-b	+13.9	-3.5
SBX 10.2Cc	D	Banded quartz and dolomite. Stage 3a-b	+13.9	-3.5
SBX 10.4Ac	D	Dolomite from vein. Stage 2b	+16.9	-4.4
SBX 10.1H	D	Dolomite and chalcopryrite. Stage 3a-b	+16.2	-4.0
SBX 10.4a	D	Dolomite and chalcopryrite. Stage 3b	+15.5	-4.5
SBX 10.1B	D	Dolomite with sulphides. Stage 3b	+15.2	-3.1
SBX 10.2Dc	D	Late banded dolomite. Stage 3b	+19.0	-5.3
SBX 10.2D	D	Late banded dolomite and calcite. Stage 3b	+16.3	-4.3
SBX 10.2D	C	Late banded dolomite and calcite. Stage 3b	+15.6	-5.0

## APPENDIX IV

Analyses of Sulphur Isotopes

A description of the analytical methods is given in Robinson and Badham (In Preparation, 1973). The samples were burnt to  $SO_2$  at  $1075^\circ C$  in a stream of pure tank oxygen. The results are reported in per mil deviation from the Canon Diablo Troilite. The data for 49 samples are presented below. Samples prefixed A and T are from the Terra Mine, and SB are from the Silver Bay Mine.

Minerals - Py = pyrite  
Mc = marcasite  
Cp = chalcopyrite  
Tet = tetrahedrite  
Mt = matildite  
Bm = bismuthinite

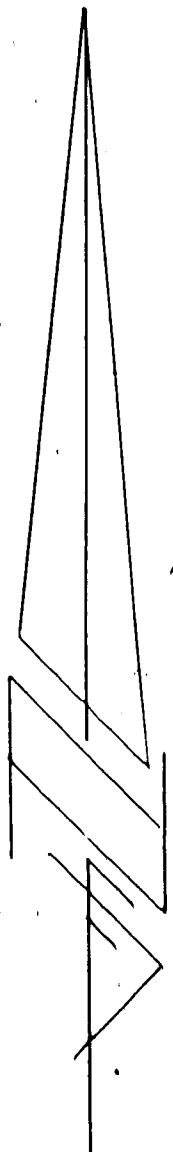
Sample Number	Mineral	Description	$\delta^{34}\text{S}_{\text{CDT}}$ (‰)
TM 24.2	Py	Scattered cubes in banded red and green tuffs	+5.1
TJ 11.2D	Cp	Scattered and massive in red cherty brecciated rock	+4.0
TX 24.7	Py	Cubes in red and green banded tuffs	+3.5
TJ 3.3A	Mc	Banded and massive in calcargillite. Stage 1	+4.0
TJ 5.1Db	Mc	Massive banded Cp and Mc. Stage 1	+3.7
TJ 5.1Dc	Cp	Massive Cp. Late Stage 1	+3.4
TJ 5.1Dd	Mc	Massive Mc. Late Stage 1	+2.8
TJ 5.1Df	Cp	Cp and carbonate in joint plane. Stage 1	+3.9
TJ 10.2Ba	Cp	Remobilised Cp and Mc banded ore. Stage 1	+3.1
TJ 10.2Bb	Mc	Remobilised Cp and Mc banded ore. Stage 1	+3.4
TX 3.1a	Cp	Banded massive Cp and Mc. Stage 1	+3.7
TX 3.1b	Mc	Banded massive Cp and Mc. Stage 1	+0.9
TX 7.2	Mc	From recrystallised banded metacalcargillite. Stage 1	+3.2
A 1.1a	Cp	Massive Cp and Mc in calcargillite. Stage 1	+1.0
A 1.1b	Mc	Massive Cp and Mc in calcargillite. Stage 1	+2.7
TM 21.4Ca	Cp	Banded and massive Cp with carbonate. Stage 3a	+2.6
TX 3.3a	Cp	Cp and Ss intergrown in carbonate. Stage 3a	+3.7
TX 3.3b	Tet	Cp and Ss intergrown in carbonate. Stage 3a	+3.7
TM 24.1	Gn	Massive fine-grained galena. Stage 3a	+4.2
TM 25.8	Mt	Massive matildite. Stage 3b	+1.9
A 2.18	Mt	From sulphosalts vein. Stage 3b	+1.4
A 2.1	Bm	Bismuthinite and bismuth vein. Stage 3b	+2.7



Sample Number	Mineral	Description	$\delta^{34}\text{S}_{\text{CDT}}$ (‰)
TM 21.10c	Cp	Late massive Cp in carbonate vein. Stage 3b-4	+5.9
TM 25.10a	Gn	Bands of Cp and Gn in late carbonate. Stage 4	+1.4
TM 25.10b	Cp	Bands of Cp and Gn in late carbonate. Stage 4	+6.4
TJ 3.1A	Cp	Associated with late carbonate rhombs. Stage 4	+4.3
TJ 11.2A	Cp	Massive late Cp in carbonate vein. Stage 4	+4.0
TJ 19.1b	Py	Late Py on carbonate. Stage 4	-26.0
SBX 10.4A	Cp	Massive Cp in brecciated country rock	-1.0
SBX 10.6a	Cp	Massive sulphides in volcanics	-10.2
SBX 10.6b	Py	Massive sulphides in volcanics	-8.4
SBX 10.6c	Py	Massive sulphides in volcanics	-9.6
SBX 10.3Fa	Py	Massive, intergrown Py and Gn with quartz and	-1.2
SBX 10.3fb	Gn	carbonate in vein. Stage 3a	-2.8
SBX 10.1Ba	Cp	Massive intergrowth of Gn and Cp with banded	-3.9
SBX 10.1Bb	Gn	quartz and carbonate vein. Stage 3a	-8.0
SBX 10.1Ca	Cp	Cp and Gn in massive carbonate vein. Stage 3a	-4.2
SBX 10.1Cb	Gn	Cp and Gn in massive carbonate vein. Stage 3a	-6.5
SBX 10.1Cc	Gn	Coarse late galena in vein. Stage 4	+1.5
NK 1.1A	Py	From vein in tuffs. Lypka	+3.8
NK 18.17B	Py	Disseminated Py cubes in andesite. Balachey	+4.2
NK 11.4A	Cp	Massive Cp in carbonate vein. Stage 3a. Norex	+2.1
NK 20.1J	Gn	Disseminated galena in vein. Stage 3a. Norex	-2.0
NX 20.1Ca	Gn	Intergrown Gn and Cp in vein. Stage 4. Norex	+0.5
NX 20.1Cb	Cp	Intergrown Gn and Cp in vein. Stage 4. Norex	+1.4

## APPENDIX V

Papers published or presently awaiting publication are contained in the back-pocket, with the enlarged figure 6 and Figure 31.

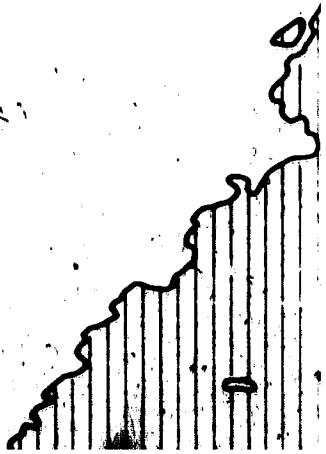


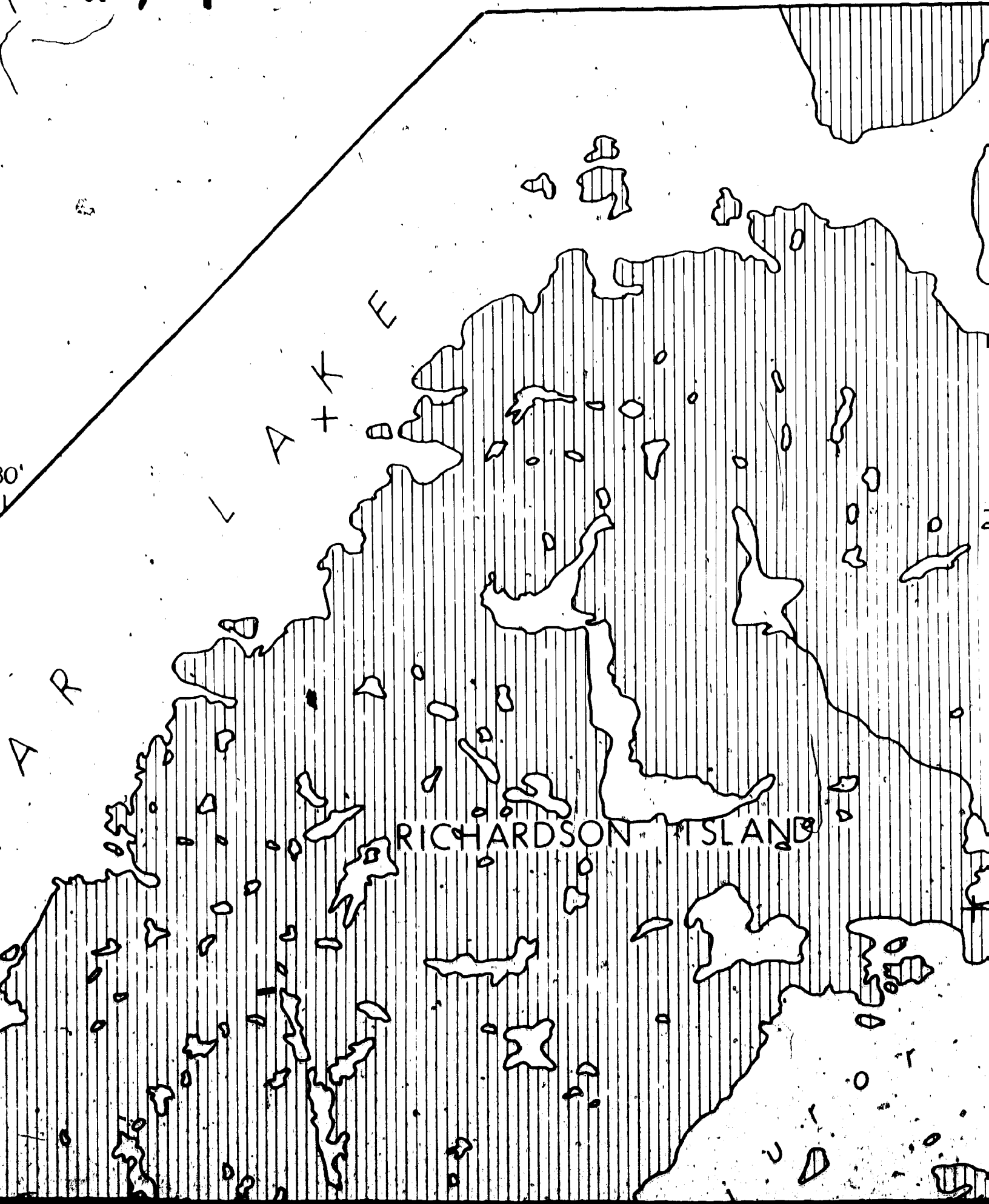
Declination:  
46° East

118° 30'

B  
E  
A

T





RICHARDSON ISLAND

A R  
L A T T E

30'




# PALEOZOIC

 Clastic sediments

# APHEBIAN


## ECHO BAY GROUP

 Conglomerate, arkose, silt & dolomite

 Acid volcanics & pyroclastics

 Intermediate tuffs & lavas

 Basic lavas

 Dominantly extrusive porphyries

 Undifferentiated rocks


## BALACHEY UNIT


 Sediments, tuffs & agglomerates

 Granitic rocks

 Dominantly Intrusive porphyries

 Porphyritic dikes

 Diabase & Gabbro

 Giant Quartz Veins

 Fault

 Fold axes

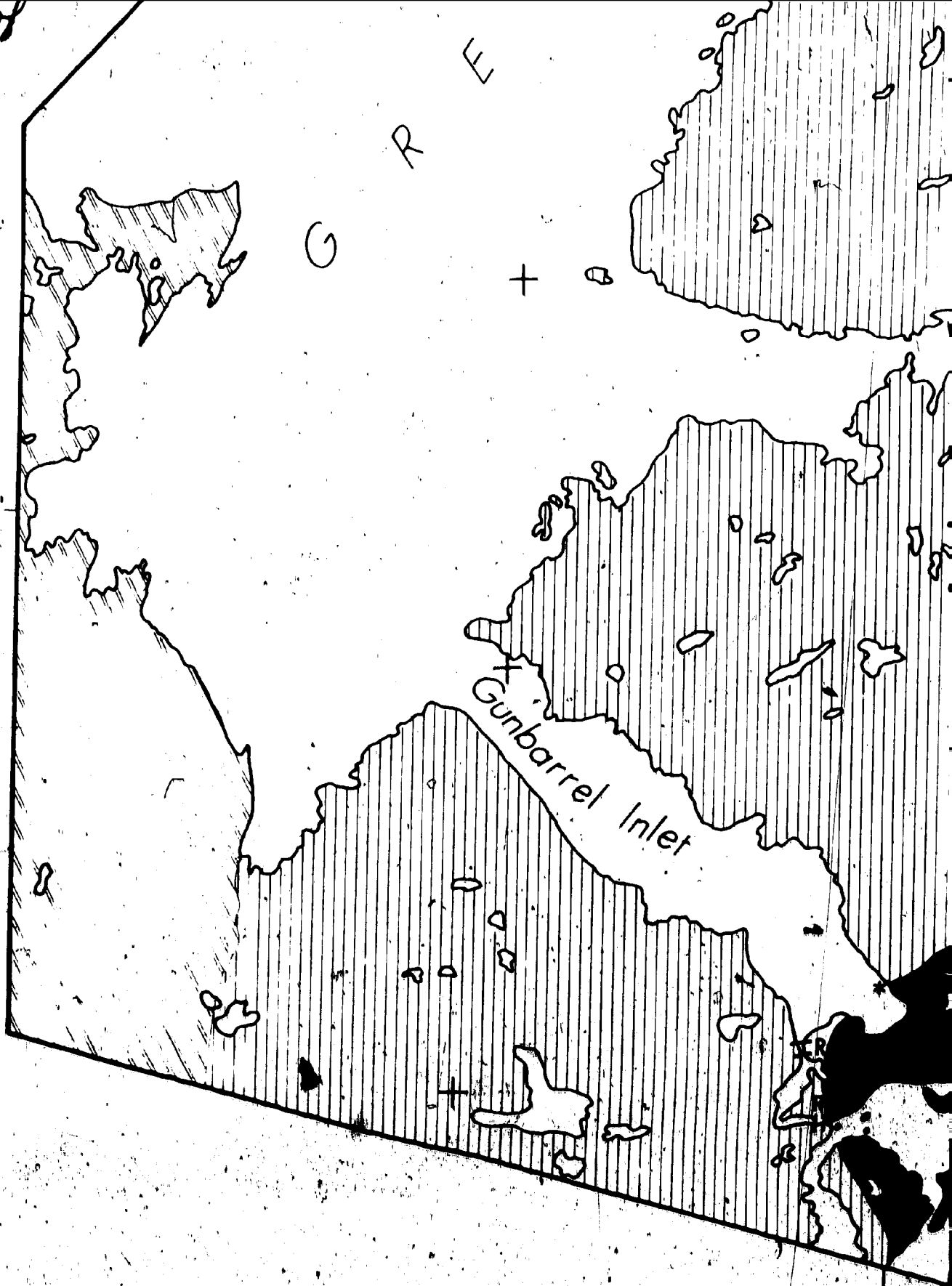
59

G R E E

65°30'

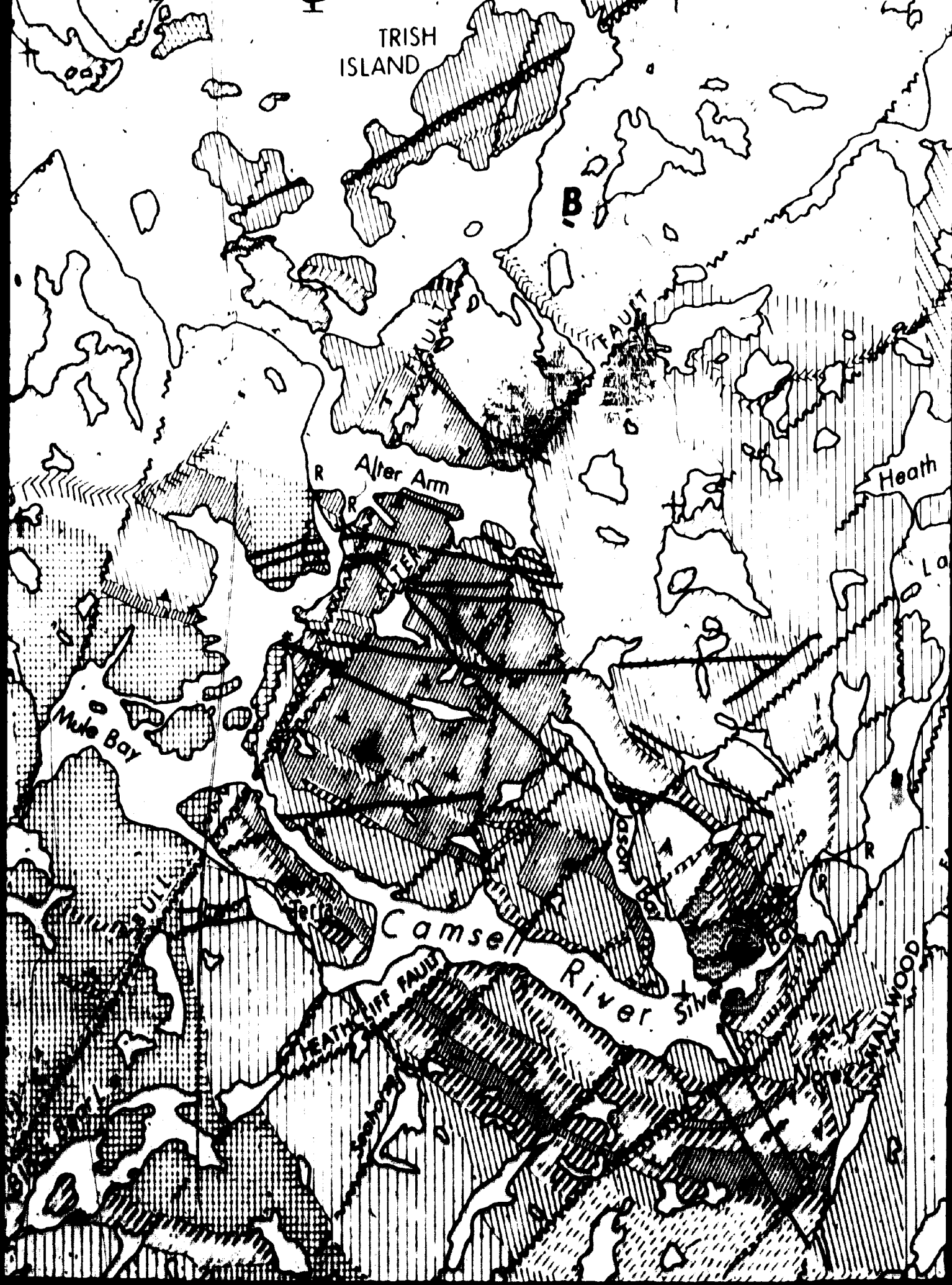
Gunbarrel Inlet

118°30'



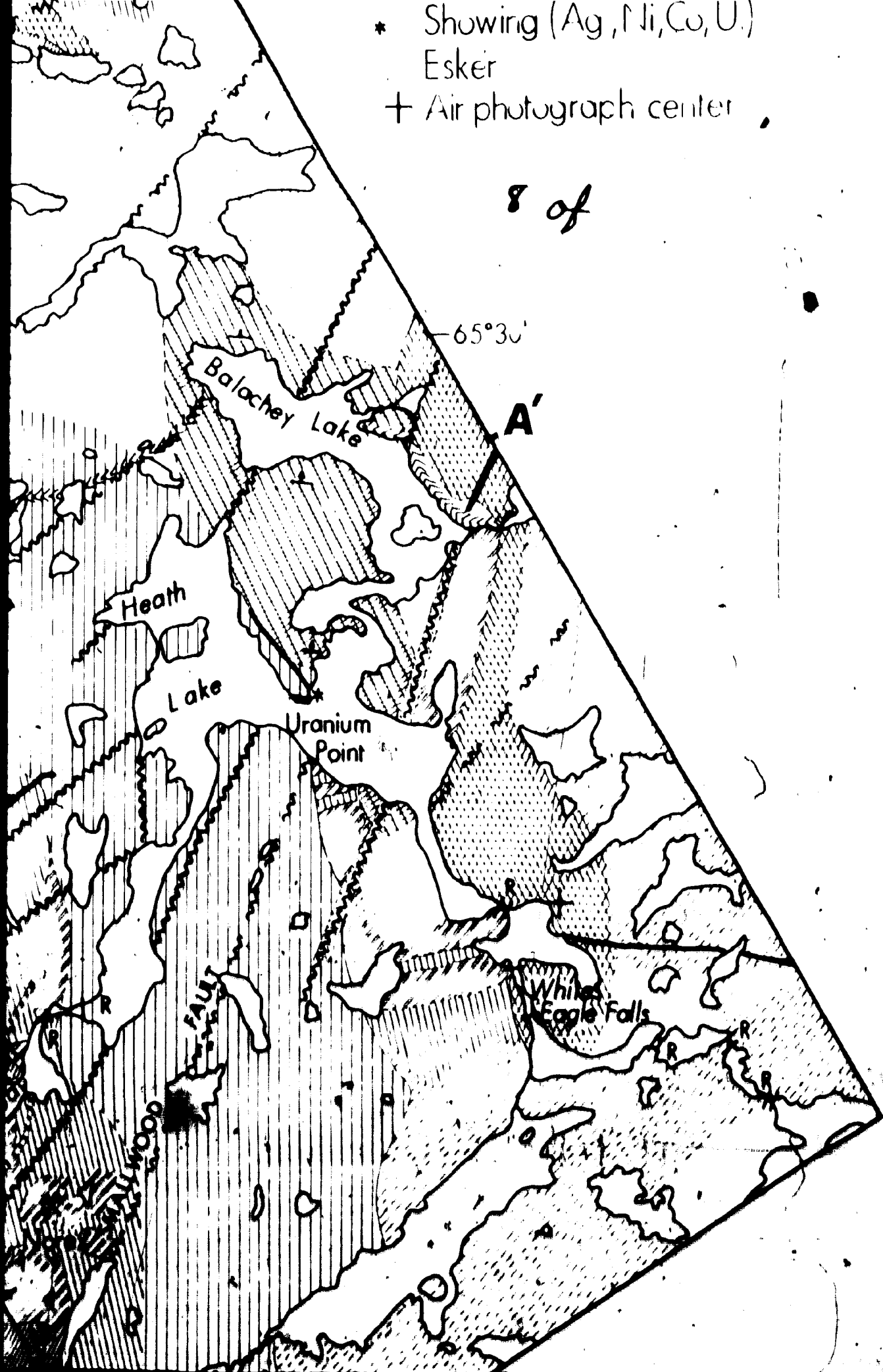


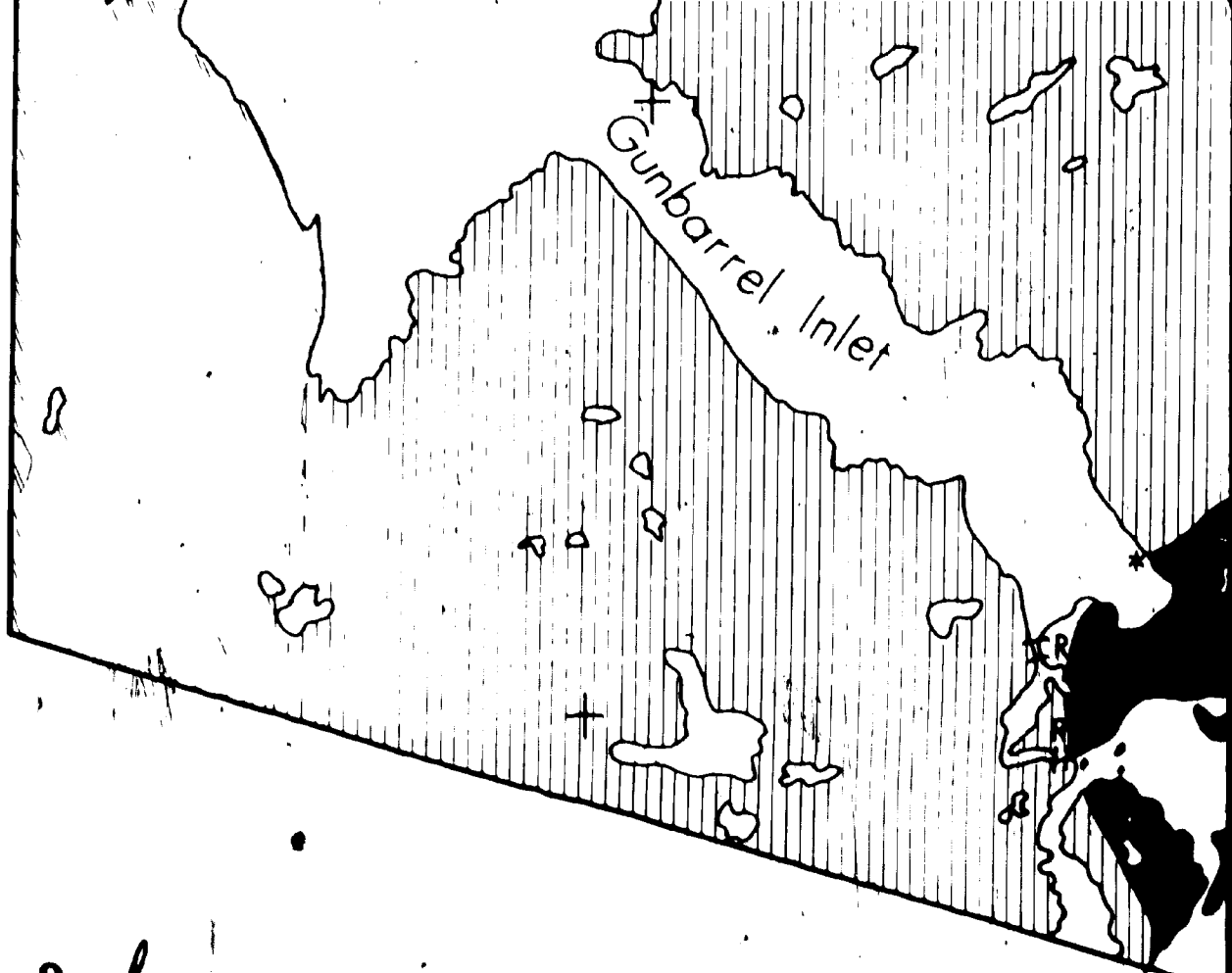




- \* Showing (Ag, Ni, Co, U.)
- Esker
- + Air photograph center

8 of

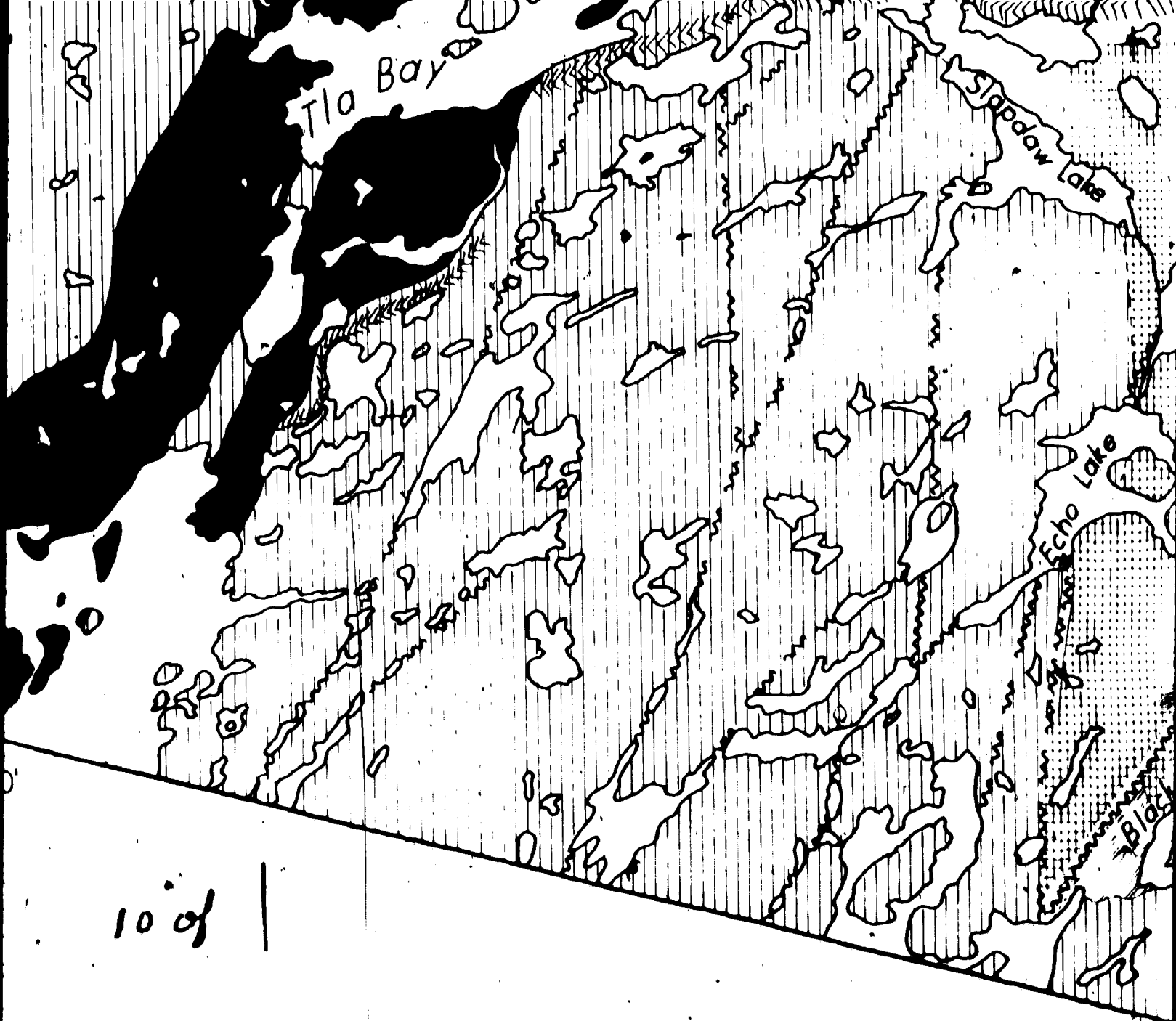




9 of

118°30'

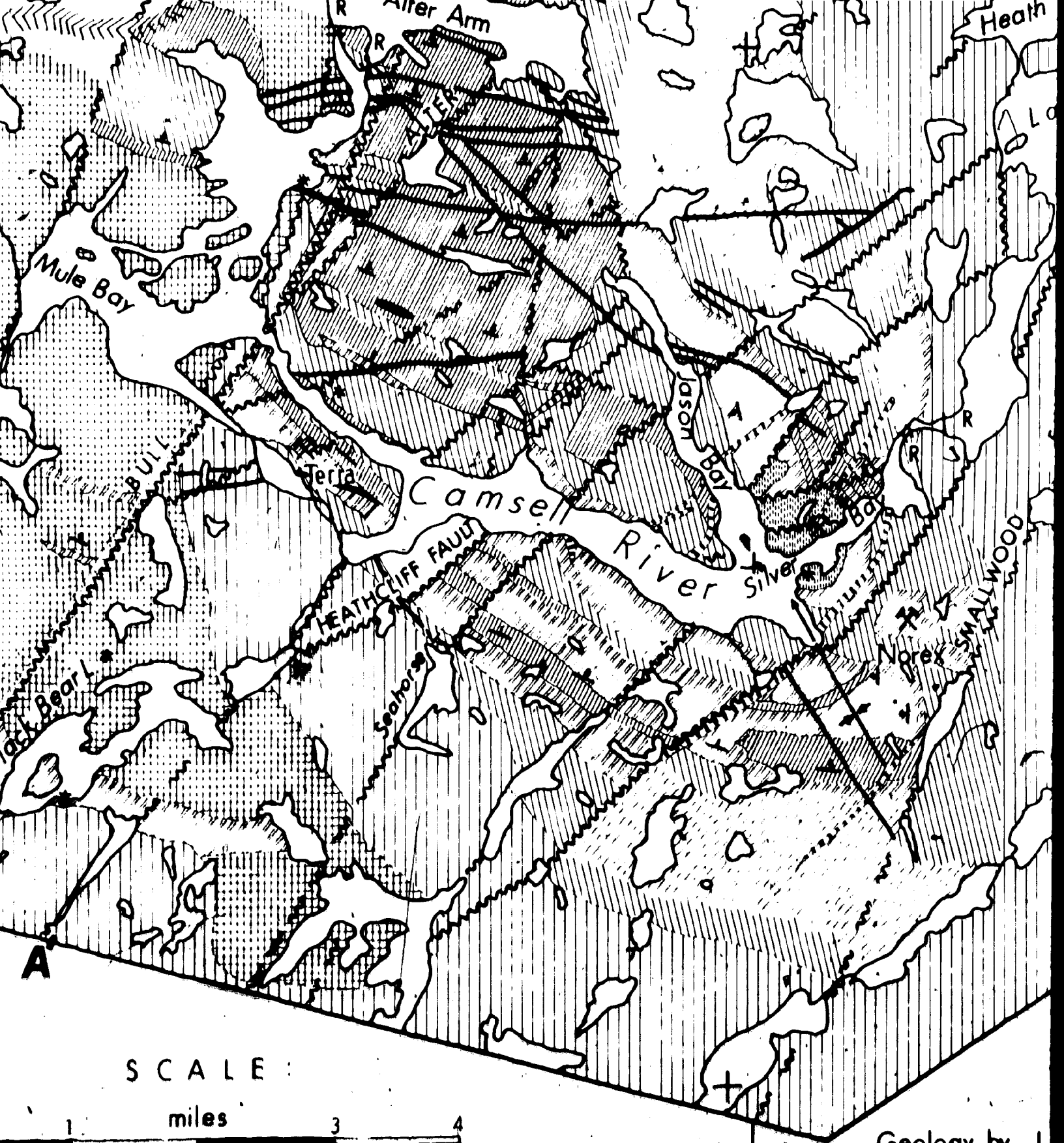
THE CAMSELL RIVER—CON.  
DISTRICT OF MACKEN



10 of 1

INJUROR BAY AREA

ENZIE, N.W.T.



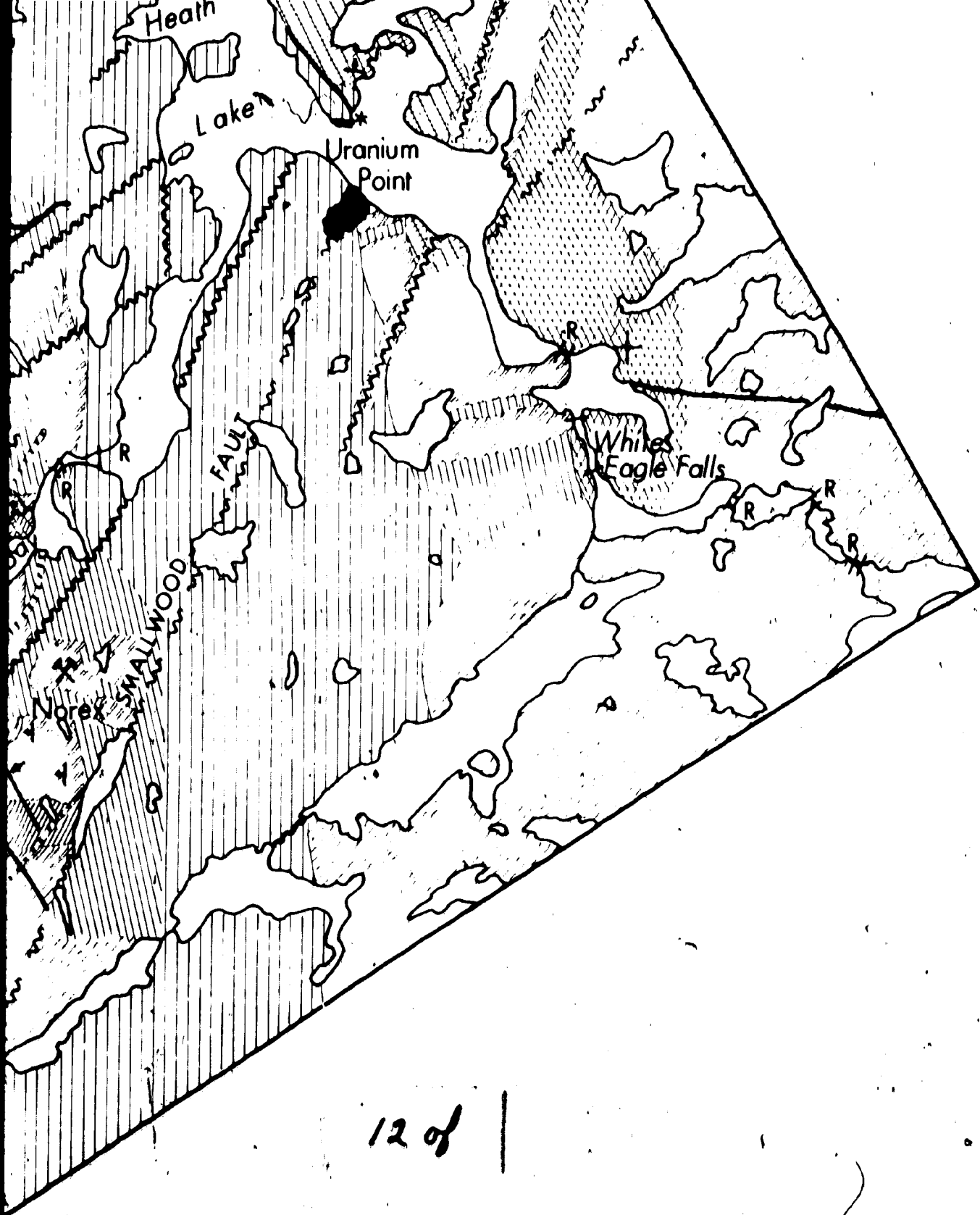
SCALE :

miles

2 kilometers

Geology by J. Gunbarrel Galt  
W. H. Parsons  
Cartography by

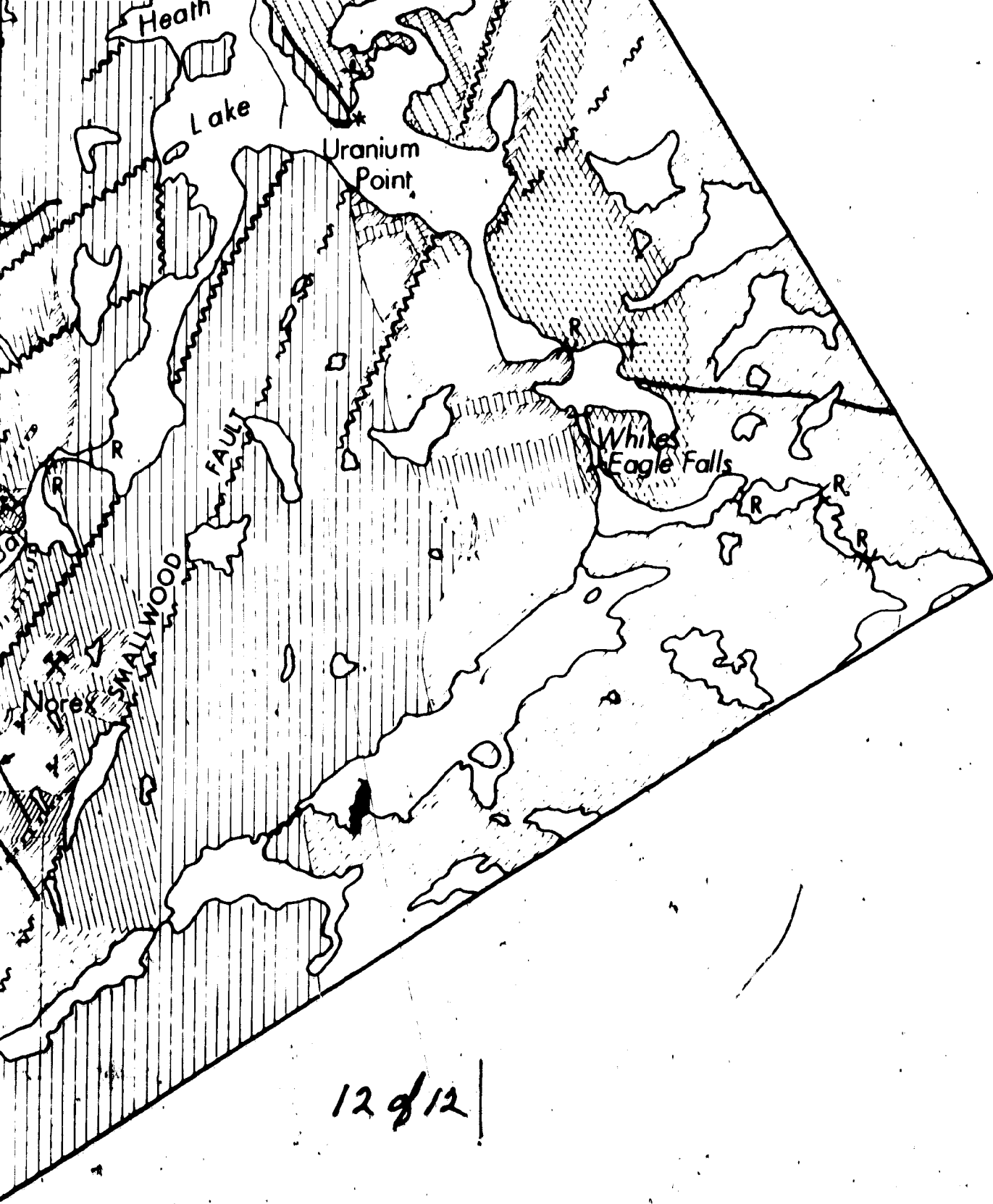
11 of



12 of 1

Geology by J.P.N. Badham (1970, 1971) after D.F. Kidd (1930, 1932, 1934), with the Gunbarrel Gabbro after G.M. Furnival (1934), and the eastern margins modified after W. H. Parsons & C. S. Lord (1947).

Cartography by J.P.N. Badham from an uncontrolled air-photograph mosaic.



12 of 12 |

Geology by J.P.N. Badham (1970, 1971) after D.F. Kidd (1930, 1932, 1934), with the Gunbarrel Gabbro after G.M. Furnival (1934), and the eastern margins modified after W. H. Parsons & C. S. Lord (1947).

• Cartography by J.P.N. Badham from an uncontrolled air-photograph mosaic.

1 of

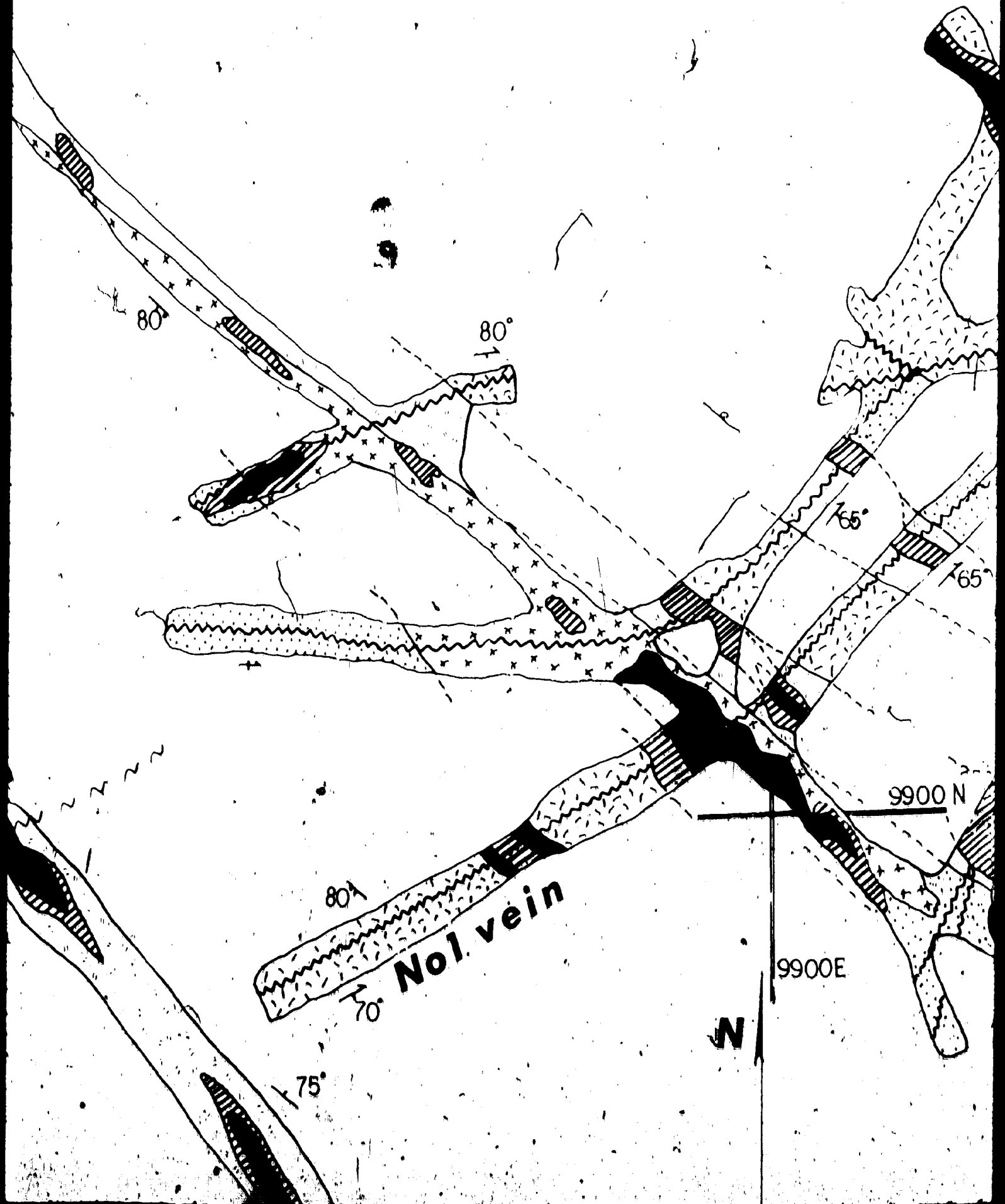


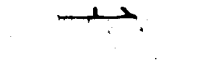
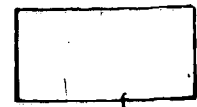
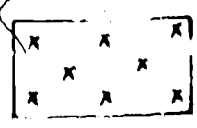
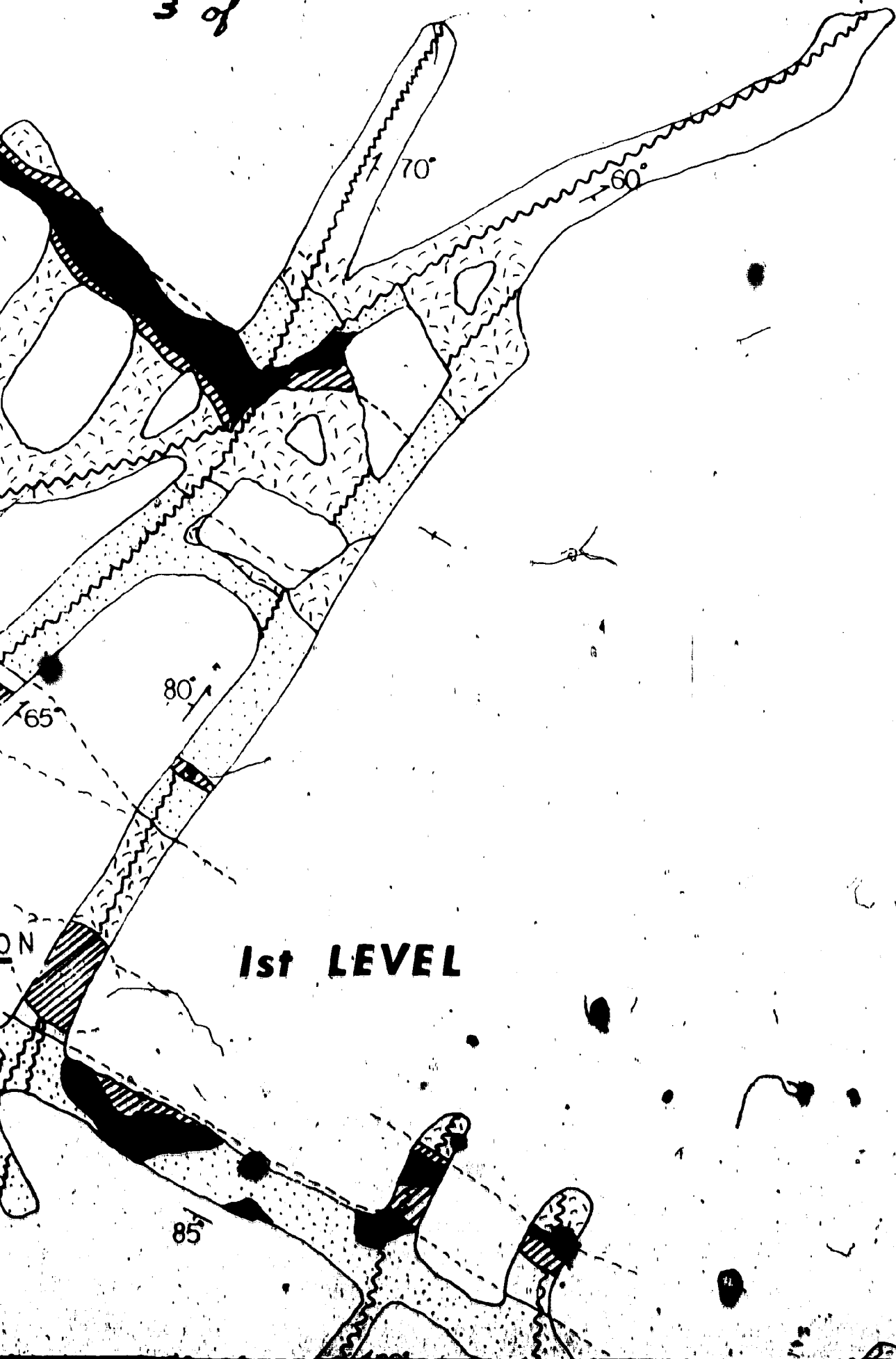
No. 9 vein

~ ~ ~ ~ ~  
70°











Banded red, green or black, silicified tuffs.



Well-bedded, coarse and fine tuffs and volcanoclastic sediments.



Massive, chloritised, intermediate lava.



Cupriferous zone  $C_p > 15\%$



Pyritiferous zone  $Pyt > 15\%$



Highly variable, banded meta-alcargillite



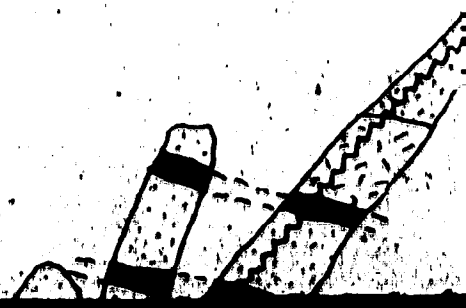
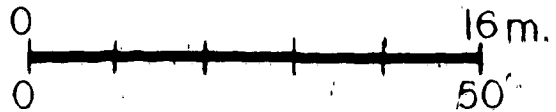
Vein



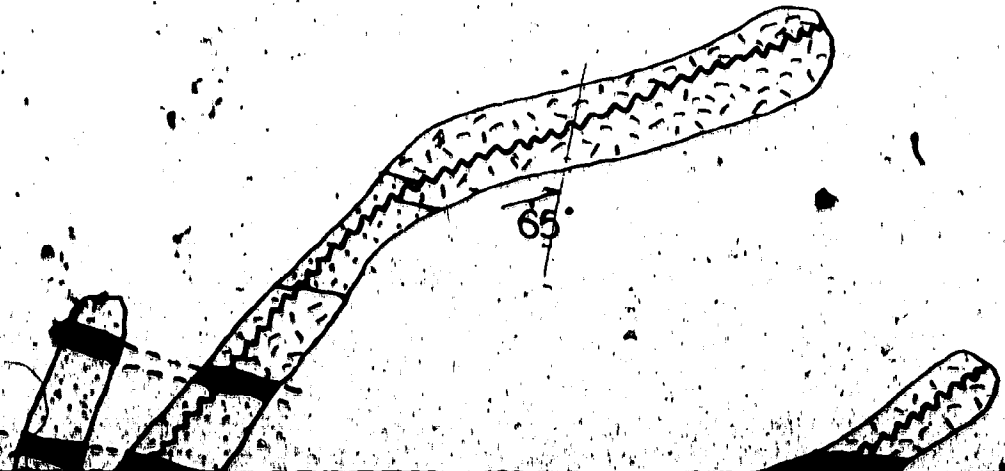
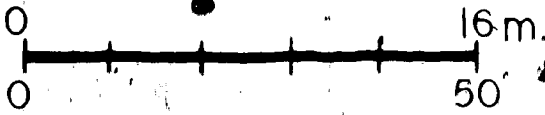
Vein dip

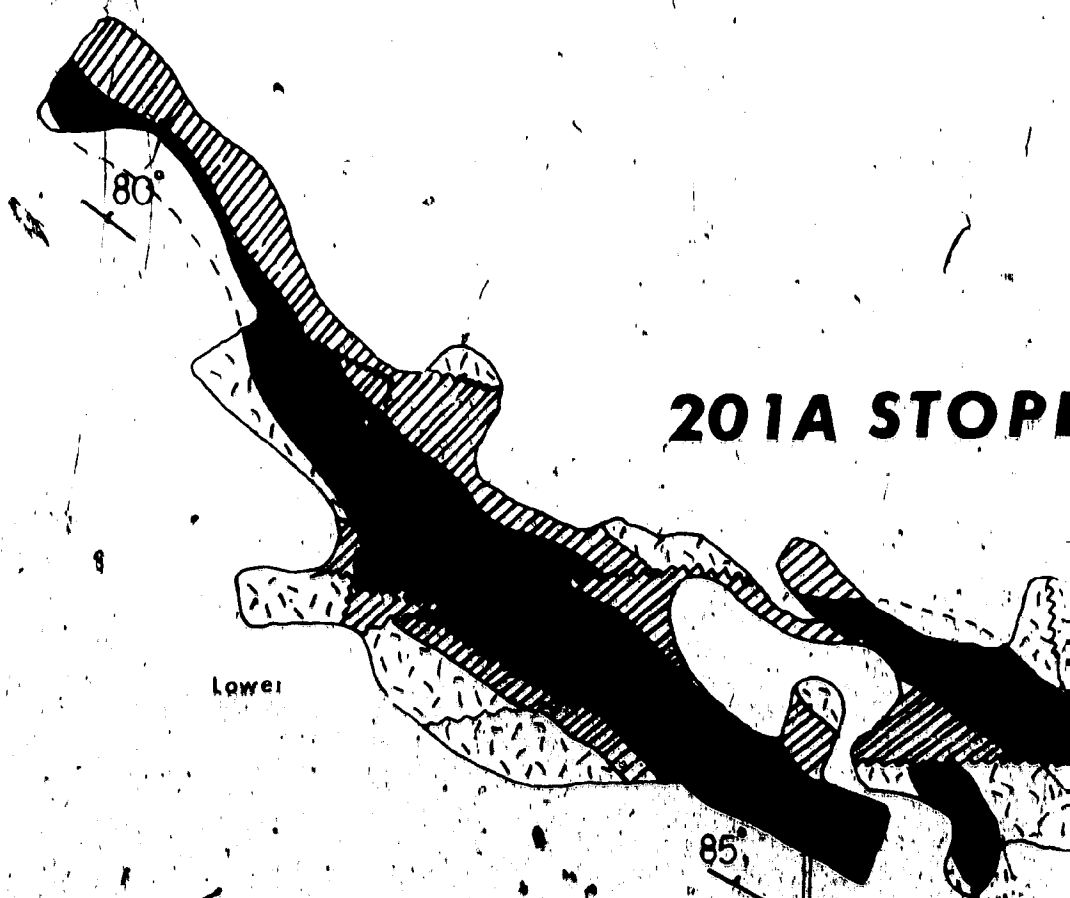
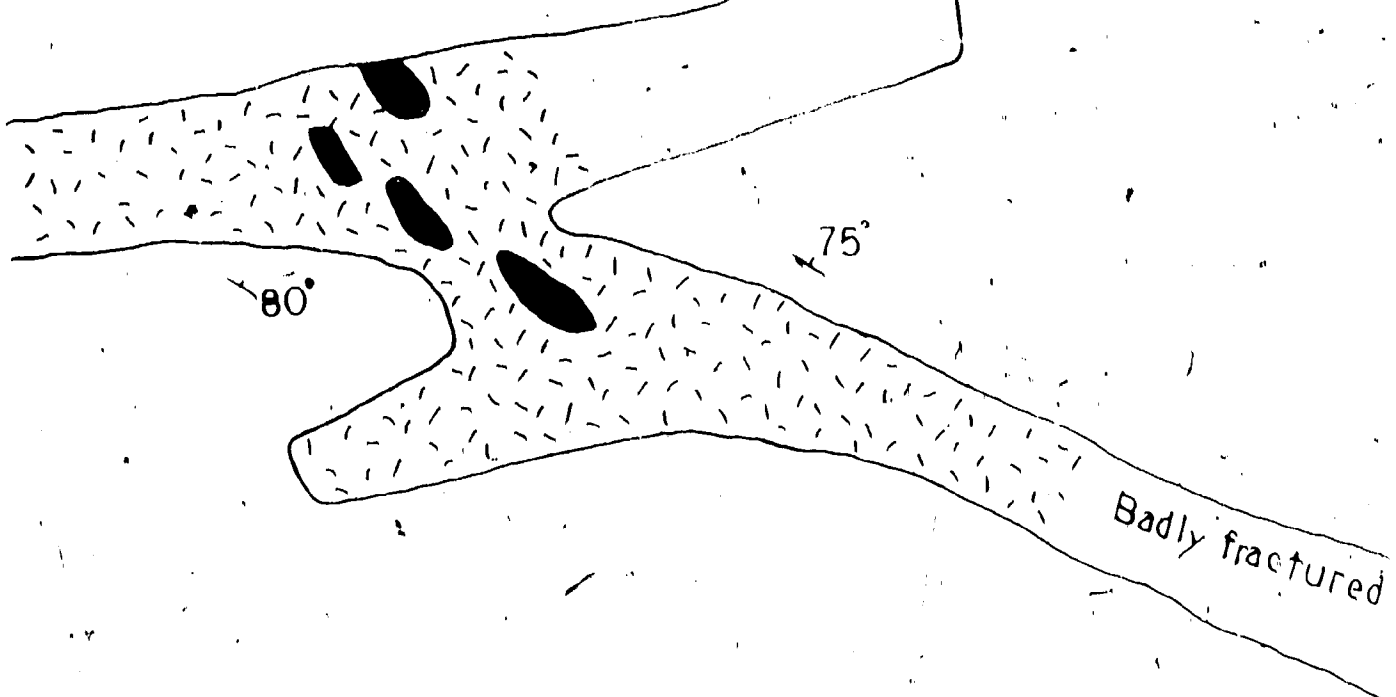


Bedding dip



5 of

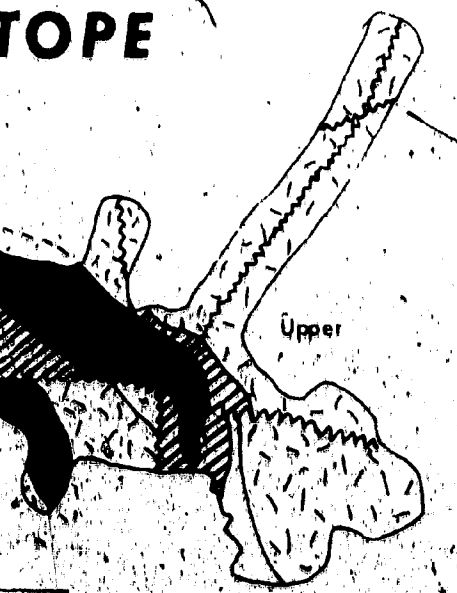




9900 N

fractured & altered rocks

TOPE



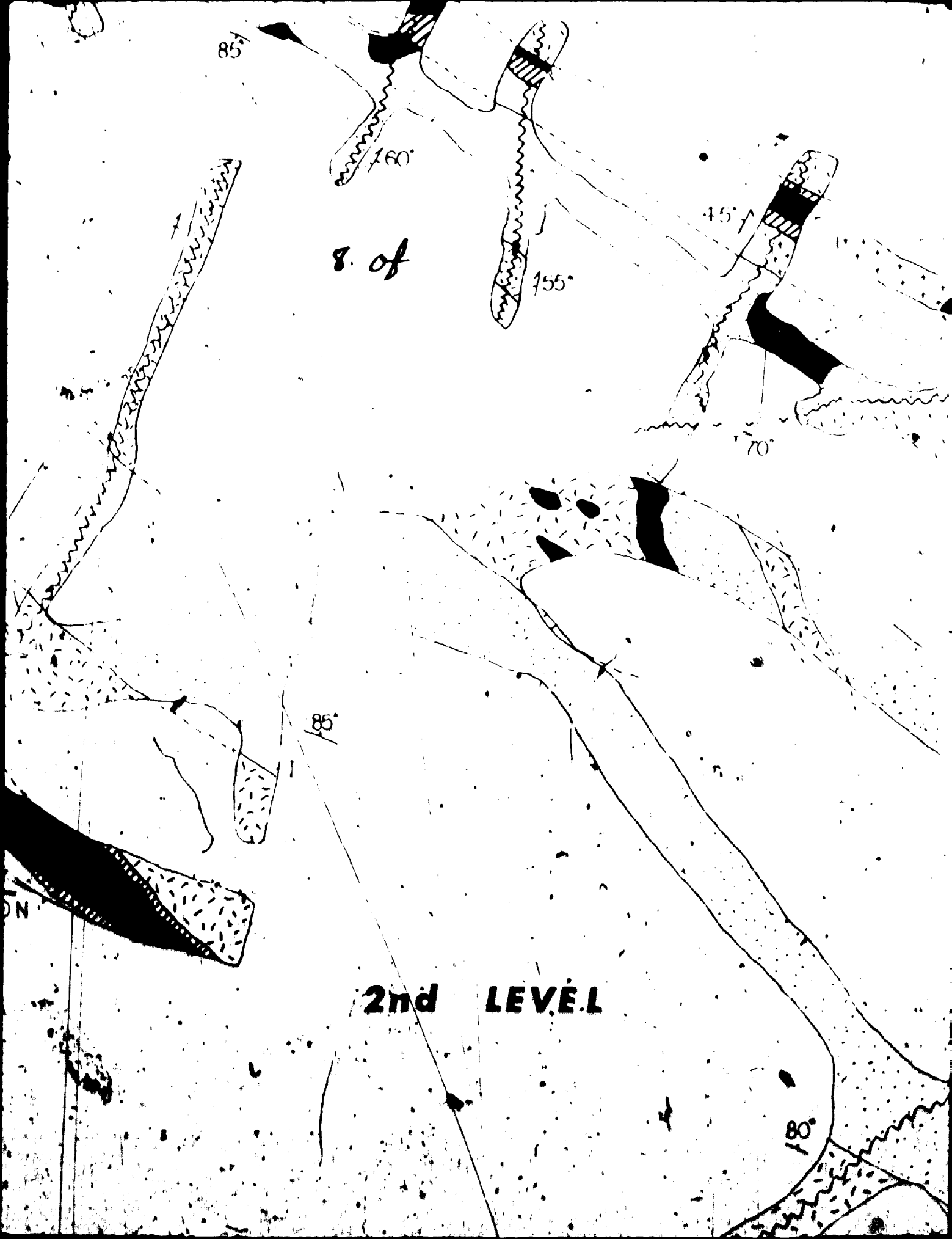
No. 1 vein

85°

9900 N

9900 E

9900 N



8. of

**2nd LEVEL**

85°

70°

75°

45°

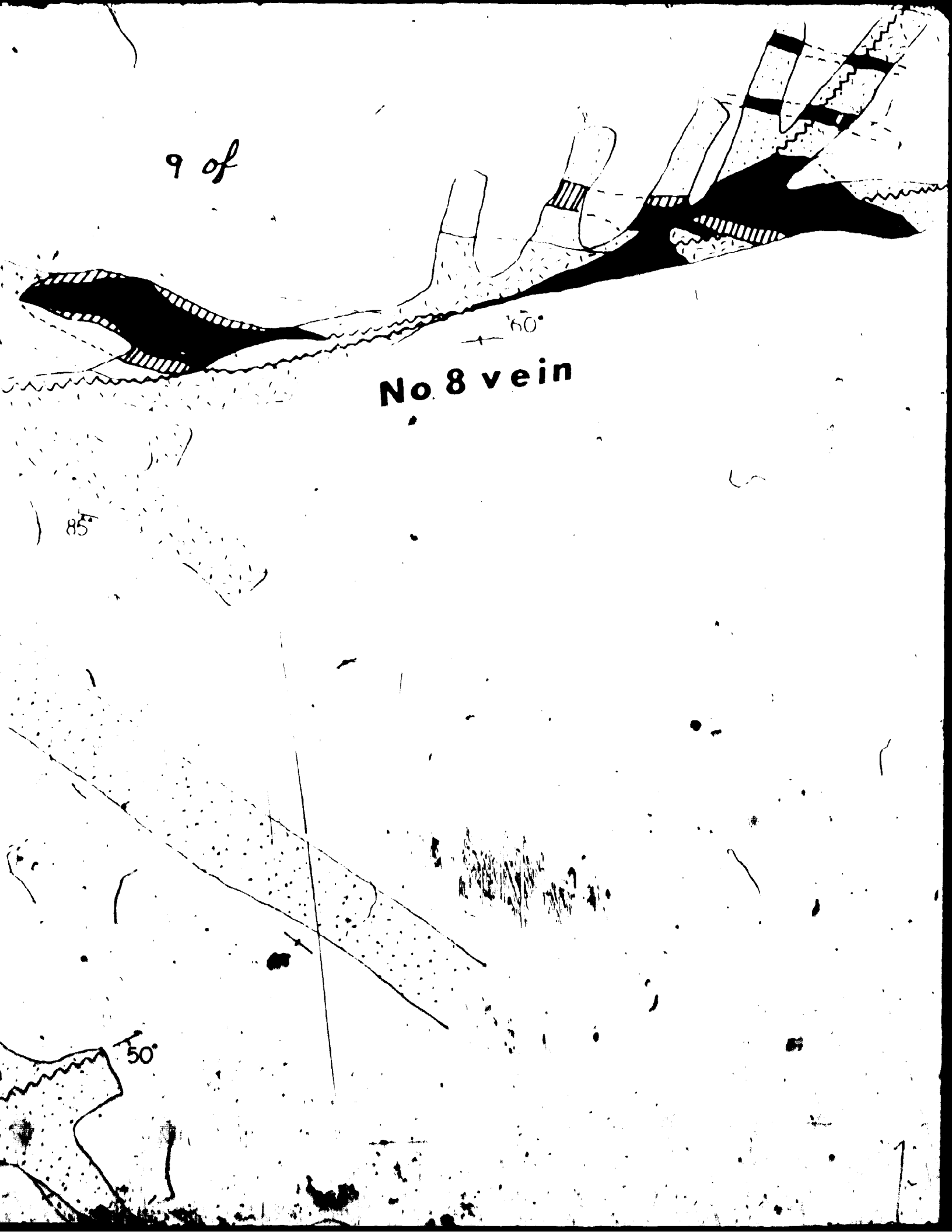
70°

85°

80°

ON

9 of



No. 8 vein

60°

85°

50°



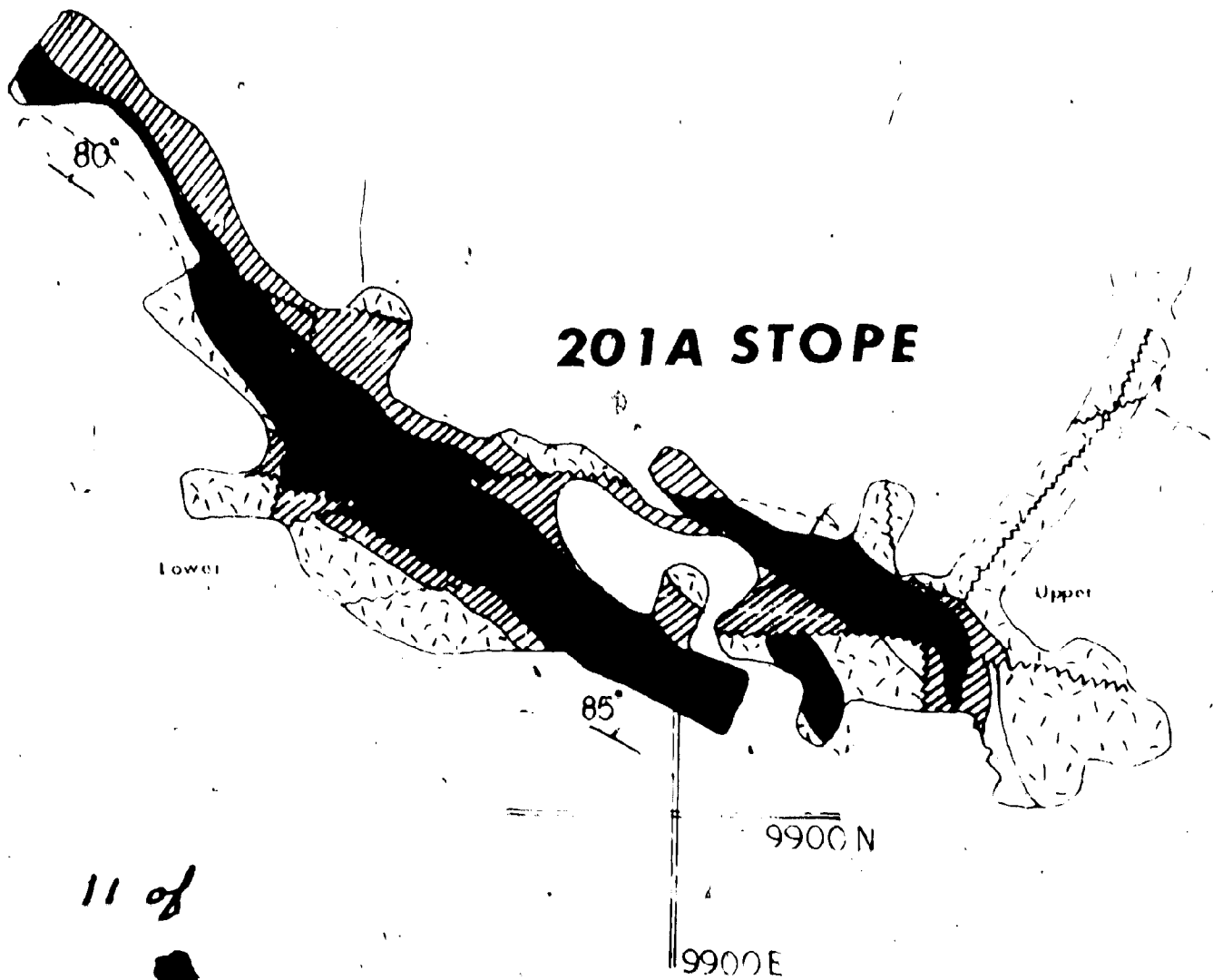


50°

ein

10 of

65°

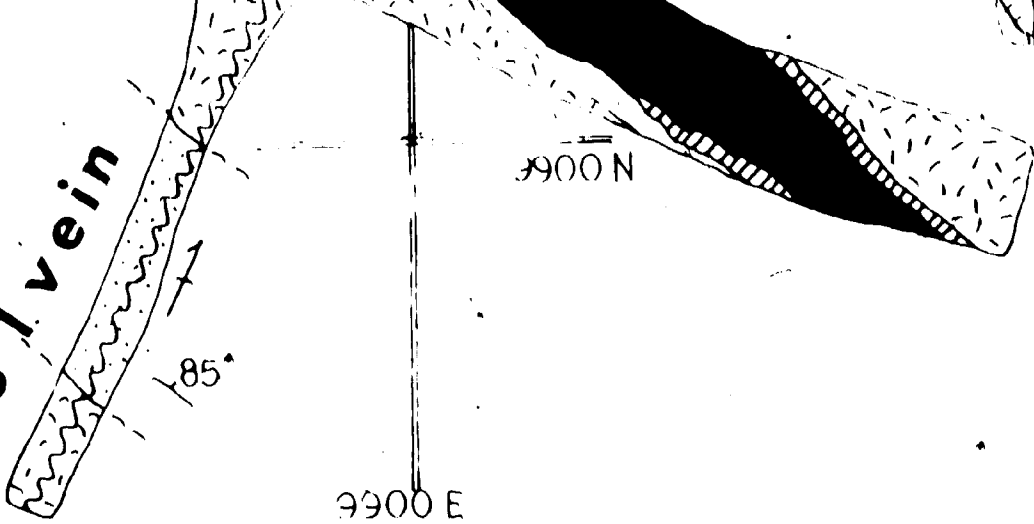


11 of

**Figure 31**

**THE TERRA MINE**

No 1 vein



85°

9900 N

85°

9900 E

2n

12 of 12

July 1970

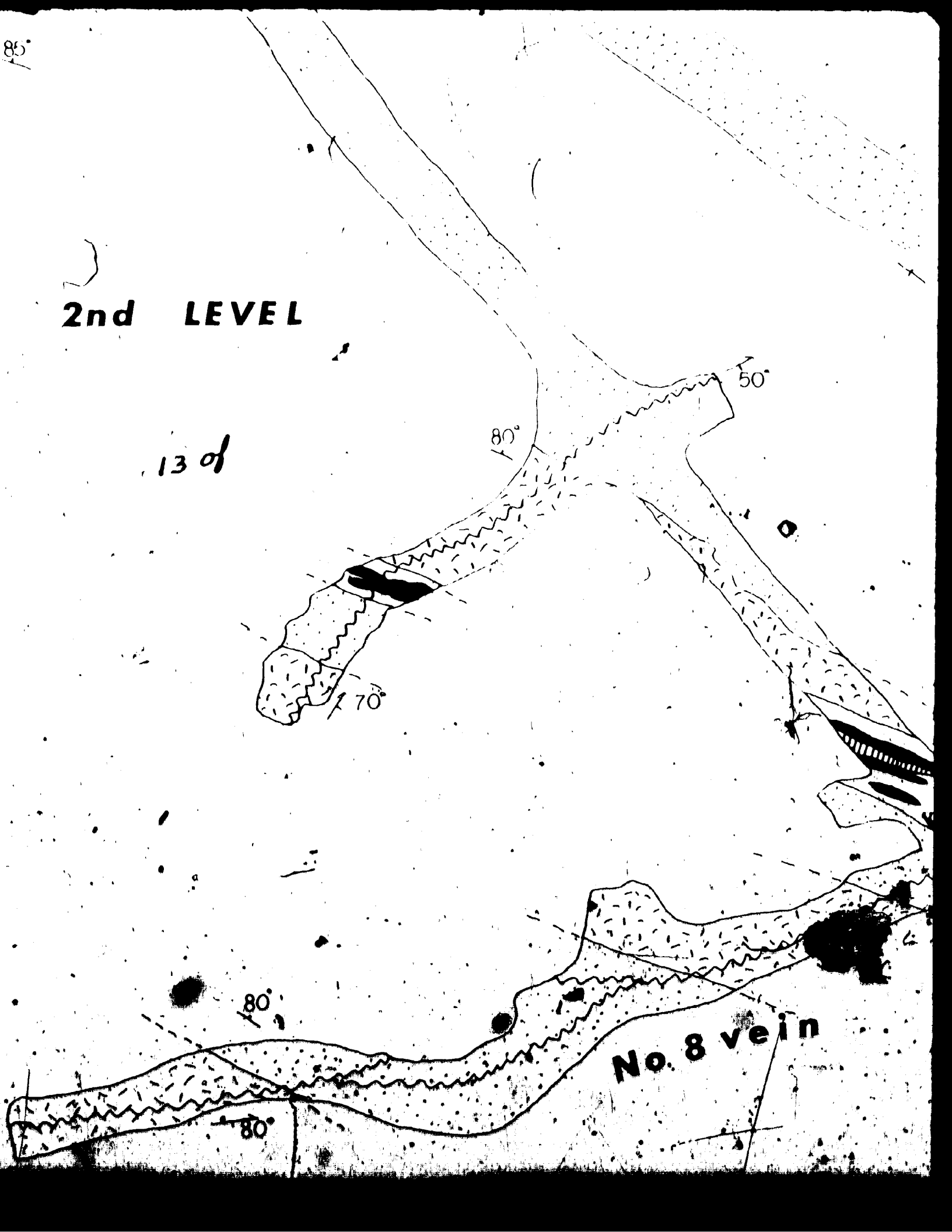
J.F.N.B.



85°

# 2nd LEVEL

13 of



50°

80°

70°

80°

80°

No. 8 vein

14 of 14

